CSC /TM-78/6010

NASA CR-183452

Computer Sciences Corporation

EVALUATION OF ONBOARD EPHEMERIS REPRESENTATIONS FOR THE SOLAR MAXIMUM MISSION (SMM) SPACECRAFT

Prepared For

NATIONAL AERONAUTICS AND SPACE ADMINISTRATION
Goddard Space Flight Center
Greenbelt, Maryland

CSC

CONTRACT NAS 5-24300
Task Assignment 893

MARCH 1978

(NASA-CR-183452) EVALUATION OF ONBOARD EPHEMERIS REPRESENTATIONS FOR THE SOLAR MAXIMUM MISSION (SMM) SPACECRAFT (Computer Sciences Corp.) 168 p

N90-70265

Unclas
00/13 0253121

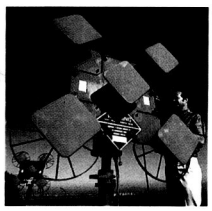

CSC/TM-78/6010

EVALUATION OF ONBOARD EPHEMERIS REPRESENTATIONS FOR THE SOLAR MAXIMUM MISSION (SMM) SPACECRAFT

Prepared for

GODDARD SPACE FLIGHT CENTER

By

COMPUTER SCIENCES CORPORATION

Under

Contract NAS 5-24300
Task Assignment 893

Prepared by:

Narendra Kumar 3/21/78
N. V. Kumar Date

Reviewed by:

David L Hall 3/21/78
David L. Hall Date

Approved by:

Anne C. Long 3/21/78
A. C. Long Date
Section Manager

ABSTRACT

This document describes the results of an evaluation of ephemeris representations for use onboard the Solar Maximum Mission (SMM) spacecraft. The proposed onboard algorithm involves a truncated Fourier series representation of the Cartesian components of the position and velocity at evenly spaced grid intervals followed by a four-point Hermite interpolation using the grid point coordinates. The numerical accuracy of this ephemeris representation was determined by comparing the interpolated ephemeris with a high precision ephemeris computed using the Goddard Trajectory Determination System (GTDS). Primary evaluation criteria are the onboard computational cost, optimization of core requirements in the onboard computer (OBC), and accuracy of representations.

TABLE OF CONTENTS

Section 1 - Introduction 1-1

Section 2 - Ephemeris Representation Algorithms 2-1

2.1 Overview of the Ephemeris Representation Process 2-1
2.1.1 Ground Support Functions 2-1
2.1.2 Onboard Functions 2-1
2.2 Mathematical Algorithms 2-2
2.2.1 Hermite Four-Point Interpolator 2-2
2.2.2 Fourier Series Cartesian Coordinate Representation 2-4
2.3 Mode of Analysis 2-5

Section 3 - Comparison of Ephemeris Representation Accuracies 3-1

3.1 Comparison of Fourier Series with and without Grid Point Residuals 3-3
3.1.1 No Residuals 3-4
3.1.2 Position Residuals 3-5
3.1.3 All Residuals 3-5
3.2 Comparison of 29- and 36-Term Fourier Series 3-72
3.2.1 No Residuals 3-72
3.2.2 Position Residuals 3-72
3.2.3 All Residuals 3-73
3.3 Comparison of 10- and 16-Minute Interpolation Grid Spacings 3-73
3.4 Effect of Changing Interpolation Interval 3-80

Section 4 - Influence of Drag, Gravity, and Orbital Eccentricity 4-1

4.1 Effect of Increased Atmospheric Drag 4-1
4.1.1 No Residuals 4-1
4.1.2 Position Residuals 4-3
4.1.3 Position and Velocity Residuals 4-3
4.2 Effect of Increased Gravity Model 4-3
4.2.1 No Residuals 4-10
4.2.2 Position Residuals 4-10
4.2.3 Position and Velocity Residuals 4-11
4.3 Effect of Orbital Eccentricity 4-11
4.3.1 No Residuals 4-11
4.3.2 Position Residuals 4-18
4.3.3 Position and Velocity Residuals 4-18

TABLE OF CONTENTS (Cont'd)

Section 4 (Cont'd)

4.4 Effect of Varying Mean Orbital Frequency 4-31
4.4.1 No Residuals 4-31
4.4.2 Position Residuals 4-31
4.4.3 Position and Velocity Residuals 4-32

Section 5 - Examination of Results 5-1

5.1 Summary of Results 5-1
5.2 Conclusions and Recommendations 5-2
5.3 Areas for Further Investigation 5-2
5.3.1 Cartesian Coordinate Representations 5-2
5.3.2 Orbital Element Representations 5-5

Appendix A - SMM Onboard Computation Algorithm

Appendix B - Recent Tracking and Data Relay Satellite (TDRS) Results

References

LIST OF ILLUSTRATIONS

Figure		
2-1	SMM Ephemeris Representation Program (SMMER)	2-6
3-1	Errors in the Representation of the Radial Component of Position Using a 29-Term Fourier Series with a 16-Minute Grid Spacing	3-6
3-2	Errors in the Representation of the Cross-Track Component of Position Using a 29-Term Fourier Series with a 16-Minute Grid Spacing	3-13
3-3	Errors in the Representation of the Along-Track Component of Position Using a 29-Term Fourier Series with a 16-Minute Grid Spacing	3-20
3-4	Errors in the Representation of the Radial Component of Velocity Using a 29-Term Fourier Series with a 16-Minute Grid Spacing	3-27
3-5	Errors in the Representation of the Cross-Track Component of Velocity Using a 29-Term Fourier Series with a 16-Minute Grid Spacing	3-34
3-6	Errors in the Representation of the Along-Track Component of Velocity Using a 29-Term Fourier Series with a 16-Minute Grid Spacing	3-41
3-7	Errors in the Representation of the Radial Component of Position Using a 29-Term Fourier Series with Position Residuals and a 16-Minute Grid Spacing	3-48
3-8	Errors in the Representation of the Cross-Track Component of Position Using a 29-Term Fourier Series with Position Residuals and a 16-Minute Grid Spacing	3-50
3-9	Errors in the Representation of the Along-Track Component of Position Using a 29-Term Fourier Series with Position Residuals and a 16-Minute Grid Spacing	3-52
3-10	Errors in the Representation of the Radial Component of Velocity Using a 29-Term Fourier Series with Position Residuals and a 16-Minute Grid Spacing	3-54
3-11	Errors in the Representation of the Cross-Track Component of Velocity Using a 29-Term Fourier Series with Position Residuals and a 16-Minute Grid Spacing	3-56

LIST OF ILLUSTRATIONS (Cont'd)

Figure

3-12 Errors in the Representation of the Along-Track Component of Velocity Using a 29-Term Fourier Series with Position Residuals and a 16-Minute Grid Spacing 3-58

3-13 Errors in the Representation of the Radial Component of Position Using a 29-Term Fourier Series with Position and Velocity Residuals and a 16-Minute Grid Spacing 3-60

3-14 Errors in the Representation of the Cross-Track Component of Position Using a 29-Term Fourier Series with Position and Velocity Residuals and a 16-Minute Grid Spacing 3-62

3-15 Errors in the Representation of the Along-Track Component of Position Using a 29-Term Fourier Series with Position and Velocity Residuals and a 16-Minute Grid Spacing 3-64

3-16 Errors in the Representation of the Radial Component of Velocity Using a 29-Term Fourier Series with Position and Velocity Residuals and a 16-Minute Grid Spacing 3-66

3-17 Errors in the Representation of the Cross-Track Component of Velocity Using a 29-Term Fourier Series with Position and Velocity Residuals and a 16-Minute Grid Spacing 3-68

3-18 Errors in the Representation of the Along-Track Component of Velocity Using a 29-Term Fourier Series with Position and Velocity Residuals and a 16-Minute Grid Spacing 3-70

3-19 Errors in the Representation of the Along-Track Component of Position Using a 36-Term Fourier Series with a 16-Minute Grid Spacing 3-74

3-20 Errors in the Representation of the Radial Component of Velocity Using a 36-Term Fourier Series with a 16-Minute Grid Spacing 3-75

3-21 Errors in the Representation of the Along-Track Component of Position Using a 36-Term Fourier Series with Position Residuals and a 16-Minute Grid Spacing 3-76

LIST OF ILLUSTRATIONS (Cont'd)

Figure

3-22 Errors in the Representation of the Radial Component of Velocity Using a 36-Term Fourier Series with Position Residuals and a 16-Minute Grid Spacing. 3-77

3-23 Errors in the Representation of the Along-Track Component of Position Using a 36-Term Fourier Series with Position and Velocity Residuals and a 16-Minute Grid Spacing 3-78

3-24 Errors in the Representation of the Radial Component of Velocity Using a 36-Term Fourier Series with Position and Velocity Residuals and a 16-Minute Grid Spacing 3-79

3-25 Errors in the Representation of the Along-Track Component of Position Using a 36-Term Fourier Series with a 10-Minute Grid Spacing 3-81

3-26 Errors in the Representation of the Radial Component of Velocity Using a 36-Term Fourier Series with a 10-Minute Grid Spacing 3-82

3-27 Errors in the Representation of the Along-Track Component of Position Using a 36-Term Fourier Series with Position Residuals and a 10-Minute Grid Spacing 3-83

3-28 Errors in the Representation of the Radial Component of Velocity Using a 36-Term Fourier Series with Position Residuals and a 10-Minute Grid Spacing 3-84

3-29 Errors in the Representation of the Along-Track Component of Position Using a 36-Term Fourier Series with Position and Velocity Residuals and a 10-Minute Grid Spacing 3-85

3-30 Errors in the Representation of the Radial Component of Velocity Using a 36-Term Fourier Series with Position and Velocity Residuals and a 10-Minute Grid Spacing 3-86

3-31 Errors in the Representation of the Along-Track Component of Position Using a 29-Term Fourier Series with a 10-Minute Grid Spacing and a (-.5, +.5) Interpolation Interval 3-88

3-32 Errors in the Representation of the Radial Component of Velocity Using a 29-Term Fourier Series with a 16-Minute Grid Spacing and a (-.5, + 5) Interpolation Interval 3-89

LIST OF ILLUSTRATIONS (Cont'd)

Figure

3-33 Errors in the Representation of the Along-Track Component of Position Using a 29-Term Fourier Series with Position Residuals, a 16-Minute Grid Spacing, and a (-.5, +.5) Interpolation Interval 3-90

3-34 Errors in the Representation of the Radial Component of Velocity Using a 29-Term Fourier Series with Position Residuals, a 16-Minute Grid Spacing, and a (-.5, +.5) Interpolation Interval 3-91

3-35 Errors in the Representation of the Along-Track Component of Position Using a 29-Term Fourier Series with Position and Velocity Residuals, a 16-Minute Grid Spacing, and a (-.5, +.5) Interpolation Interval 3-92

3-36 Errors in the Representation of the Radial Component of Velocity Using a 29-Term Fourier Series with Position and Velocity Residuals, a 16-Minute Grid Spacing, and a (-.5, +.5) Interpolation Interval 3-93

4-1 Errors in the Representation of the Along-Track Component of Position Using a 29-Term Fourier Series and a 16-Minute Grid Spacing in the Case of Increased Drag Effects 4-4

4-2 Errors in the Representation of the Radial Component of Velocity Using a 29-Term Fourier Series and a 16-Minute Grid Spacing in the Case of Increased Drag Effects 4-5

4-3 Errors in the Representation of the Along-Track Component of Position Using a 29-Term Fourier Series with Position Residuals and a 16-Minute Grid Spacing in the Case of Increased Drag Effects 4-6

4-4 Errors in the Representation of the Radial Component of Velocity Using a 29-Term Fourier Series with Position Residuals and a 16-Minute Grid Spacing in the Case of Increased Drag Effects 4-7

4-5 Errors in the Representation of the Along-Track Component of Position Using a 29-Term Fourier Series with Position and Velocity Residuals and a 16-Minute Grid Spacing in the Case of Increased Drag Effects 4-8

LIST OF ILLUSTRATIONS (Cont'd)

Figure

4-6 Errors in the Representation of the Radial Component of Velocity Using a 29-Term Fourier Series with Position and Velocity Residuals and a 16-Minute Grid Spacing in the Case of Increased Drag Effects 4-9

4-7 Errors in the Representation of the Along-Track Component of Position Using a 29-Term Fourier Series with a 16-Minute Grid Spacing in the Case of Increased Gravitational Effects 4-12

4-8 Errors in the Representation of the Radial Component of Velocity Using a 29-Term Fourier Series with a 16-Minute Grid Spacing in the Case of Increased Gravitational Effects 4-13

4-9 Errors in the Representation of the Along-Track Component of Position Using a 29-Term Fourier Series with Position Residuals and a 16-Minute Grid Spacing in the Case of Increased Gravitational Effects 4-14

4-10 Errors in the Representation of the Radial Component of Velocity Using a 29-Term Fourier Series with Position Residuals and a 16-Minute Grid Spacing in the Case of Increased Gravitational Effects 4-15

4-11 Errors in the Representation of the Along-Track Component of Position Using a 29-Term Fourier Series with Position and Velocity Residuals and a 16-Minute Grid Spacing in the Case of Increased Gravitational Effects 4-16

4-12 Errors in the Representation of the Radial Component of Velocity Using a 29-Term Fourier Series with Position and Velocity Residuals and a 16-Minute Grid Spacing in the Case of Increased Gravitational Effects 4-17

4-13 Errors in the Representation of the Along-Track Component of Position Using a 29-Term Fourier Series with a 16-Minute Grid Spacing for Case 4 4-19

4-14 Errors in the Representation of the Radial Component of Velocity Using a 29-Term Fourier Series with a 16-Minute Grid Spacing for Case 4 4-21

4-15 Errors in the Representation of the Along-Track Component of Position Using a 29-Term Fourier Series with Position Residuals and a 16-Minute Grid Spacing for Case 4 4-23

LIST OF ILLUSTRATIONS (Cont'd)

Figure

4-16 Errors in the Representation of the Radial Component of Velocity Using a 29-Term Fourier Series with Position Residuals and a 16-Minute Grid Spacing for Case 4 4-25

4-17 Errors in the Representation of the Along-Track Component of Position Using a 29-Term Fourier Series with Position and Velocity Residuals and a 16-Minute Grid Spacing for Case 4 4-27

4-18 Errors in the Representation of the Radial Component of Velocity Using a 29-Term Fourier Series with Position and Velocity Residuals and a 16-Minute Grid Spacing for Case 4 4-29

5-1 Difference Between High-Precision and Ephemeris Representation of X Component of Position 5-4

LIST OF TABLES

Table

1-1 Summary of Previous SMM Ephemeris Representation Studies 1-3

3-1 SMM Test Cases 3-2

3-2 Summary of SMM Representation Accuracies Varying Interpolation Parameters for Case 1 3-4

4-1 Comparison of SMM Representation Accuracies for Different Force Models 4-2

5-1 Summary of SMM Results 5-3

SECTION 1 - INTRODUCTION

The concept of Multimission Modular Spacecraft (MMS) was developed in response to an increasing demand for standardization of spacecraft and detailed mission design. In this concept a spacecraft will use modular, standardized hardware components and onboard software which will be adaptable to a variety of missions. Many of these missions require ground based orbit determination and prediction with subsequent transmission of a 3-4 day span of predicted ephemeris data to the spacecraft. This ephemeris data when used in conjunction with computational algorithms available in the onboard computer (OBC) must be sufficient to reconstruct the predicted spacecraft trajectory to within some specified degree of accuracy. The transmitted data plus the OBC ephemeris reconstruction algorithms is referred to as an "ephemeris representation". Onboard the spacecraft, the ephemeris representation can be used in real time to compute information required in the attitude and control algorithms, to compute the line-of-sight vector to Tracking and Data Relay Satellites (TDRS), and to annotate the scientific data.

Results from a general investigation of ephemeris representations from MMS missions are presented in References 1, 2, and 3. In that study the relationship of representation accuracy to OBC core and time requirements and uplink data transmission requirements was identified. Use of the NASA Standard Spacecraft Computer-1 (NSSC-1) as the OBC for Landsat-D and the Solar Maximum Mission (SMM) were given particular attention. Ephemeris representations for TDRS type spacecraft were previously evaluated and documented in Reference 4.

Two constraints, in addition to an accuracy requirement, influence the design of an ephemeris representation for early MMS missions such as SMM. First, the size of the ground-to-spacecraft data transmission is limited. Therefore, a highly accurate ephemeris cannot be simply computed on the ground and

transmitted to the spacecraft for every time of interest (every 30 seconds at a minimum). Second, the computational ability of the NSSC-1 is limited. Hence, a highly accurate analytical (or quadrature) formulation is probably too complex for onboard computation of the spacecraft position and velocity at the desired times.

To satisfy both constraints, a compromise between a completely analytical and a completely numerical ephemeris representation was adopted which is nearly identical to the Block 5D algorithm (Reference 5). In this approach a simple analytical approximation to the ephemeris and a file of residuals are computed on the ground and transmitted to the spacecraft. The residuals are the differences between accurate ephemeris coordinates and the analytical approximation at the interpolation grid points. Each residual is constrained to fit in a single precision OBC word. The analytical approximation acts as a data compression device which decreases the required data transmission. The OBC algorithm consists of evaluating the analytical approximation and adding the residuals to reconstruct the interpolation grid points and interpolating for the times of interest.

Several possible analytic approximations to the ephemeris data were considered in the previous study and are listed in Table 1-1. From a physical viewpoint, it is natural to consider an analytic representation of classical orbital elements because there exists an enormous theoretical background detailing how classical elements evolve in time due to various gravitational, drag, etc., perturbations. However, the computation time required by the NSSC-1 to convert from classical to Cartesian elements is relatively large. For missions such as SMM which require Cartesian elements at the times of interest (e.g., every 30 seconds), the first study indicates that it is advantageous to directly model the Cartesian coordinates rather than mean or osculating classical elements.

An analytic representation consisting of a set of Chebyshev time series polynomials was considered but found to be inappropriate because the data span of

Table 1-1. Summary of Previous SMM Ephemeris Representation Studies

AREA STUDIED	RECOMMENDATIONS
EPHEMERIS FORMULATIONS: • OSCULATING ORBITAL ELEMENTS • MEAN ORBITAL ELEMENTS • CARTESIAN COORDINATES • FOURIER SERIES FIT TO $\vec{r}, \dot{\vec{r}}$ WITH RESIDUALS AT GRID POINTS • FOURIER SERIES FIT TO $\vec{r}, \dot{\vec{r}}$	CARTESIAN COORDINATES
INTERPOLATORS: • 5-POINT LAGRANGE • 2-, 3-, 4-POINT HERMITE	4-POINT HERMITE
INTERPOLATION GRID SPACING	16 MINUTES

3 to 4 days includes 45 revolutions of the SMM spacecraft. Since Cartesian components of position and velocity exhibit periodicities on the order of the spacecraft period, Chebyshev time series representation requires too many coefficients to be efficient.[1] Instead, a truncated Fourier-power series was indicated.

Various interpolators were also studied. A four-point Hermite interpolation used with a 16-minute interpolation interval was found to yield an interpolation error below 300 m when compared with the reference ephemeris for SMM-type orbits.

Thus, the basic result of Reference 1 is to suggest that a truncated Fourier series with grid point residuals coupled with a Hermite interpolation scheme is a good candidate ephemeris representation for SMM.

The current evaluation begins with this concept and concentrates on refinement of the Cartesian coordinate representation to meet the SMM accuracy requirements with minimum data transmission. For the Sun-pointing SMM, mission requirements are satisfied if the predicted representation is in agreement with the exact ephemeris to within 7 kilometers. The representation must maintain this accuracy for a data span of 3 to 4 days. This 7-kilometer accuracy requirement is dictated primarily by the ground-based experimenters. Since the error in the reference SMM predicted ephemeris has a root-mean-squared (rms) value of about 5 km over a 3-day span, the ephemeris representation is constrained to add no more than 2 km rms additional error (Reference 6).

Several variations in the Cartesian coordinate representation were investigated including: (1) uplink only the Fourier-power series coefficients and evaluate the series directly to obtain position and velocity at the present times; (2) uplink only the Fourier power series coefficients, evaluate the series to

---

[1] Even breaking the data set into several subintervals would not alleviate the problem of too many coefficients.

obtain grid-point values of the position and velocity, and interpolate for position and velocity at the request times; and (3) uplink Fourier-power series coefficients and grid-point residuals for the position and velocity, reconstruct the grid-point coordinates using the Fourier-power series and residuals, and interpolate for position and velocity at the request times.

The primary evaluation criteria are

- Interpolation accuracy
- Onboard computational speed and core requirements
- Data transmission requirements from the ground

This required software is coded in FORTRAN. It has also been recoded from the original FORTRAN version into the assembly language for the NSSC-1. The present analysis was performed on the IBM S/360-95 computer. Section 2 discusses the mathematical algorithms used in the analysis. Numerical results of the evaluation are presented in Section 3 and 4 of this document. Graphs of these results, obtained using the Goddard Trajectory Determination System (GTDS) Ephemeris Comparison (COMPARE) program, are also presented. Section 5 summarizes the study, discusses the results in terms of accuracy and computational times for the NSSC, and suggests areas for future investigation.

Appendix A presents a copy of the specification for the "SMM Onboard Ephemeris Computation Algorithm", revised according to the recommendations expressed in the present document. In Appendix B additional TDRS results are discussed as an extension of work presented in Reference 4.

SECTION 2 - EPHEMERIS REPRESENTATION ALGORITHMS

The present study is an extension of the study described in Reference 1. The purpose of this study is to evaluate the accuracy of an ephemeris representation for SMM consisting of a Hermite four-point interpolator used in conjunction with a Fourier Series Cartesian coordinate representation of the grid points. The numerical accuracy of the ephemeris representation was determined by comparison with a high precision ephemeris file using the GTDS COMPARE program. An overview of the ground support and spacecraft functions is given in this section. The details of the algorithms are presented, and an overview of the evaluation procedure is described.

2.1 OVERVIEW OF THE EPHEMERIS REPRESENTATION PROCESS

2.1.1 Ground Support Functions

A 3-day file of Cartesian ephemeris data is generated by a numerical integration. This data is analyzed to determine the mean orbital frequency and least-squares fit to the truncated Fourier power series discussed in Section 2.2.2. An optional step is to compute the coordinate residuals or differences between the accurate ephemeris and Fourier series. The Fourier coefficients, mean orbital frequency, reference times, grid spacing and (perhaps) residuals are to be transmitted to the spacecraft.

2.1.2 Onboard Functions

The Fourier series are evaluated for $\bar{r}$ and $\dot{\bar{r}}$ at specified grid point times. An option at this point is to add the residuals to reconstruct the accurate ephemeris data. Each time a new grid point value is computed, i.e., about every 16 minutes, new Hermitean interpolation coefficients are computed. At each request time, which is on the order of every 30 seconds for SMM, Hermitean interpolation is performed for the position and velocity coordinates. The Hermitean interpolation formulas are discussed in Section 2.2.1.

The direct evaluation of the Fourier series at each request time was found to be too costly computationally[1] for SMM and hence not considered in detail.

2.2 MATHEMATICAL ALGORITHMS

This section describes the Hermite four-point interpolator and the Fourier series Cartesian coordinate representation.

2.2.1 Hermite Four-Point Interpolator

A Hermite four-point interpolation is used to obtain the value of a position or velocity component at an arbitrary time, t, within a grid of four equally-spaced times t_1, t_2, t_3, t_4. For each position-velocity pair $(x, \dot{x})$, interpolation is performed by the expressions

$$x(t) = x_2 + p\left\{g\dot{x}_2 + p\left[y_1 + p\left(y_2 + p\left(y_3 + p(y_4 + p(y_5 + py_6))\right)\right)\right]\right\} \quad (2\text{-}1)$$

$$\dot{x}(t) = \dot{x}_2 + \frac{p\left\{2y_1 + p\left[3y_2 + p\left(4y_3 + p(5y_4 + p(6y_5 + 7py_6))\right)\right]\right\}}{g} \quad (2\text{-}2)$$

where g is the time interval between grid points, and $p = \left[(t - t_2)/g\right]$. This algorithm requires $(7j + 10.2\,k + 1)$ multiplications and $(7j + 5k + 1)$ additions, where j and k are the number of interpolated position and velocity components, respectively.

---

[1] The estimated cost in the NSSC-1 is 85 milliseconds for evaluation of a 29-term Fourier series, 40 milliseconds for computation of the 4-point Hermitean interpolation coefficients, and 20 milliseconds for the interpolation for position and velocity at the request time. Thus, to directly evaluate the 29-term Fourier series every 30 seconds over a 16 minute interval requires approximately 2700 milliseconds, while the Fourier series/Hermite scheme requires approximately 1000 milliseconds to generate the same points (Reference 7).

The interpolation coefficients $y_1, y_2, \ldots, y_6$ are determined by the following relations

$$(y_1, y_2, y_3, y_4, y_5, y_6) = (x_1, x_2, x_3, x_4)A + g(\dot{x}_1, \dot{x}_2, \dot{x}_3, \dot{x}_4)B \quad (2\text{-}3)$$

where x stands for any position coordinate and $\dot{x}$ is the corresponding velocity coordinate, the subscripts refer to various grid points, and A and B are the 4×6 matrices

$$A = \begin{bmatrix} \frac{56}{108} & -\frac{124}{108} & \frac{50}{108} & \frac{59}{108} & -\frac{52}{108} & \frac{11}{108} \\ -\frac{11}{4} & \frac{1}{4} & \frac{10}{4} & \frac{1}{2} & \frac{3}{4} & \frac{1}{4} \\ 2 & 1 & \frac{5}{2} & \frac{1}{4} & 1 & \frac{1}{4} \\ \frac{25}{108} & -\frac{11}{108} & -\frac{50}{108} & \frac{22}{108} & \frac{25}{108} & -\frac{11}{108} \end{bmatrix}$$

and

$$B = \begin{bmatrix} \frac{1}{9} & \frac{2}{9} & \frac{1}{36} & \frac{7}{36} & \frac{5}{36} & \frac{1}{36} \\ -1 & \frac{7}{4} & 2 & \frac{1}{2} & -1 & \frac{1}{4} \\ -1 & 0 & \frac{7}{4} & \frac{1}{4} & \frac{3}{4} & \frac{1}{4} \\ -\frac{1}{18} & \frac{1}{36} & \frac{1}{9} & -\frac{1}{18} & -\frac{1}{18} & \frac{1}{36} \end{bmatrix}$$

When written out explicitly, these equations involve 32n multiplications and 41n additions, where n is the number of position-velocity pairs.

2.2.2 Fourier Series Cartesian Coordinate Representation

In order to represent the Cartesian ephemeris data at the equispaced grid points, a Fourier-power series is chosen of the form

$$\sum_{i=0}^{N=3} \sum_{j=0}^{M=5} \left[a_{ij} t^j \sin(iwt) + b_{ij} t^j \cos(iwt) \right] \tag{2-4}$$

The mean orbital frequency, w, is assumed to be the same for each Cartesian coordinate. Such a representation is consistent with modeling the variation of the Cartesian coordinates due to second and third degree zonal geopotential effects and atmospheric drag. In practice, the series is used in the nested form

$$\begin{aligned}
X(t) = {} & A_1 + t\left\{A_2 + t\left[A_3 + t\left(A_4 + t(A_5 + tA_6)\right)\right]\right\} \\
& + \left\{A_7 + t\left[A_8 + t\left(A_9 + t\left(A_{10} + t(A_{11} + tA_{12})\right)\right)\right]\right\} \sin(wt) \\
& + \left\{A_{13} + t\left[A_{14} + t\left(A_{15} + t\left(A_{16} + t(A_{17} + tA_{18})\right)\right)\right]\right\} \cos(wt) \\
& + \left\{A_{19} + t\left[A_{20} + t\left(A_{21} + t(A_{22} + tA_{23})\right)\right]\right\} \sin^2(wt) \\
& + \left\{A_{24} + t\left[A_{25} + t\left(A_{26} + t(A_{27} + tA_{28})\right)\right]\right\} \sin(wt)\cos(wt) \\
& + \left\{A_{29} + t\left[A_{30} + t(A_{31} + tA_{32})\right]\right\} \sin^3(wt) \\
& + \left\{A_{33} + t\left[A_{34} + t(A_{35} + tA_{36})\right]\right\} \sin^2(wt)\cos(wt)
\end{aligned} \tag{2-5}$$

where X is any position or velocity component and t is the time relative to the reference time for the span. This form is obtained by making use of the fact that trigonometric functions of multiple angles are simple polynomials

in the functions of the fundamental angle. This computation requires 2 sines/cosines, $[(2N + 1) Mn + 2Nn + 2N - 2]$ multiplications, and $[(2N + 1) Mn + 2Nn]$ additions, where N and M are the highest harmonic and the highest power of t, respectively, and n is the number of position and velocity components.

The coefficients A_i are obtained by a least-squares fit of Equation (2-5) to the accurate ephemeris file generated by numerical integration. The frequency w is assumed known, either from a priori knowledge of the orbital period or by spectral analysis (such as by the Maximum Entropy Method described in Reference 8) of the ephemeris file.

2.3 MODE OF ANALYSIS

In the current study, the following procedure was adopted to evaluate ephemeris representations for SMM OBC applications.

1. Given precision ephemeris data at a specified grid spacing determine the coefficients and residuals for a Fourier series Cartesian coordinate representation. This determination was accomplished using the SMM Ephemeris Representation (SMMER) program developed by CSC personnel. A flow diagram of SMMER is given in Figure 2-1.

2. Study three possible representations for the Cartesian coordinates at the grid points.

    a. Fourier series with no residuals at grid points

    b. Fourier series with position residuals at grid points

    c. Fourier series with position and velocity residuals at grid points

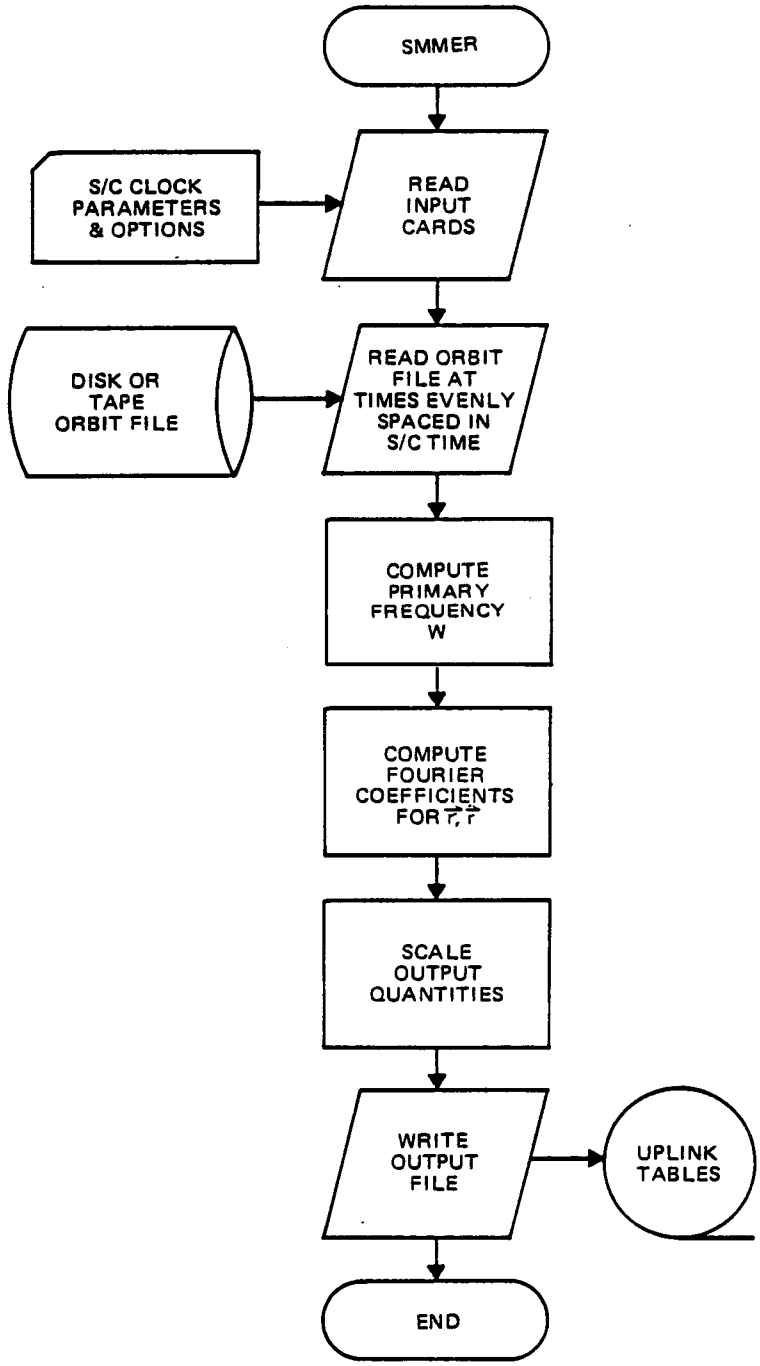

Figure 2-1. SMM Ephemeris Representation Program (SMMER)

3. Using any one of the above representations compute the Cartesian coordinates at the specified grid points. Interpolate on the coordinates thus obtained using the Hermite four-point interpolation scheme. Create an ORB1 file using the OBC software and compare it with a previously created high precision ORB1 file using the GTDS COMPARE program. Further, graphical plots are obtained using the plotting option of the COMPARE routine. Appendix A gives the technical details of the OBC software.

SECTION 3 - COMPARISON OF EPHEMERIS REPRESENTATION ACCURACIES

The accuracy of a SMM trajectory computed by the OBC algorithm was evaluated by comparison at one minute intervals with a 3-day high precision trajectory. The results from these comparisons are presented below.

The four nominal SMM state vectors used for the above analysis are given in Table 3-1. It should be noted that Case 2 will be more affected by atmospheric drag than Case 1, Case 3 will be more affected by nonspherical gravitational forces than Cases 1 or 2, and Case 4 is more circular than Case 1. For Cases 1, 2, and 3, the mean orbital frequency (used in the Fourier series) was computed using the numerical osculating-to-mean element conversion process available in the Goddard Trajectory Determination System (GTDS). In Case 4 the mean orbital frequency was computed using the Maximum Entropy Method (MEM) spectral analysis technique (Reference 8).

Several variations in this Cartesian representation algorithm were tested. These are:

- Two choices for the set of Fourier series coefficients:
  - 36-set {all 36-coefficients of the Fourier series given in Equation (2-5)}
  - 29-set {excluding the 7-coefficients (A_6, A_{12}, A_{18}, A_{23}, A_{28}, A_{32}, and A_{36})}
- Two choices for grid point spacing:
  - 10 minutes
  - 16 minutes

Table 3-1. SMM Test Cases

PARAMETER	CASE I	CASE II	CASE III	CASE IV
EPOCH	710930.0	710930.0	710930.0	710930.0
SEMIMAJOR AXIS (km)	6832.91	6832.91	6832.91	6933.74
ECCENTRICITY	0.018	0.018	0.018	0.001
INCLINATION (DEG)	33.144	33.144	33.144	33.0
LONGITUDE OF ASCENDING NODE (DEG)	306.714	306.714	306.714	270.0
ARGUMENT OF PERIGEE (DEG)	66.575	66.575	66.575	90.0
MEAN ANOMALY (DEG)	88.002	88.002	88.002	0.0
SPACECRAFT AREA (m^2)	10	17.3	17.3	17.3
SPACECRAFT MASS (kg)	1000	735	735	735
SOLAR FLUX VALUE	150	175	175	175
DRAG COEFFICIENT	2.0	2.5	2.5	2.5
GRAVITY MODEL	8x8	8x8	15x15	15x15
MEAN ORBITAL FREQUENCY (SEC^{-1})	0.0011177905	0.0011177905	0.00118344	0.001094782

- Three choices of grid point residuals
  - No residuals
  - Position and velocity residuals
  - Only position residuals
- Two choices for interpolation interval:
  - Interpolate using an equal distribution (±0.5) of points to the left and right of the second grid point.
  - Interpolate using a quarter three-quarter (±0.25, ±0.75) distribution of data points to the left and right of the second grid point.

These choices were based on results presented in References 1, 2, and 3.

3.1 COMPARISON OF FOURIER SERIES WITH AND WITHOUT GRID POINT RESIDUALS

For this analysis comparison of the trajectories from 29-term Fourier series were made every minute over a 71-hour duration with a high precision trajectory. The nominal state vector is Case 1 in Table 3-1. The reference solution included the effects of a nonspherical geopotential field, Sun, Moon, and atmospheric drag. The interpolation interval was (-0.25, +0.75) from the second grid point and the grid-point spacing was 16 minutes.

3.1.1 No Residuals

The first entry of Table 3-2 contains the error statistics for this case. The rms position errors are 0.139 kilometers for the radial component, 0.127 kilometers for the cross-track component, and 0.472 kilometers for the along-track component. The rms errors in velocity are 0.665×10^{-3} kilometers/second in the radial, 0.135×10^{-3} in the cross-track, and 0.43×10^{-3} kilometers/second in the along-track components. The minimum and maximum position differences are 0.376×10^{-4} and 0.486 kilometers, 0.227×10^{-3} and 0.345 kilometers, and

Table 3-2. Summary of SMM Representation Accuracies Varying Interpolation Parameters for Case 1

FOURIER SERIES (TERMS)	GRID INTERVAL (MIN)	RESIDUALS	INTERPOLATION INTERVAL	RMS POSITION ERROR				RMS VELOCITY ERROR				MAXIMUM POSITION ERROR			
				H (km)	C (km)	L (km)	$\Delta\vec{R}$ (km)	H (m/s)	C (m/s)	L (m/s)	$\Delta\dot{\vec{R}}$ (m/s)	H (km)	C (km)	L (km)	$\Delta\vec{R}$ (km)
29	16	NONE	(−0.25, +0.75)	0.13981	0.12783	0.47265	0.50920	0.66590	0.13530	0.43062	0.80441	0.48634	0.34587	1.29999	1.34217
29	16	$\vec{r}$	(−0.25, +0.75)	0.11701	0.02176	0.10037	0.15569	0.57511	0.10881	0.45273	0.73997	0.51335	0.11638	0.37958	0.55224
29	16	$\vec{r}, \dot{\vec{r}}$	(−0.25, +0.75)	0.10063	0.00056	0.08352	0.13078	0.45444	0.00264	0.41318	0.61420	0.29867	0.00314	0.20893	0.30323
36	16	NONE	(−0.25, +0.75)	0.14022	0.12336	0.47084	0.50653	0.66498	0.12975	0.43067	0.80281	0.52418	0.33244	1.30767	1.33844
36	16	$\vec{r}$	(−0.25, +0.75)	0.11674	0.02024	0.10024	0.15520	0.57415	0.10318	0.45340	0.73883	0.52531	0.10399	0.40007	0.56466
36	16	$\vec{r}, \dot{\vec{r}}$	(−0.25, +0.75)	0.10063	0.00056	0.08352	0.13078	0.45444	0.00264	0.41318	0.61420	0.29867	0.00313	0.20893	0.30323
36	10	NONE	(−0.25, +0.75)	0.09656	0.12352	0.46412	0.48989	0.48704	0.12967	0.11709	0.51742	0.27274	0.33651	1.26470	1.26618
36	10	$\vec{r}$	(−0.25, +0.75)	0.08529	0.02374	0.04030	0.09727	0.37605	0.10530	0.16482	0.42387	0.28399	0.08894	0.14617	0.29178
36	10	$\vec{r}, \dot{\vec{r}}$	(−0.25, +0.75)	0.08703	0.02319	0.03253	0.09501	0.06276	0.02855	0.10908	0.12905	0.21031	0.06573	0.11934	0.21303
29	16	NONE	(−0.5, +0.5)	0.18776	0.12787	0.49103	0.54103	0.82587	0.13533	0.67927	1.07790	0.78588	0.34587	1.89107	1.93334
29	16	$\vec{r}$	(−0.5, +0.5)	0.18698	0.03463	0.18062	0.26226	0.75686	0.11724	0.70776	1.04280	0.99781	0.17222	1.16262	1.26827
29	16	$\vec{r}, \dot{\vec{r}}$	(−0.5, +0.5)	0.16077	0.00092	0.16072	0.22733	0.66713	0.00381	0.66878	0.94464	0.71715	0.00812	0.71826	0.80306
36	16	NONE	(−0.5, +0.5)	0.18809	0.12333	0.48945	0.53866	0.82516	0.12990	0.67985	1.07700	0.77838	0.33244	1.90190	1.93501
36	16	$\vec{r}$	(−0.5, +0.5)	0.18655	0.03293	0.18106	0.26205	0.75587	0.11145	0.70877	1.04220	1.00403	0.16791	1.19404	1.28898
36	16	$\vec{r}, \dot{\vec{r}}$	(−0.5, +0.5)	0.16077	0.00092	0.16072	0.22733	0.66713	0.00381	0.66878	0.94464	0.71715	0.00812	0.71826	0.80306

NOTE ALL COMPARISONS ARE OVER A 3 DAY ARC.

0.453×10^4 and 1.299 kilometers, respectively, for the radial, cross-track, and along-track components.

3.1.2 Position Residuals

The rms position errors in this case are 0.117 kilometers for the radial, 0.021 kilometers for the cross-track, and 0.100 kilometer for the along-track components. The velocity rms errors are 0.575×10^{-3} kilometers/second for the radial, 0.108×10^{-3} kilometers/second for the cross-track, and 0.452×10^{-3} kilometers/second for the along-track components. The minimum and maximum position differences are 0.2×10^{-5} and 0.513 kilometers for the radial, 0.658×10^{-8} and 0.116 kilometers for the cross-track, and 0.877×10^{-8} and 0.379 kilometers for the along-track components.

3.1.3 All Residuals

The rms position errors are found to be 0.100 kilometers, 0.569×10^{-3} kilometers, 0.083 kilometers for the radial, cross-track, and along-track components. The rms velocity errors are found to be 0.454×10^{-3} kilometers/second for the radial, 0.264×10^{-5} kilometers/second for the cross-track, and 0.413×10^{-3} kilometers/second for the along-track components. The minimum and maximum position differences are 0.2×10^{-5} and 0.298 kilometers for the radial, 0.341×10^{-8} and 0.314×10^{-2} kilometers for the cross-track, 0.874×10^{-8} and 0.208 kilometers for the along-track components.

The plots showing the differences between the high-precision and the SMM-OBC interpolated trajectories using a 29-term Fourier series are presented in Figures 3-1 through 3-6 for the case of no residuals, Figures 3-7 through 3-12 for the case of position residuals, and Figures 3-13 through 3-18 for the case of position and velocity residuals. In cases for which residuals are used, the OBC ephemeris errors arise from local interpolation error and therefore do not demonstrate any secular or long-period behavior. In cases for which residuals are not used, the OBC ephemeris errors arise primarily from effects

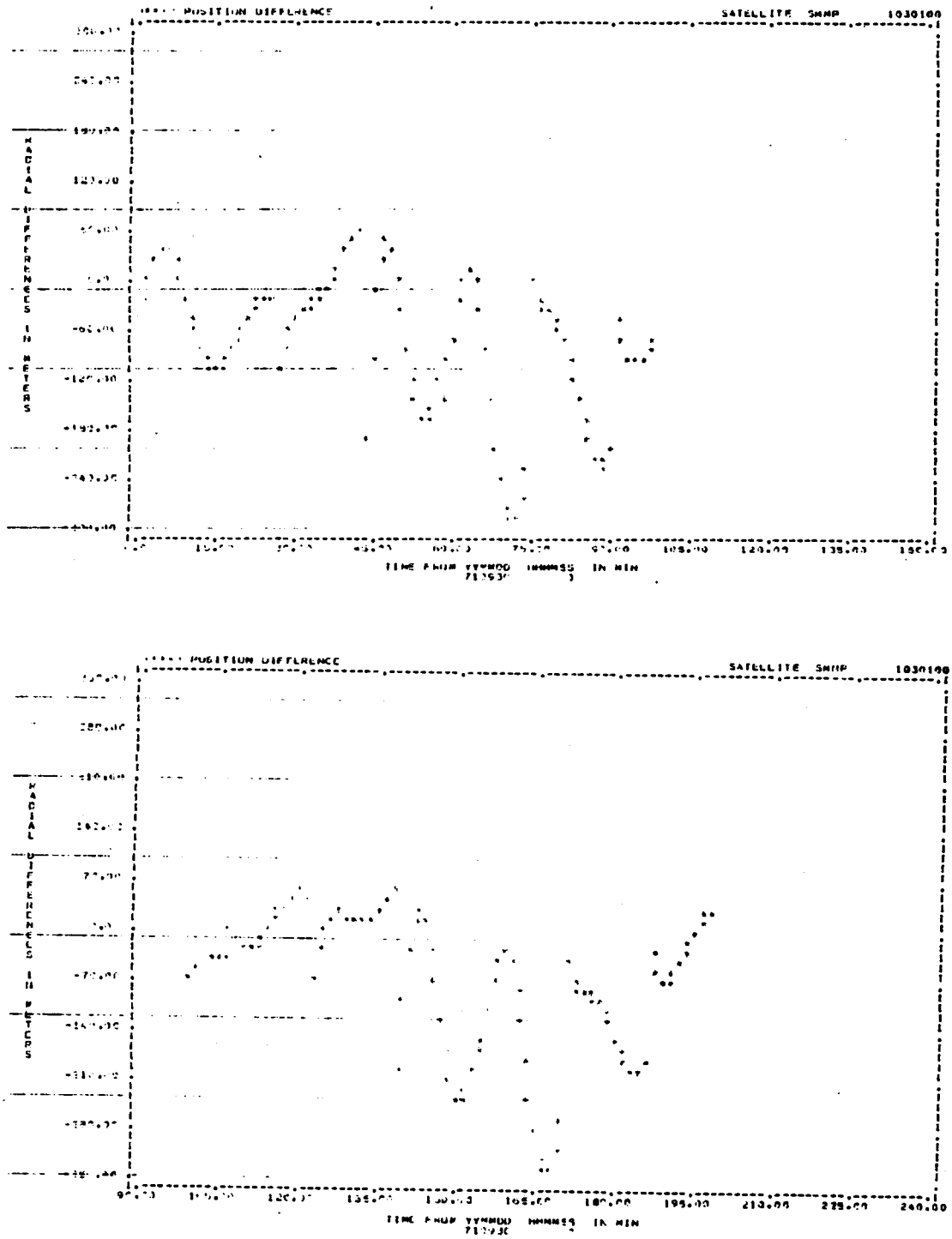

Figure 3-1. Errors in the Representation of the Radial Component of Position Using a 29-Term Fourier Series with a 16-Minute Grid Spacing (1 of 7)

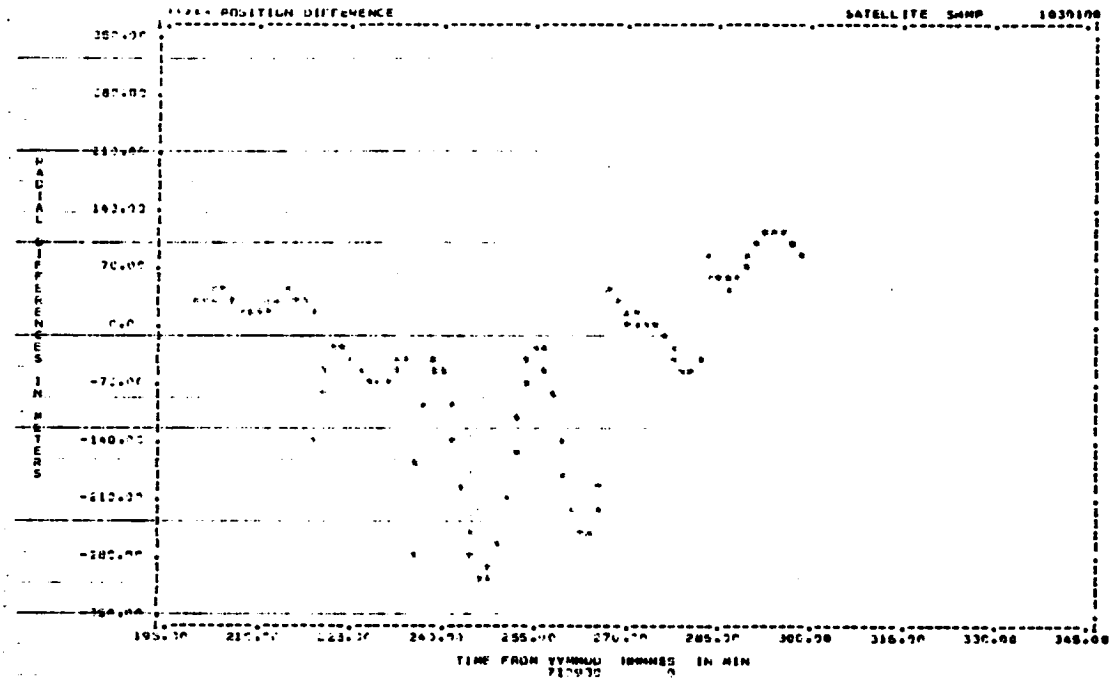

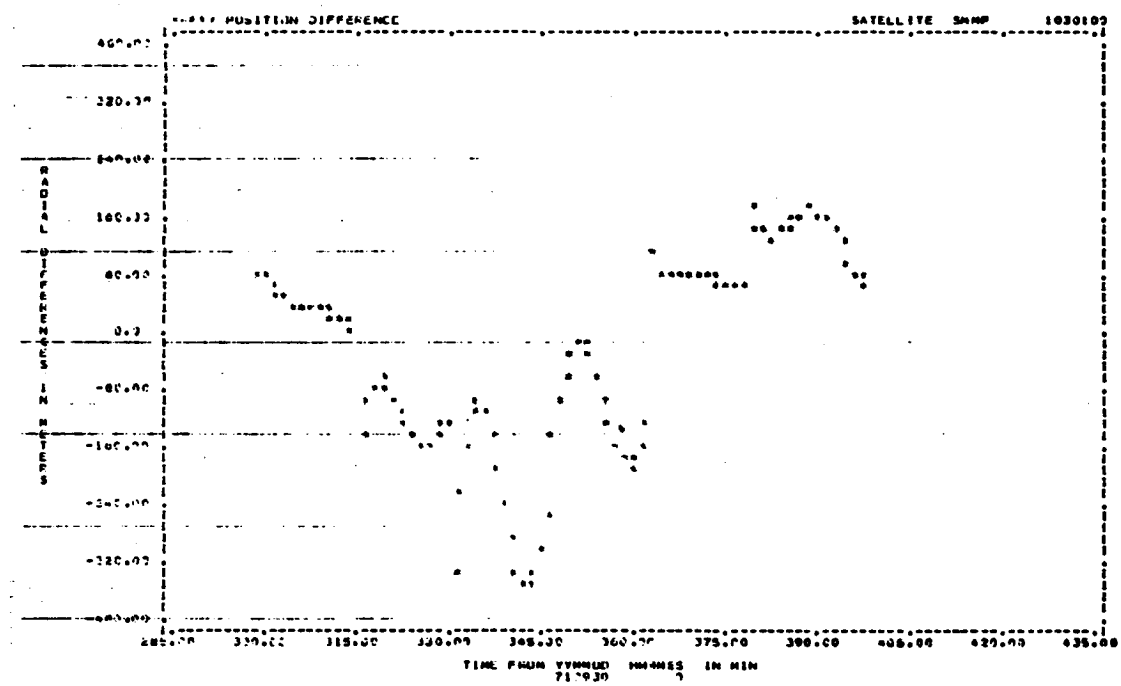

Figure 3-1. Errors in the Representation of the Radial Component of Position Using a 29-Term Fourier Series with a 16-Minute Grid Spacing (2 of 7)

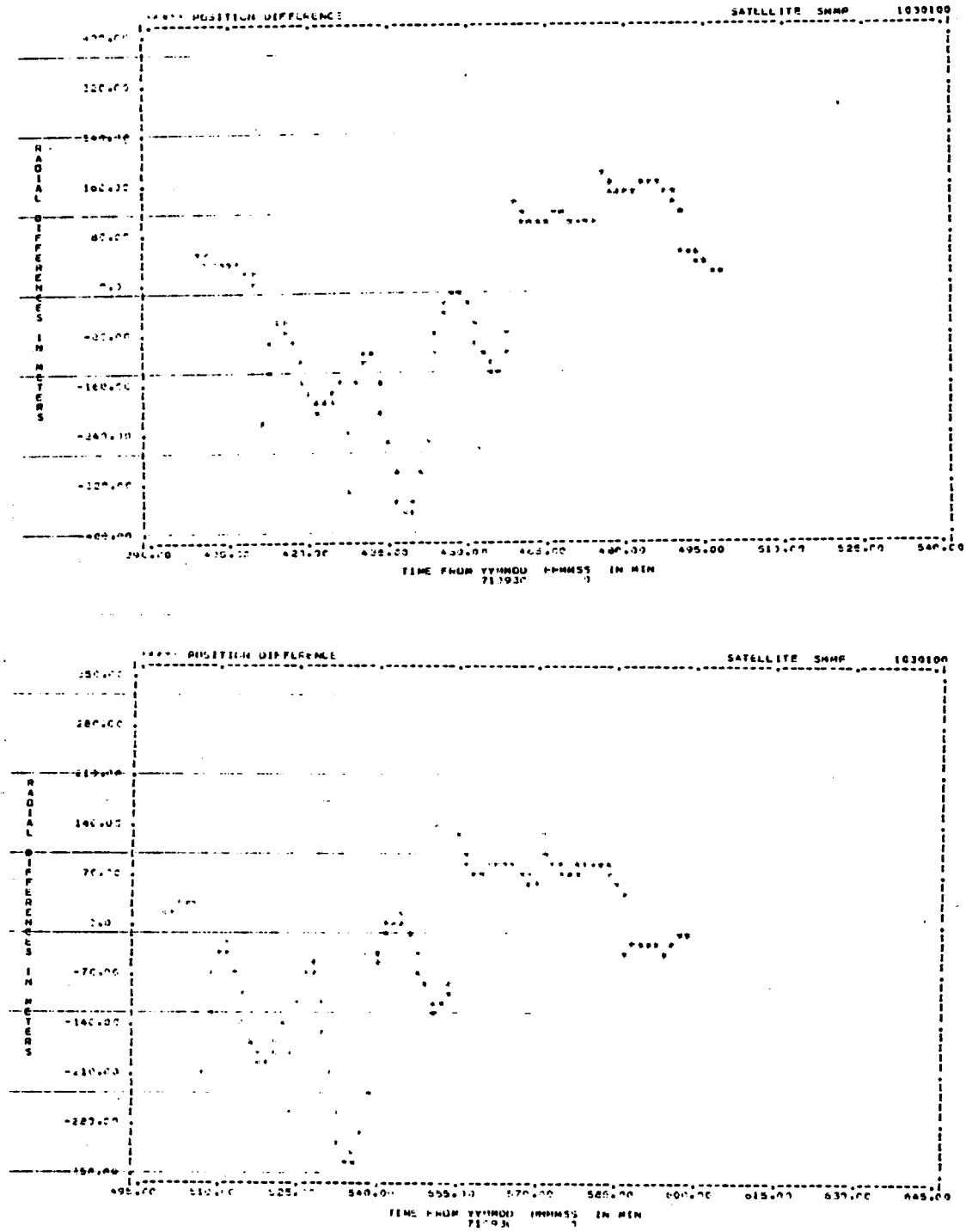

Figure 3-1. Errors in the Representation of the Radial Component of Position Using a 29-Term Fourier Series with a 16-Minute Grid Spacing (3 of 7)

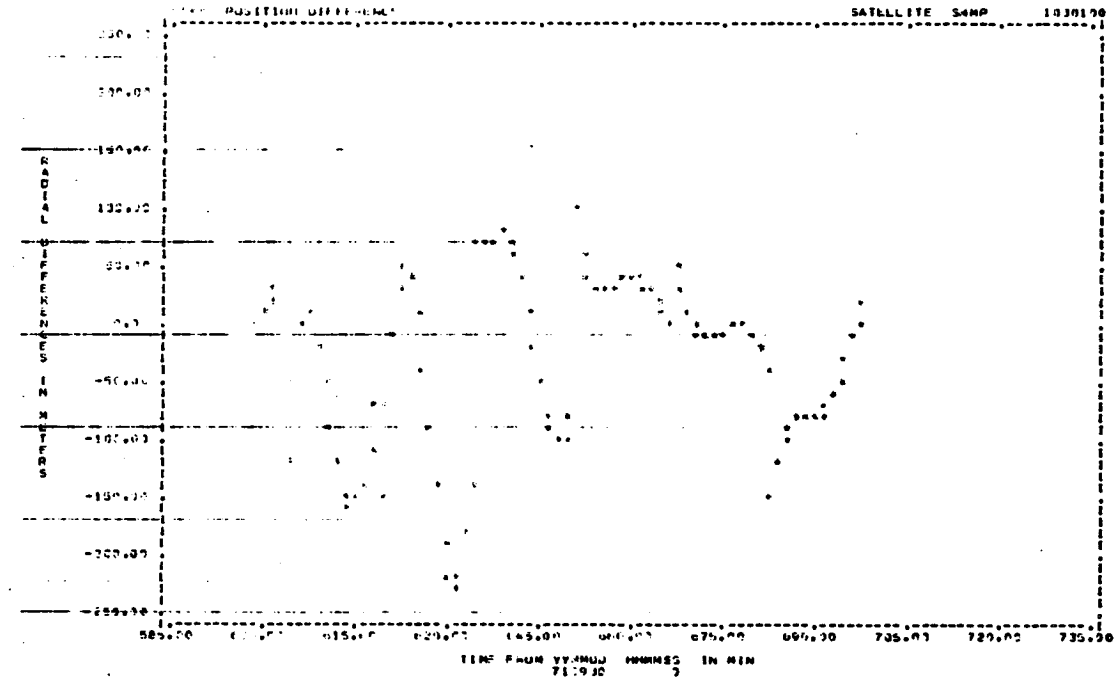

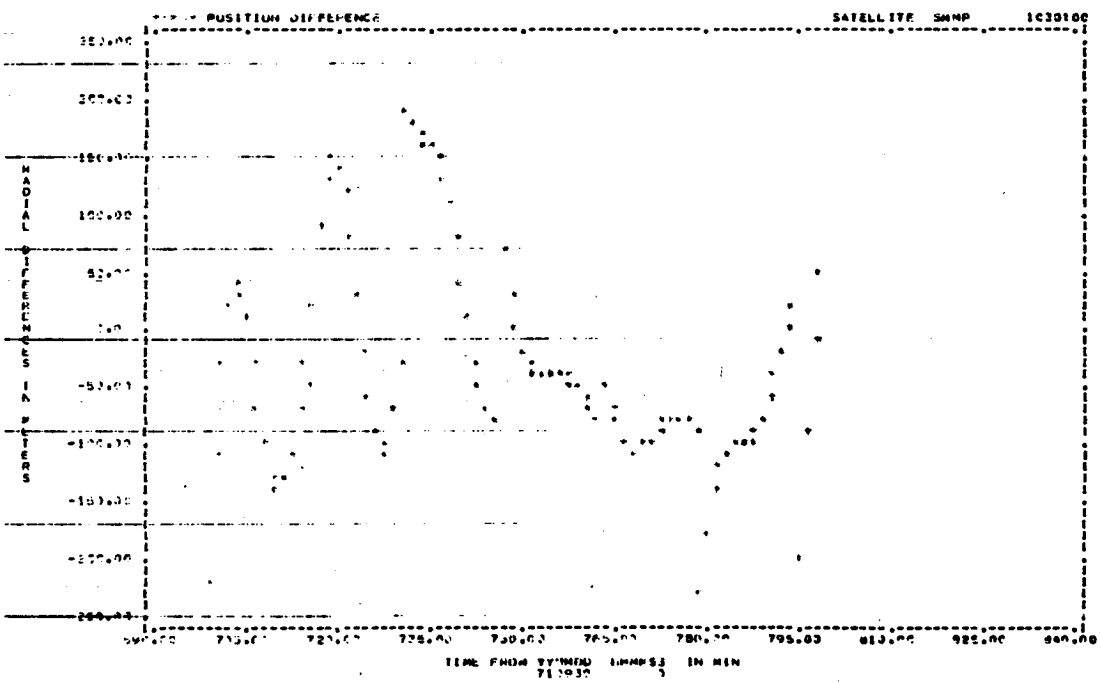

Figure 3-1. Errors in the Representation of the Radial Component of Position Using a 29-Term Fourier Series with a 16-Minute Grid Spacing (4 of 7)

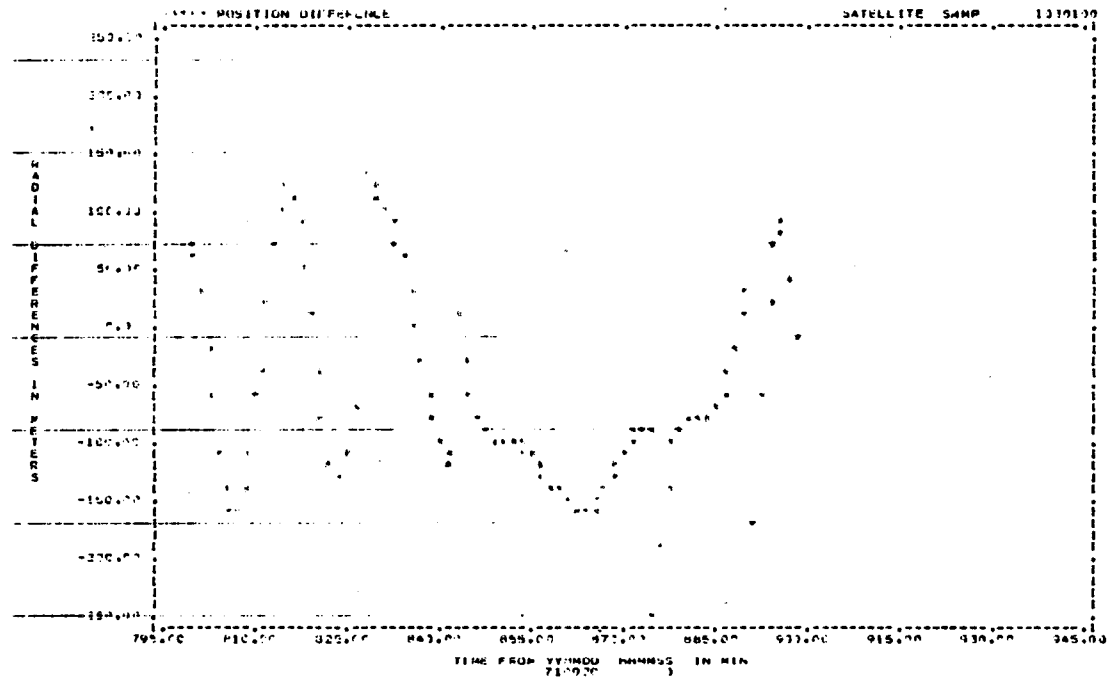

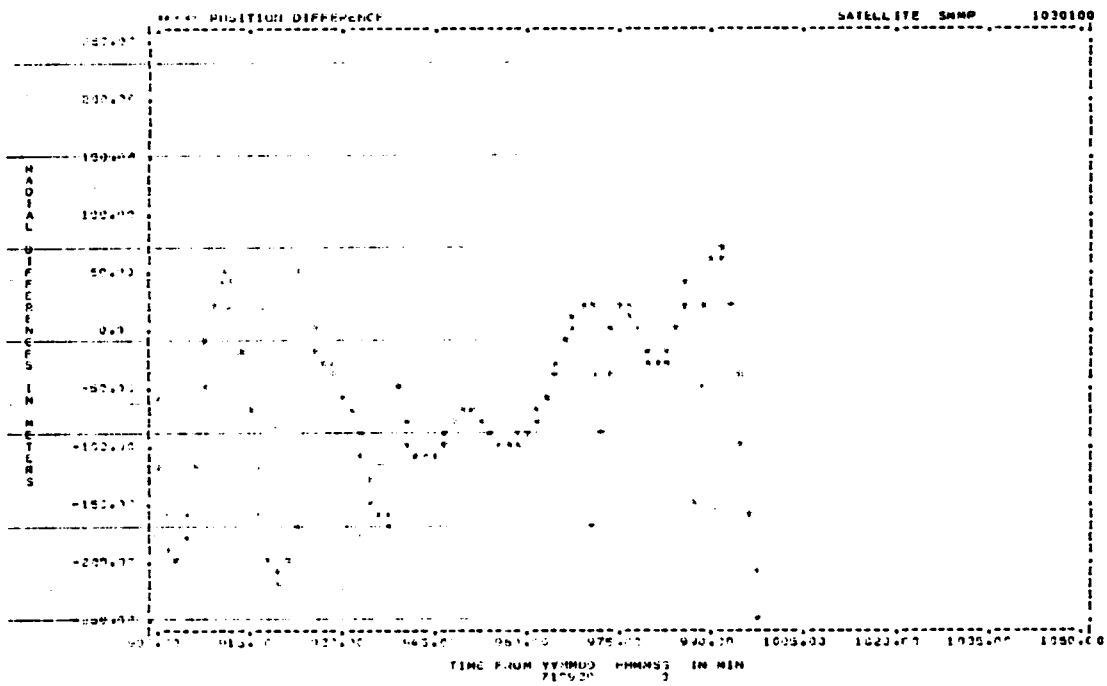

Figure 3-1. Errors in the Representation of the Radial Component of Position Using a 29-Term Fourier Series with a 16-Minute Grid Spacing (5 of 7)

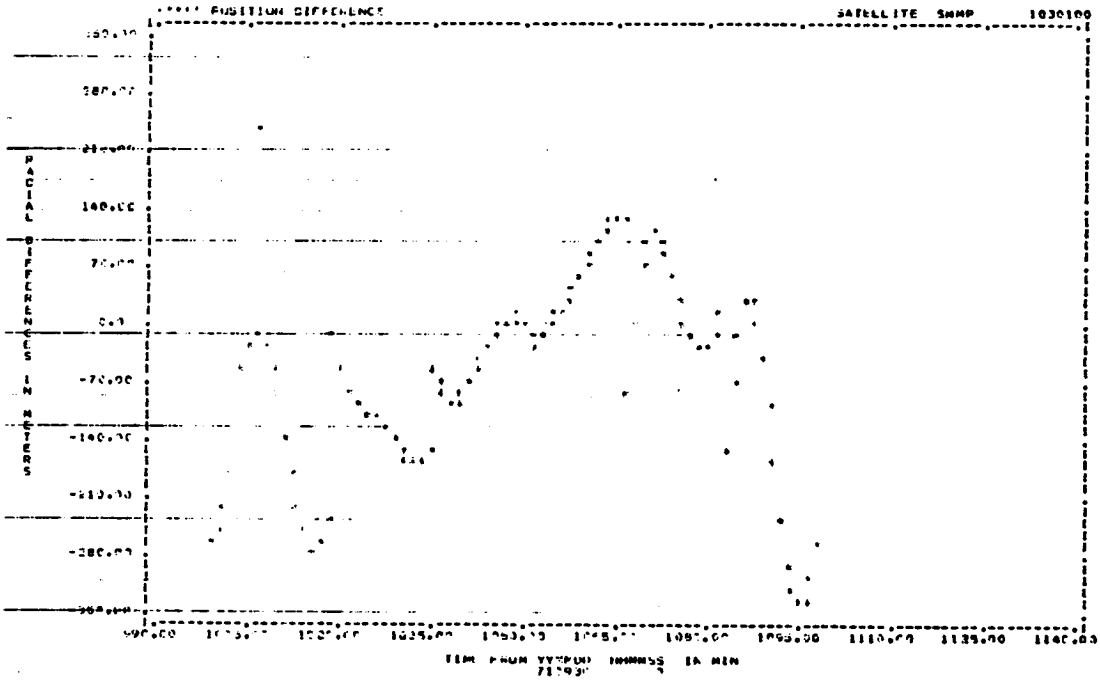

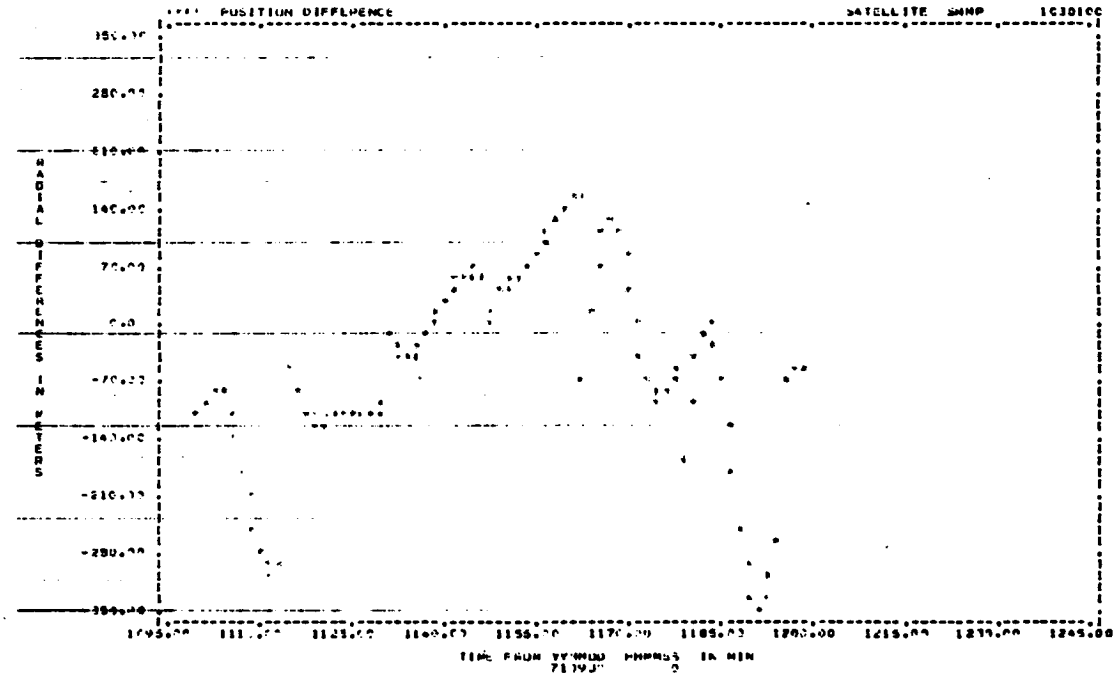

Figure 3-1. Errors in the Representation of the Radial Component of Position Using a 29-Term Fourier Series with a 16-Minute Grid Spacing (6 of 7)

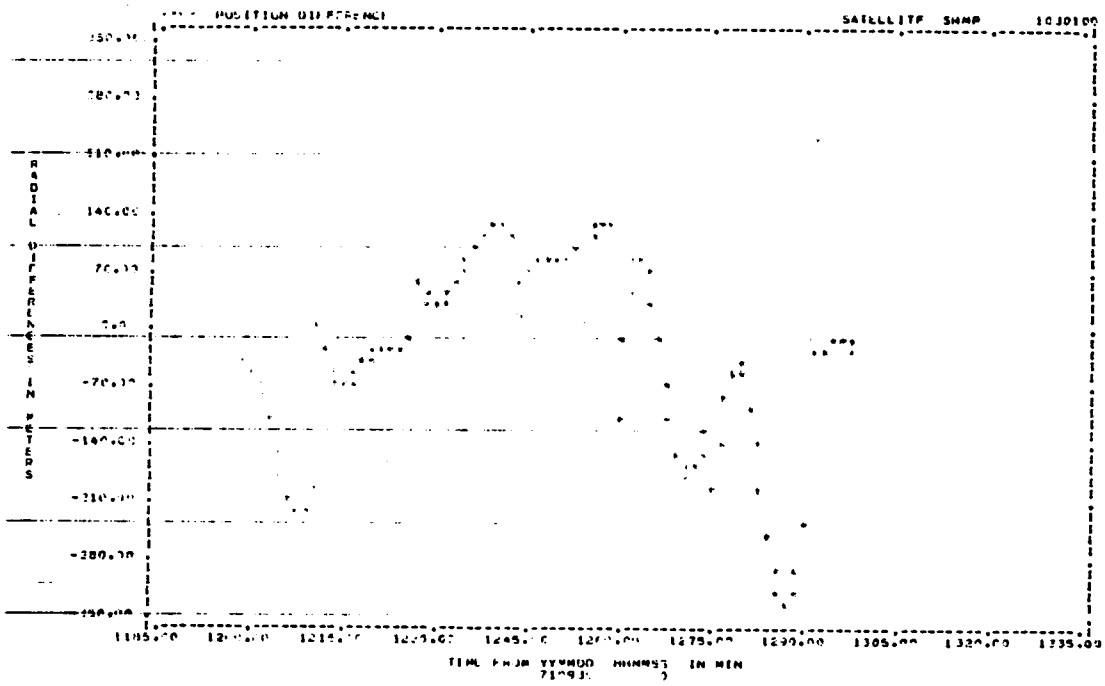

Figure 3-1. Errors in the Representation of the Radial Component of Position Using a 29-Term Fourier Series with a 16-Minute Grid Spacing (7 of 7)

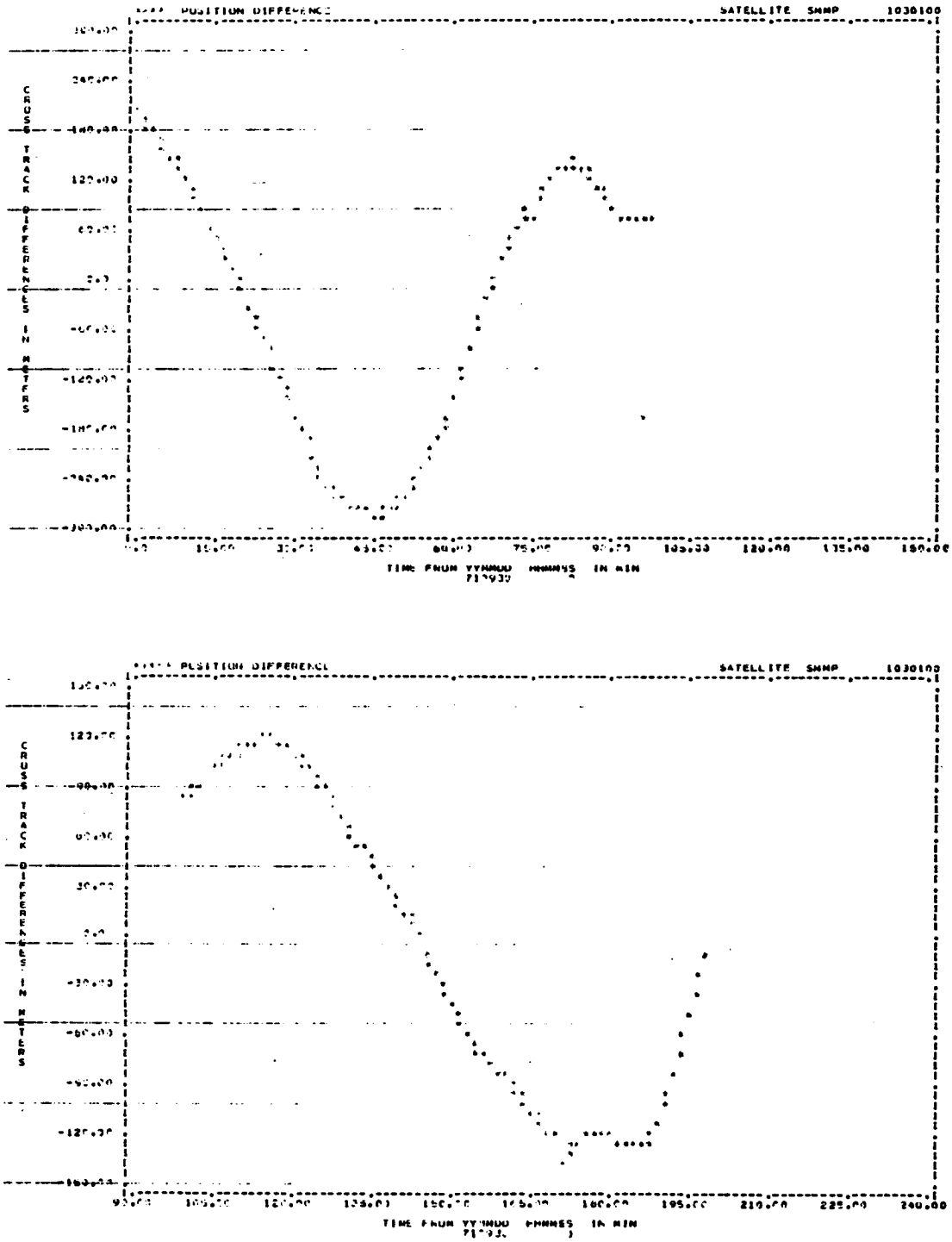

Figure 3-2. Errors in the Representation of the Cross-Track Component of Position Using a 29-Term Fourier Series with a 16-Minute Grid Spacing (1 of 7)

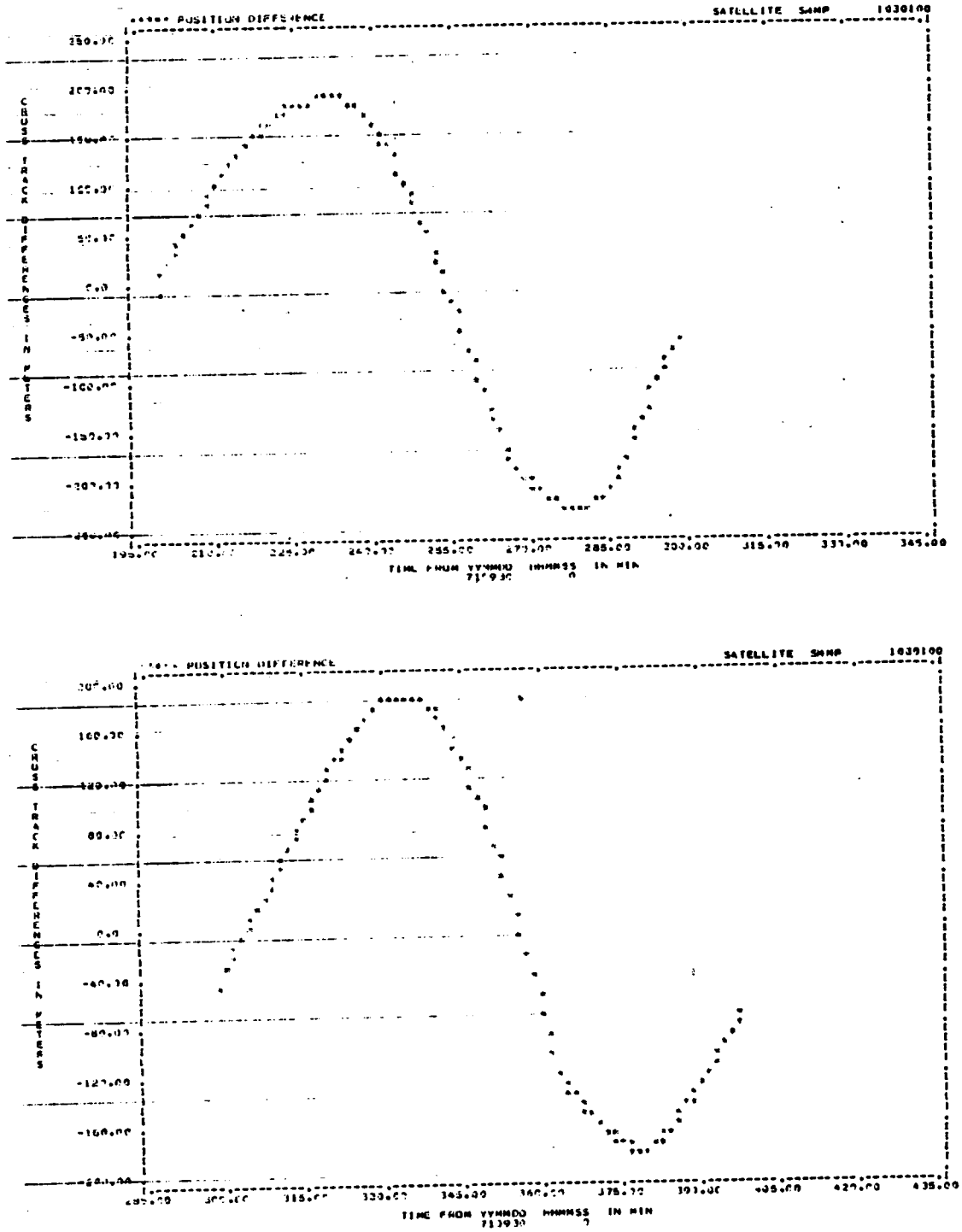

Figure 3-2. Errors in the Representation of the Cross-Track Component of Position Using a 29-Term Fourier Series with a 16-Minute Grid Spacing (2 of 7)

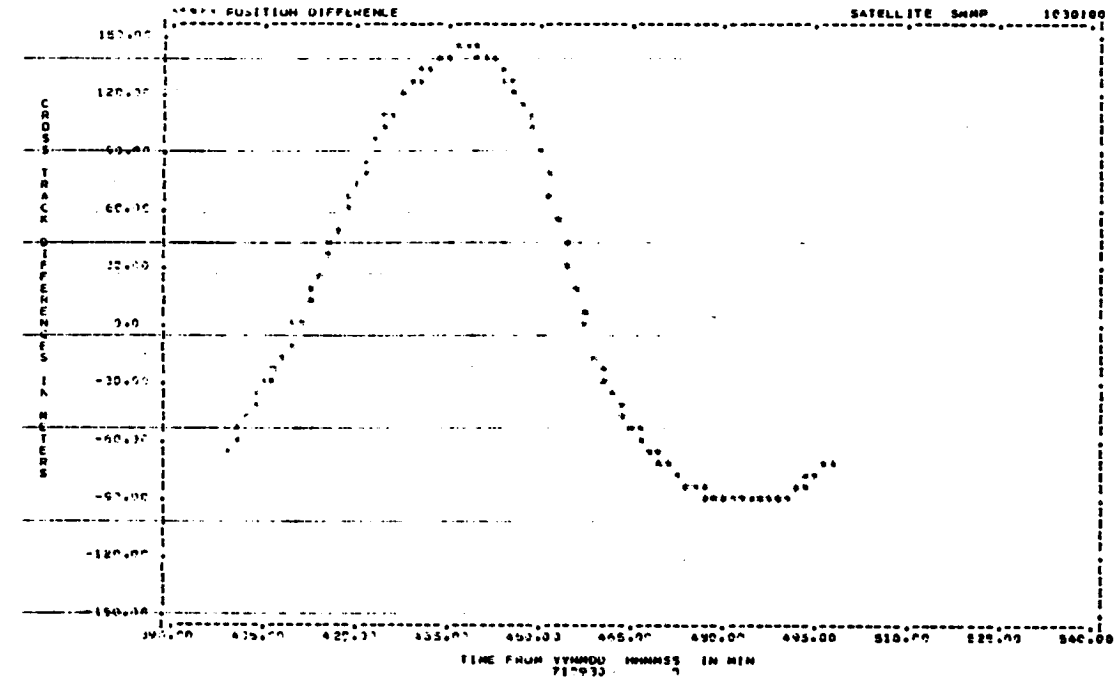

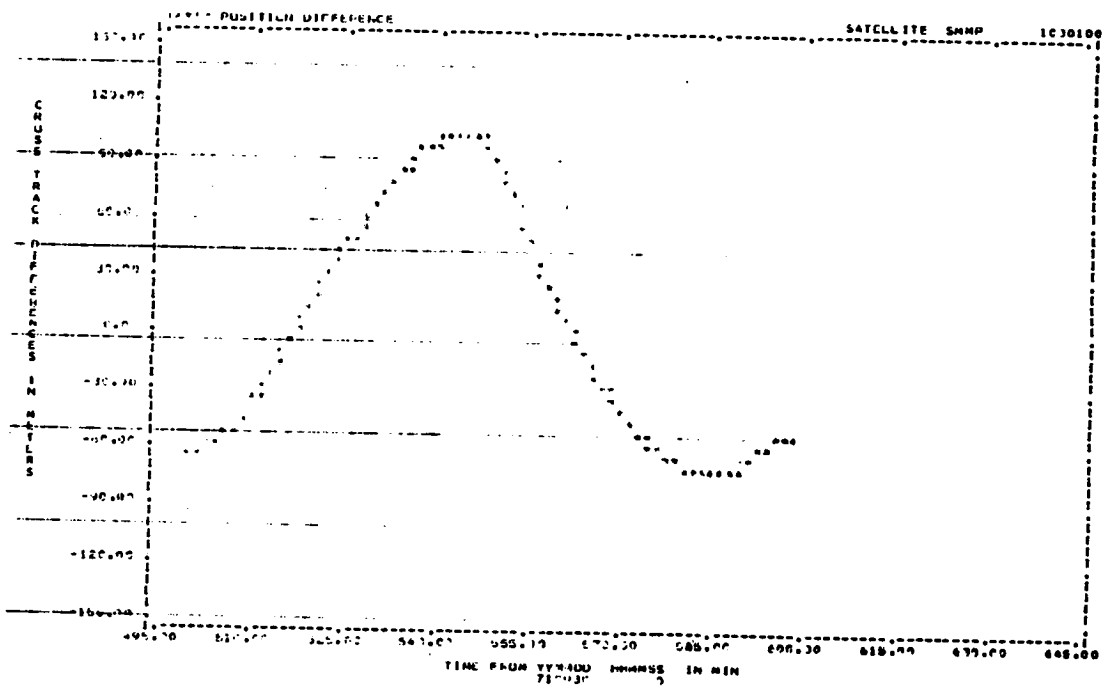

Figure 3-2. Errors in the Representation of the Cross-Track Component of Position Using a 29-Term Fourier Series with a 16-Minute Grid Spacing (3 of 7)

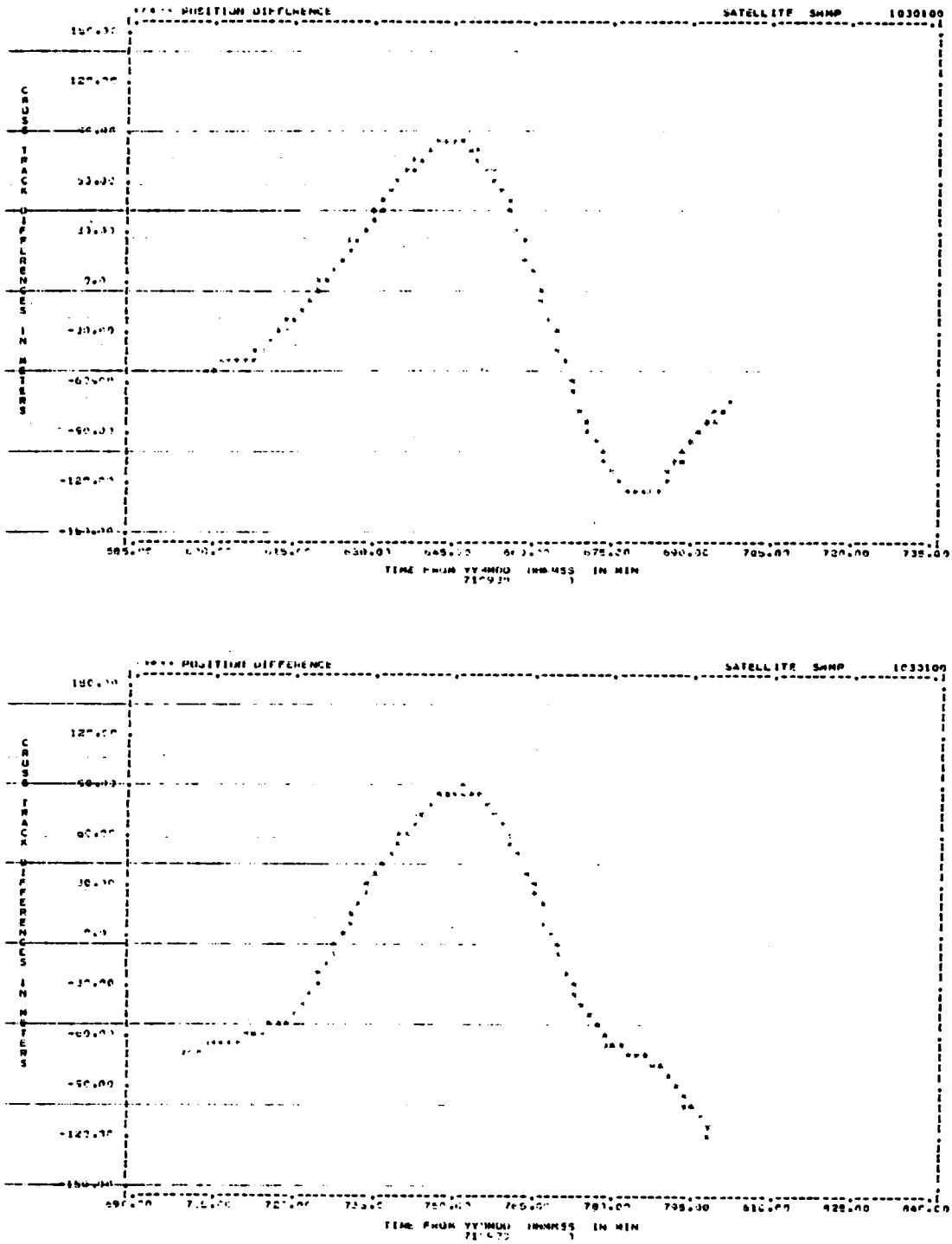

Figure 3-2. Errors in the Representation of the Cross-Track Component of Position Using a 29-Term Fourier Series with a 16-Minute Grid Spacing (4 of 7)

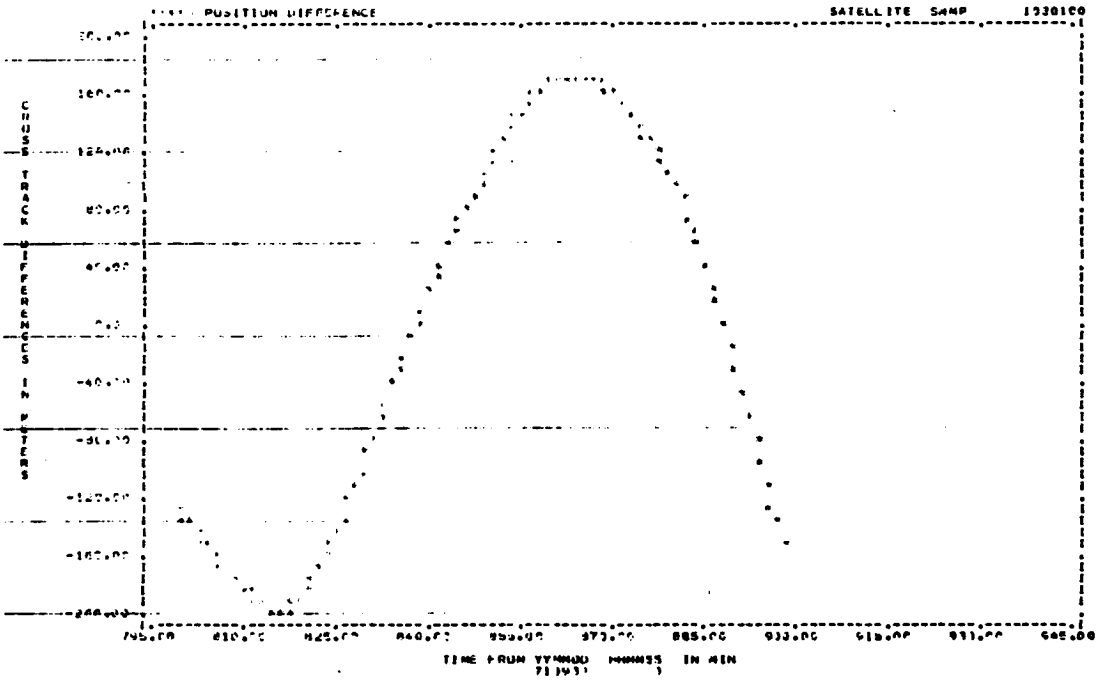

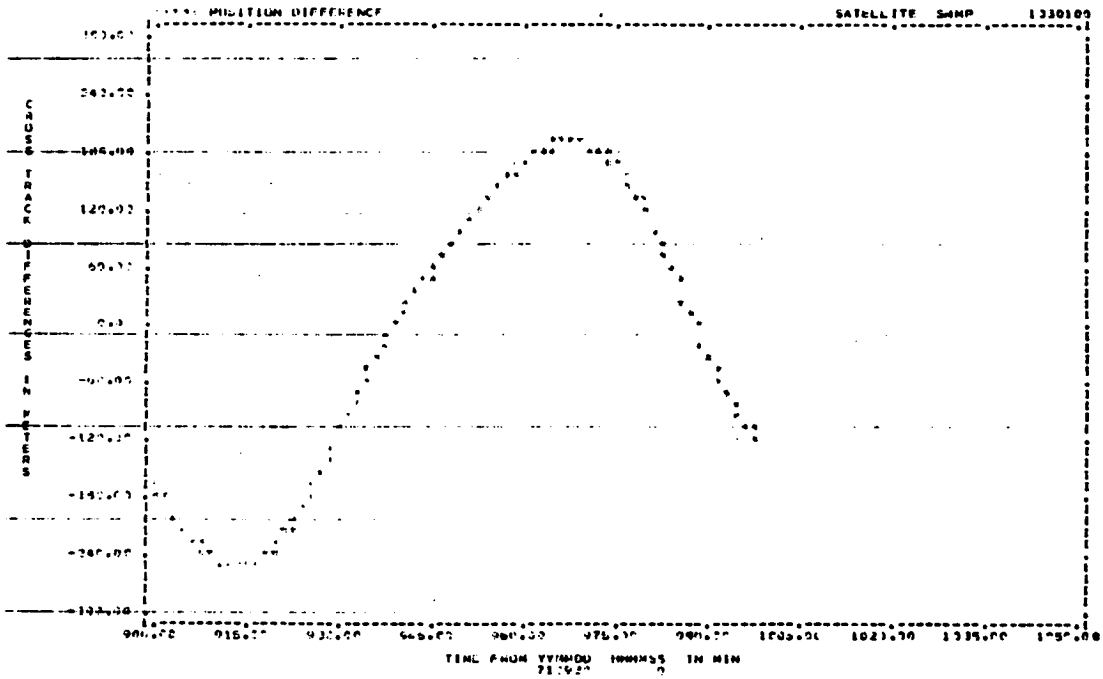

Figure 3-2. Errors in the Representation of the Cross-Track Component of Position Using a 29-Term Fourier Series with a 16-Minute Grid Spacing (5 of 7)

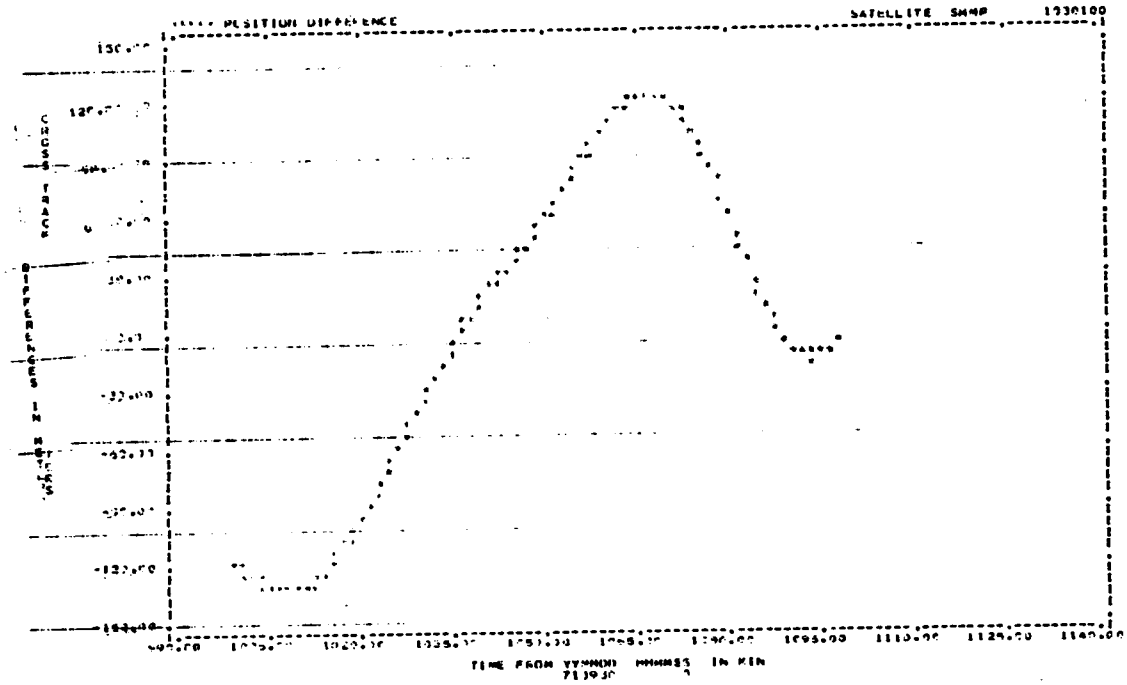

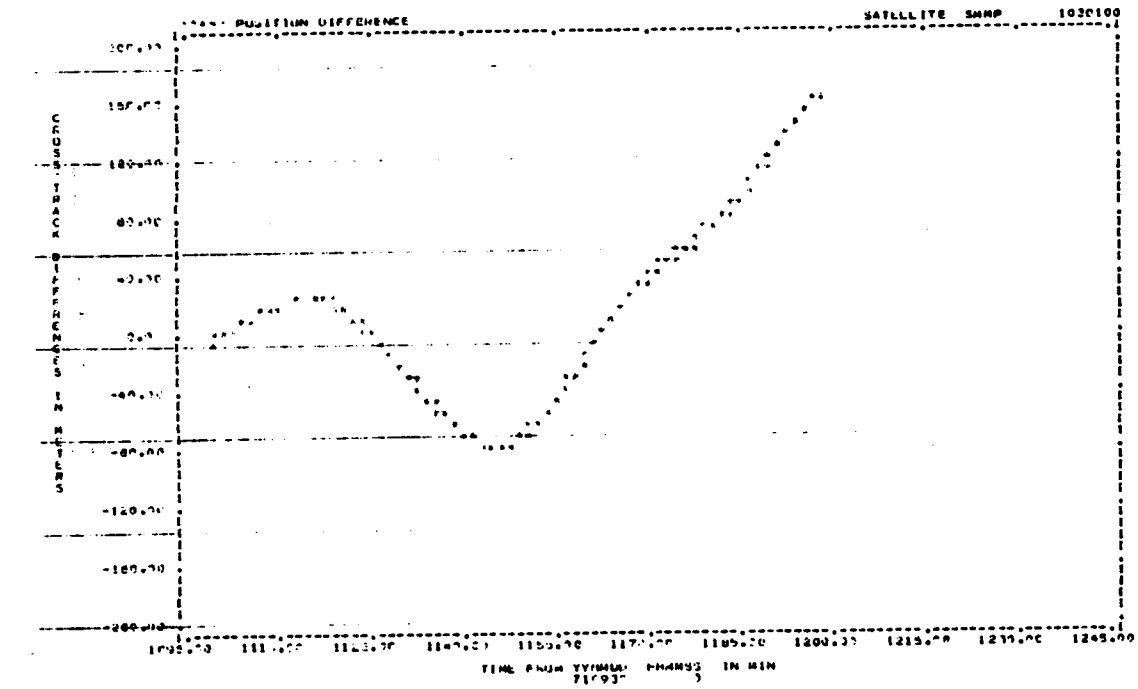

Figure 3-2. Errors in the Representation of the Cross-Track Component of Position Using a 29-Term Fourier Series with a 16-Minute Grid Spacing (6 of 7)

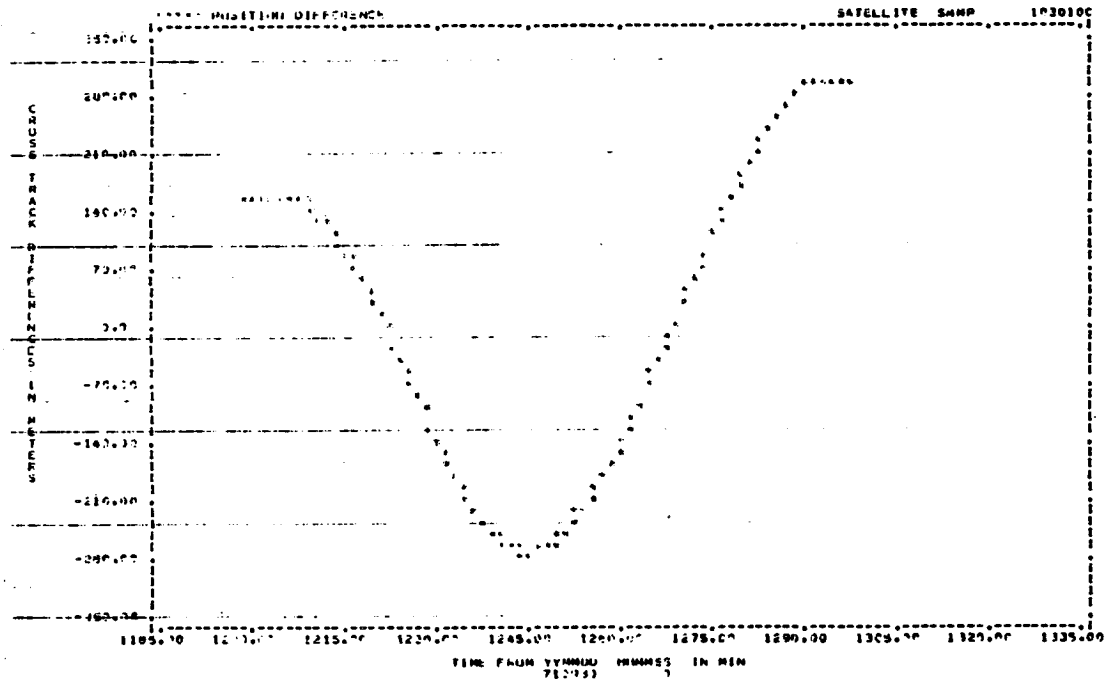

Figure 3-2. Errors in the Representation of the Cross-Track Component of Position Using a 29-Term Fourier Series with a 16-Minute Grid Spacing (7 of 7)

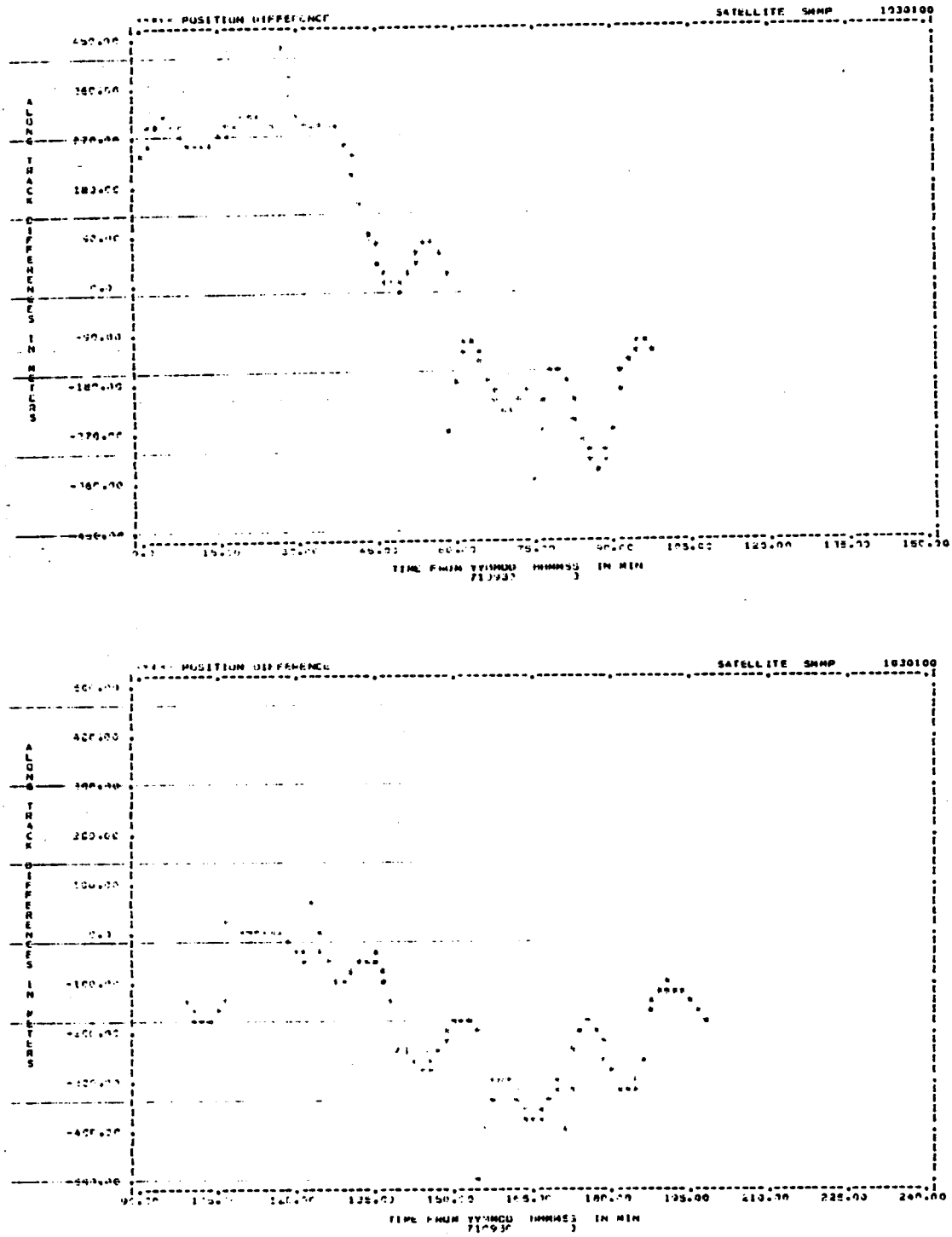

Figure 3-3. Errors in the Representation of the Along-Track Component of Position Using a 29-Term Fourier Series with a 16-Minute Grid Spacing (1 of 7)

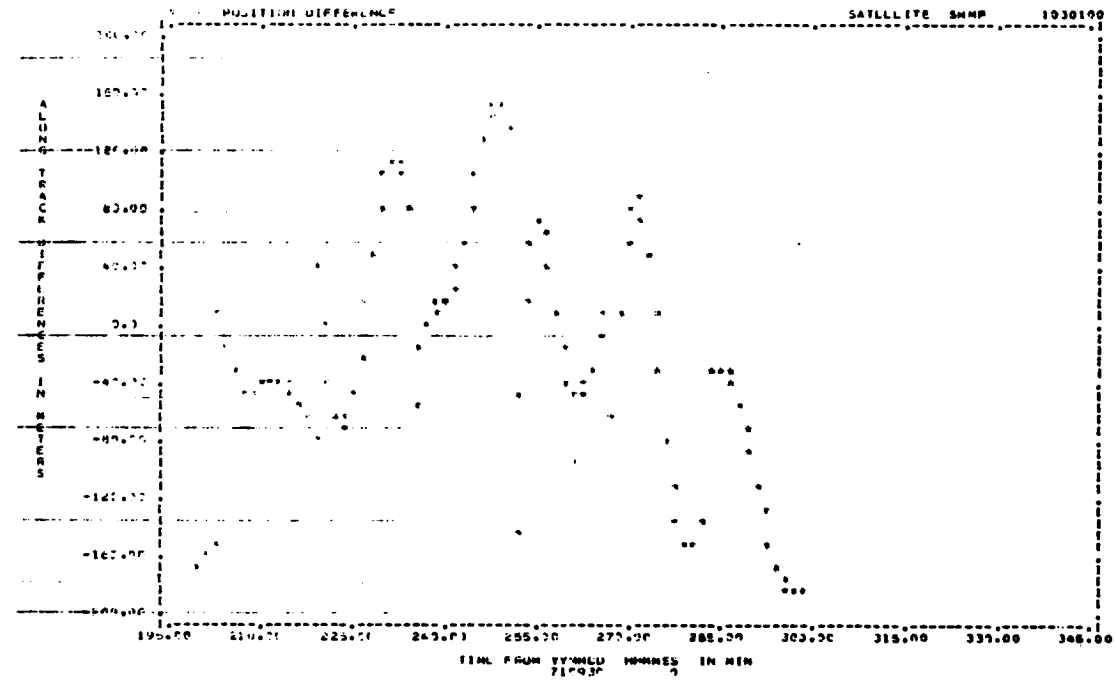

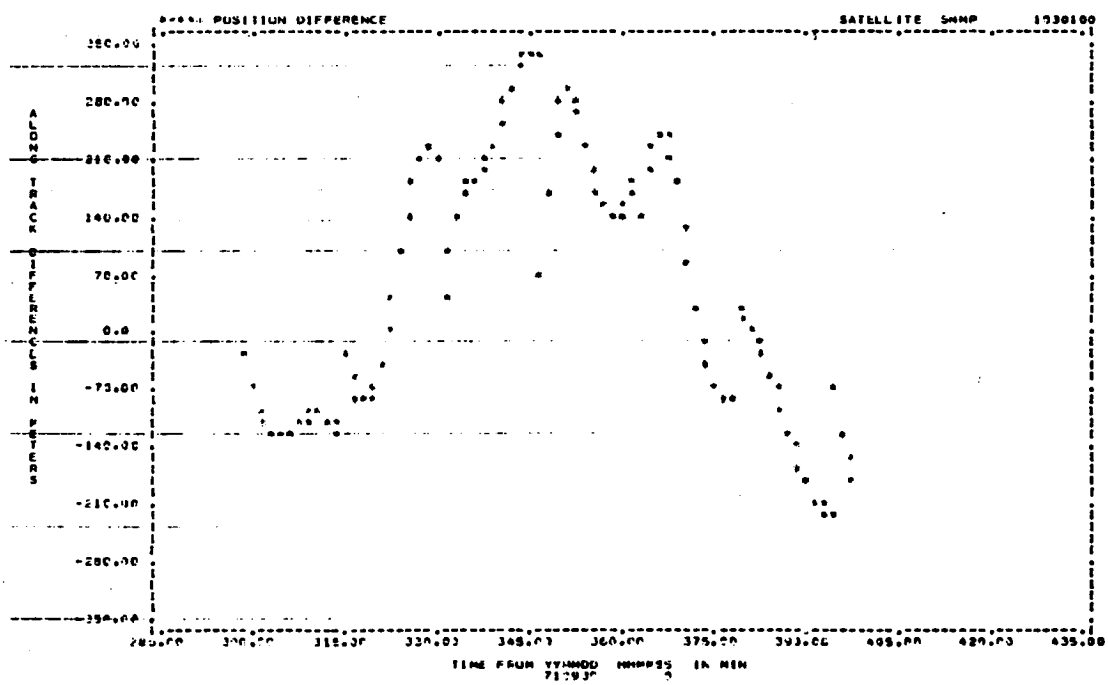

Figure 3-3. Errors in the Representation of the Along-Track Component of Position Using a 29-Term Fourier Series with a 16-Minute Grid Spacing (2 of 7)

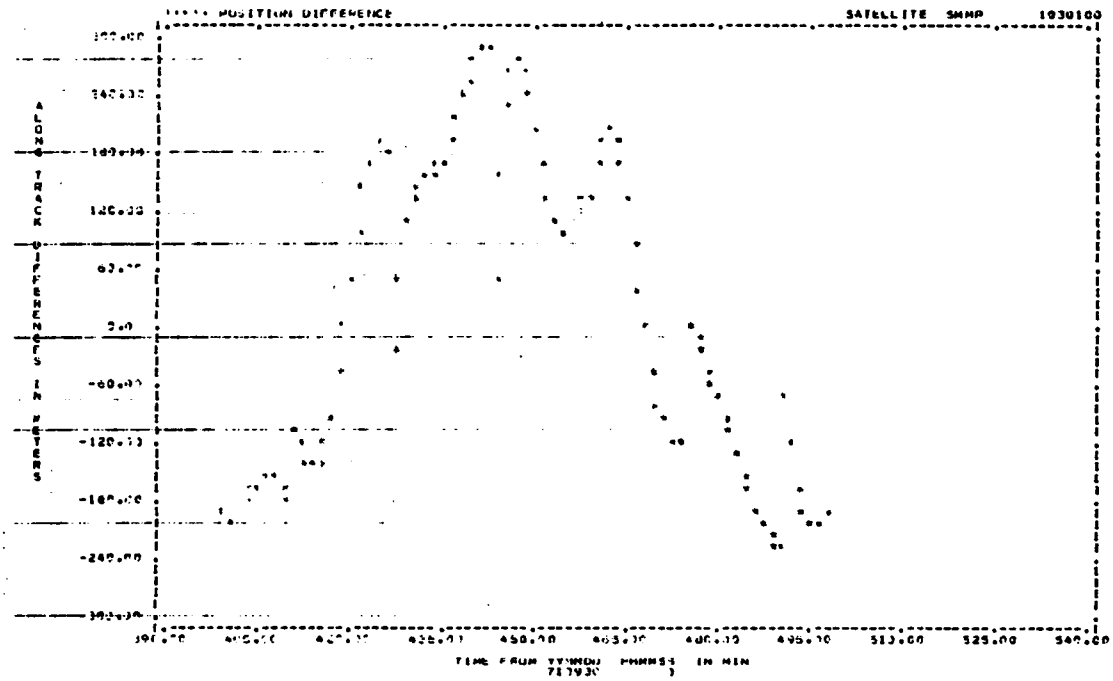

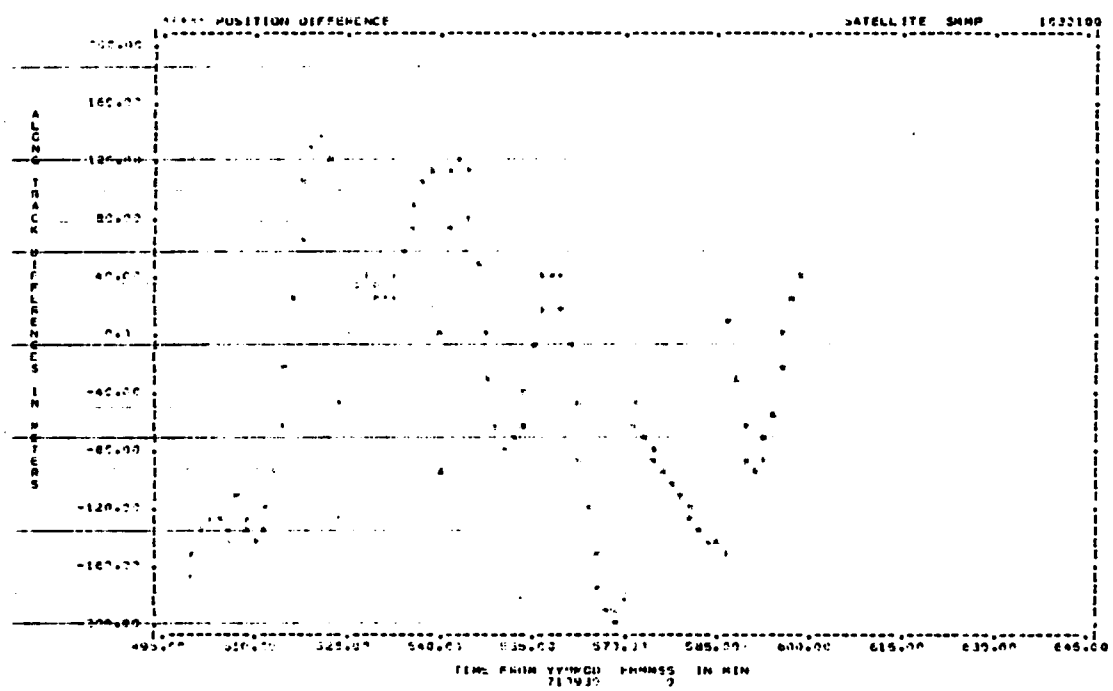

Figure 3-3. Errors in the Representation of the Along-Track Component of Position Using a 29-Term Fourier Series with a 16-Minute Grid Spacing (3 of 7)

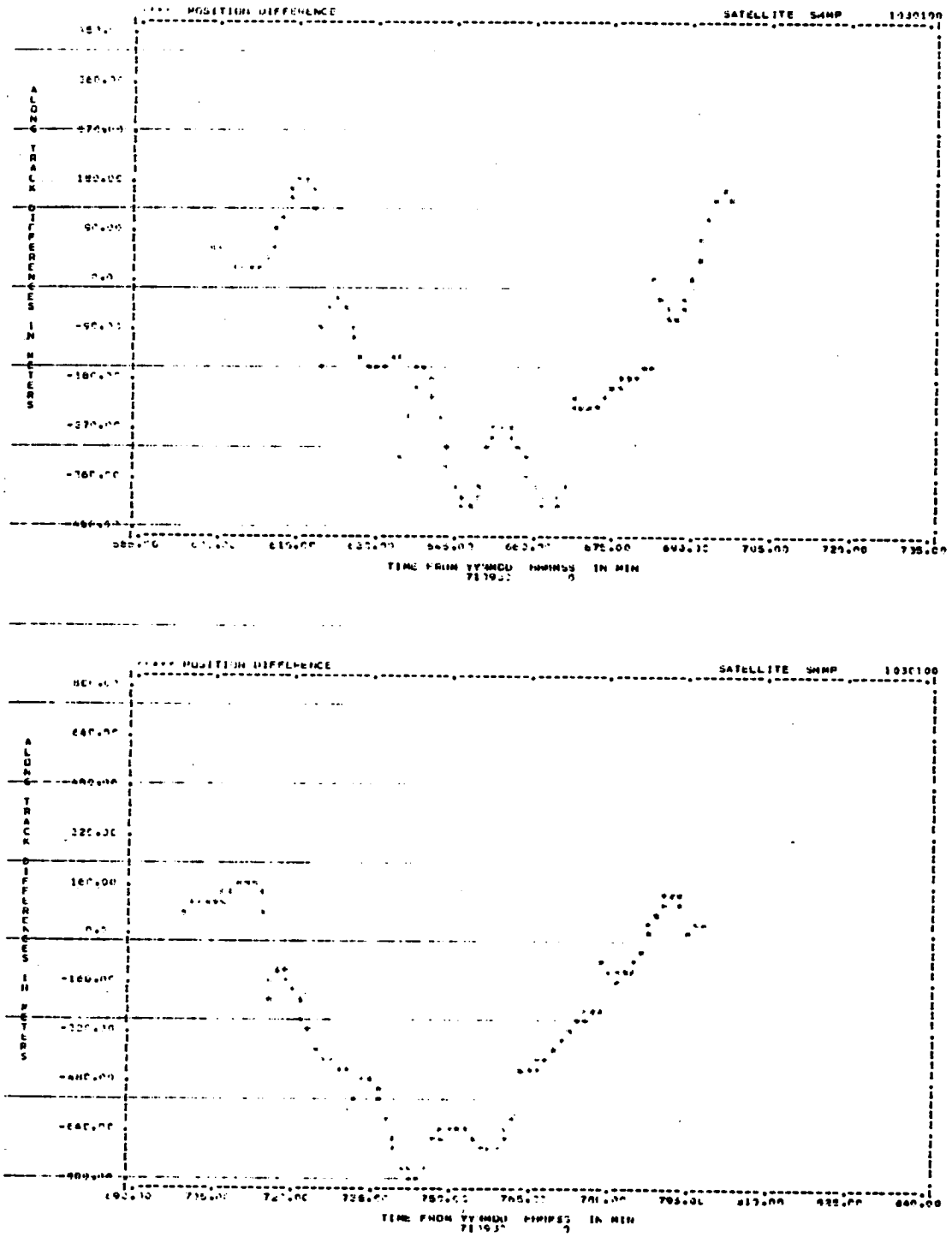

Figure 3-3. Errors in the Representation of the Along-Track Component of Position Using a 29-Term Fourier Series with a 16-Minute Grid Spacing (4 of 7)

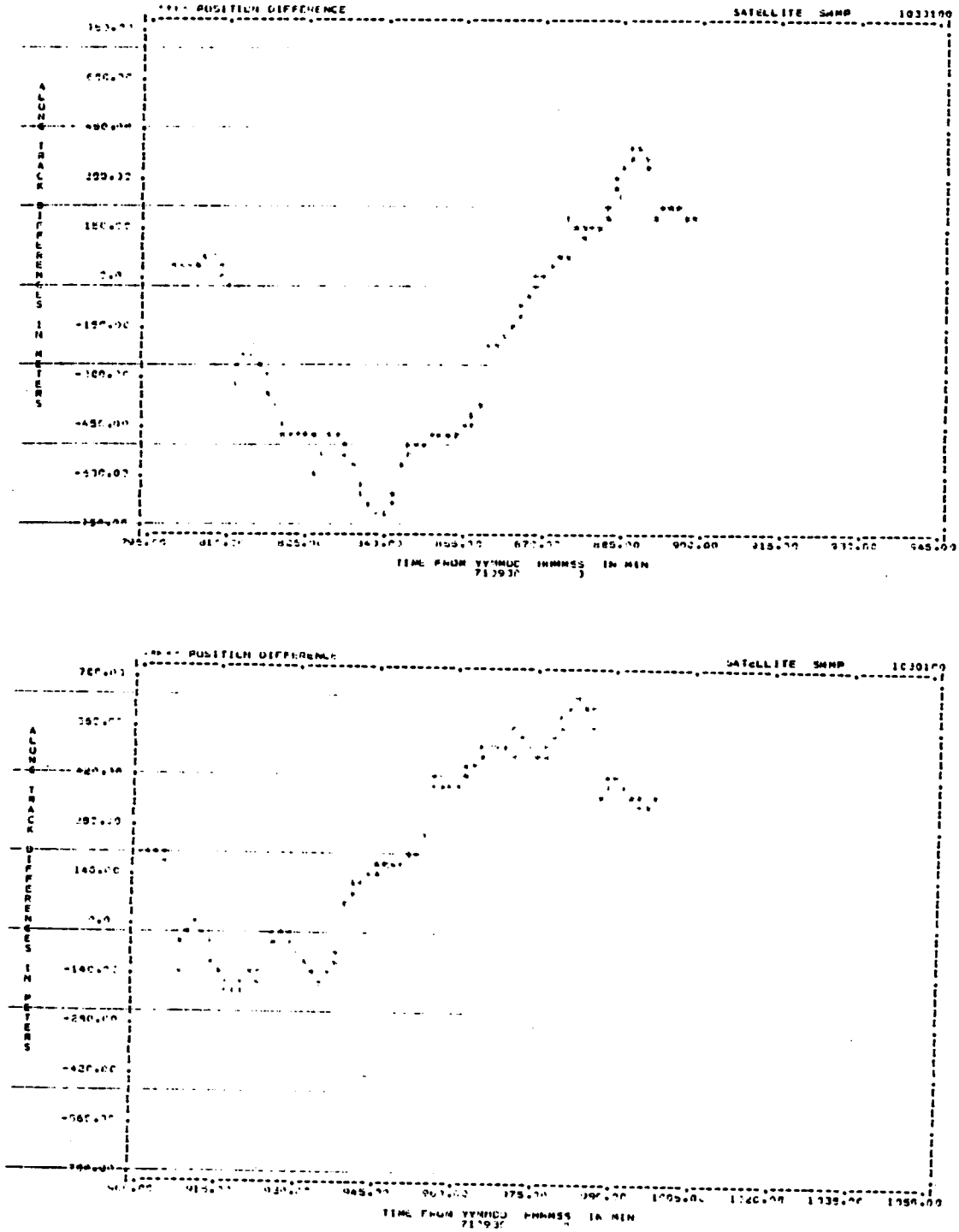

Figure 3-3. Errors in the Representation of the Along-Track Component of Position Using a 29-Term Fourier Series with a 16-Minute Grid Spacing (5 of 7)

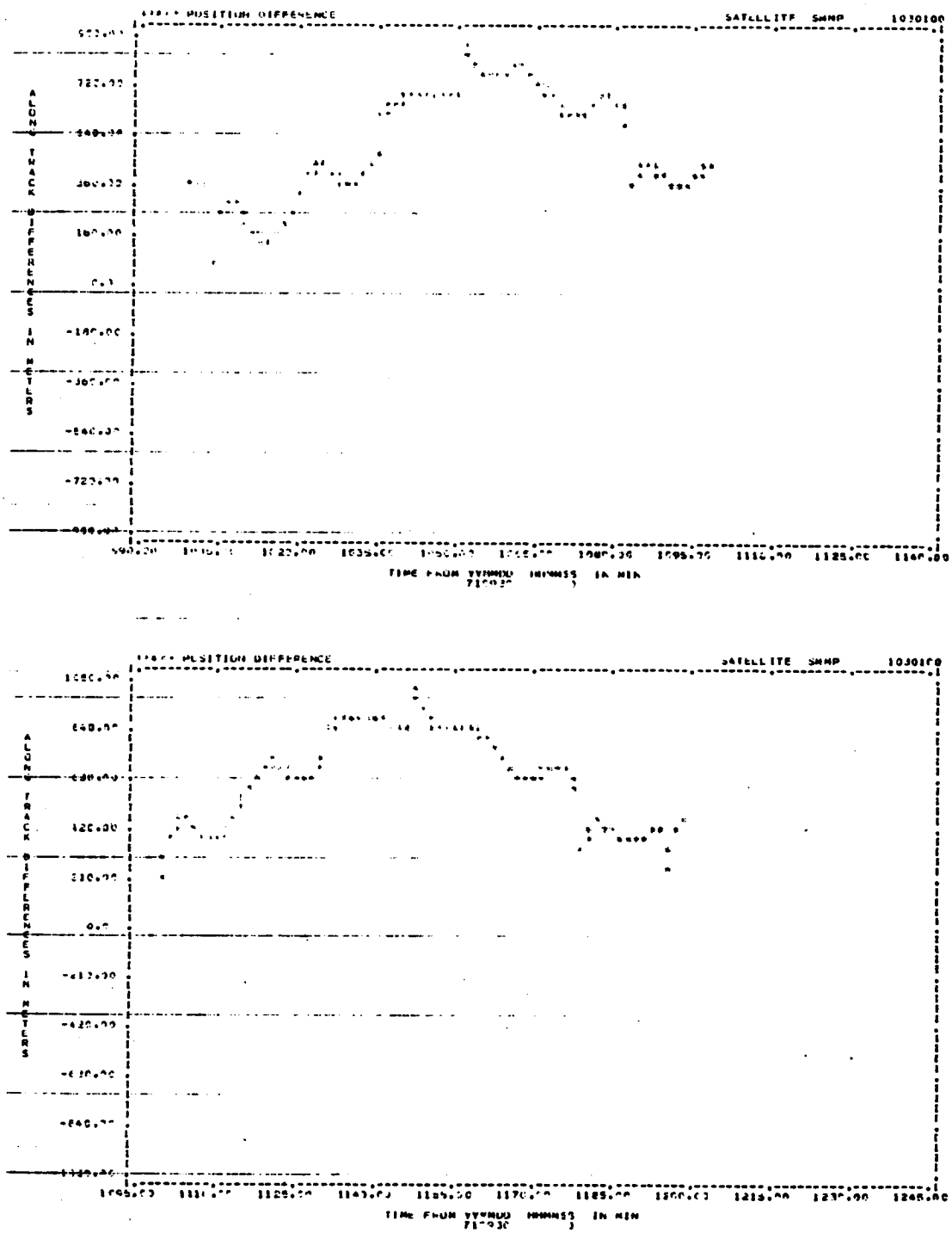

Figure 3-3. Errors in the Representation of the Along-Track Component of Position Using a 29-Term Fourier Series with a 16-Minute Grid Spacing (6 of 7)

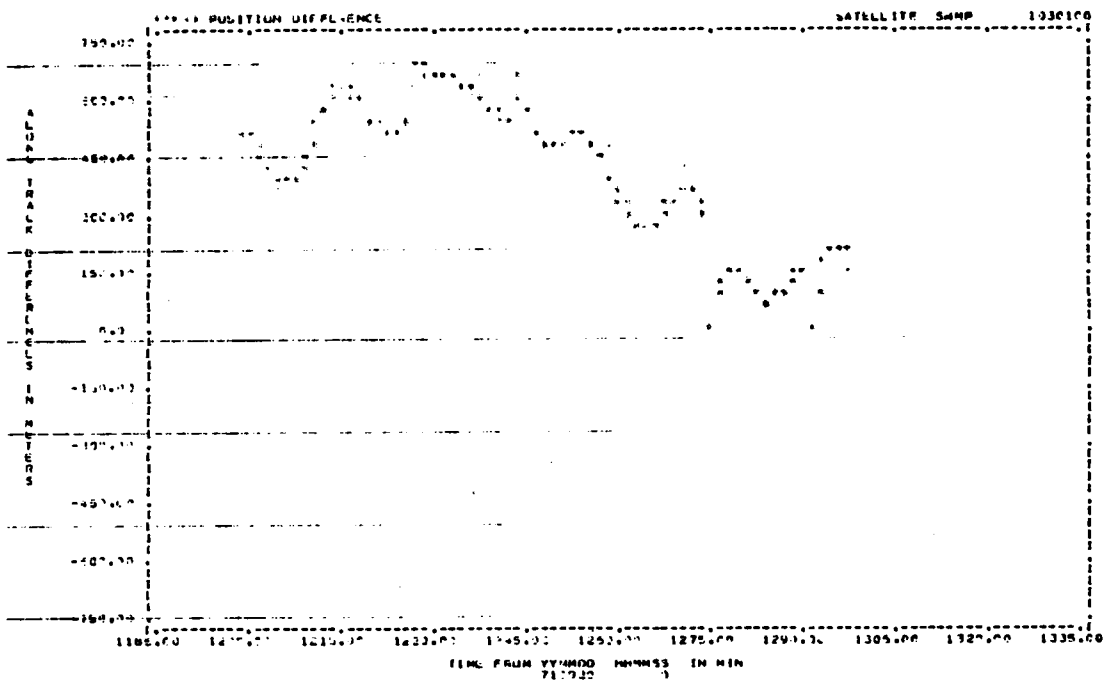

Figure 3-3. Errors in the Representation of the Along-Track Component of Position Using a 29-Term Fourier Series with a 16-Minute Grid Spacing (7 of 7)

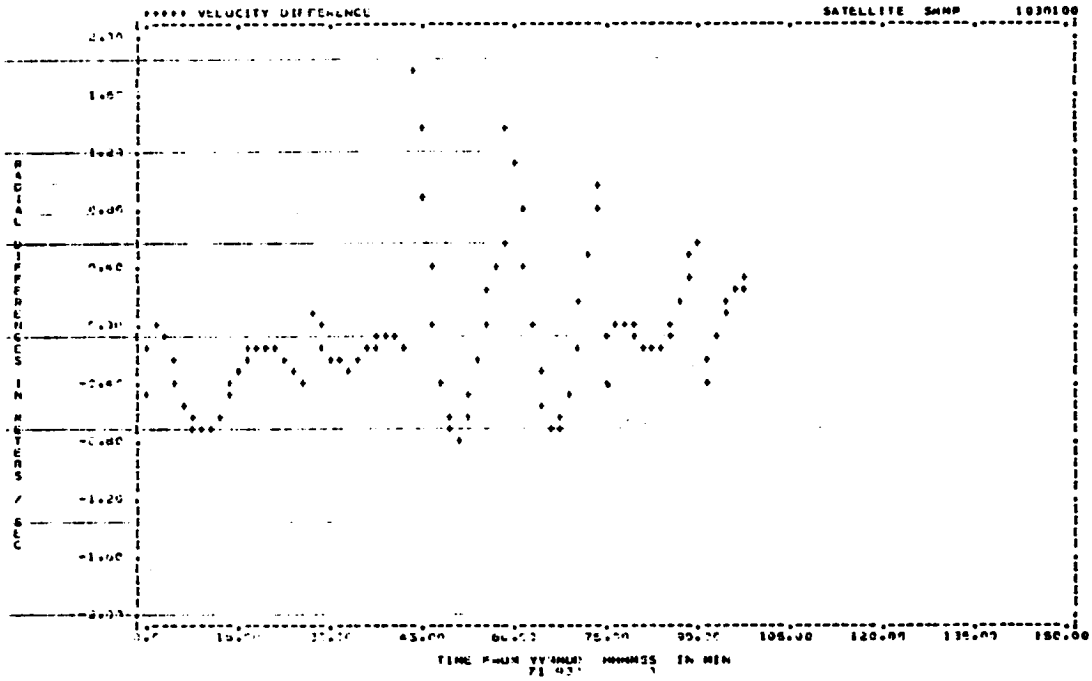

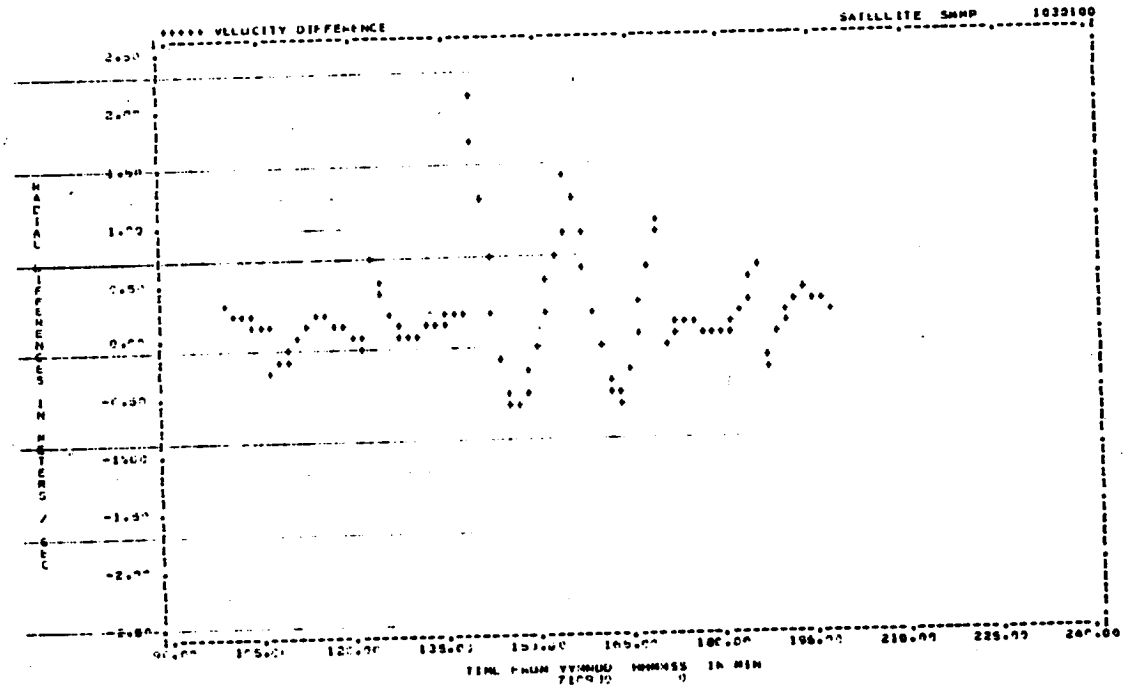

Figure 3-4. Errors in the Representation of the Radial Component of Velocity Using a 29-Term Fourier Series with a 16-Minute Grid Spacing (1 of 7)

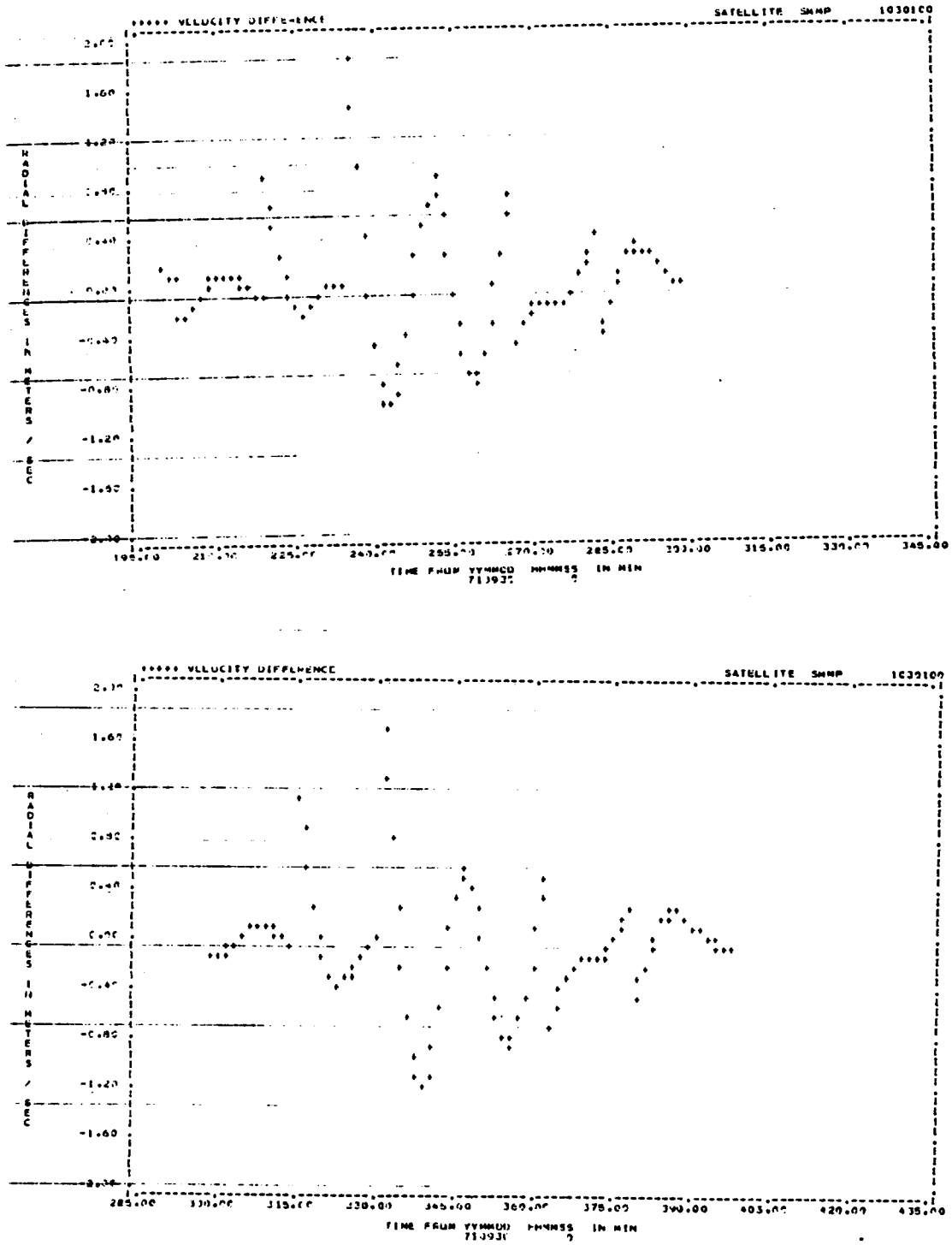

Figure 3-4. Errors in the Representation of the Radial Component of Velocity Using a 29-Term Fourier Series with a 16-Minute Grid Spacing (2 of 7)

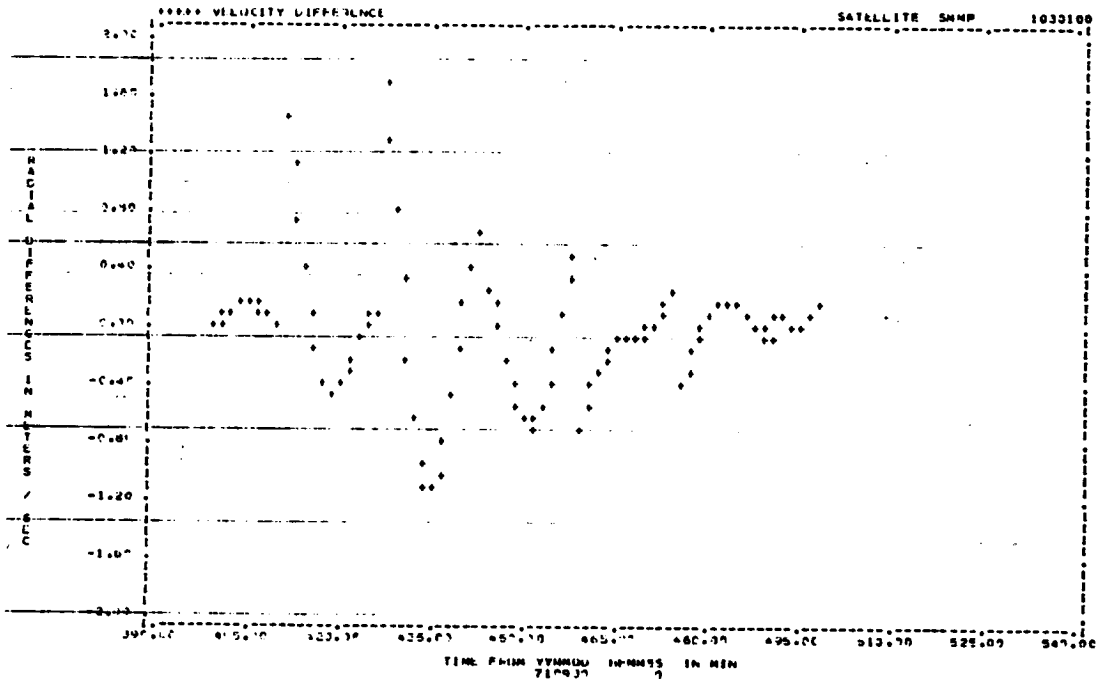

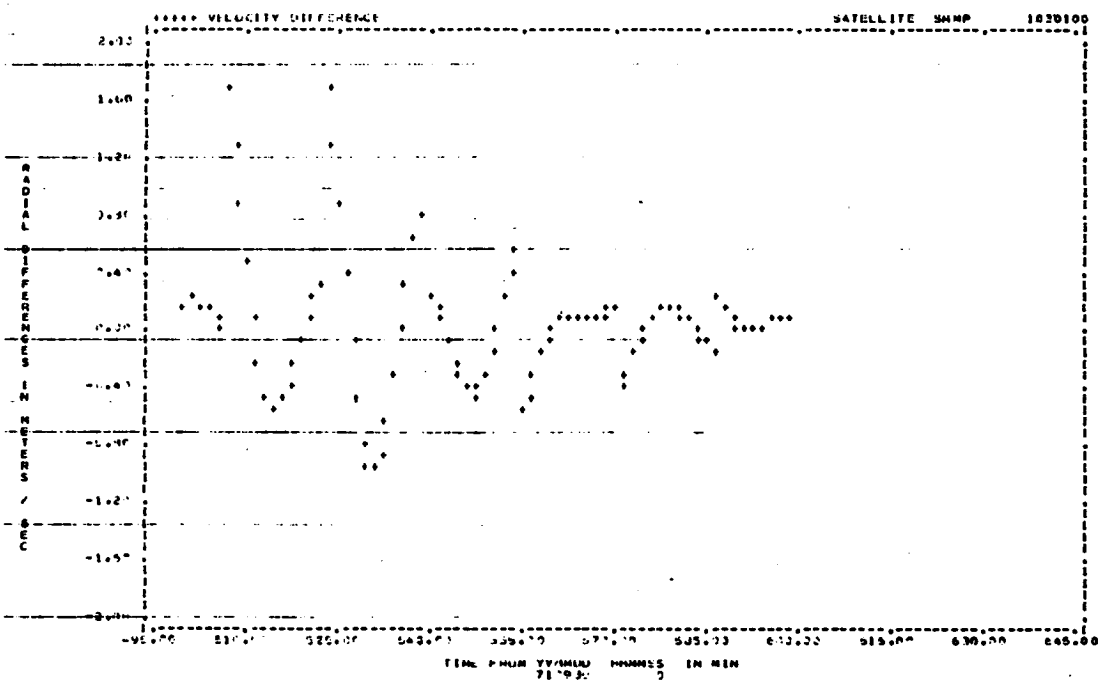

Figure 3-4. Errors in the Representation of the Radial Component of Velocity Using a 29-Term Fourier Series with a 16-Minute Grid Spacing (3 of 7)

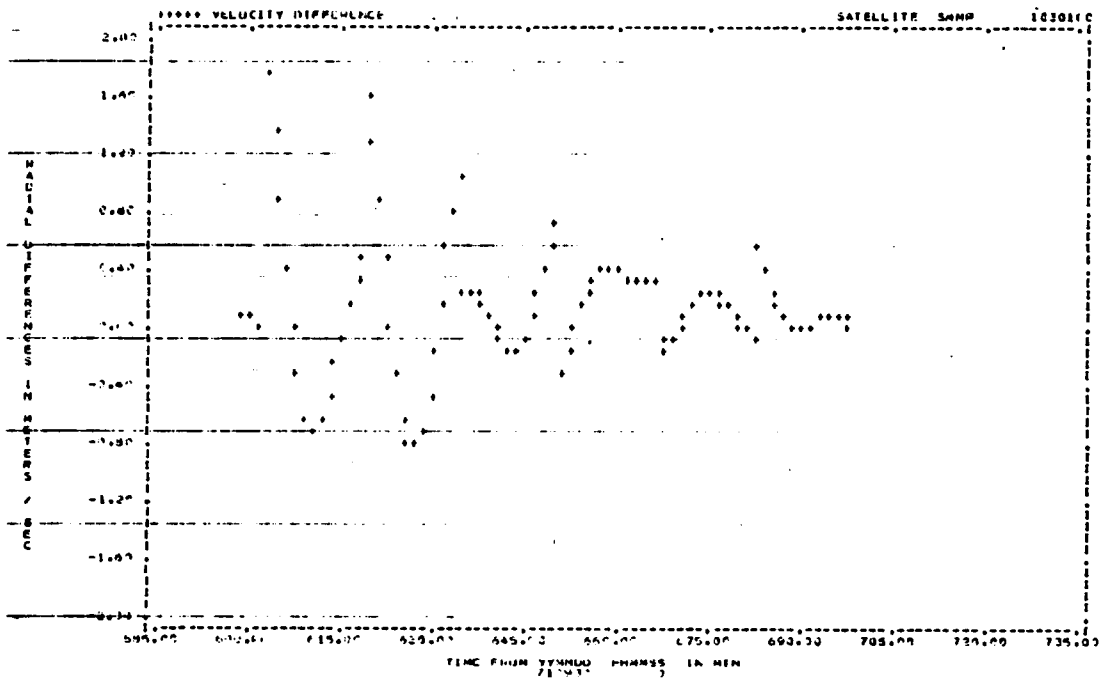

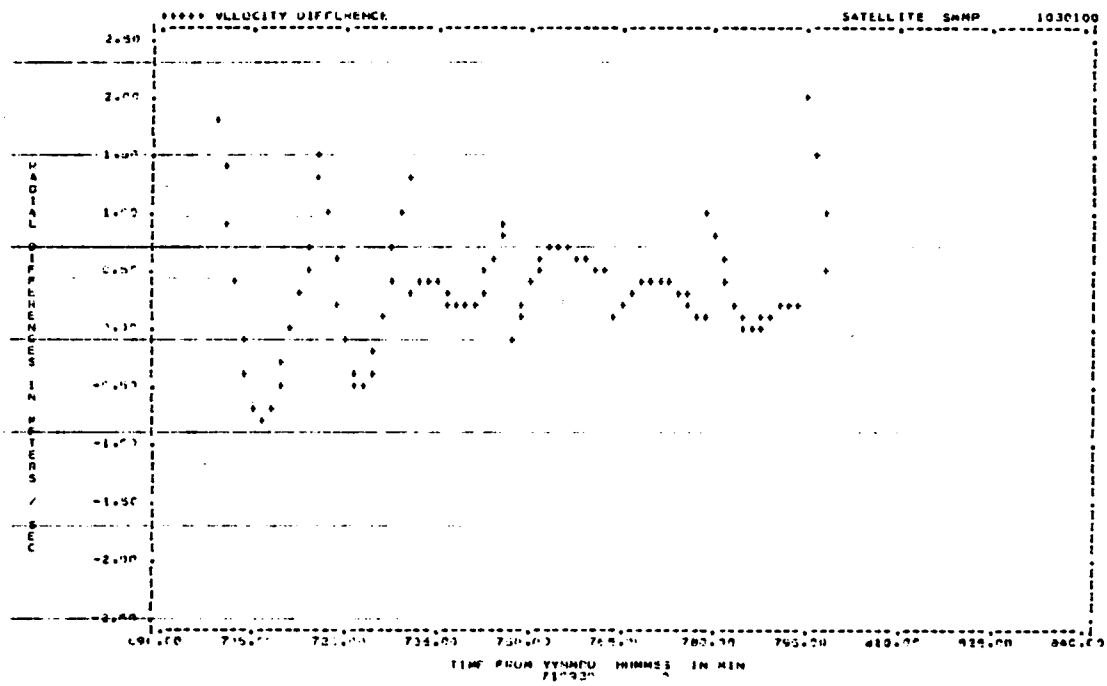

Figure 3-4. Errors in the Representation of the Radial Component of Velocity Using a 29-Term Fourier Series with a 16-Minute Grid Spacing (4 of 7)

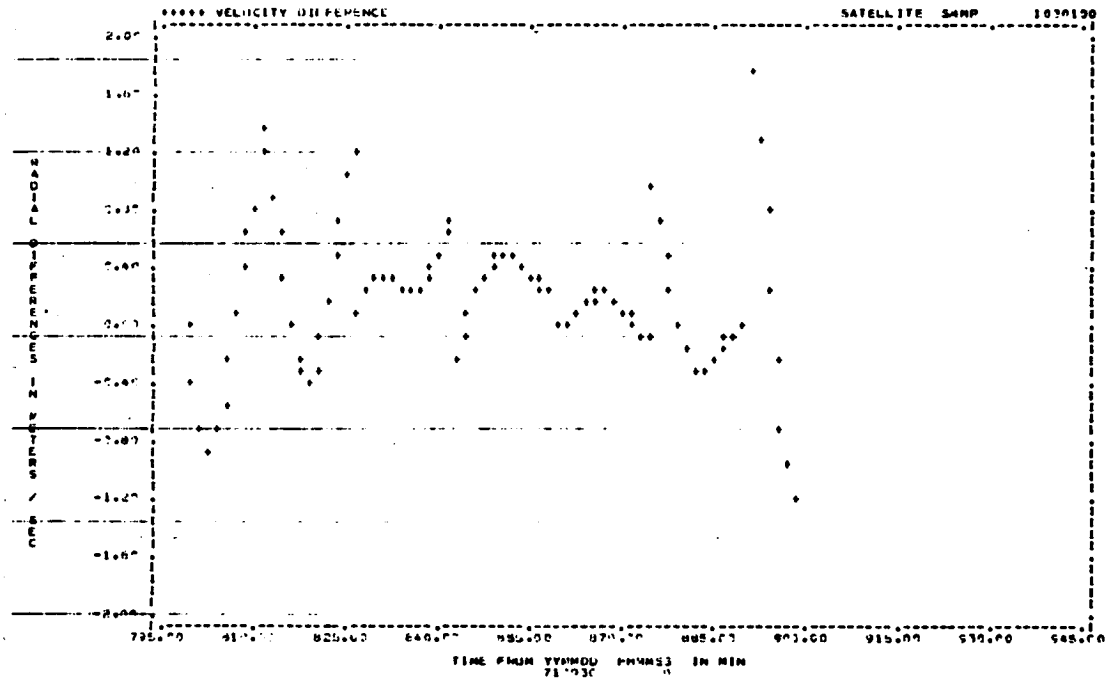

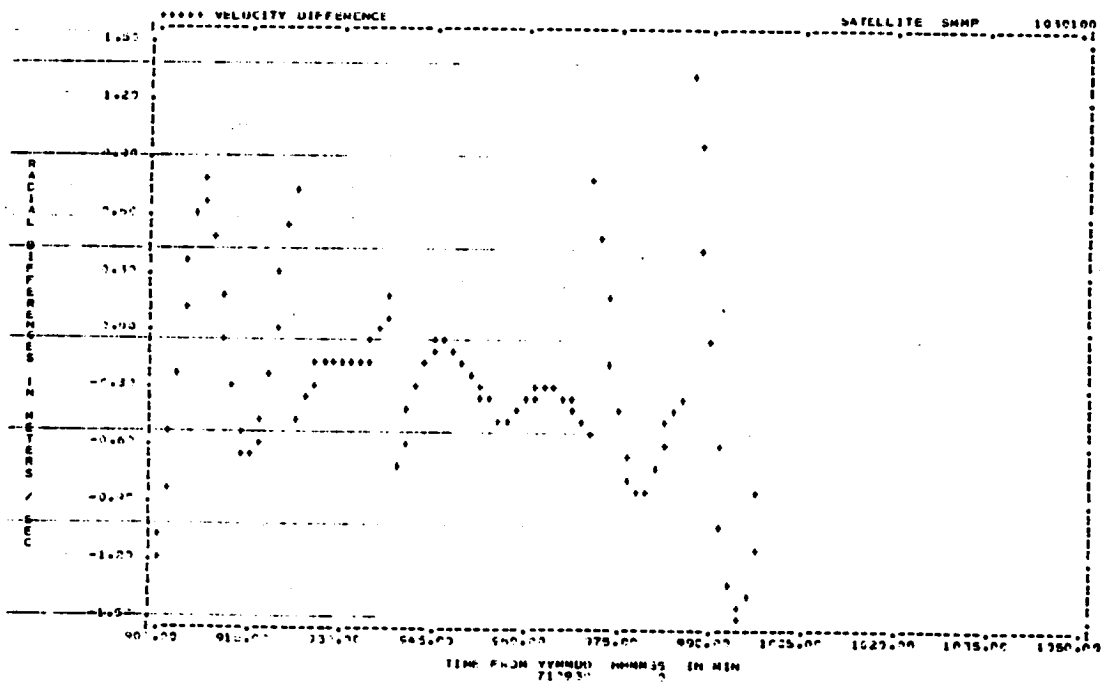

Figure 3-4. Errors in the Representation of the Radial Component of Velocity Using a 29-Term Fourier Series with a 16-Minute Grid Spacing (5 of 7)

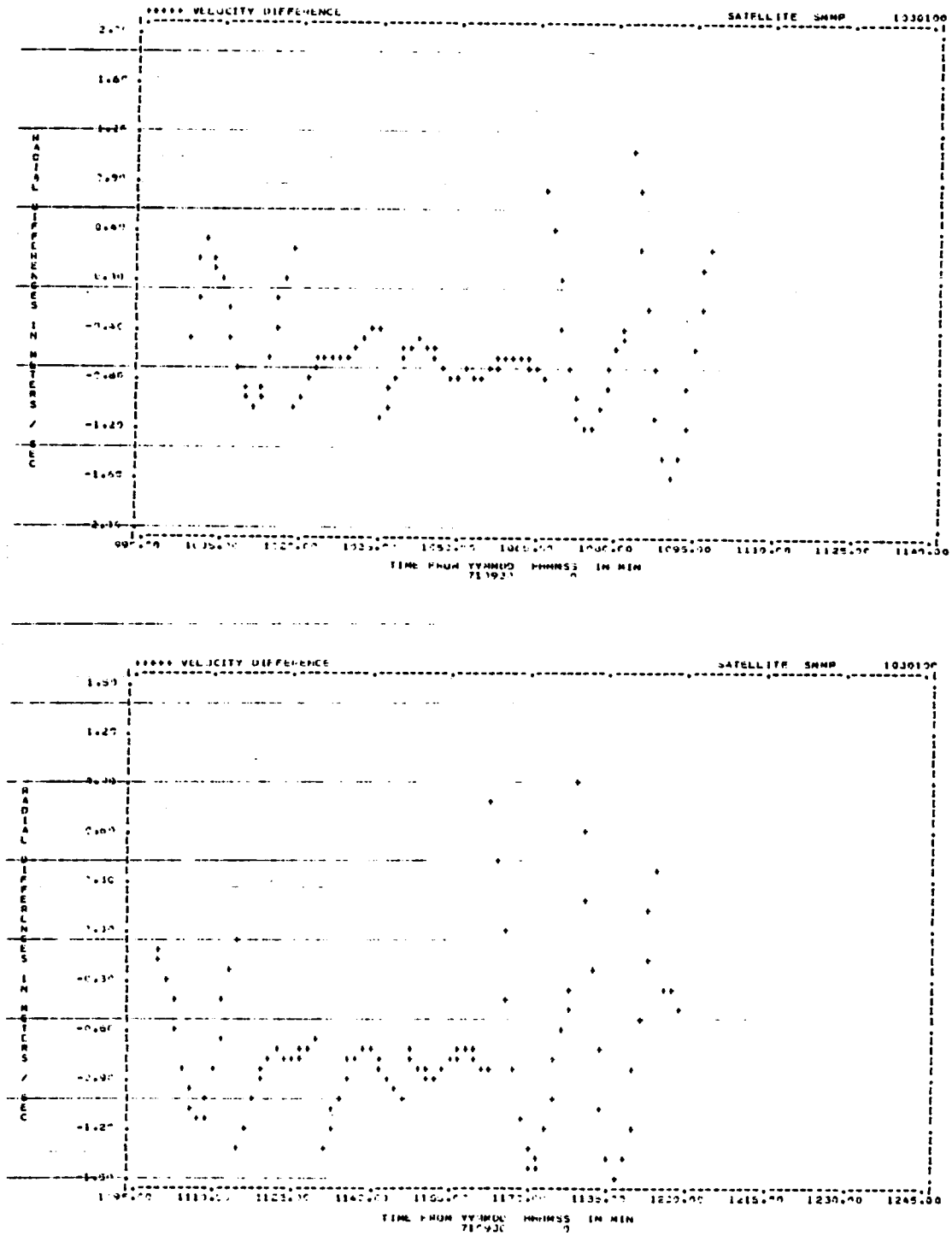

Figure 3-4. Errors in the Representation of the Radial Component of Velocity Using a 29-Term Fourier Series with a 16-Minute Grid Spacing (6 of 7)

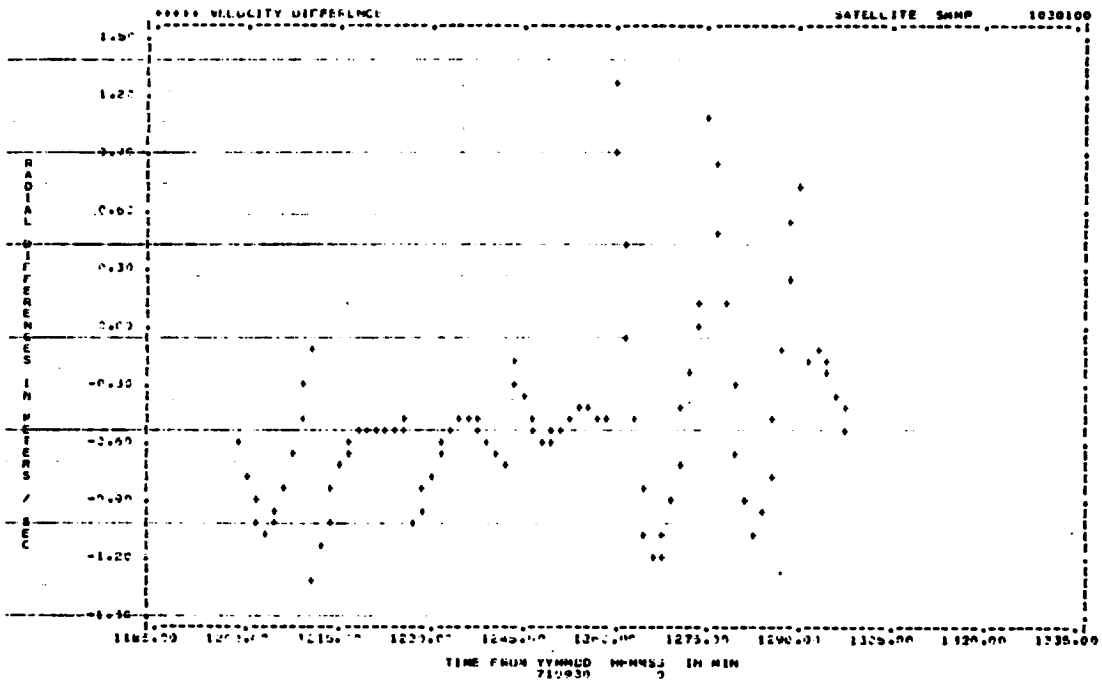

Figure 3-4. Errors in the Representation of the Radial Component of Velocity Using a 29-Term Fourier Series with a 16-Minute Grid Spacing (7 of 7)

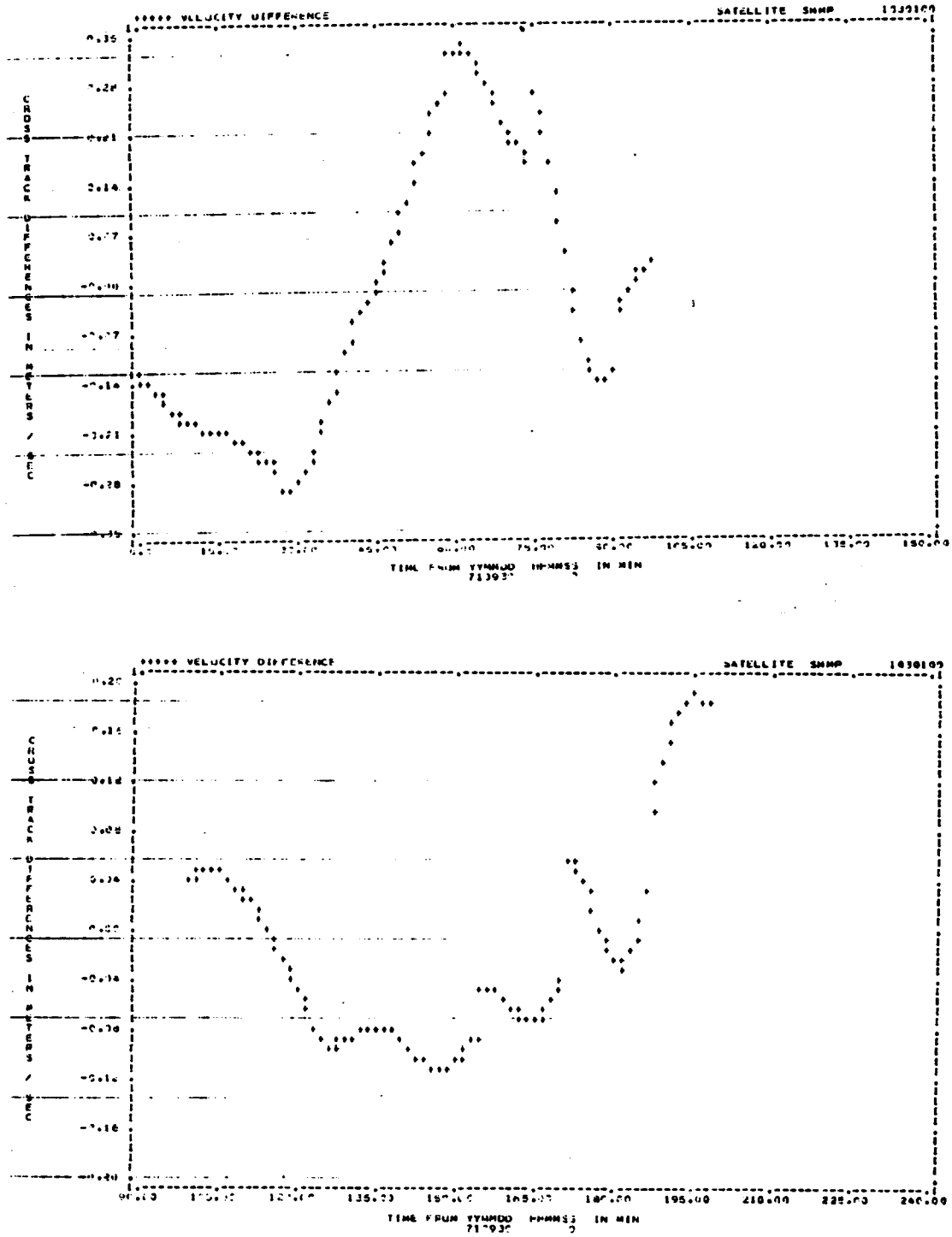

Figure 3-5. Errors in the Representation of the Cross-Track Component of Velocity Using a 29-Term Fourier Series with a 16-Minute Grid Spacing (1 of 7)

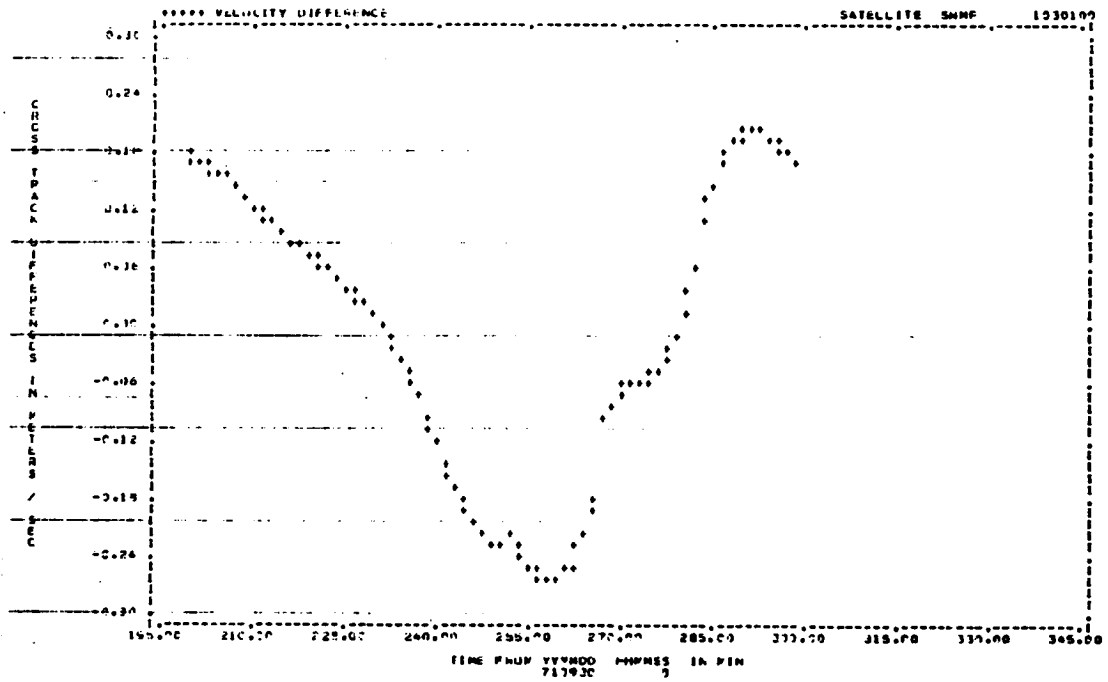

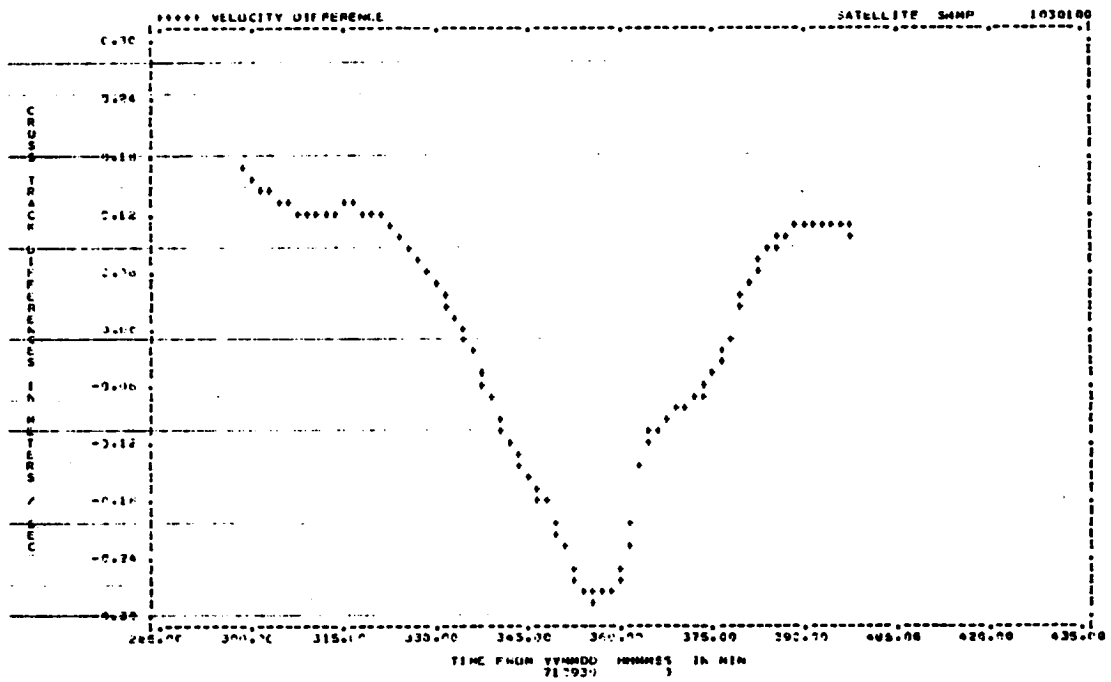

Figure 3-5. Errors in the Representation of the Cross-Track Component of Velocity Using a 29-Term Fourier Series with a 16-Minute Grid Spacing (2 of 7)

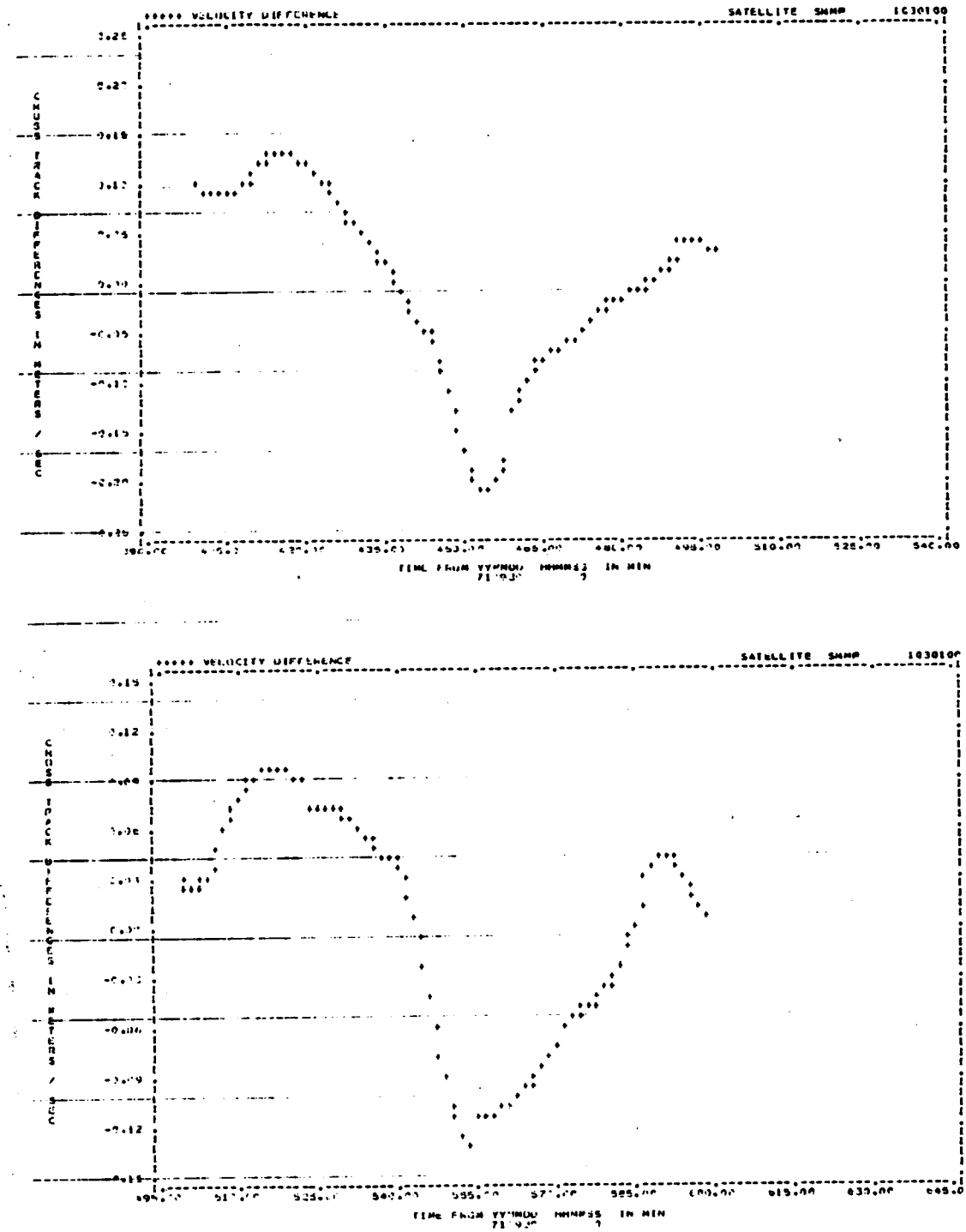

Figure 3-5. Errors in the Representation of the Cross-Track Component of Velocity Using a 29-Term Fourier Series with a 16-Minute Grid Spacing (3 of 7)

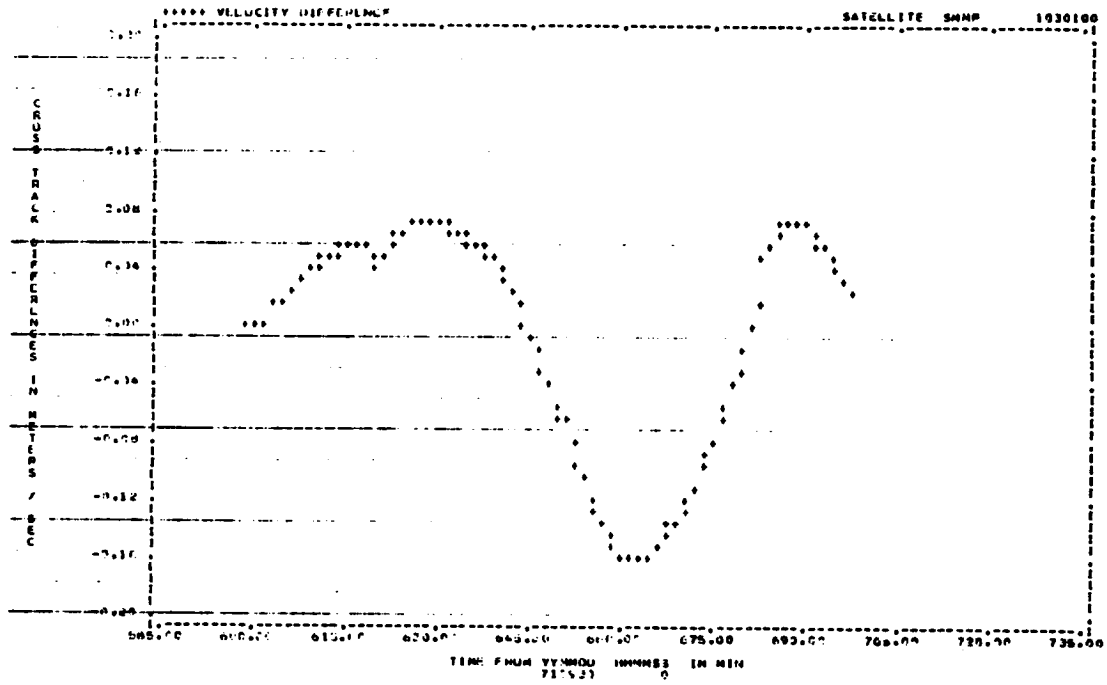

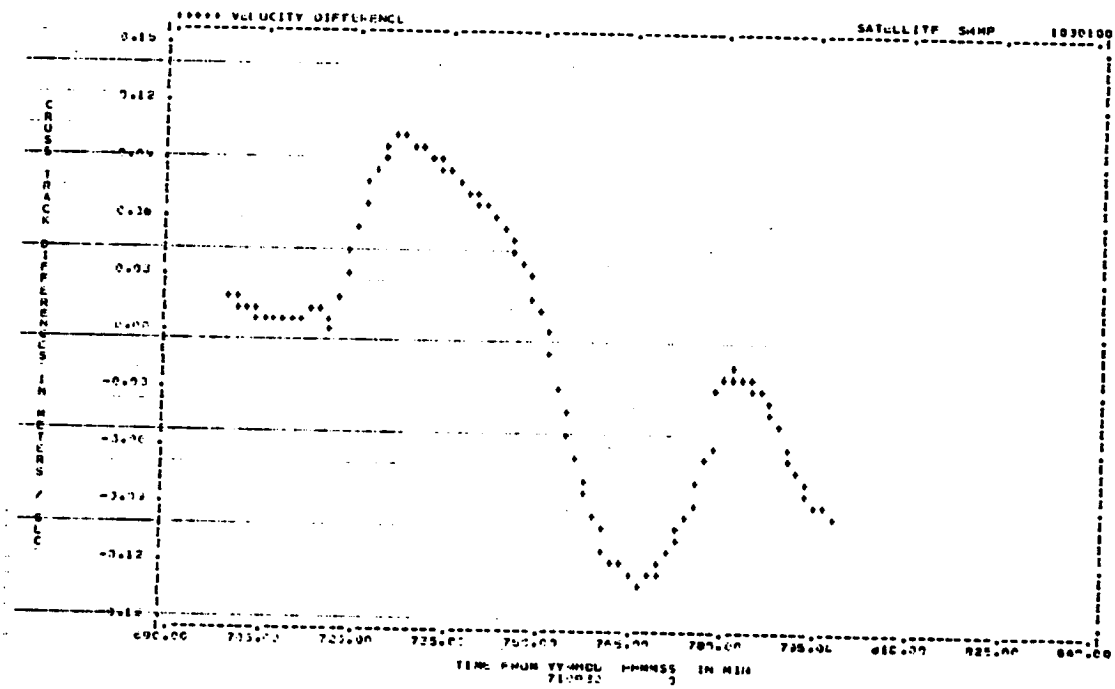

Figure 3-5. Errors in the Representation of the Cross-Track Component of Velocity Using a 29-Term Fourier Series with a 16-Minute Grid Spacing (4 of 7)

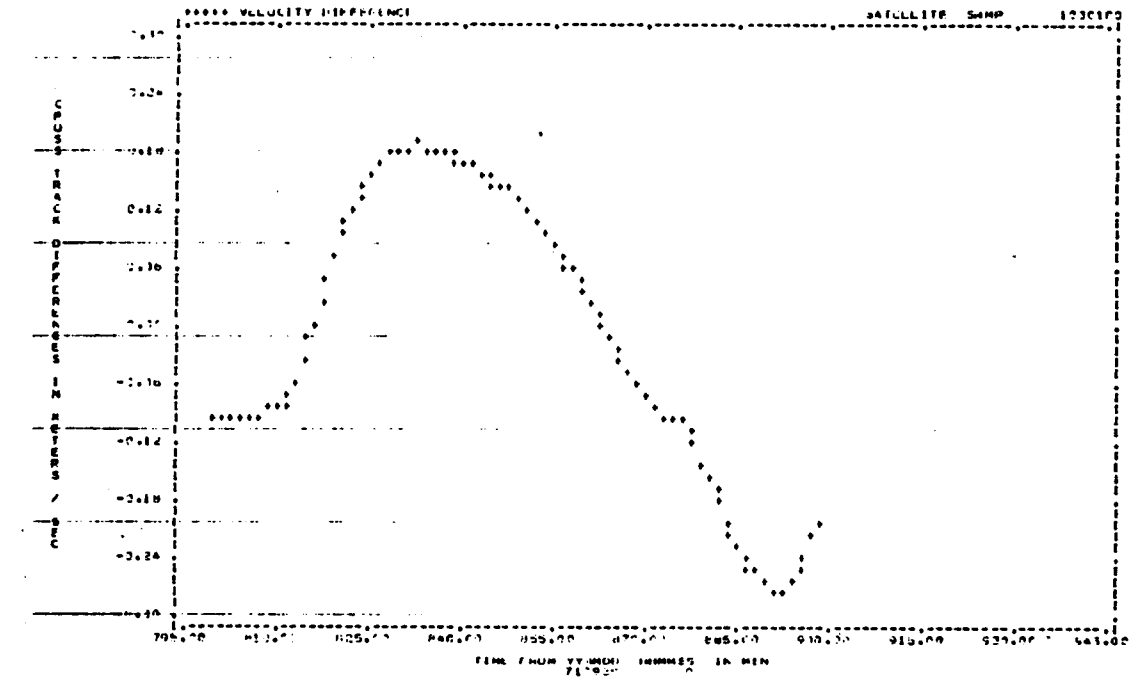

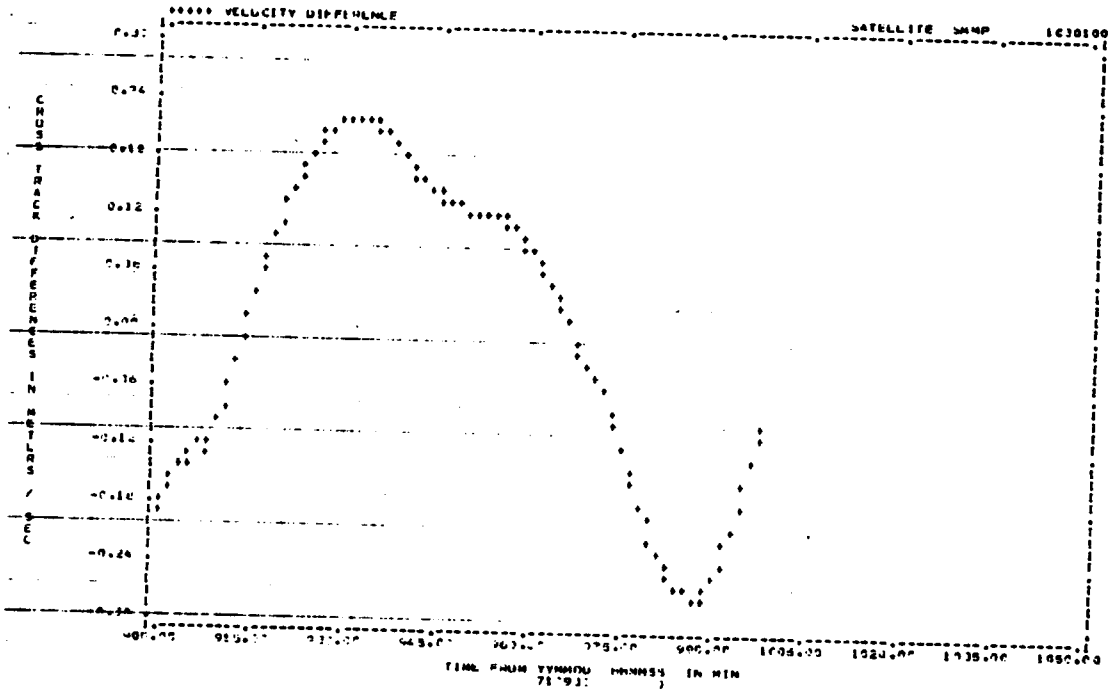

Figure 3-5. Errors in the Representation of the Cross-Track Component of Velocity Using a 29-Term Fourier Series with a 16-Minute Grid Spacing (5 of 7)

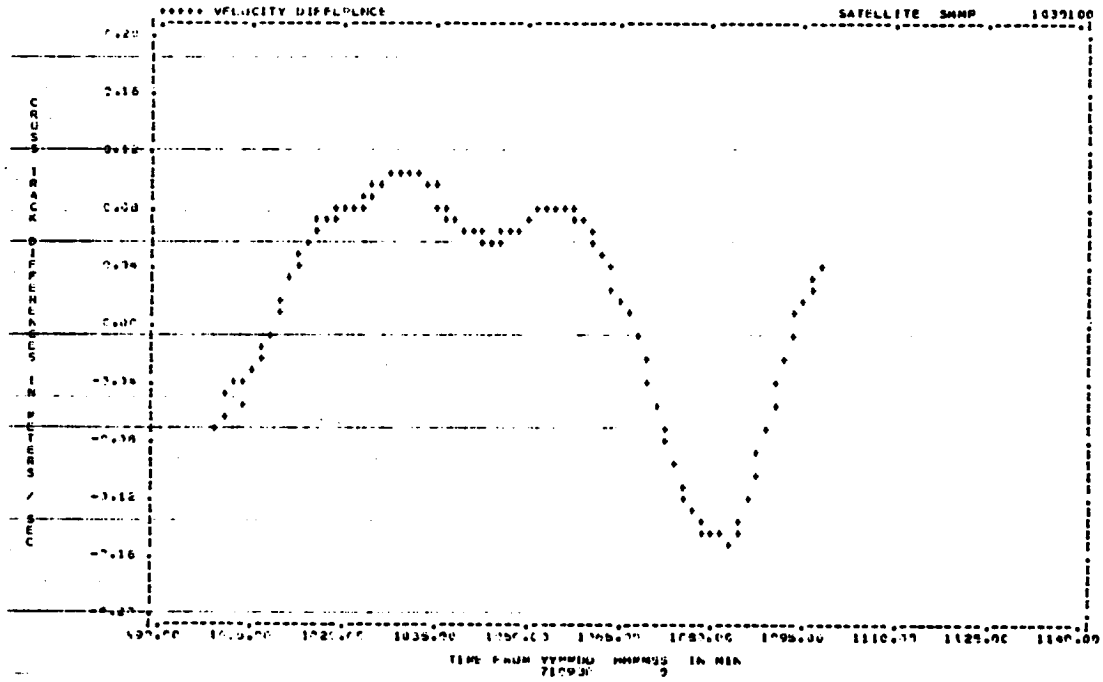

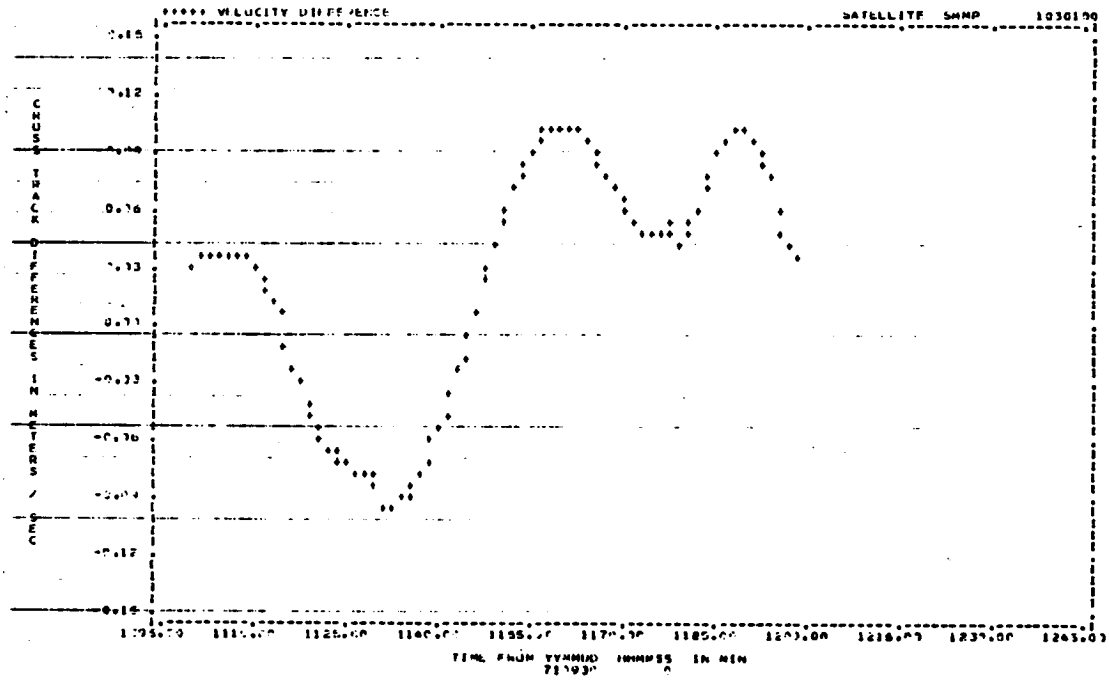

Figure 3-5. Errors in the Representation of the Cross-Track Component of Velocity Using a 29-Term Fourier Series with a 16-Minute Grid Spacing (6 of 7)

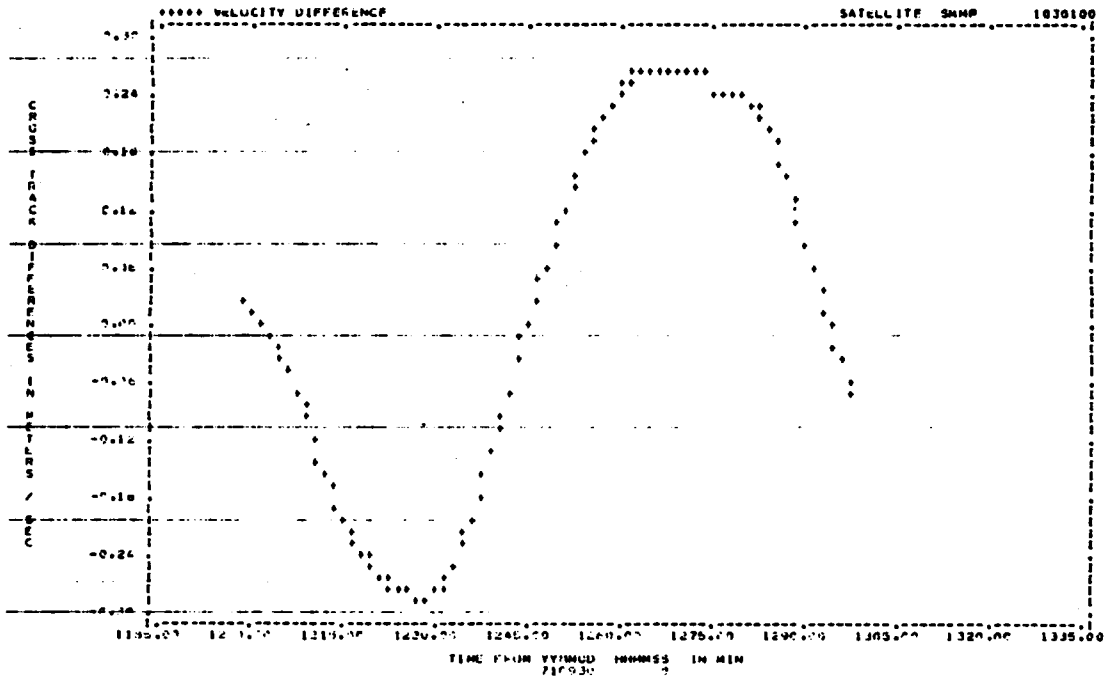

Figure 3-5. Errors in the Representation of the Cross-Track Component of Velocity Using a 29-Term Fourier Series with a 16-Minute Grid Spacing (7 of 7)

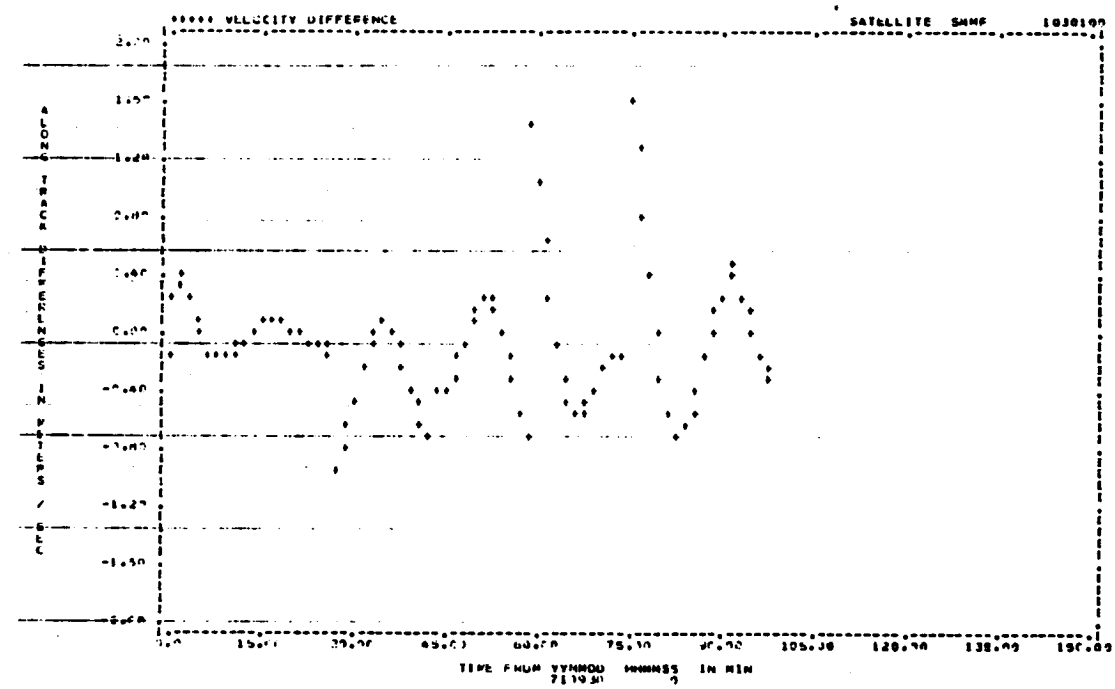

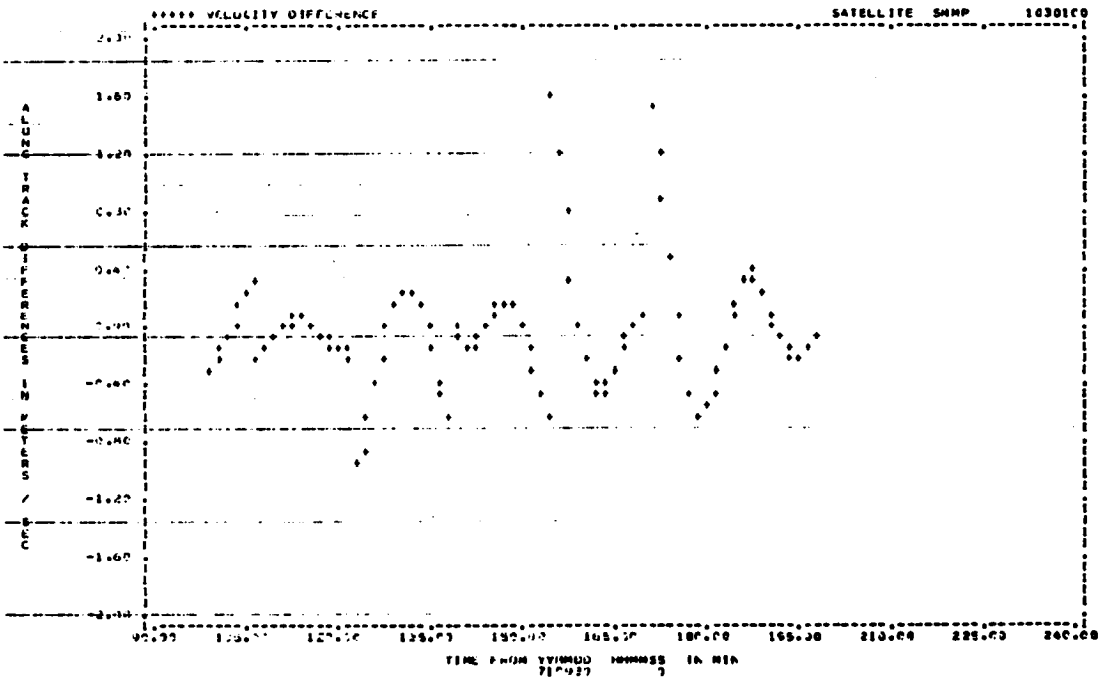

Figure 3-6. Errors in the Representation of the Along-Track Component of Velocity Using a 29-Term Fourier Series with a 16-Minute Grid Spacing (1 of 7)

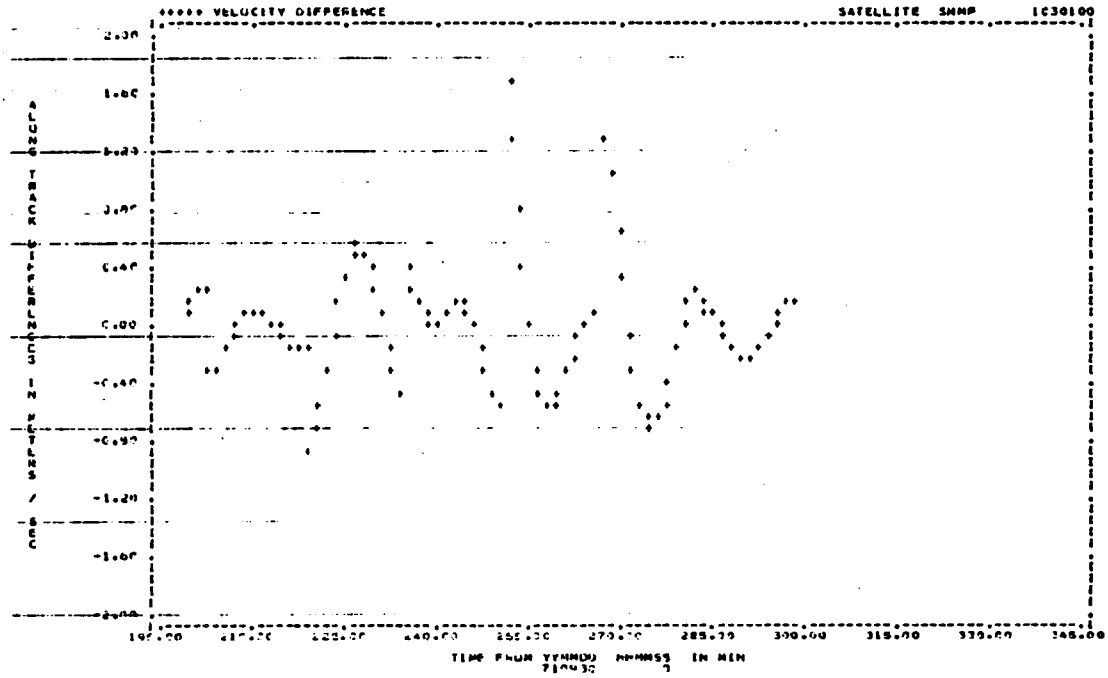

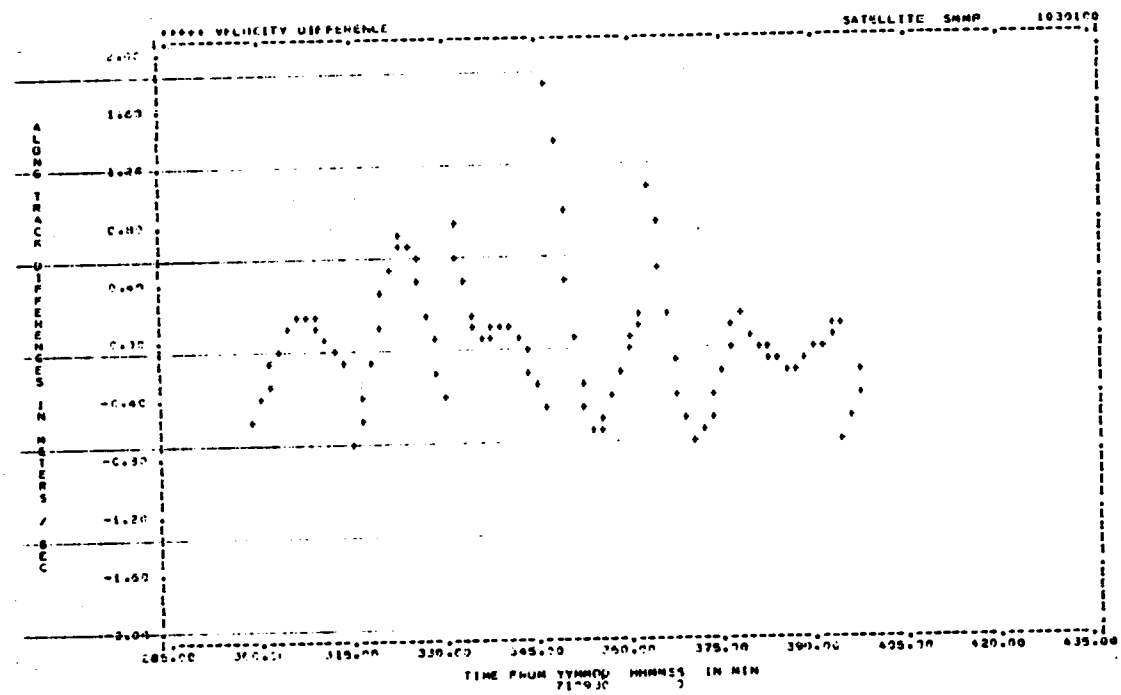

Figure 3-6. Errors in the Representation of the Along-Track Component of Velocity Using a 29-Term Fourier Series with a 16-Minute Grid Spacing (2 of 7)

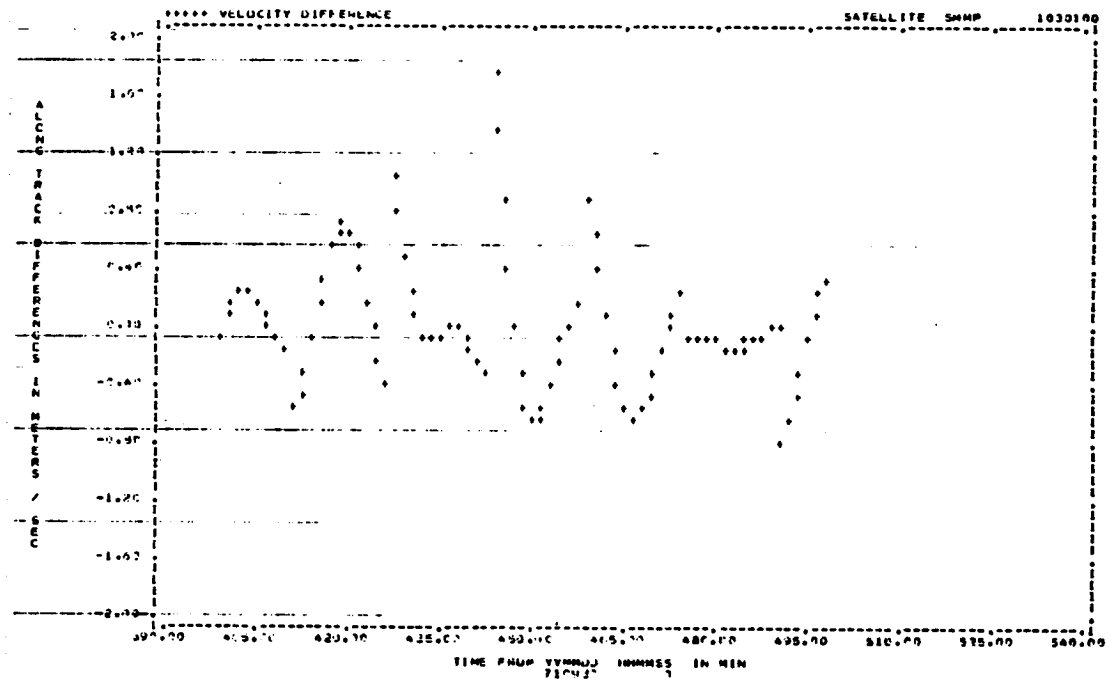

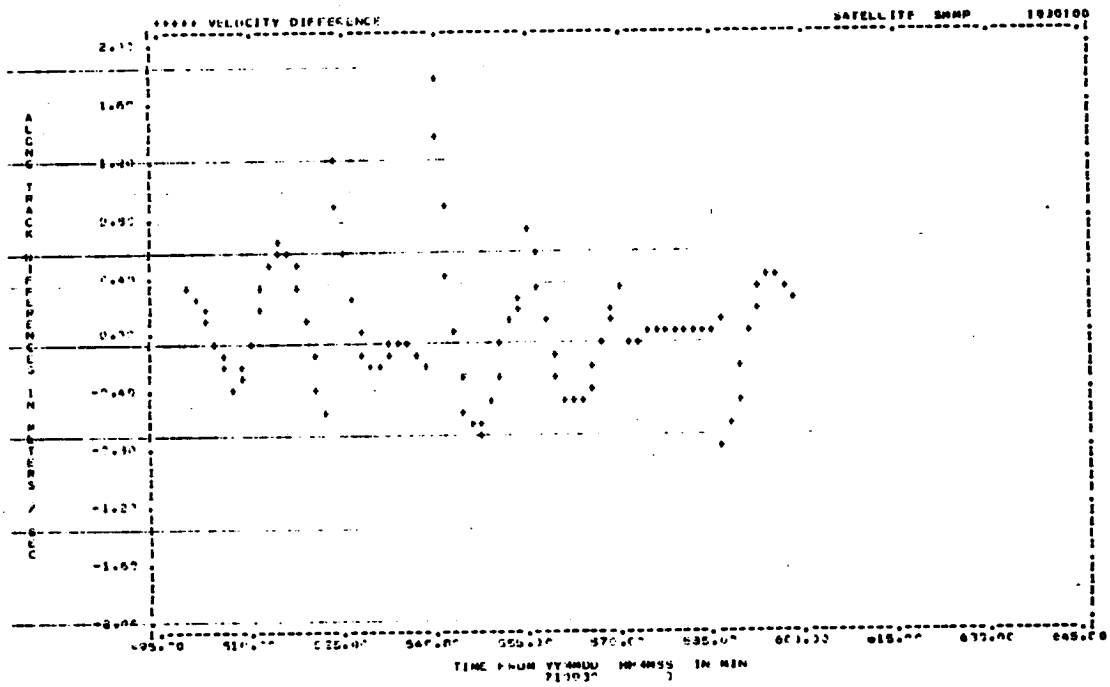

Figure 3-6. Errors in the Representation of the Along-Track Component of Velocity Using a 29-Term Fourier Series with a 16-Minute Grid Spacing (3 of 7)

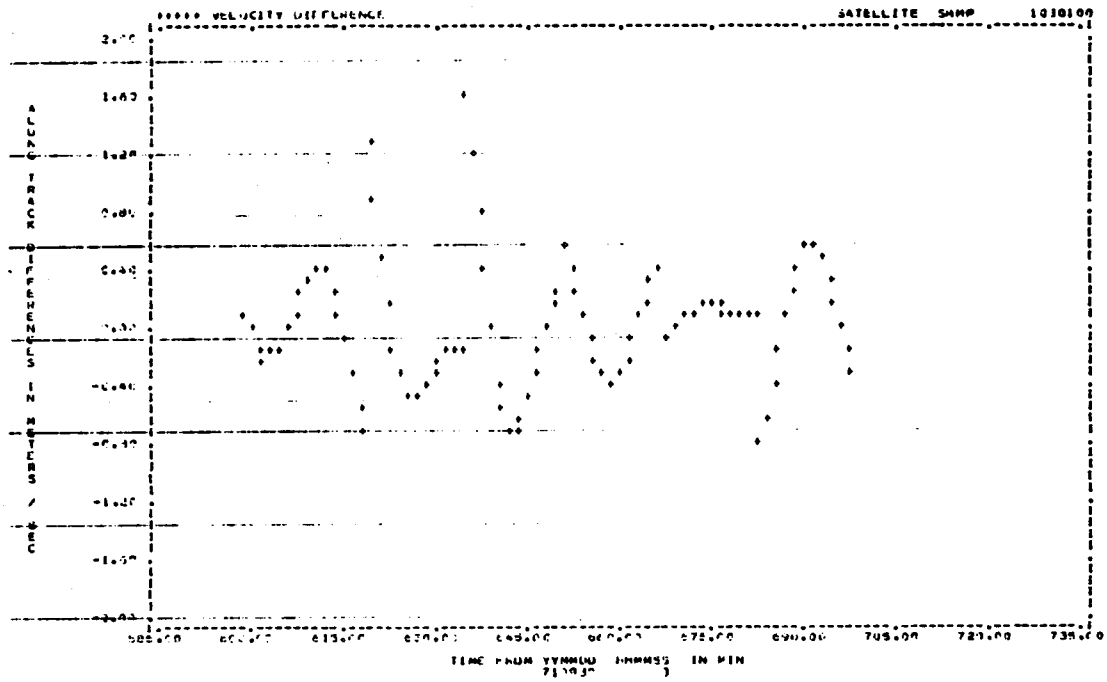

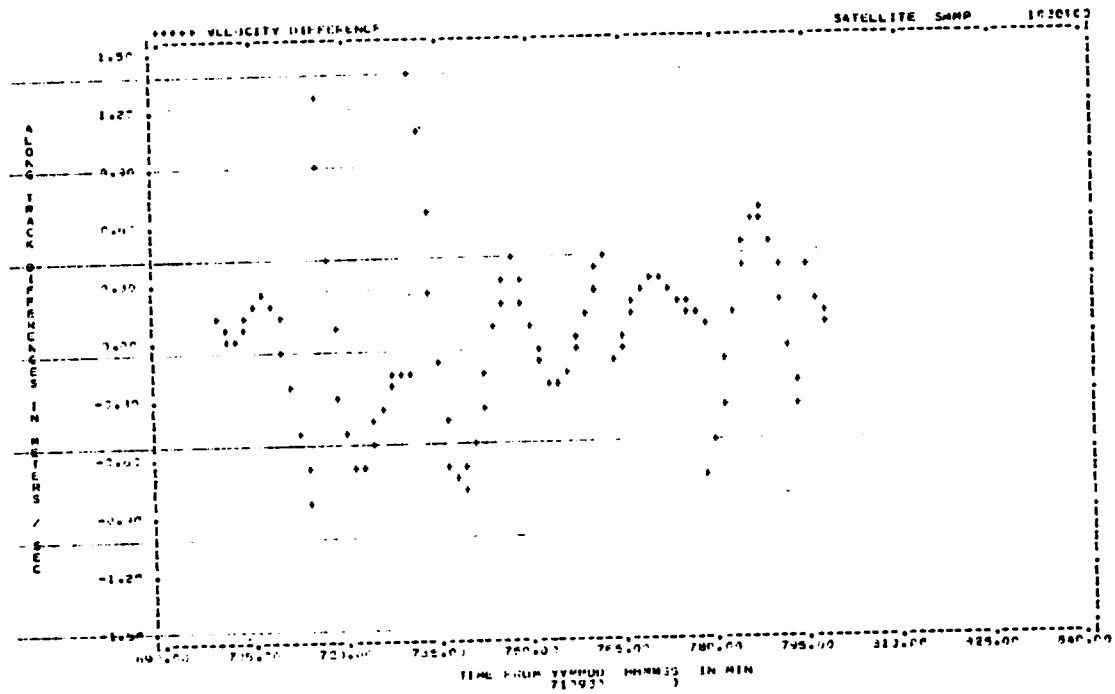

Figure 3-6. Errors in the Representation of the Along-Track Component of Velocity Using a 29-Term Fourier Series with a 16-Minute Grid Spacing (4 of 7)

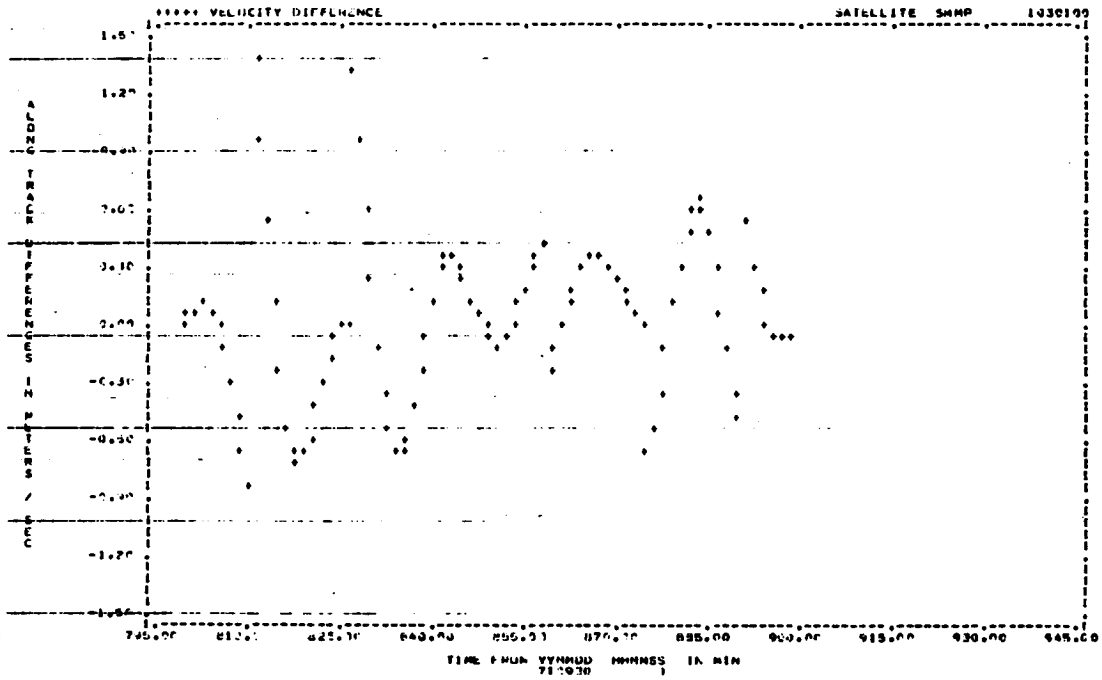

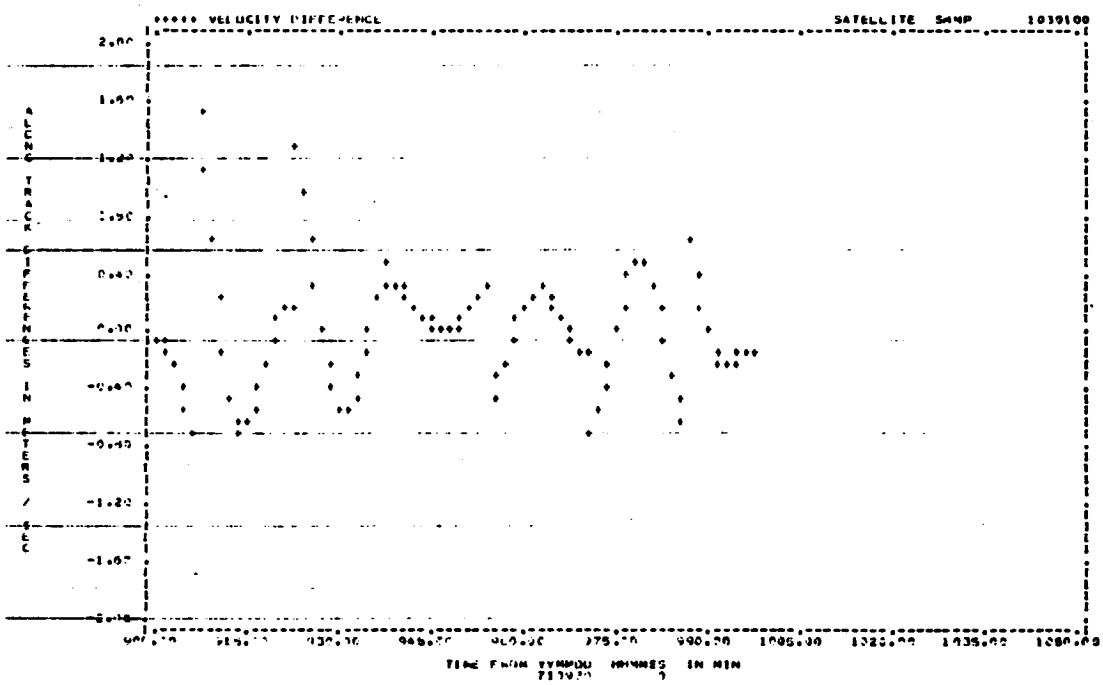

Figure 3-6. Errors in the Representation of the Along-Track Component of Velocity Using a 29-Term Fourier Series with a 16-Minute Grid Spacing (5 of 7)

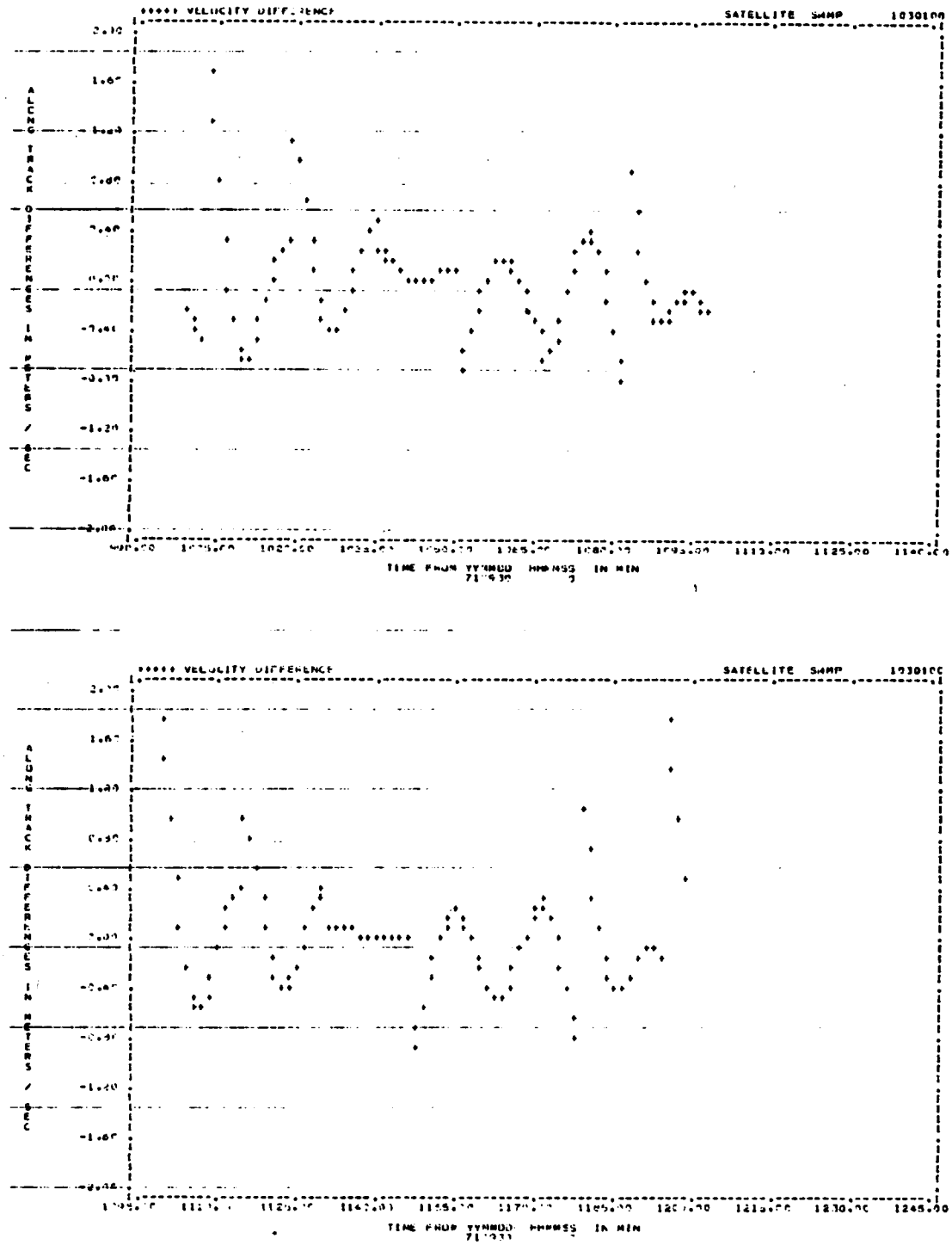

Figure 3-6. Errors in the Representation of the Along-Track Component of Velocity Using a 29-Term Fourier Series with a 16-Minute Grid Spacing (6 of 7)

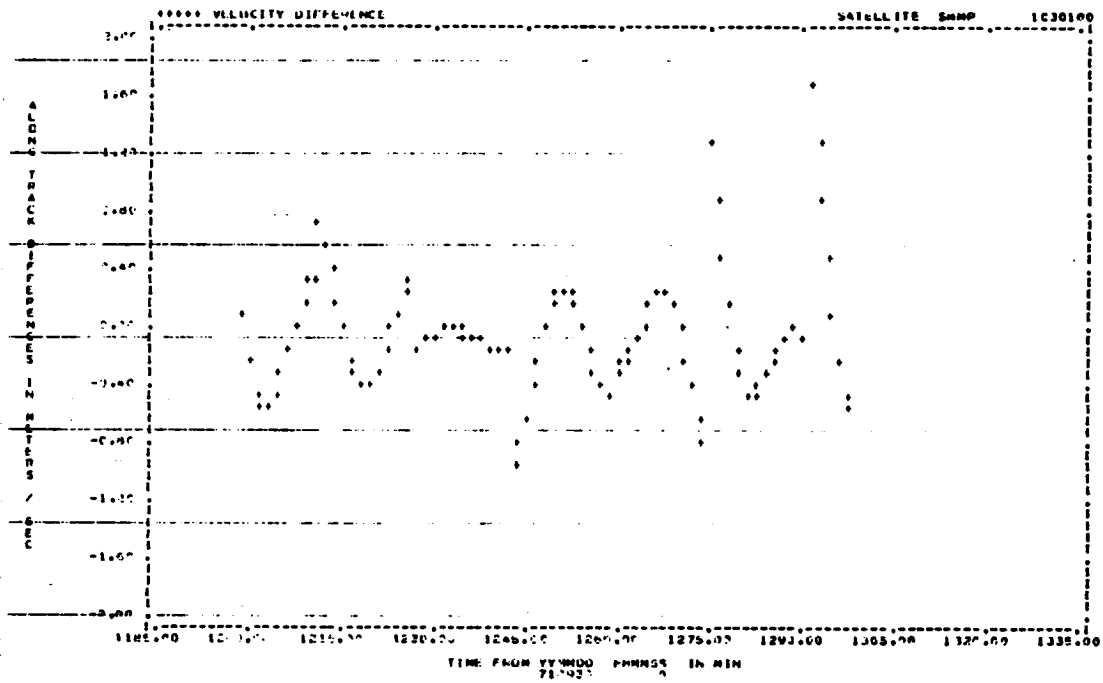

Figure 3-6. Errors in the Representation of the Along-Track Component of Velocity Using a 29-Term Fourier Series with a 16-Minute Grid Spacing (7 of 7)

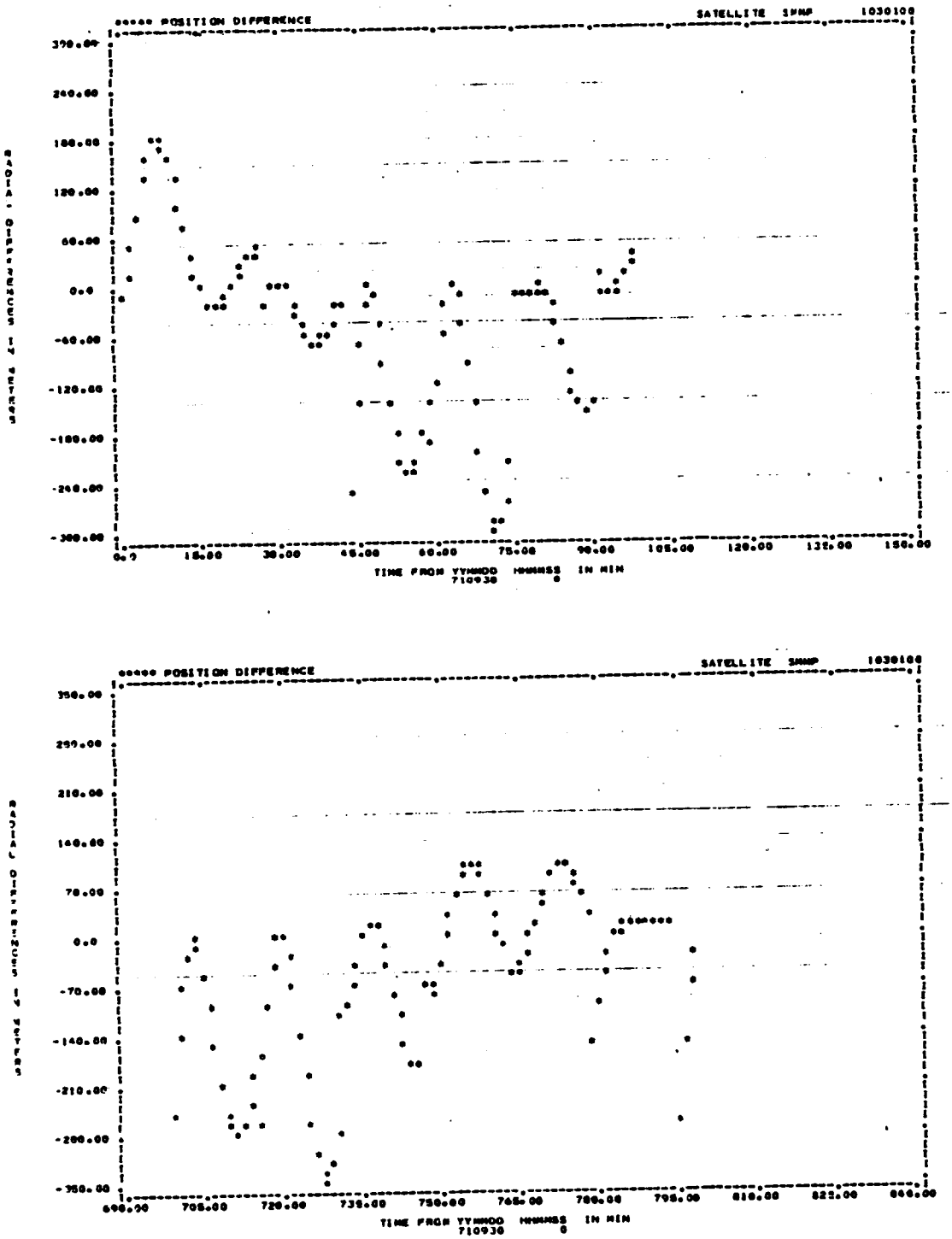

Figure 3-7. Errors in the Representation of the Radial Component of Position Using a 29-Term Fourier Series with Position Residuals and a 16-Minute Grid Spacing (1 of 2)

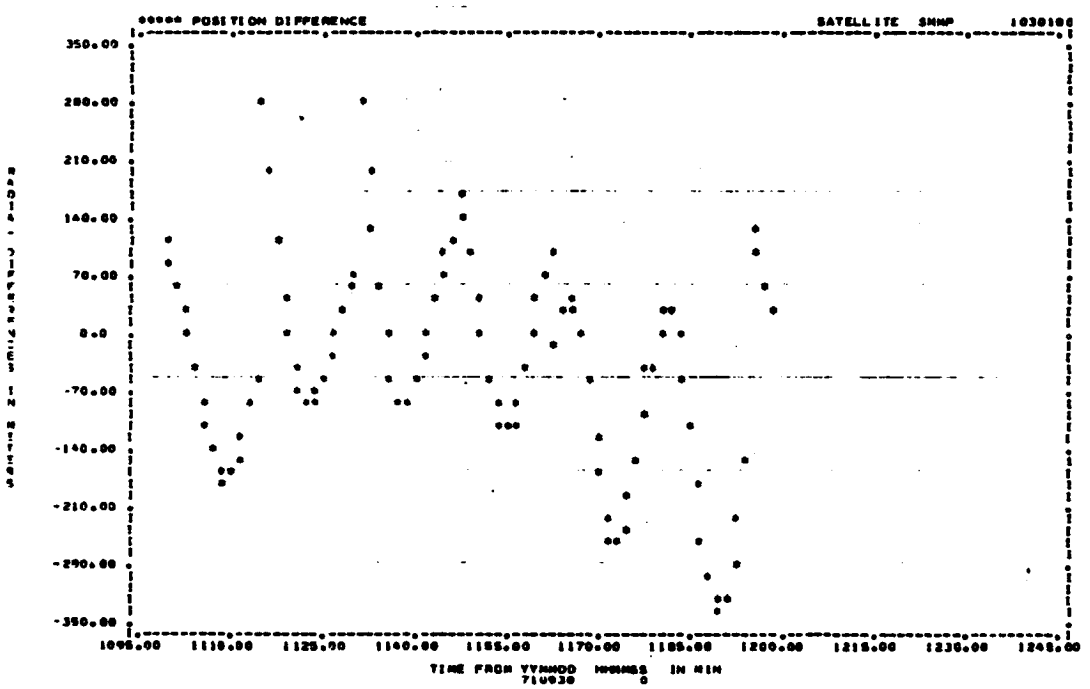

Figure 3-7. Errors in the Representation of the Radial Component of Position Using a 29-Term Fourier Series with Position Residuals and a 16-Minute Grid Spacing (2 of 2)

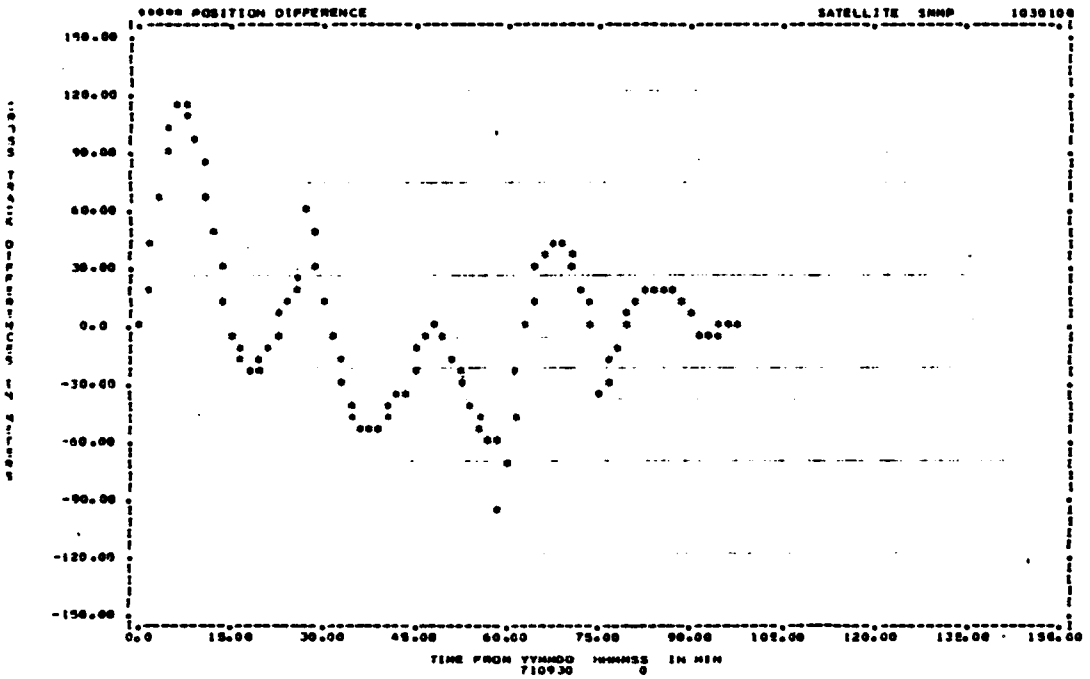

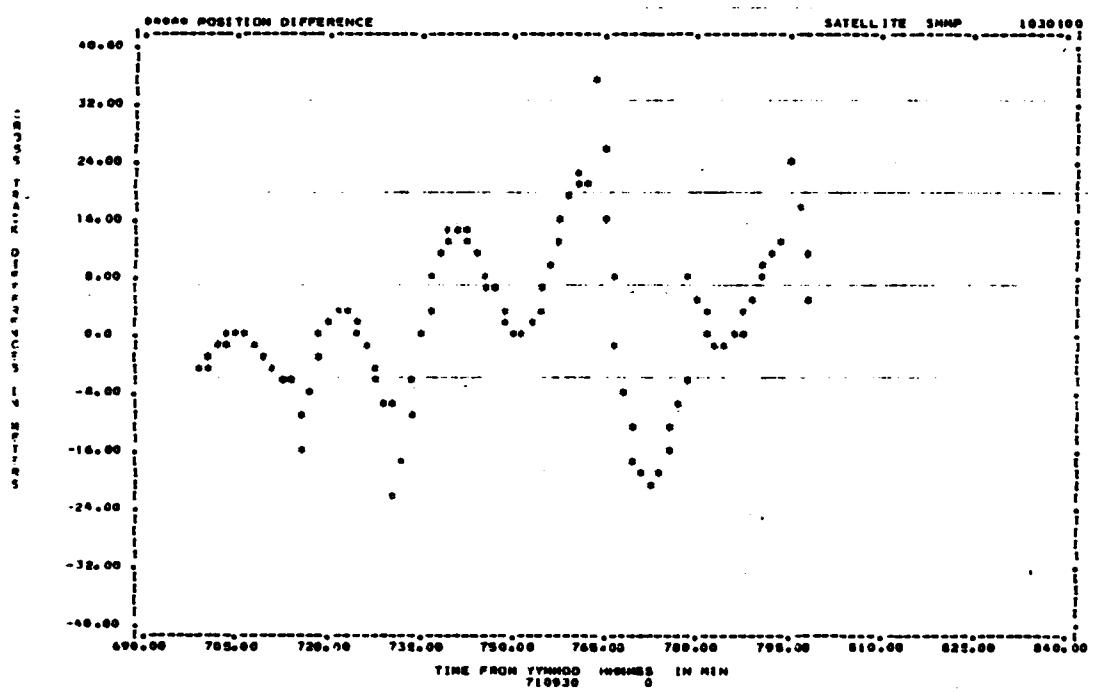

Figure 3-8. Errors in the Representation of the Cross-Track Component of Position Using a 29-Term Fourier Series with Position Residuals and a 16-Minute Grid Spacing (1 of 2)

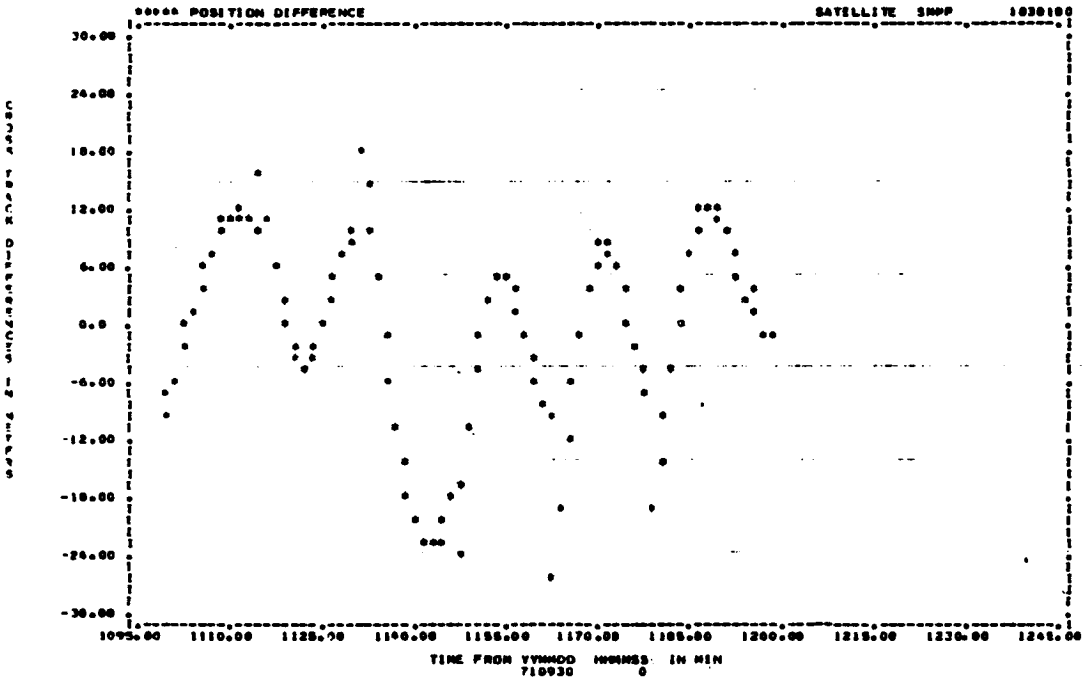

Figure 3-8. Errors in the Representation of the Cross-Track Component of Position Using a 29-Term Fourier Series with Position Residuals and a 16-Minute Grid Spacing (2 of 2)

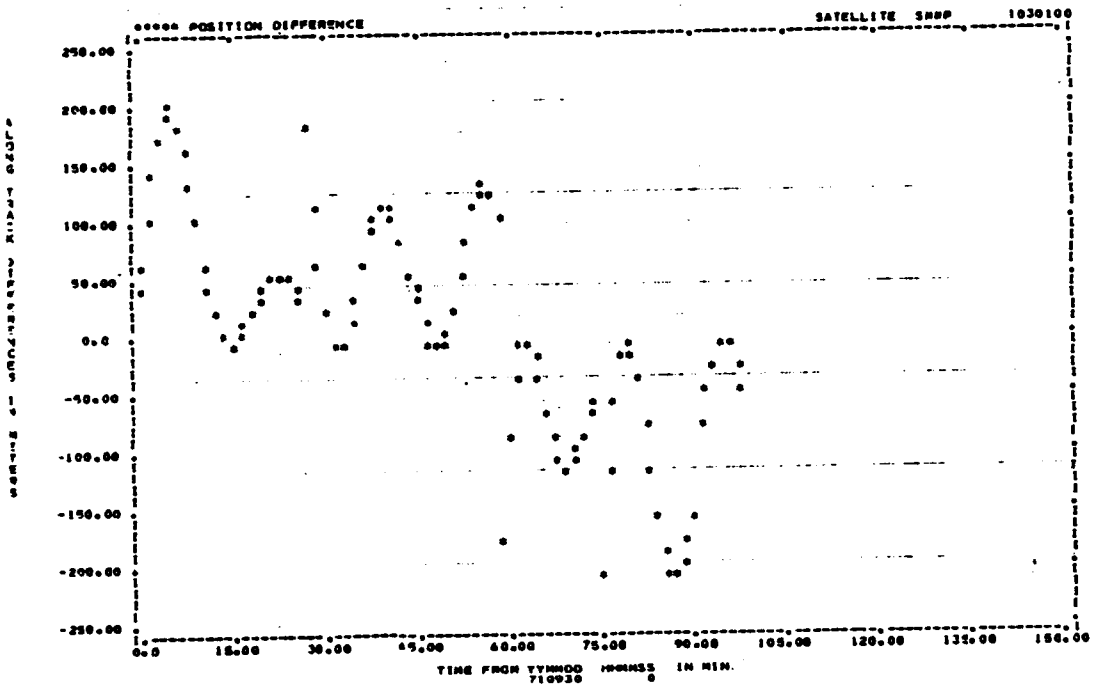

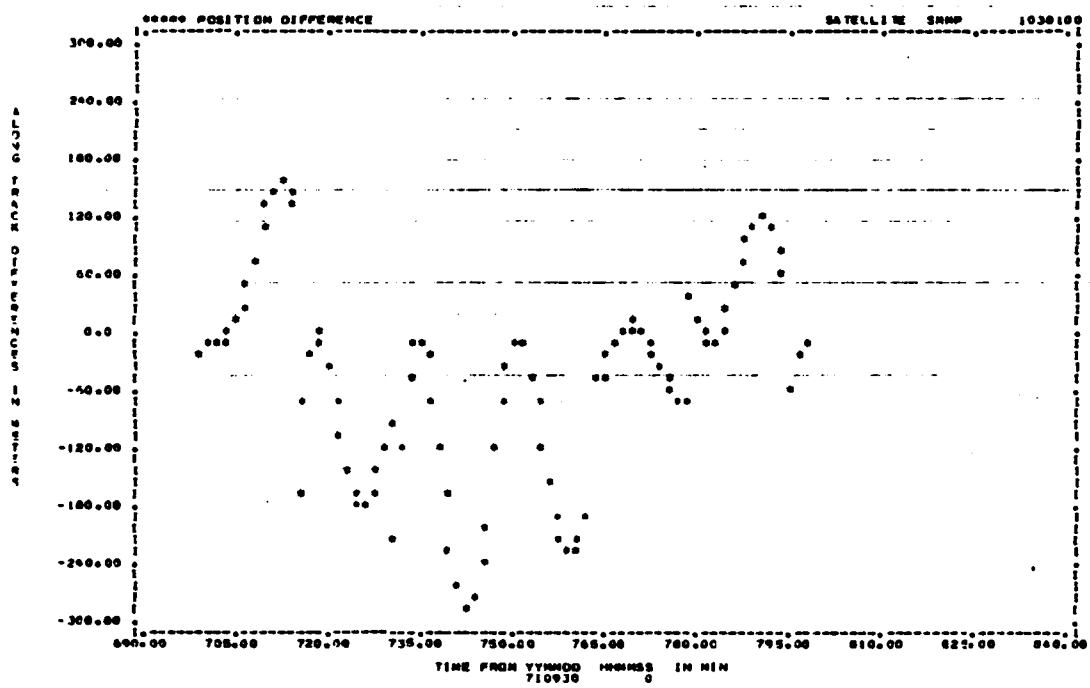

Figure 3-9. Errors in the Representation of the Along-Track Component of Position Using a 29-Term Fourier Series with Position Residuals and a 16-Minute Grid Spacing (1 of 2)

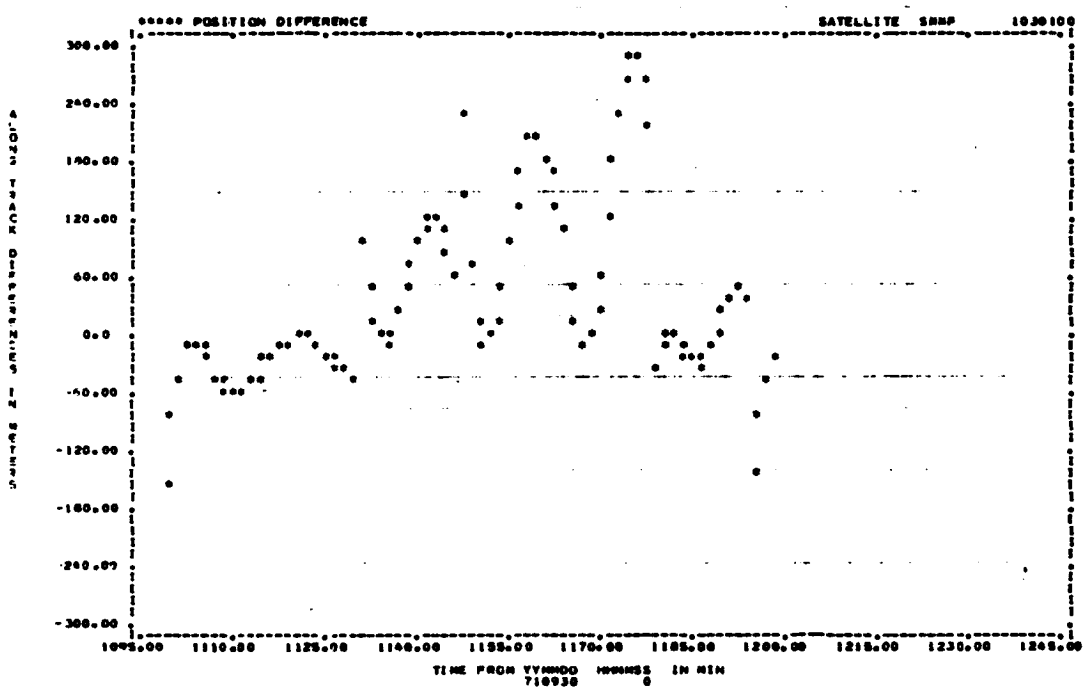

Figure 3-9. Errors in the Representation of the Along-Track Component of Position Using a 29-Term Fourier Series with Position Residuals and a 16-Minute Grid Spacing (2 of 2)

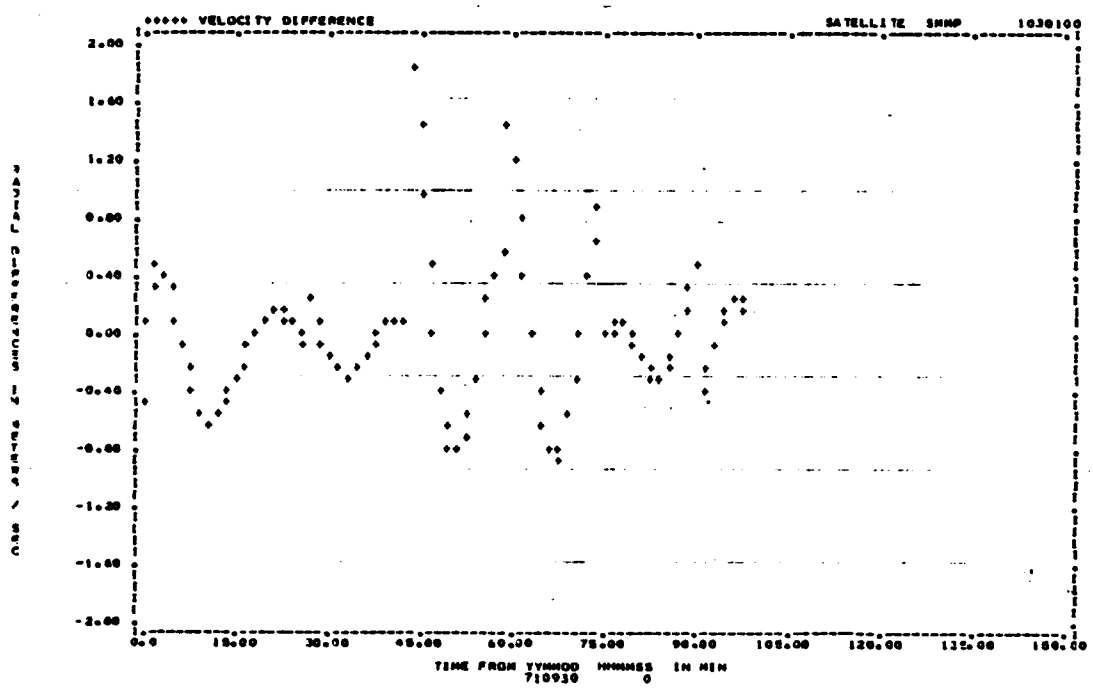

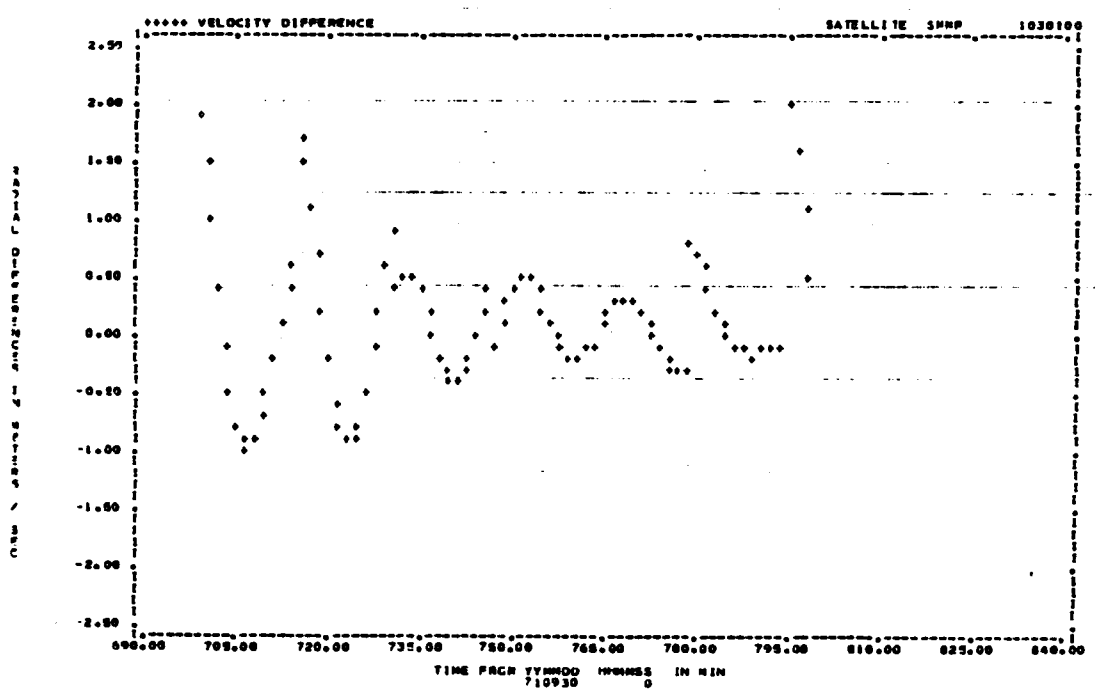

Figure 3-10. Errors in the Representation of the Radial Component of Velocity Using a 29-Term Fourier Series with Position Residuals and a 16-Minute Grid Spacing (1 of 2)

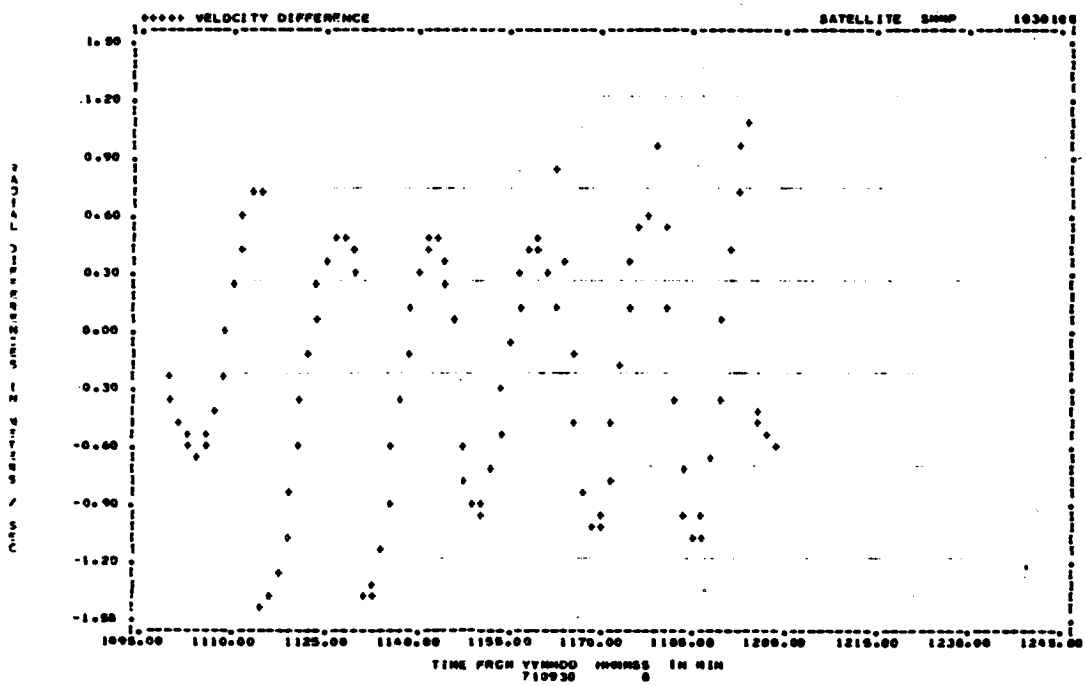

Figure 3-10. Errors in the Representation of the Radial Component of Velocity Using a 29-Term Fourier Series with Position Residuals and a 16-Minute Grid Spacing (2 of 2)

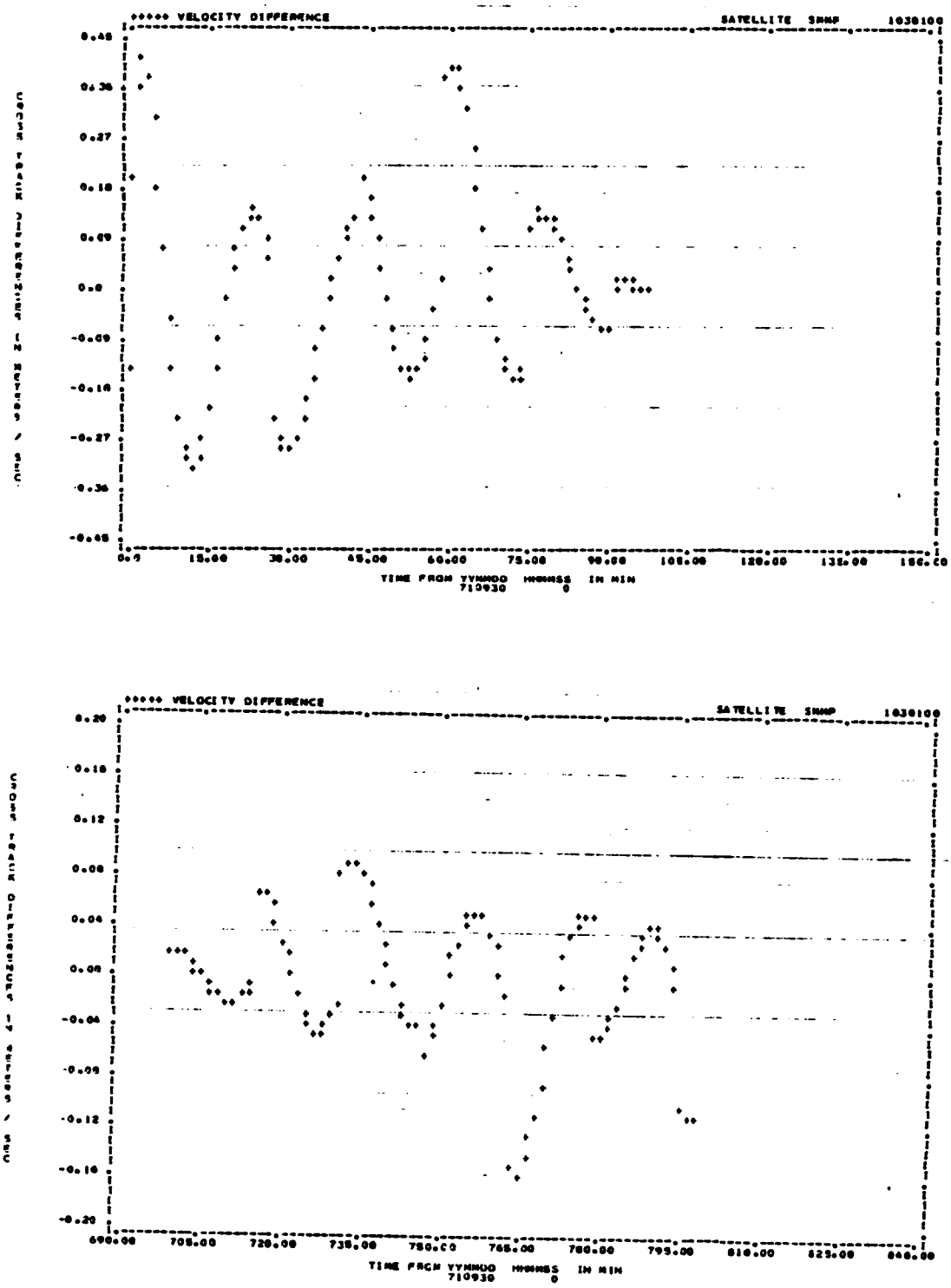

Figure 3-11. Errors in the Representation of the Cross-Track Component of Velocity Using a 29-Term Fourier Series with Position Residuals and a 16-Minute Grid Spacing (1 of 2)

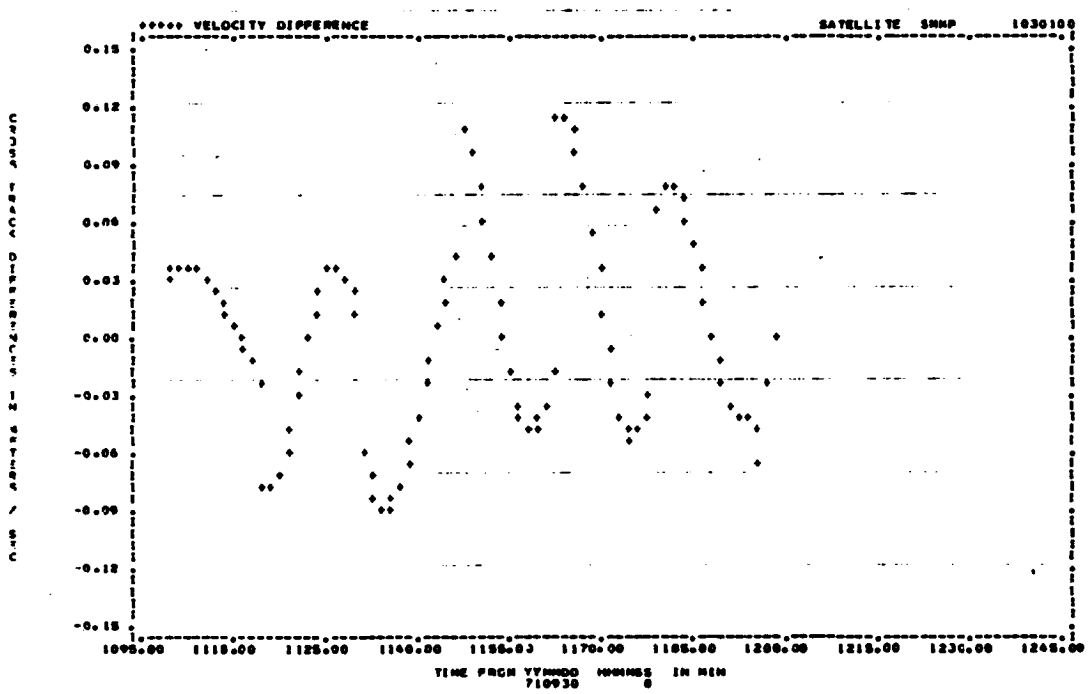

Figure 3-11. Errors in the Representation of the Cross-Track Component of Velocity Using a 29-Term Fourier Series with Position Residuals and a 16-Minute Grid Spacing (2 of 2)

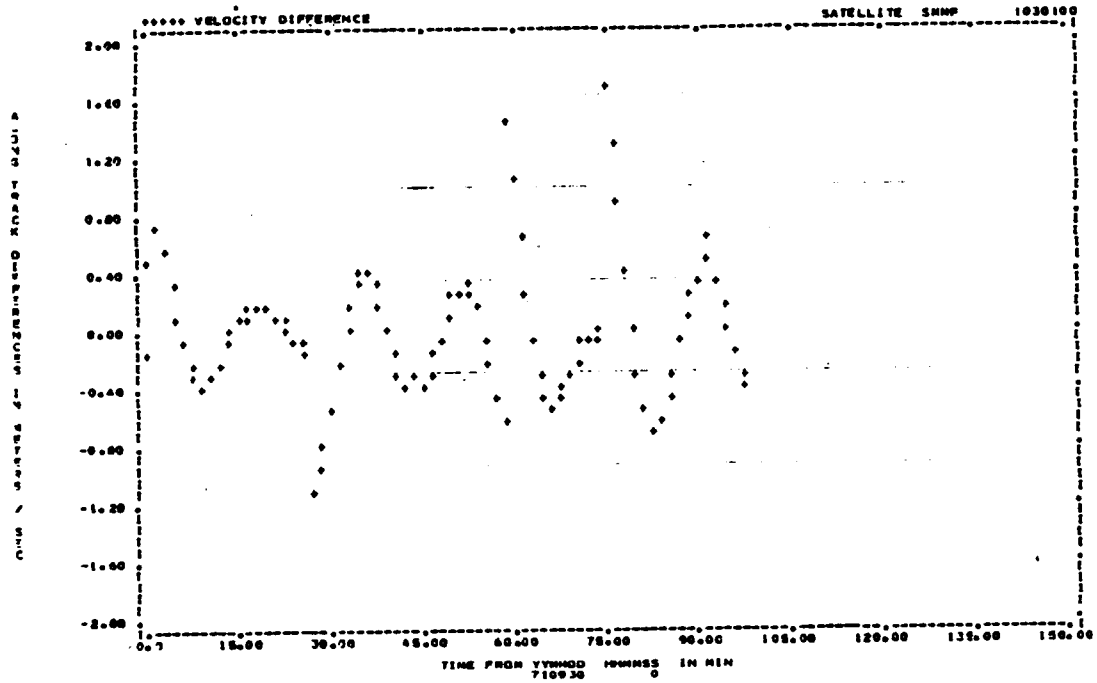

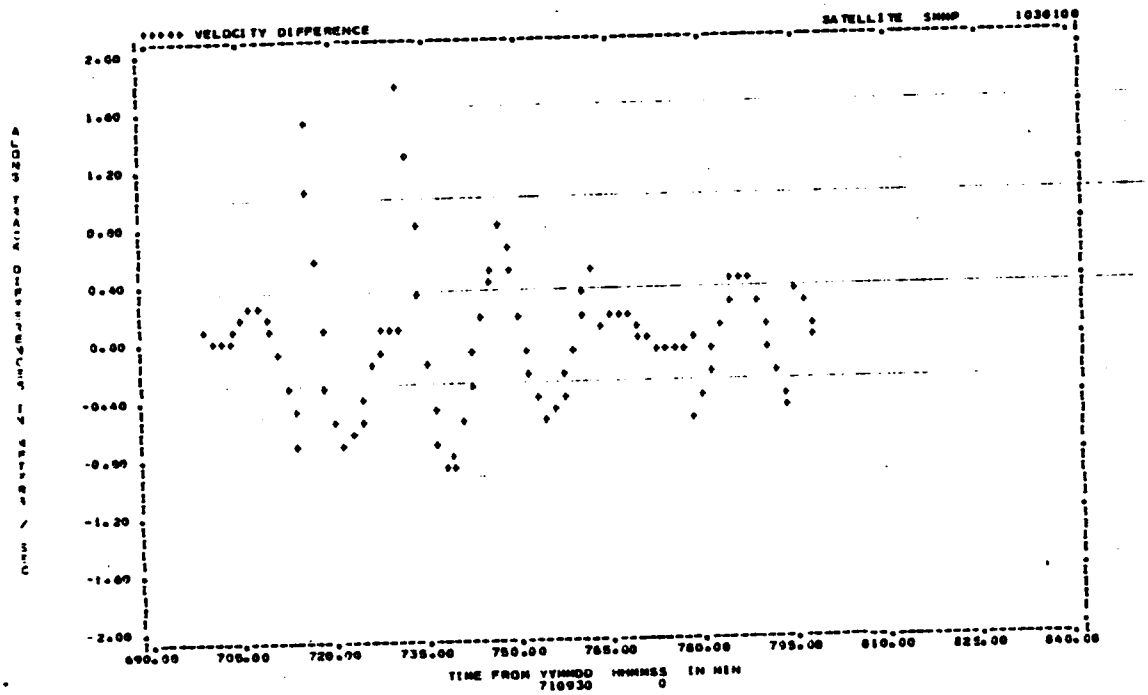

Figure 3-12. Errors in the Representation of the Along-Track Component of Velocity Using a 29-Term Fourier Series with Position Residuals and a 16-Minute Grid Spacing (1 of 2)

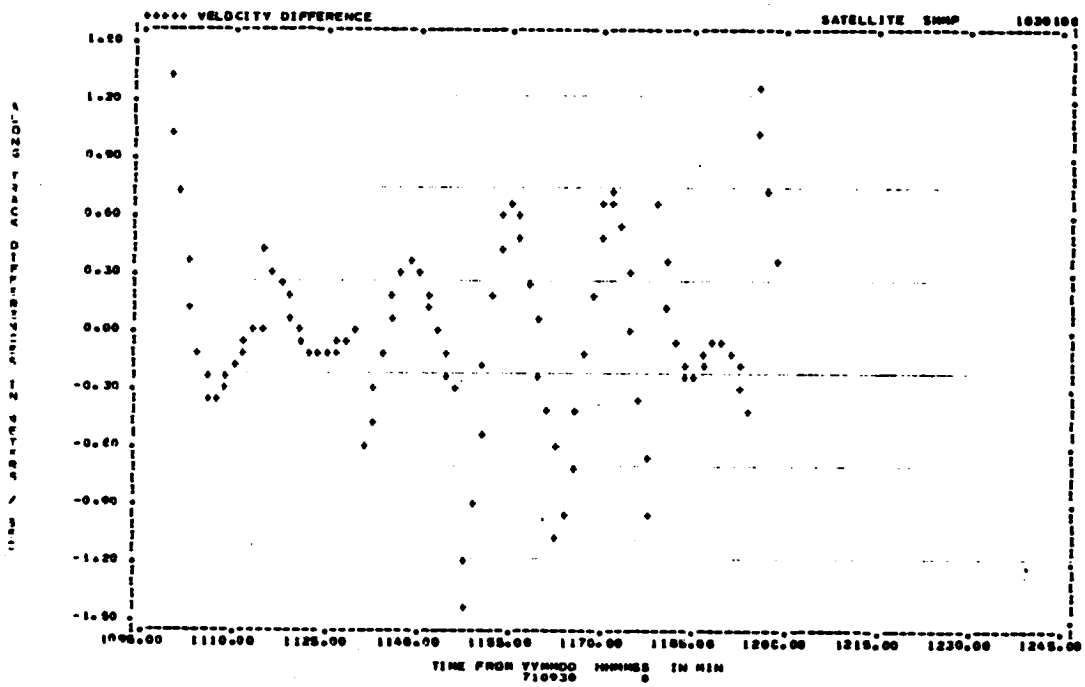

Figure 3-12. Errors in the Representation of the Along-Track Component of Velocity Using a 29-Term Fourier Series with Position Residuals and a 16-Minute Grid Spacing (2 of 2)

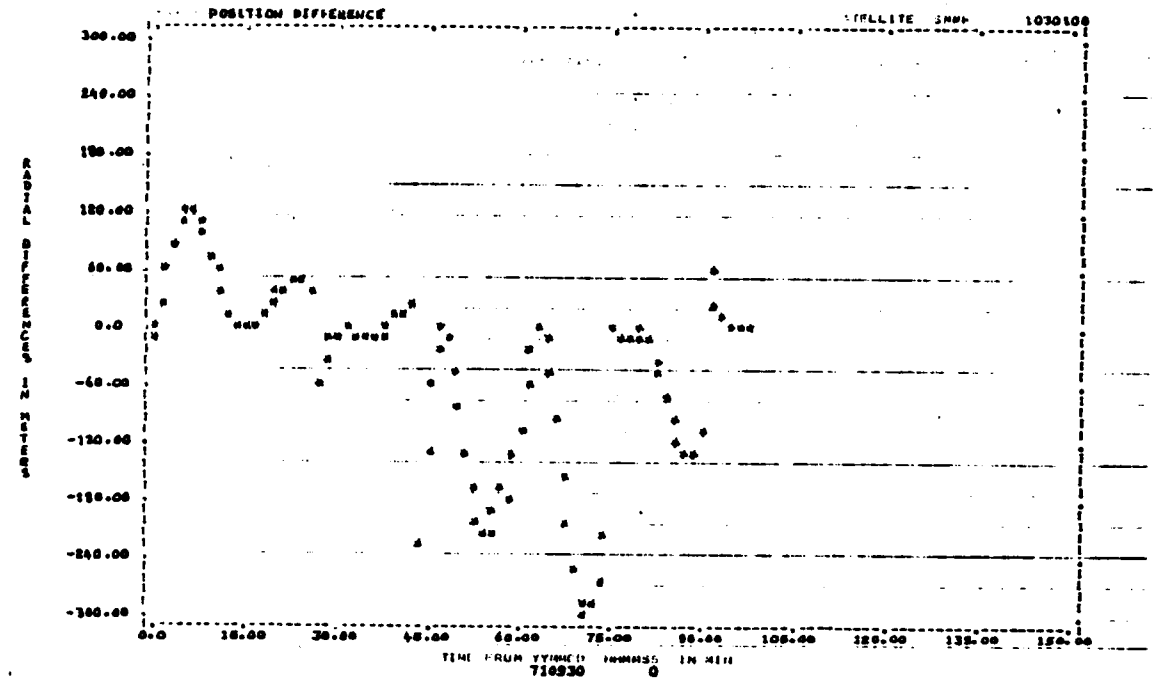

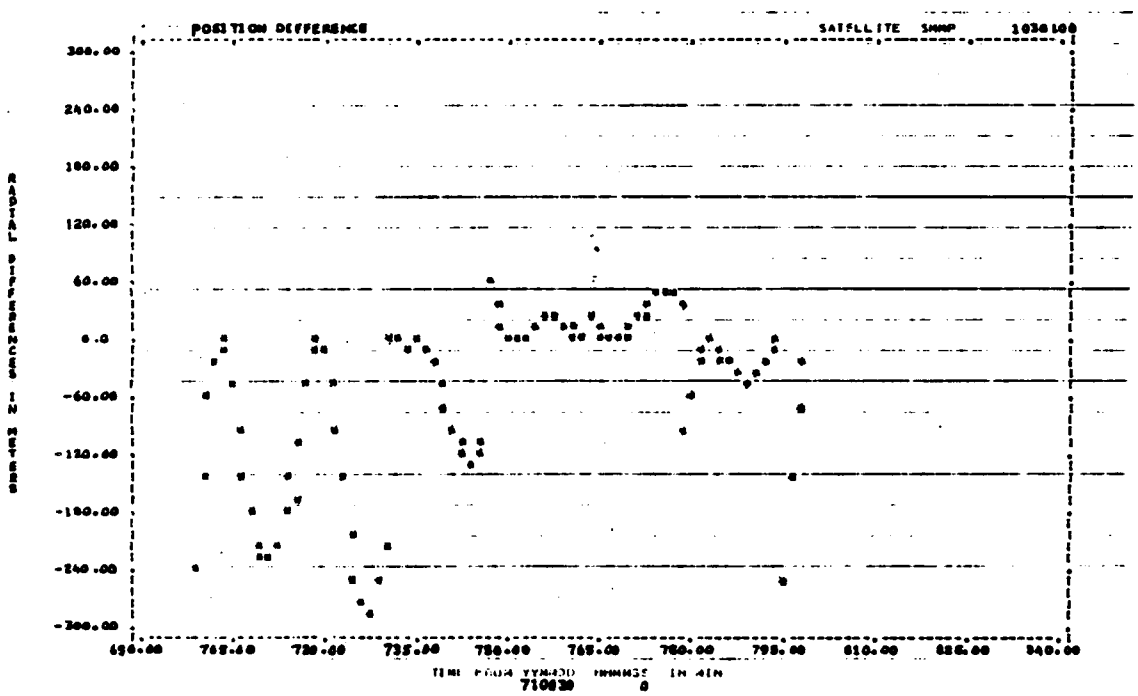

Figure 3-13. Errors in the Representation of the Radial Component of Position Using a 29-Term Fourier Series with Position and Velocity Residuals and a 16-Minute Grid Spacing (1 of 2)

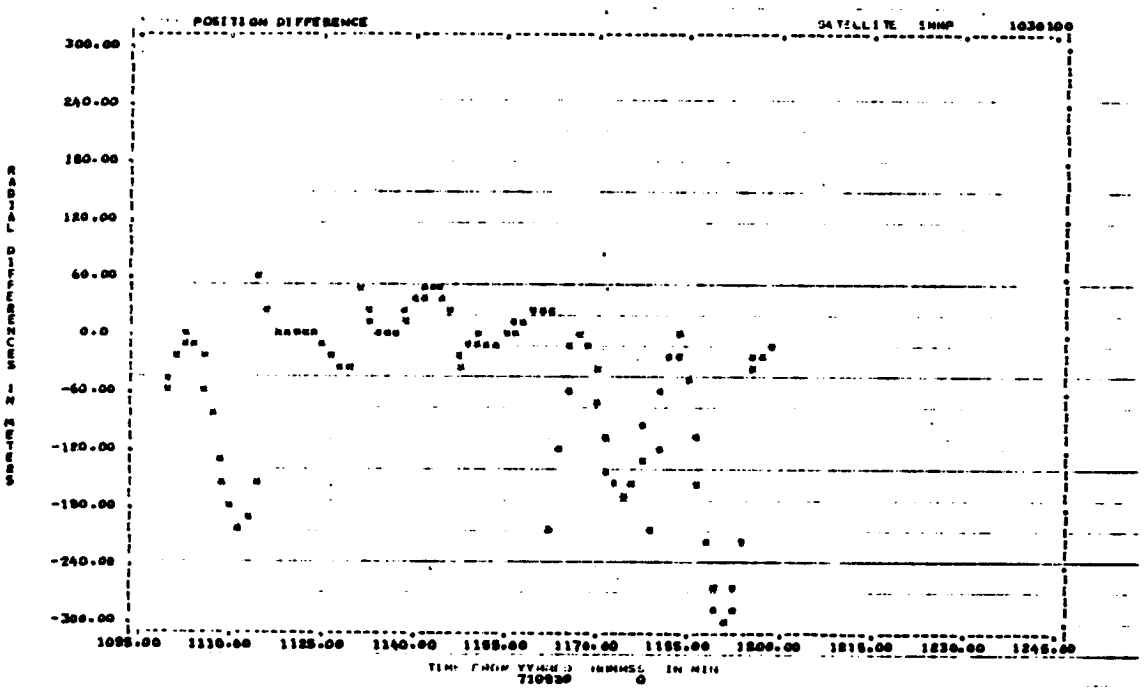

Figure 3-13. Errors in the Representation of the Radial Component of Position Using a 29-Term Fourier Series with Position and Velocity Residuals and a 16-Minute Grid Spacing (2 of 2)

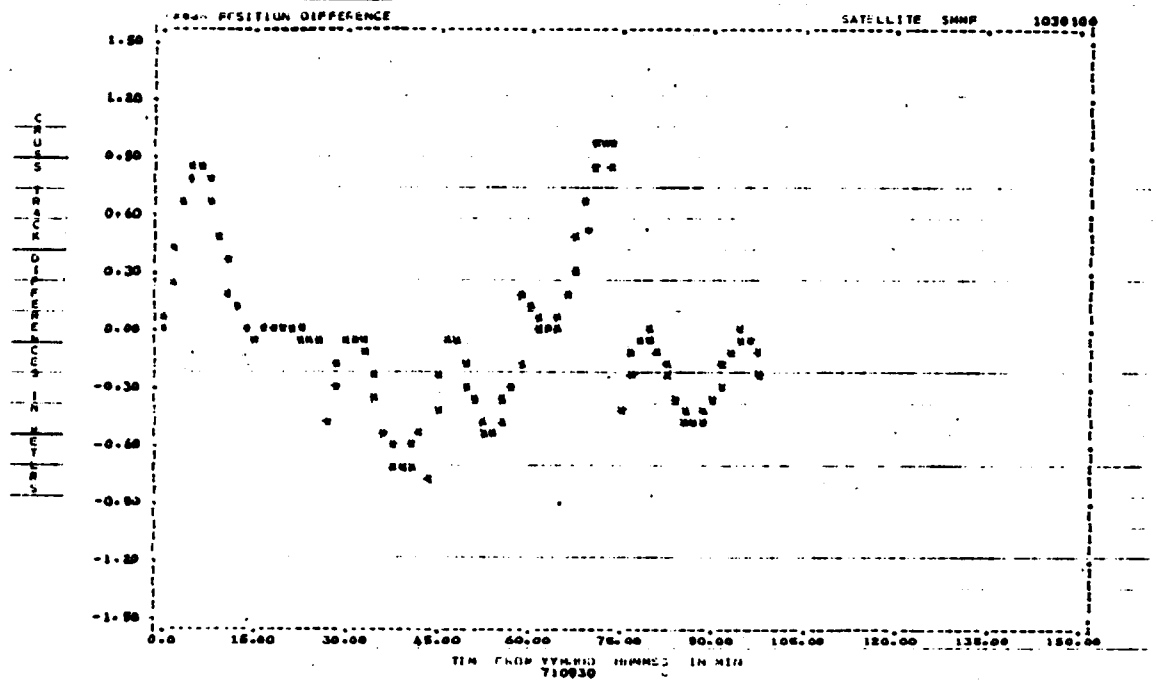

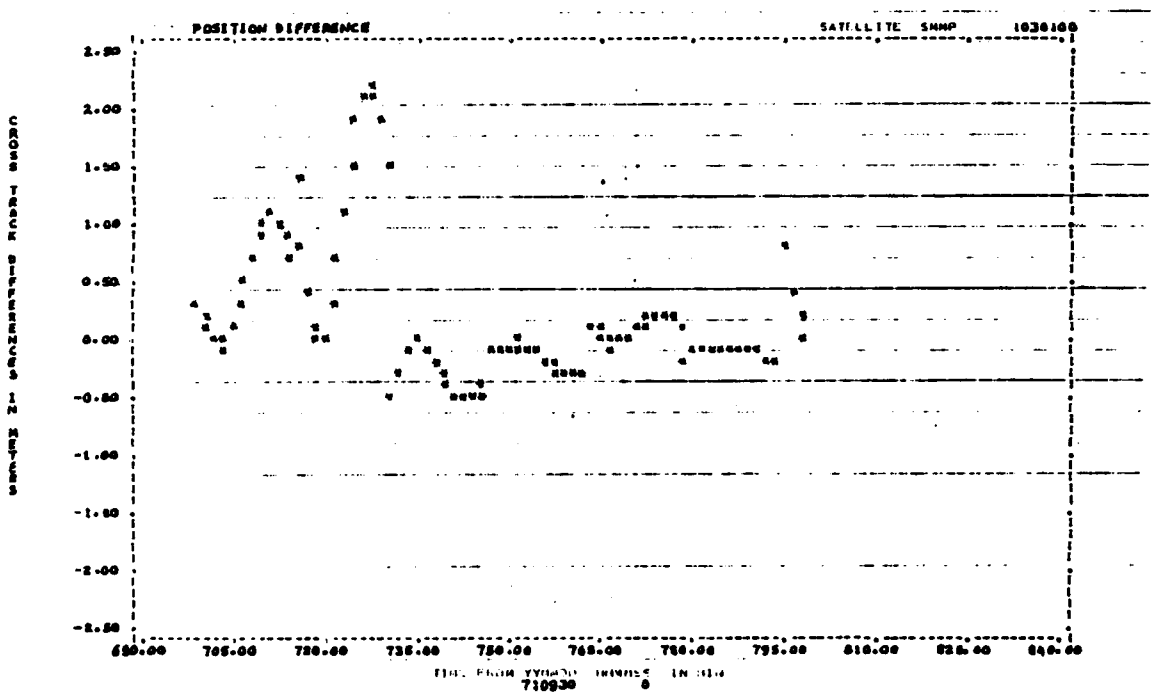

Figure 3-14. Errors in the Representation of the Cross-Track Component of Position Using a 29-Term Fourier Series with Position and Velocity Residuals and a 16-Minute Grid Spacing (1 of 2)

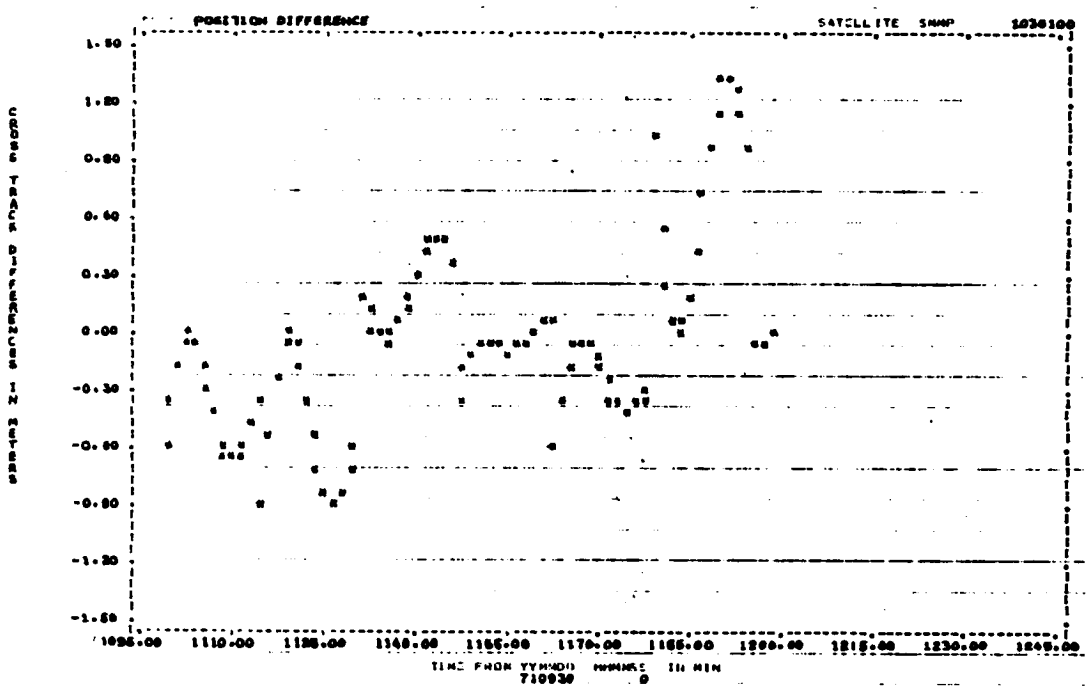

Figure 3-14. Errors in the Representation of the Cross-Track Component of Position Using a 29-Term Fourier Series with Position and Velocity Residuals and a 16-Minute Grid Spacing (2 of 2)

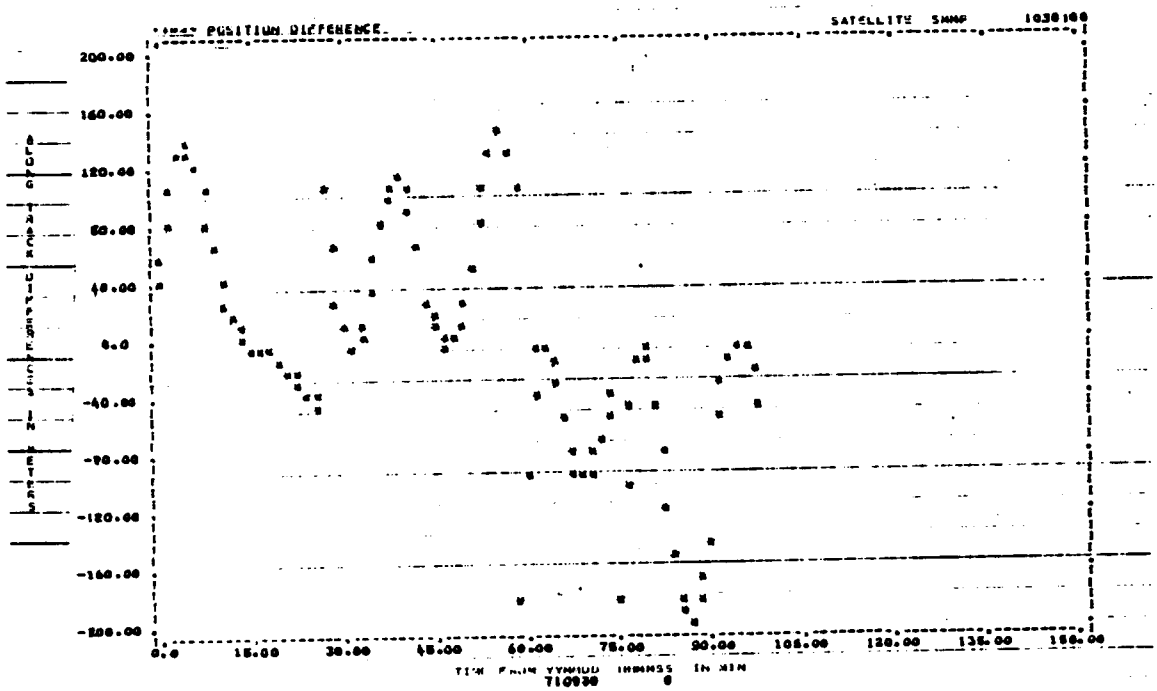

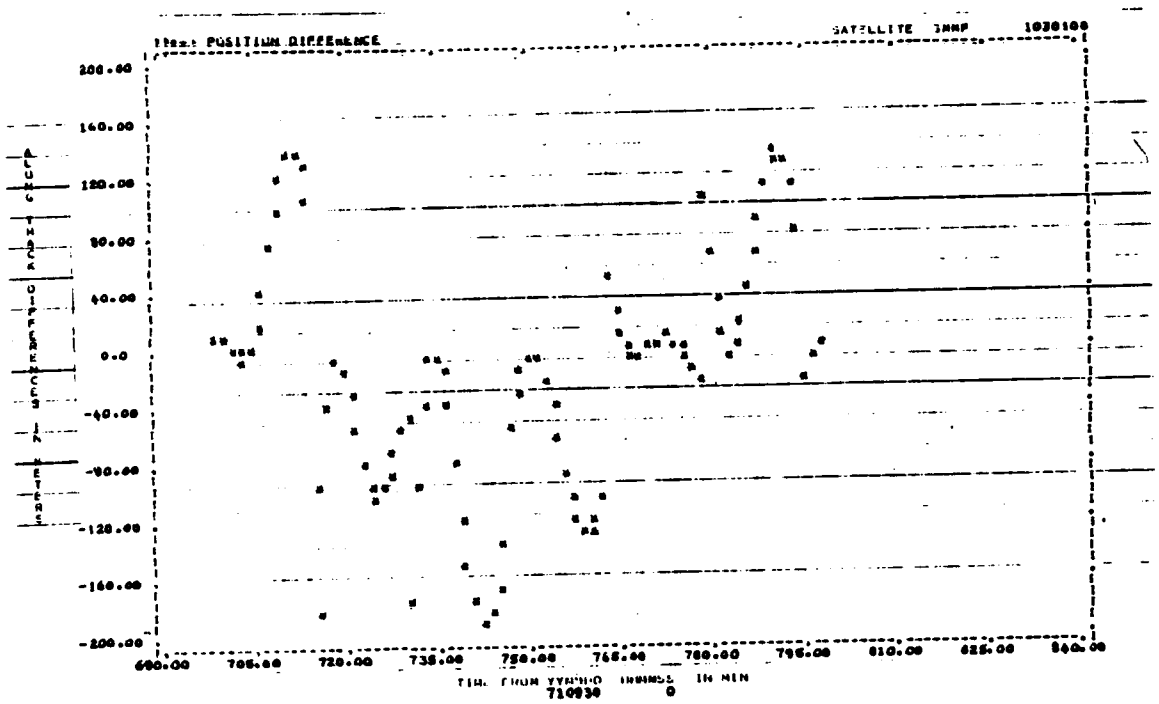

Figure 3-15. Errors in the Representation of the Along-Track Component of Position Using a 29-Term Fourier Series with Position and Velocity Residuals and a 16-Minute Grid Spacing (1 of 2)

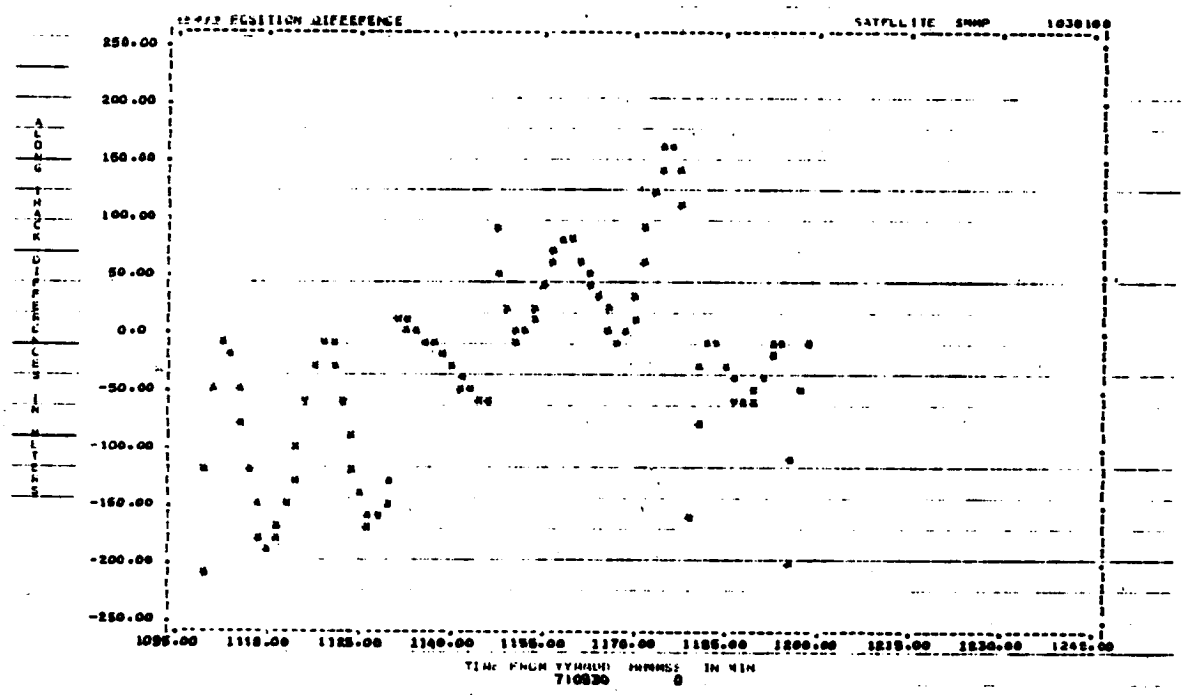

Figure 3-15. Errors in the Representation of the Along Track Component of Position Using a 29-Term Fourier Series with Position and Velocity Residuals and a 16-Minute Grid Spacing (2 of 2)

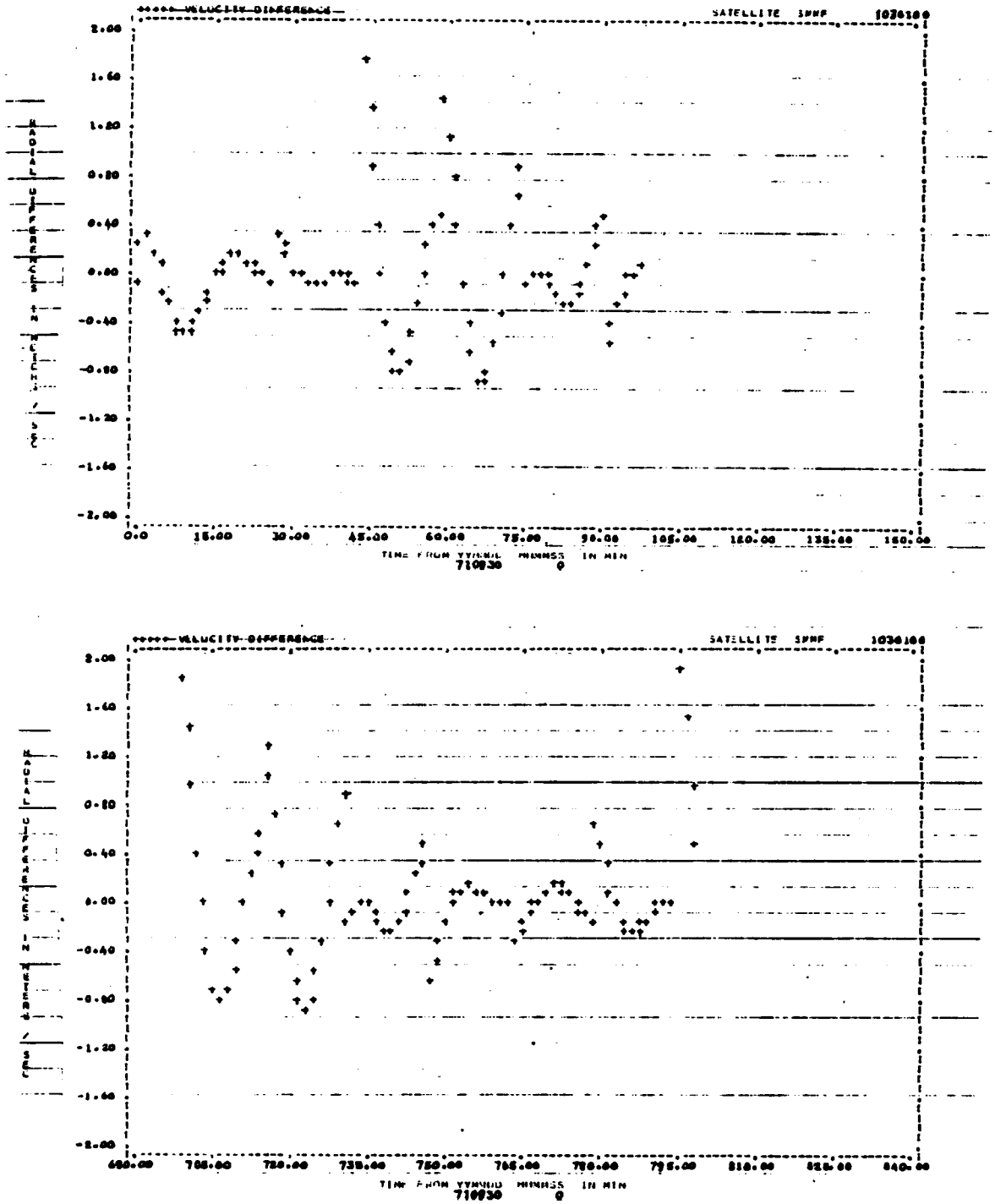

Figure 3-16. Errors in the Representation of the Radial Component of Velocity Using a 29-Term Fourier Series with Position and Velocity Residuals and a 16-Minute Grid Spacing (1 of 2)

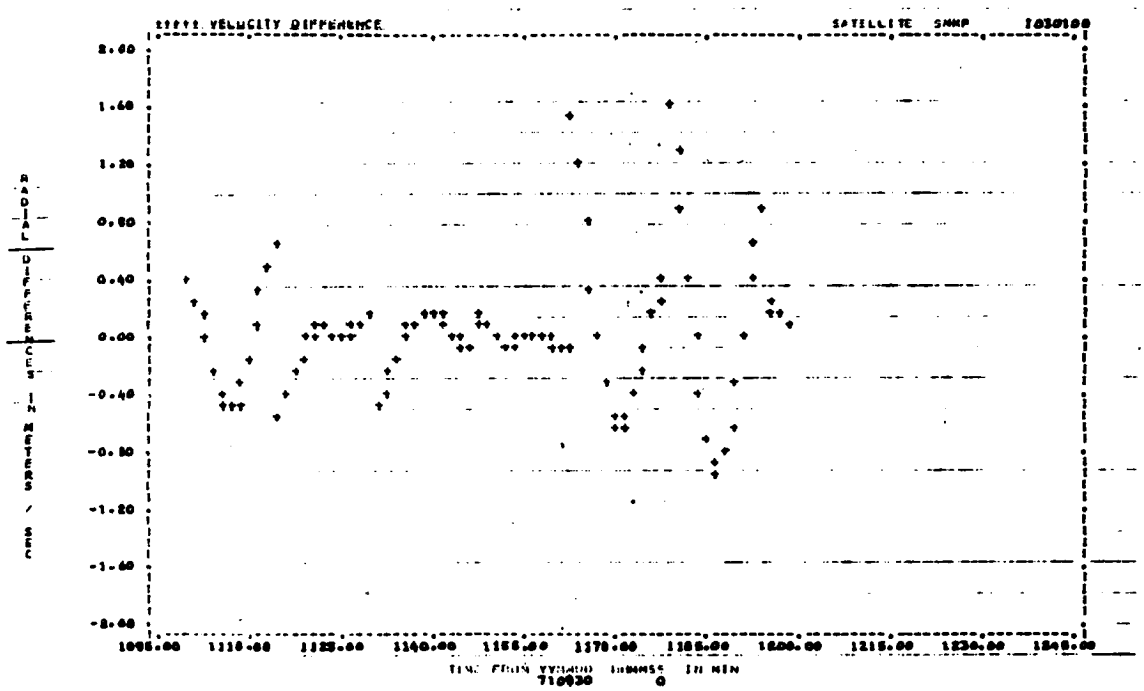

Figure 3-16. Errors in the Representation of the Radial Component of Velocity Using a 29-Term Fourier Series with Position and Velocity Residuals and a 16-Minute Grid Spacing (2 of 2)

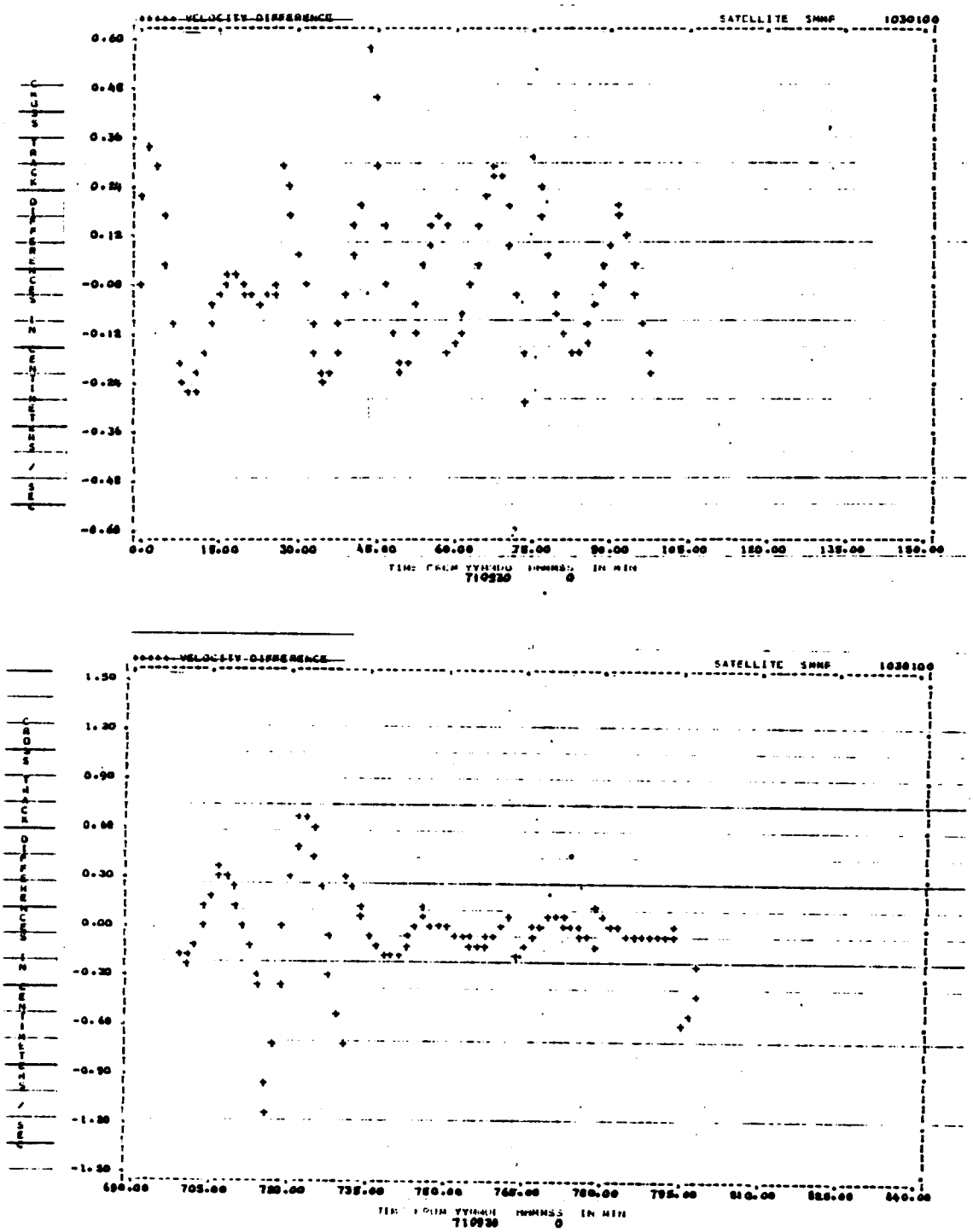

Figure 3-17. Errors in the Representation of the Cross-Track Component of Velocity Using a 29-Term Fourier Series with Position and Velocity Residuals and a 16-Minute Grid Spacing (1 of 2)

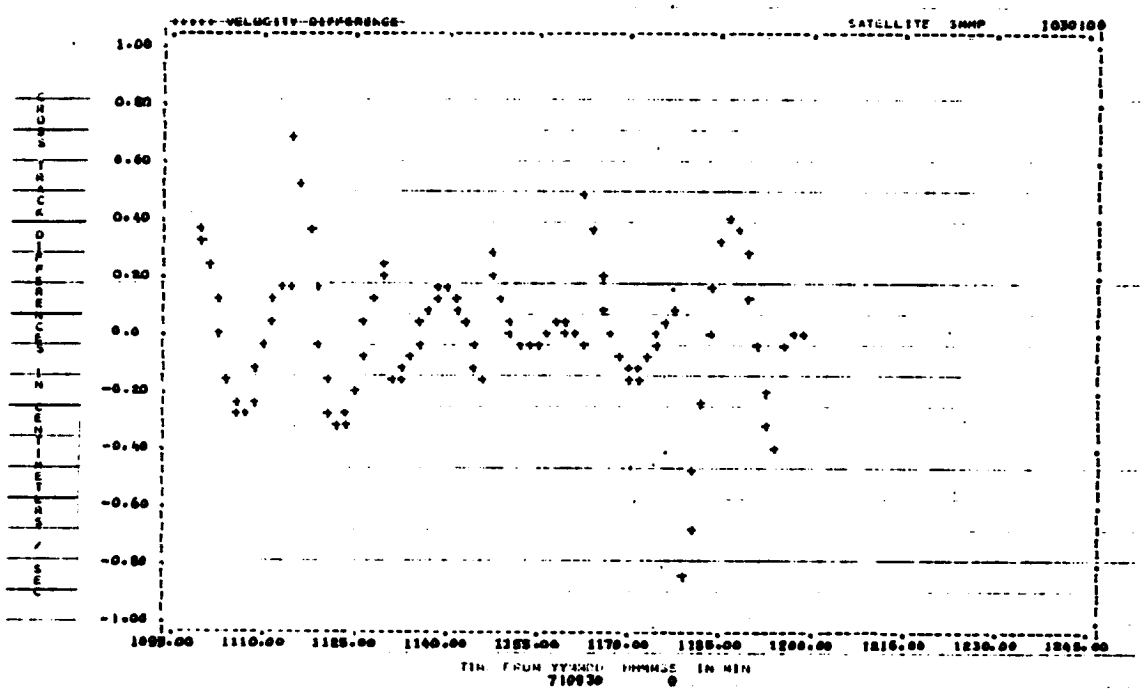

Figure 3-17. Errors in the Representation of the Cross-Track Component of Velocity Using a 29-Term Fourier Series With Position and Velocity Residuals and a 16-Minute Grid Spacing (2 of 2)

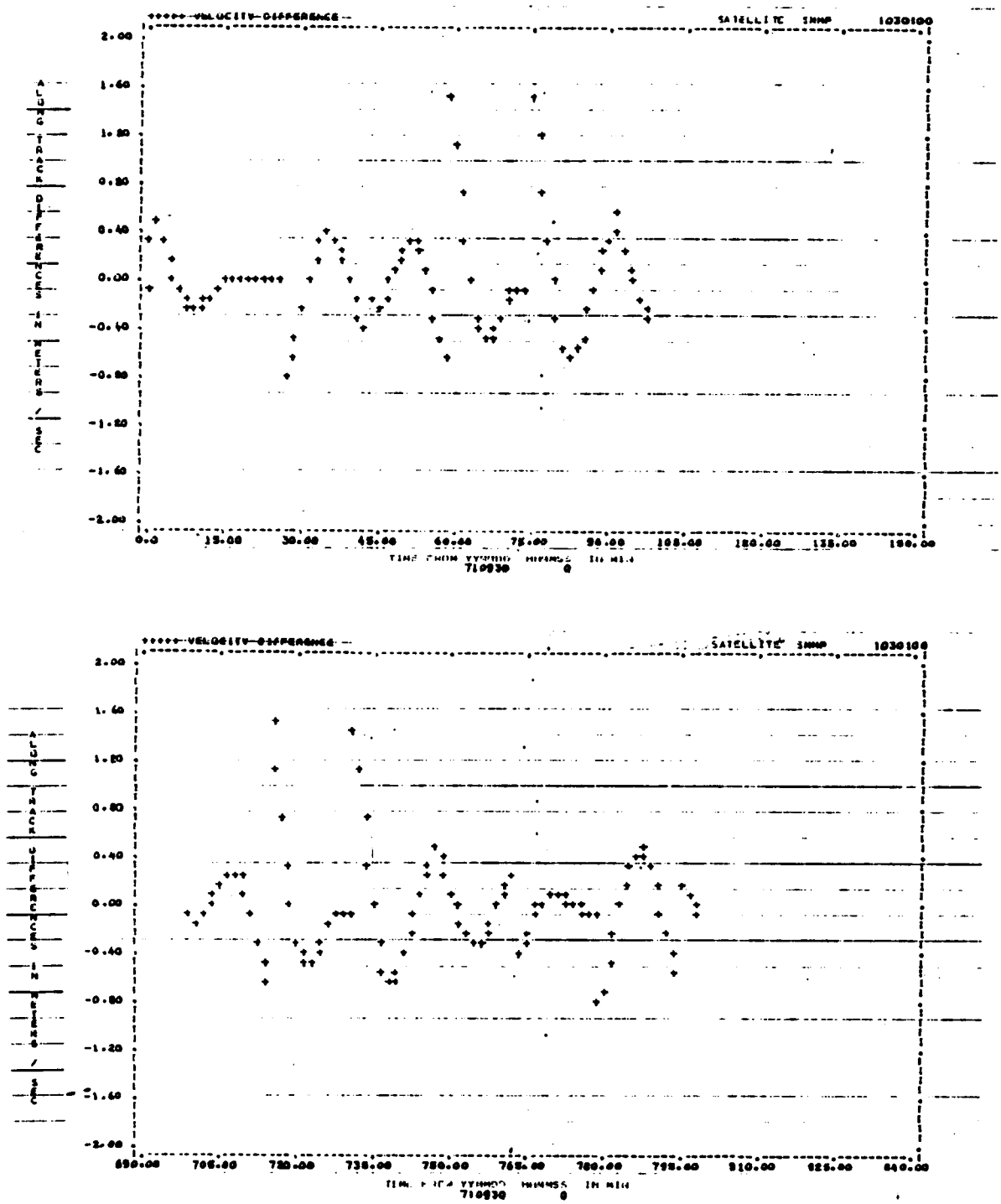

Figure 3-18. Errors in the Representation of the Along-Track Component of Velocity Using a 29-Term Fourier Series with Position and Velocity Residuals and a 16-Minute Grid Spacing (1 of 2)

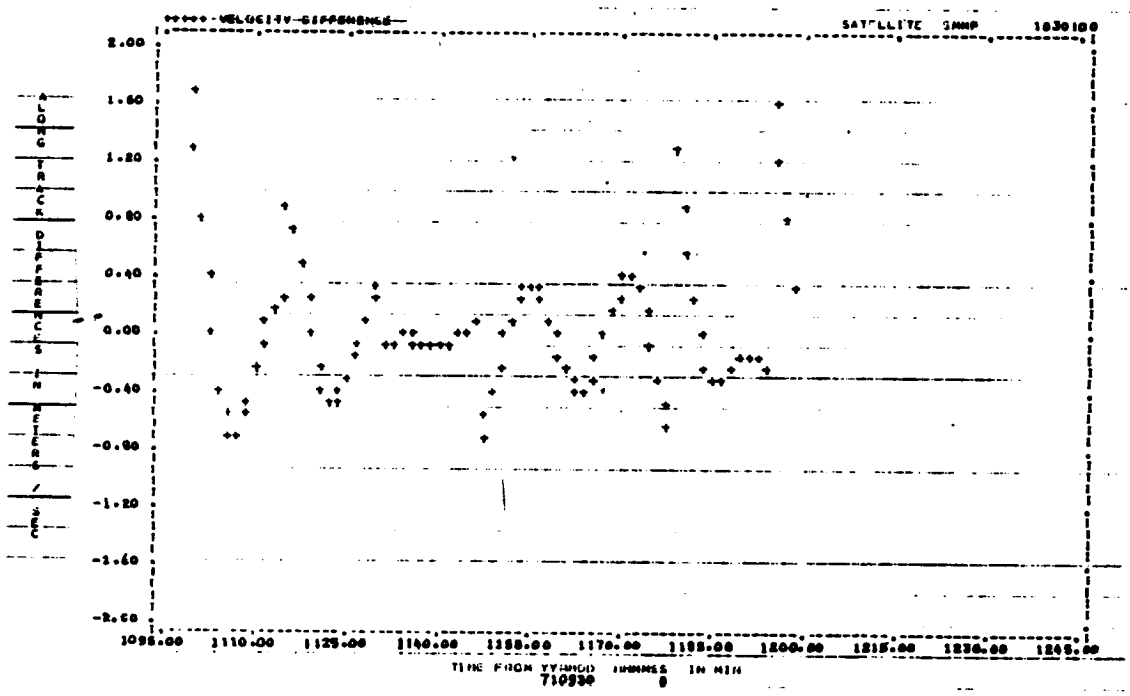

Figure 3-18. Errors in the Representation of the Along-Track Component of Velocity Using a 29-Term Fourier Series with Position and Velocity Residuals and a 16-Minute Grid Spacing (2 of 2)

not absorbed by the Fourier series. For example, examination of the long-track position error growth indicates that there is an effect with a period of 1 day and amplitude of 0.5 km which is not modeled in the Fourier series. This effect probably arises from the C_{21} and S_{21} terms in the geopotential model.

3.2 COMPARISON OF 29- AND 36- TERM FOURIER SERIES

The state vector and reference trajectory are the same as those used in Section 3.1; however, the Fourier series is constructed of 36 coefficients. The results are discussed below. The interpolation scheme follows a (0.25, + 0.75) span on either side of the second grid point. The grid points are 16-minutes apart.

3.2.1 No Residuals

For the case of no grid-point residuals, the comparison statistics are presented in the fourth entry of Table 3-2. The rms position errors are 0.14 kilometers for the radial, 0.123 kilometers for the cross-track, and 0.47 kilometers for the along-track components. The velocity rms errors are 0.664×10^{-3}, $.129 \times 10^{-3}$, and $.430 \times 10^{-3}$ for the radial, cross-track, and along-track components respectively. The minimum and maximum position differences for the radial, cross-track, and along-track components are 0.243×10^{-4} and 0.524 kilometers, 0.341×10^{-4} and 0.332 kilometers, and 0.865×10^{-4} and 1.307 kilometers respectively.

3.2.2 Position Residuals

The results using only position residuals are given in the fifth entry of Table 3-2. The rms position errors are 0.116 kilometers for the radial component, 0.02 kilometers for the cross-track component, and 0.100 kilometers for the along-track component. The rms velocity errors are 0.574×10^{-3} kilometers/second, 0.103×10^{-3} kilometers/second and 0.453×10^{-3} kilometers/second, for the radial, cross-track, and along-track components respectively. The minimum and maximum position differences for the radial, cross-track, and

along-track components are 0.195×10^{-5} and 0.525 kilometers, 0.271×10^{-8} and 0.103 kilometers, and 0.801×10^{-8} and 0.400 kilometers, respectively.

3.2.3 All Residuals

The statistics, when both position and velocity residuals are used, are given in the sixth entry of Table 3-2. The rms position errors are 0.100 kilometers for the radial component, 0.0005 kilometers for the cross-track component, 0.83 kilometers for the along-track components. The velocity rms errors are 0.454×10^{-3} kilometers/second, 0.264×10^{-5} kilometers, and 0.413×10^{-3} kilometers/second, for the radial, cross-track, and along-track components respectively. The minimum and maximum position differences for the radial, cross-track, and along-track components are 0.195×10^{-5} and 0.298 kilometers, 0.271×10^{-8} and 0.313×10^{-2} kilometers, and 0.802×10^{-8} and 0.208 kilometers, respectively.

For comparison with results obtained using a 29-term Fourier series, the along-track position and radial velocity differences between the high-precision and OBC interpolated trajectories using a 36-term Fourier series are given in Figures 3-19 through 3-24 for representative time spans.

Comparison of the results obtained using a 29-term Fourier series with results using a 36-term Fourier series indicates that the 29-term series is as accurate over the 3-day span.

3.3 COMPARISON OF 10- AND 16- MINUTE INTERPOLATION GRID SPACINGS

A 36-term Fourier series and (-0.25, + 0.75) interpolation interval was used in this comparison. The nominal state vector is Case 1 in Table 3-1. Comparisons of trajectories were made every minute over a 71-hour duration, with a high precision trajectory.

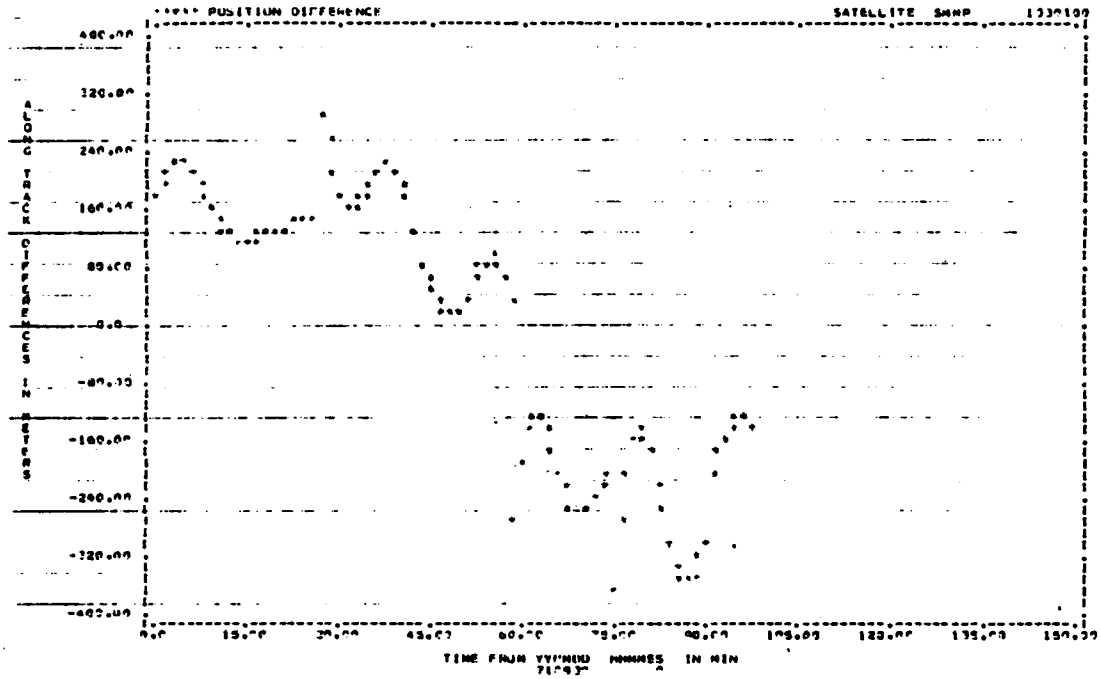

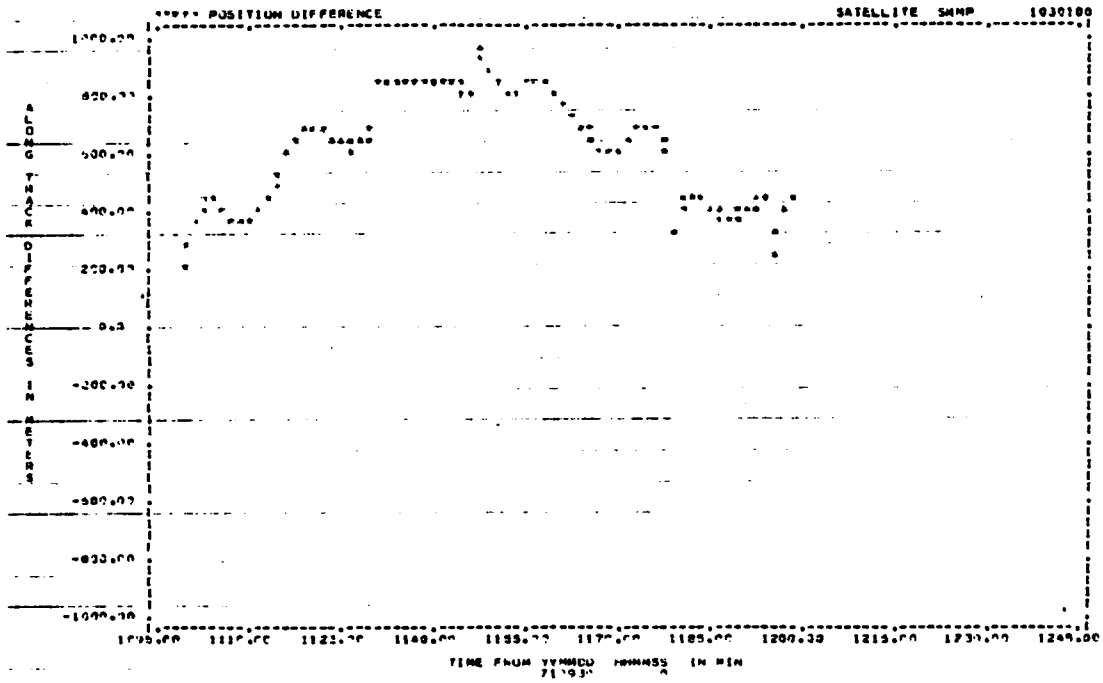

Figure 3-19. Errors in the Representation of the Along-Track Component of Position Using a 36-Term Fourier Series with a 16-Minute Grid Spacing

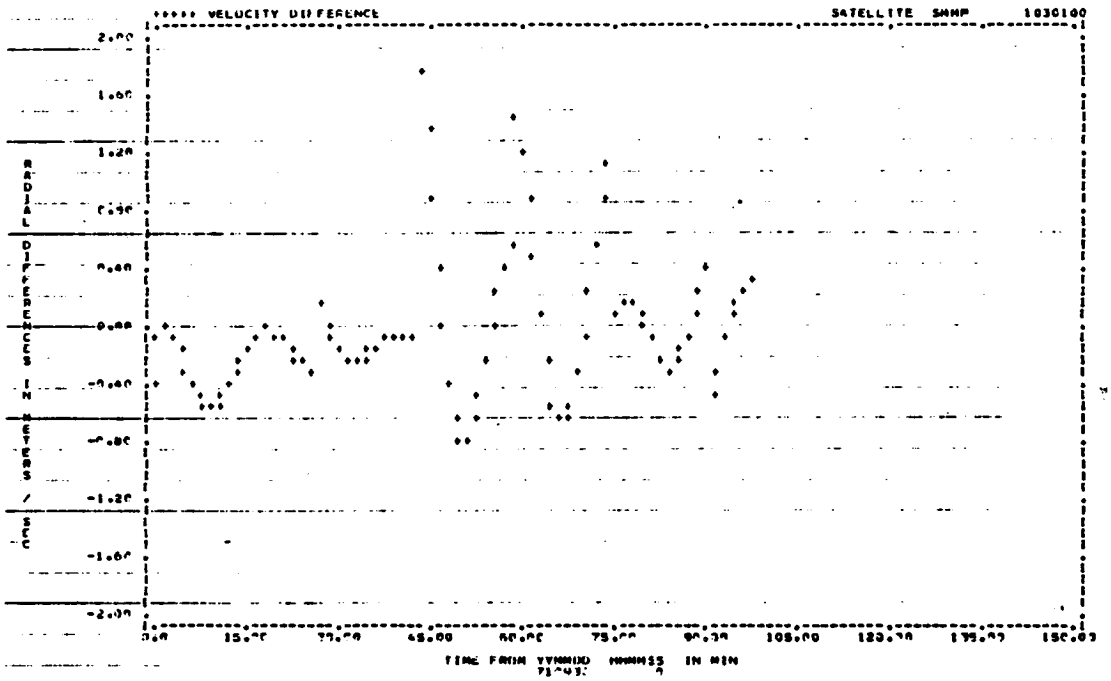

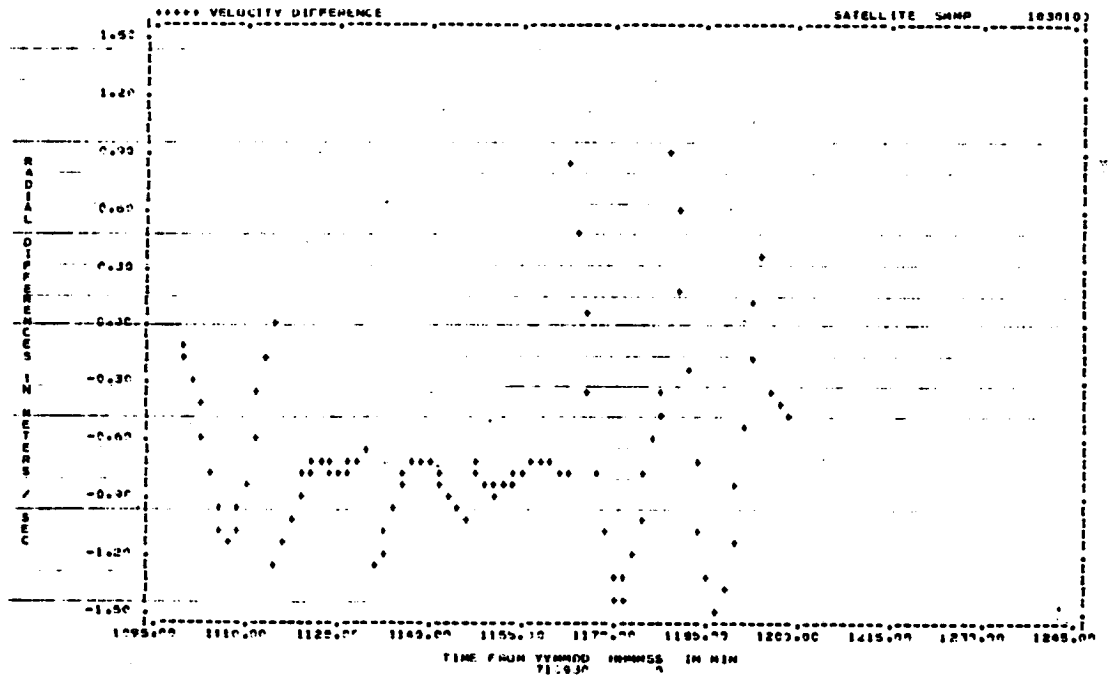

Figure 3-20. Errors in the Representation of the Radial Component of Velocity Using a 36-Term Fourier Series with a 16-Minute Grid Spacing

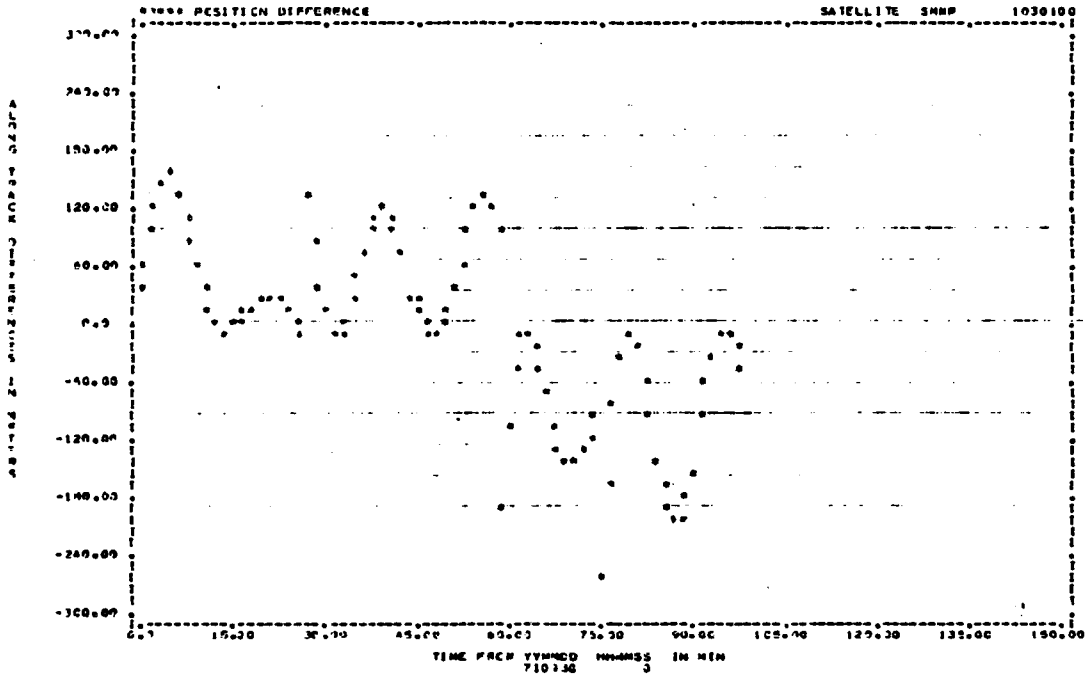

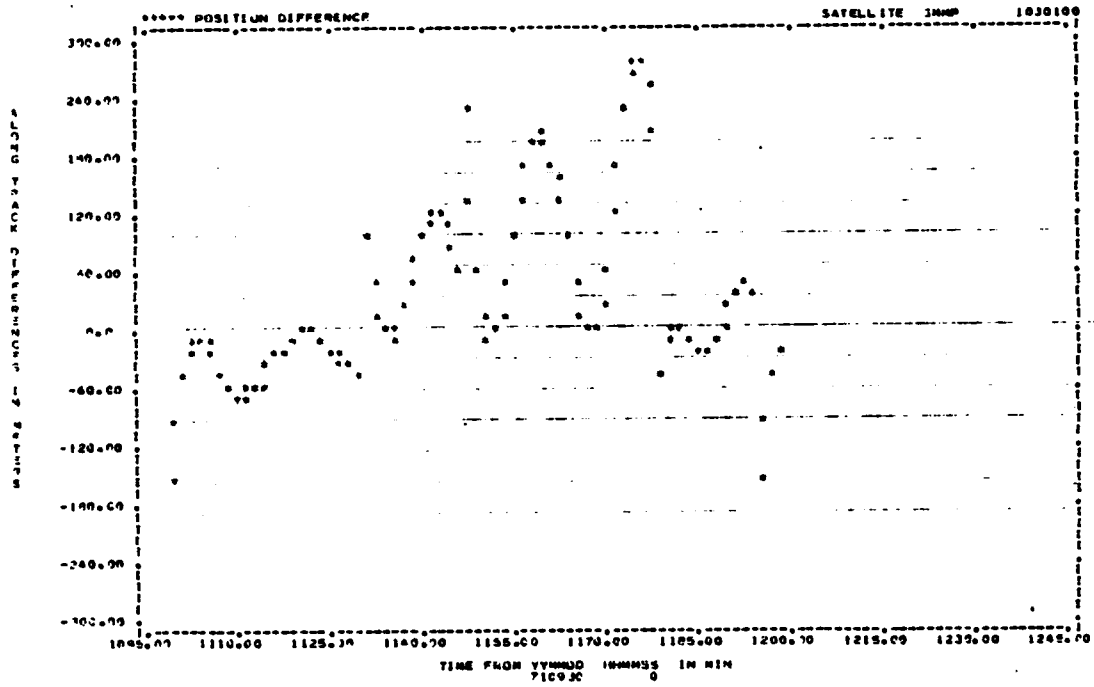

Figure 3-21. Errors in the Representation of the Along-Track Component of Position Using a 36-Term Fourier Series with Position Residuals and a 16-Minute Grid Spacing

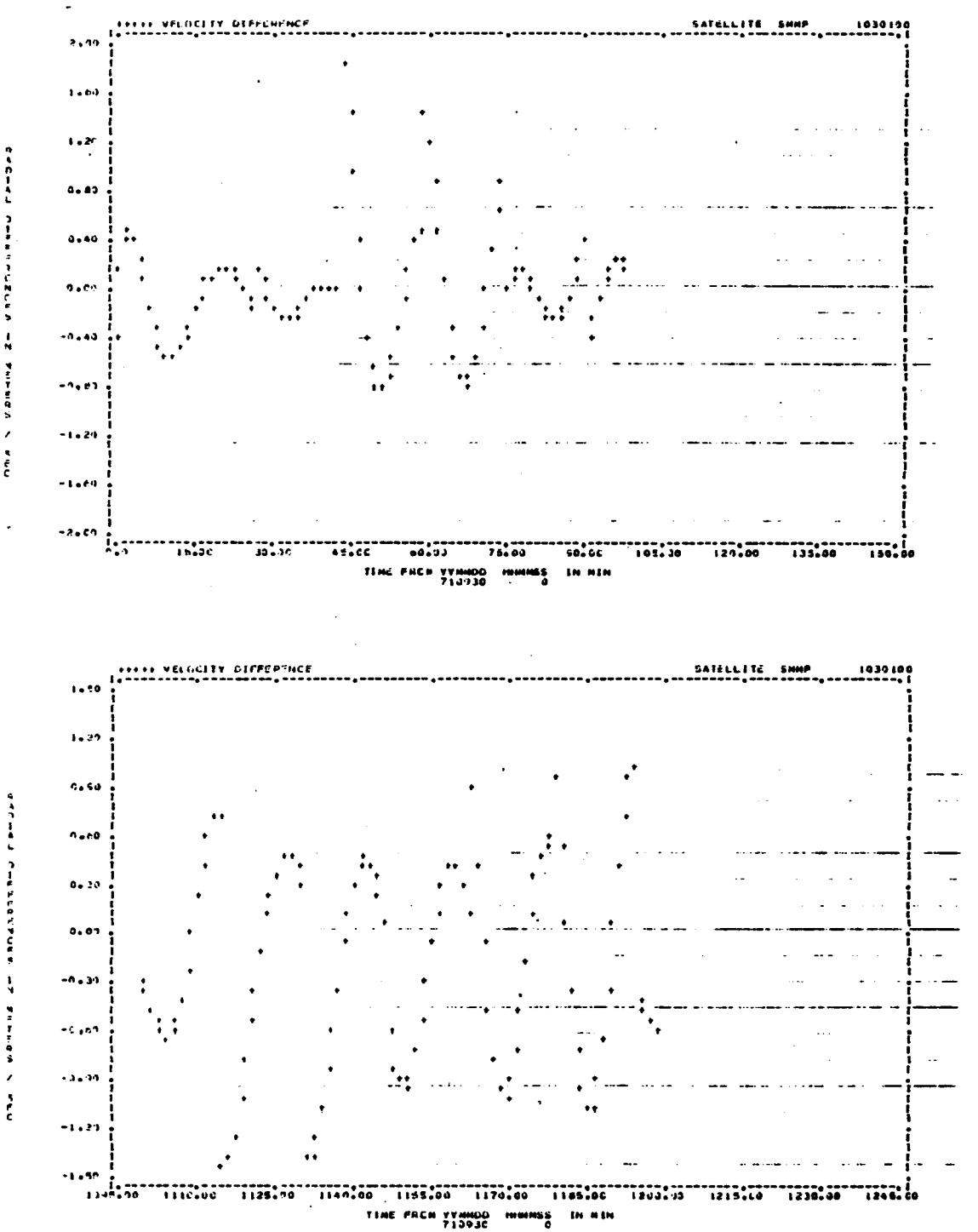

Figure 3-22. Errors in the Representation of the Radial Component of Velocity Using a 36-Term Fourier Series with Position Residuals and a 16-Minute Grid Spacing

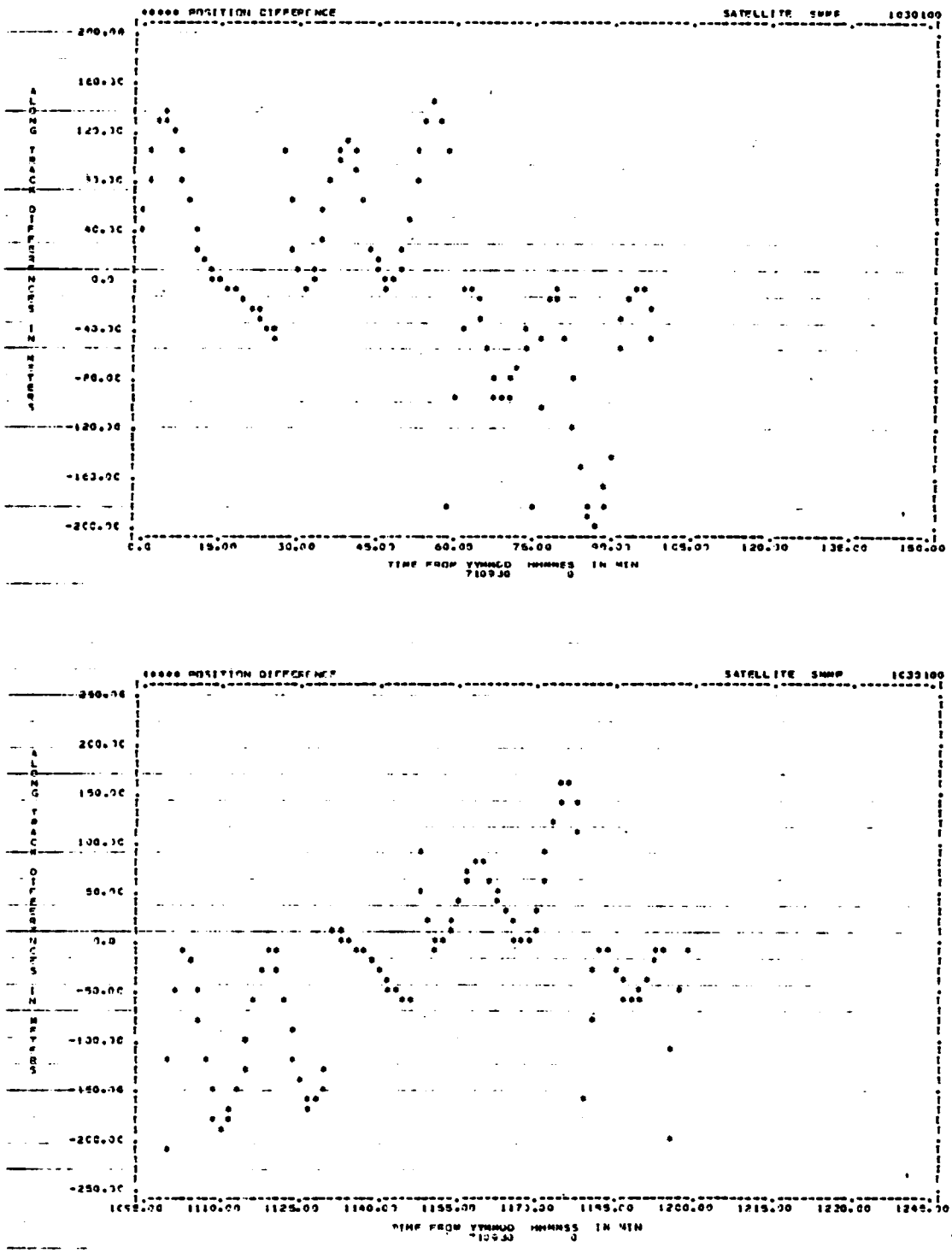

Figure 3-23. Errors in the Representation of the Along-Track Component of Position Using a 36-Term Fourier Series with Position and Velocity Residuals and a 16-Minute Grid Spacing

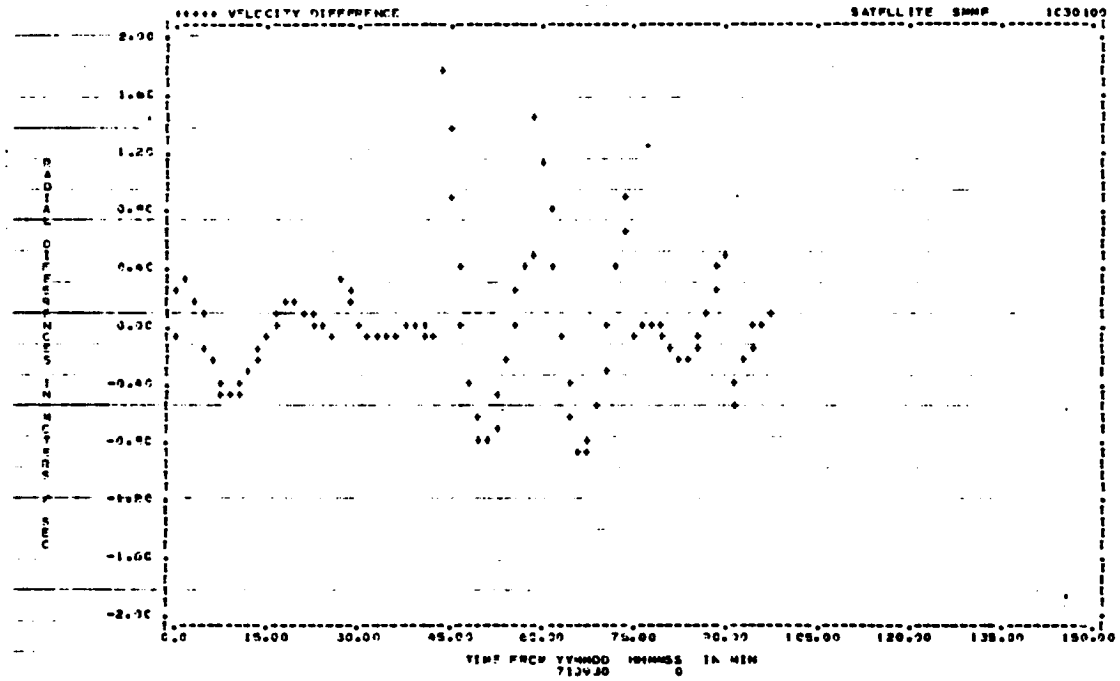

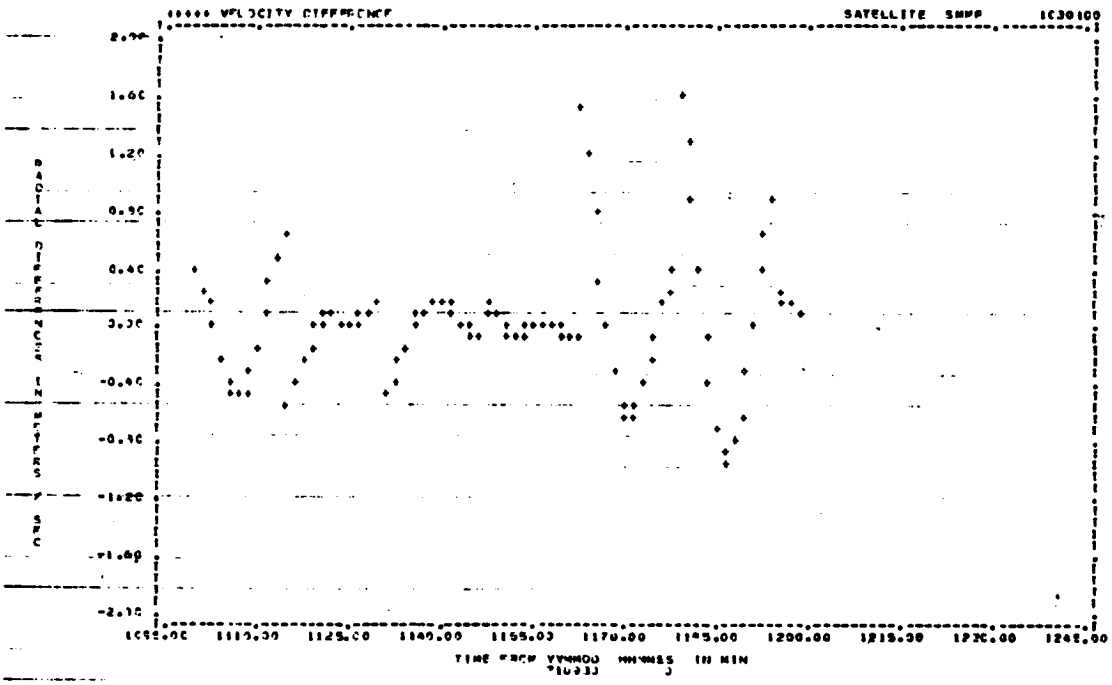

Figure 3-24. Errors in the Representation of the Radial Component of Velocity Using a 36-Term Fourier Series with Position and Velocity Residuals and a 16-Minute Grid Spacing

The statistics from this comparison are given in Table 3-2. Without residuals the root-mean-square (rms) position errors are 0.096 kilometers for the radial (H) component, 0.123 kilometers for the cross-track (C) component, and 0.464 kilometers for the along-track (L) component. The rms velocity errors are 0.487×10^{-3} kilometers/second, 0.129×10^{-3} kilometers/second and 0.117×10^{-3} kilometers/second, respectively, for the radial, cross-track, and along-track components. The minimum and maximum position differences for the radial, cross-track, and along-track components are 0.163×10^{-4} and 0.273 kilometers, 0.133×10^{-4} and 0.336 kilometers, and 0.663×10^{-5} and 1.265 kilometers, respectively.

The statistics of analysis with position residuals, and position and velocity residuals are also presented in Table 3-2. Comparison with results obtained using a 16-minute grid spacing indicates that the 16-minute spacing yields nearly the same accuracy as the 10 minute spacing if grid point residuals are not used. The improvement seen in the cases using residuals is an indication of a somewhat smaller interpolation error in the case of a 10-minute grid spacing. For comparison with previous results, the along-track position and radial velocity errors obtained using a 10-minute grid spacing are plotted in Figures 3-25 through 3-30 for representative spans.

3.4 EFFECT OF CHANGING INTERPOLATION INTERVAL

A 29-term Fourier series and a 71-hour comparison span were used in this study. The state vectors are the same as in the earlier analysis. However, the interpolation scheme follows a ± 0.5 span on either side of the second grid point. The results are discussed below, and are presented in Table 3-2.

Without residuals the rms position errors are found to be 0.187 kilometers, 0.127 kilometers, 0.491 kilometers for the radial, cross-track, and along-track components, respectively. The rms velocity errors are 0.825×10^{-2} kilometers/second for the radial component, 0.135×10^{-3} kilometers/

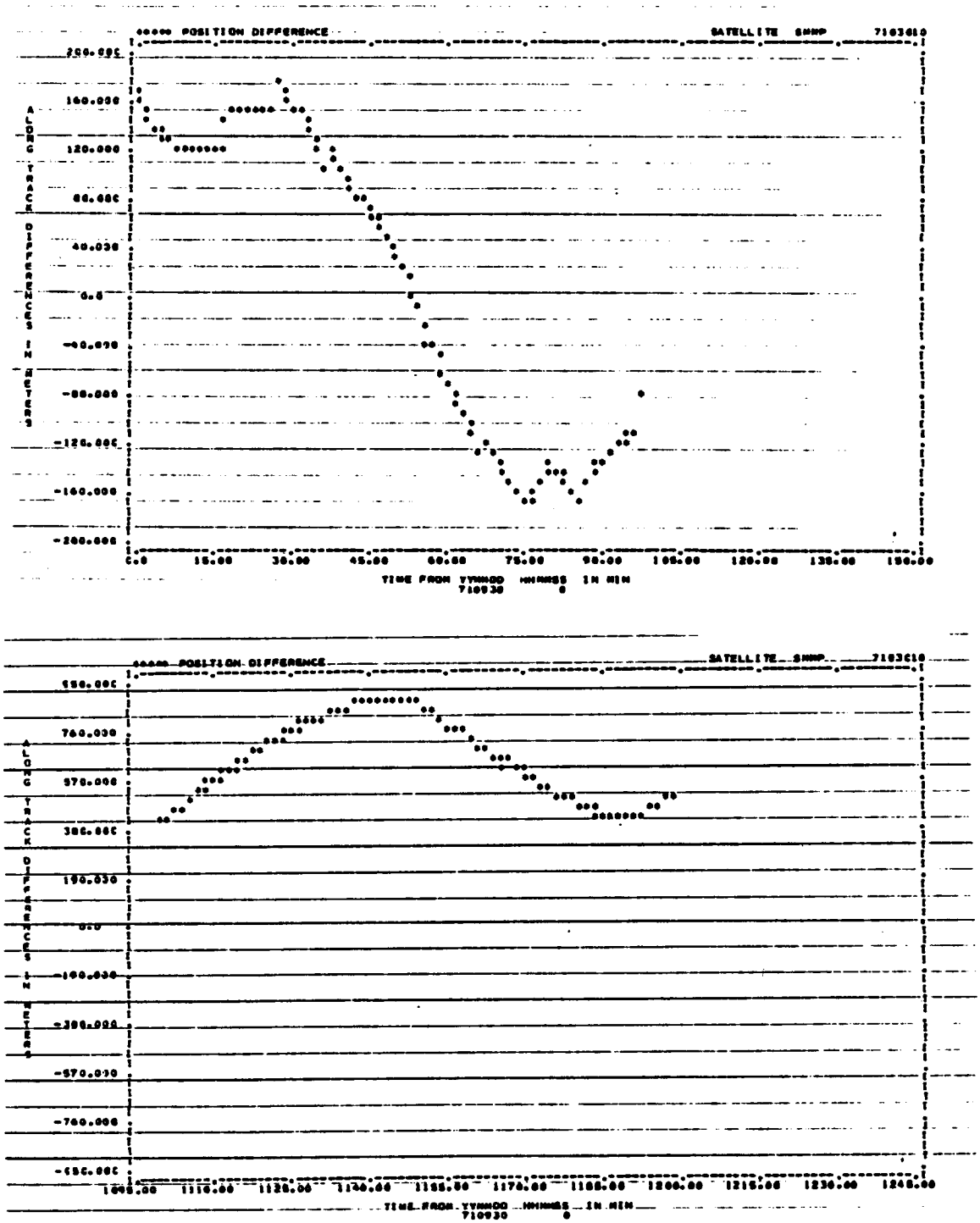

Figure 3-25. Errors in the Representation of the Along-Track Component of Position Using a 36-Term Fourier Series with a 10-Minute Grid Spacing

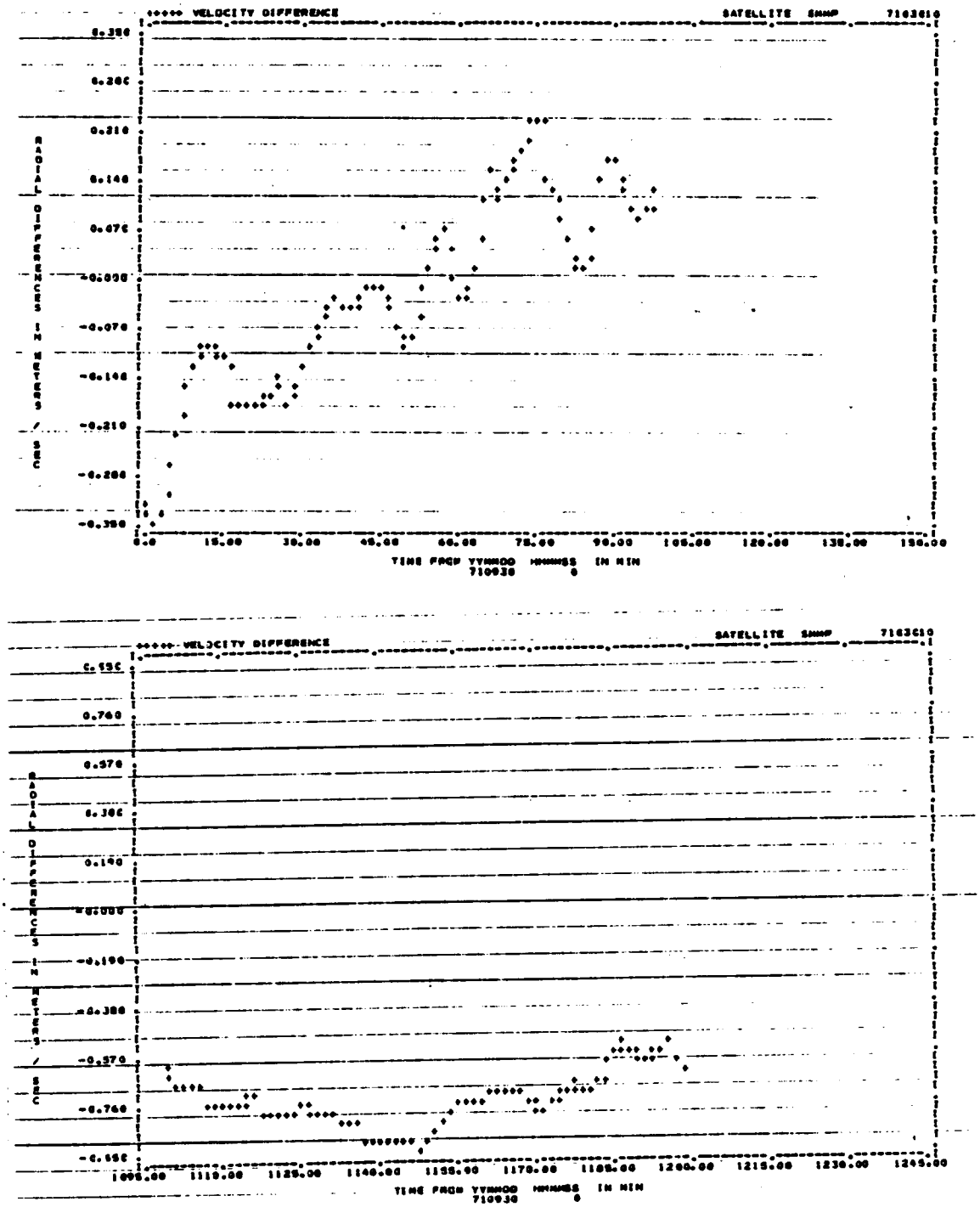

Figure 3-26. Errors in the Representation of the Radial Component of Velocity Using a 36-Term Fourier Series with a 10-Minute Grid Spacing

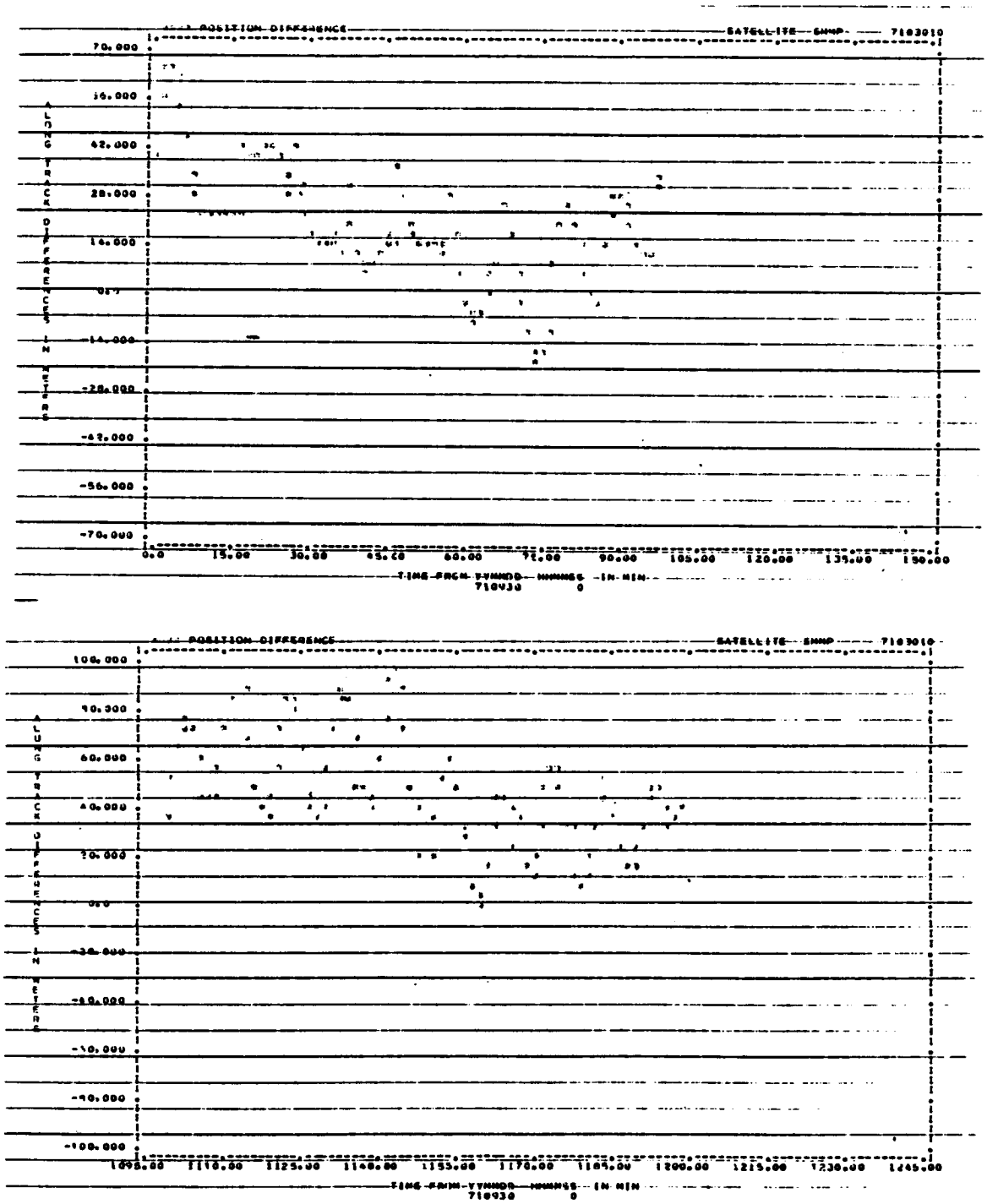

Figure 3-27. Errors in the Representation of the Along-Track Component of Position Using a 36-Term Fourier Series with Position Residuals and a 10-Minute Grid Spacing

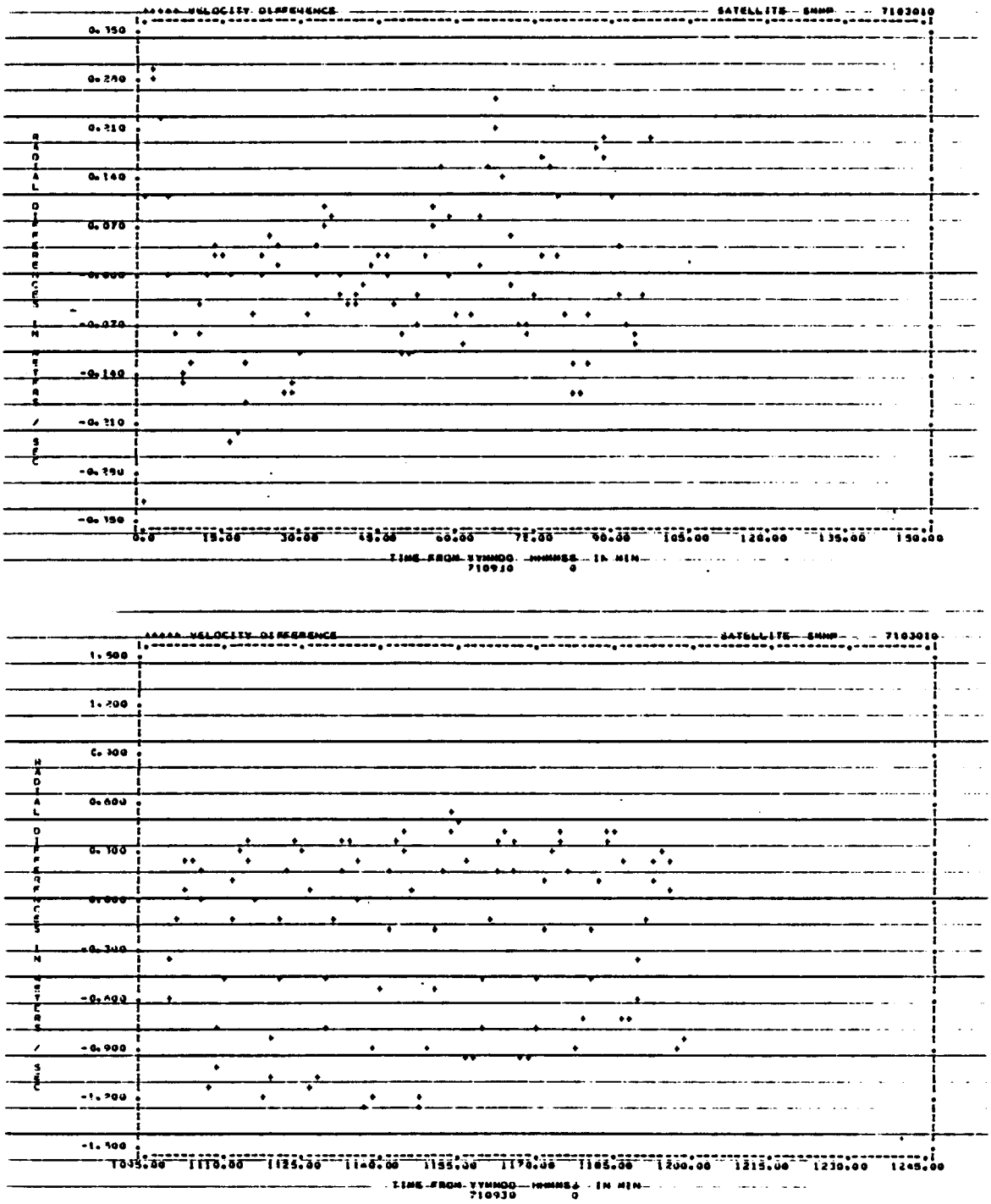

Figure 3-28. Errors in the Representation of the Radial Component of Velocity Using a 36-Term Fourier Series with Position Residuals and a 10-Minute Grid Spacing

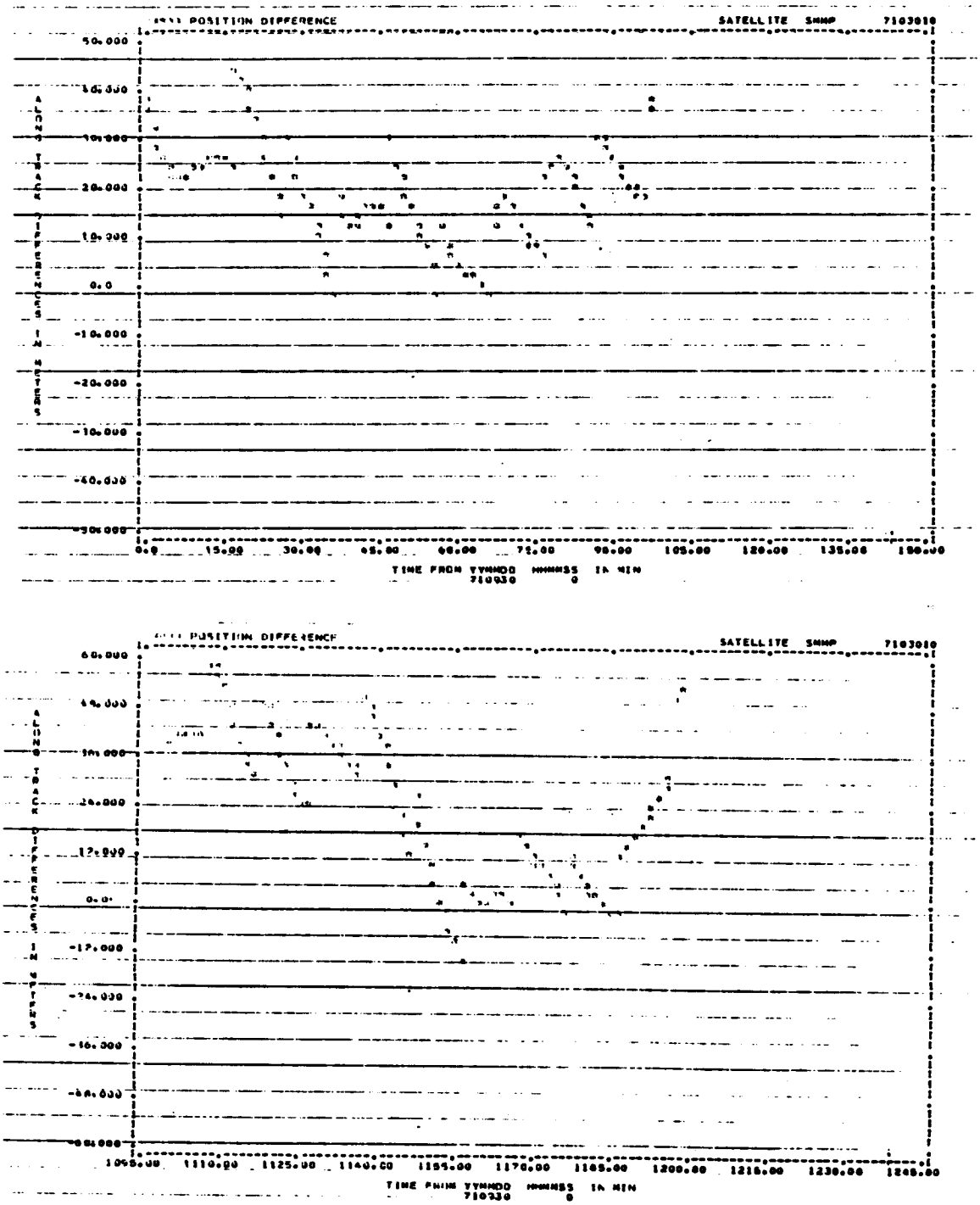

Figure 3-29. Errors in the Representation of the Along-Track Component of Position Using a 36-Term Fourier Series with Position and Velocity Residuals and a 10-Minute Grid Spacing

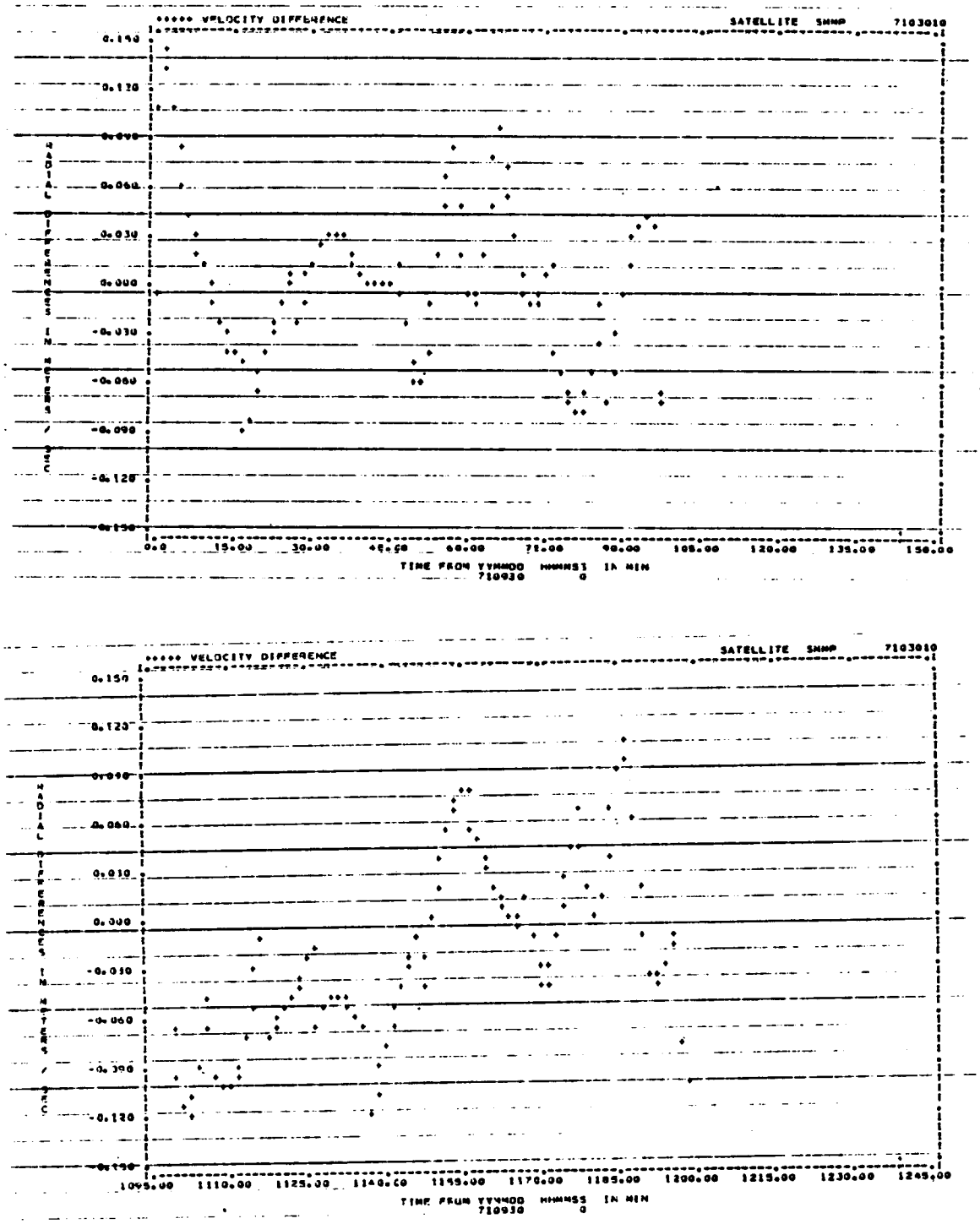

Figure 3-30. Errors in the Representation of the Radial Component of Velocity Using a 36-Term Fourier Series with Position and Velocity Residuals and a 10-Minute Grid Spacing

second for the cross-track component, and 0.679×10^{-3} kilometers/second for the along-track component. The minimum and maximum position differences are 0.496×10^{-5} and 0.785 kilometers for the radial, 0.227×10^{-3} and 0.345 kilometers for the cross-track, and 0.453×10^{-4} and 1.891 kilometers for the along-track components.

For completeness the statistics for analysis involving position, and position and velocity residuals are also given in Table 3-2. Comparison with results obtained using an interpolation interval of (-0.25, +0.75) indicates that the latter produces more accurate interpolation results in all cases.

The plots showing the along-track position differences between the high-precision and the SMM-OBC interpolated trajectories using the ±.5 interpolation interval are presented in Figure 3-31 through 3-36.

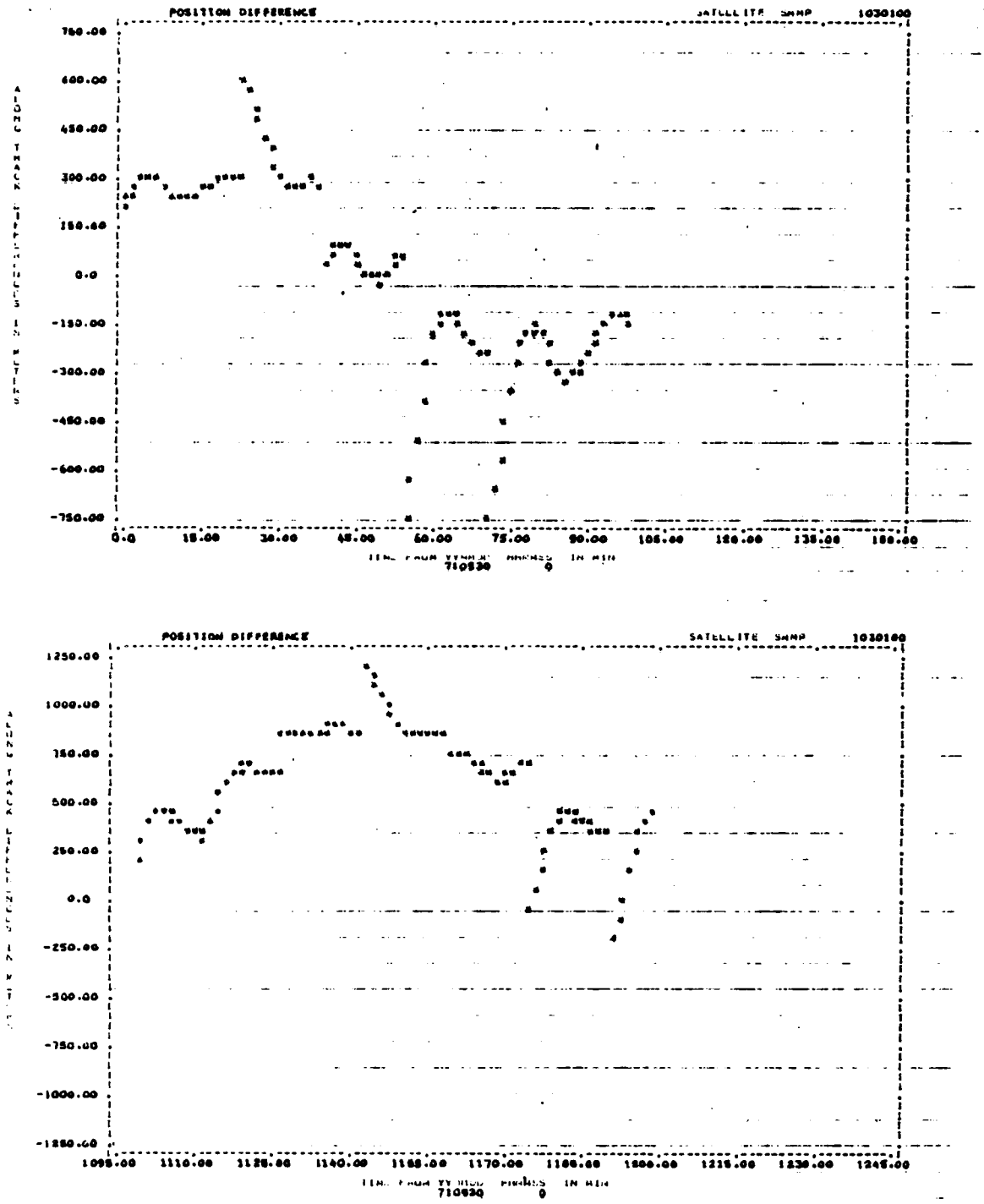

Figure 3-31. Errors in the Representation of the Along-Track Component of Position Using a 29-Term Fourier Series with a 10-Minute Grid Spacing and a (-.5, +.5) Interpolation Interval

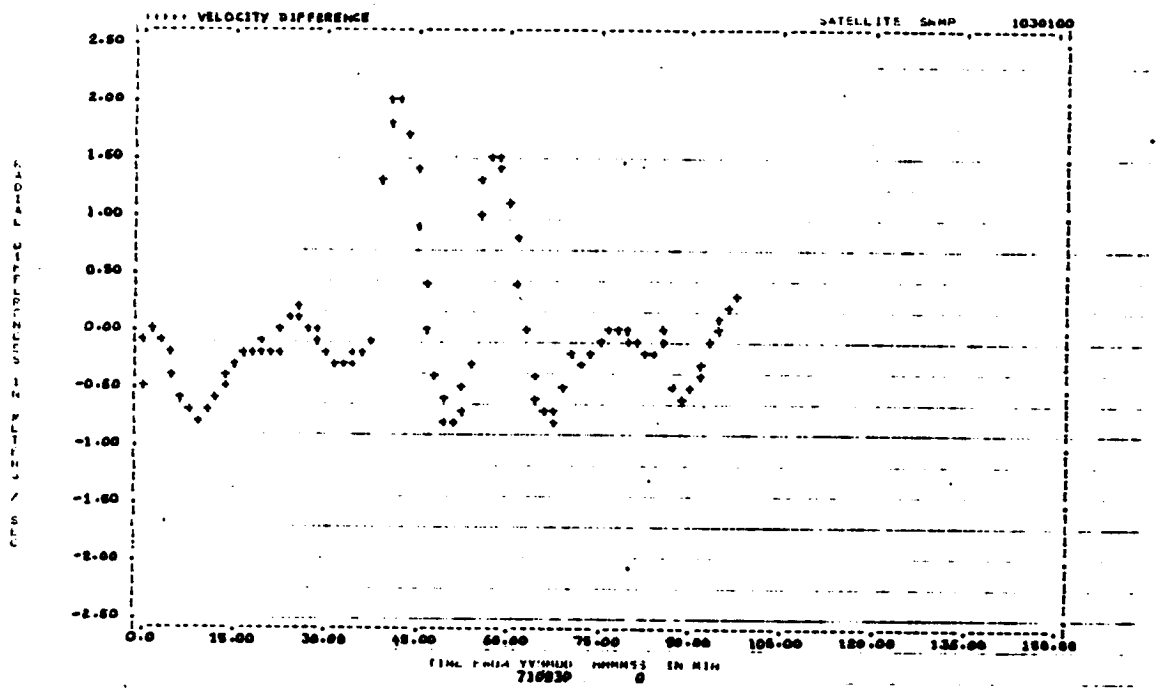

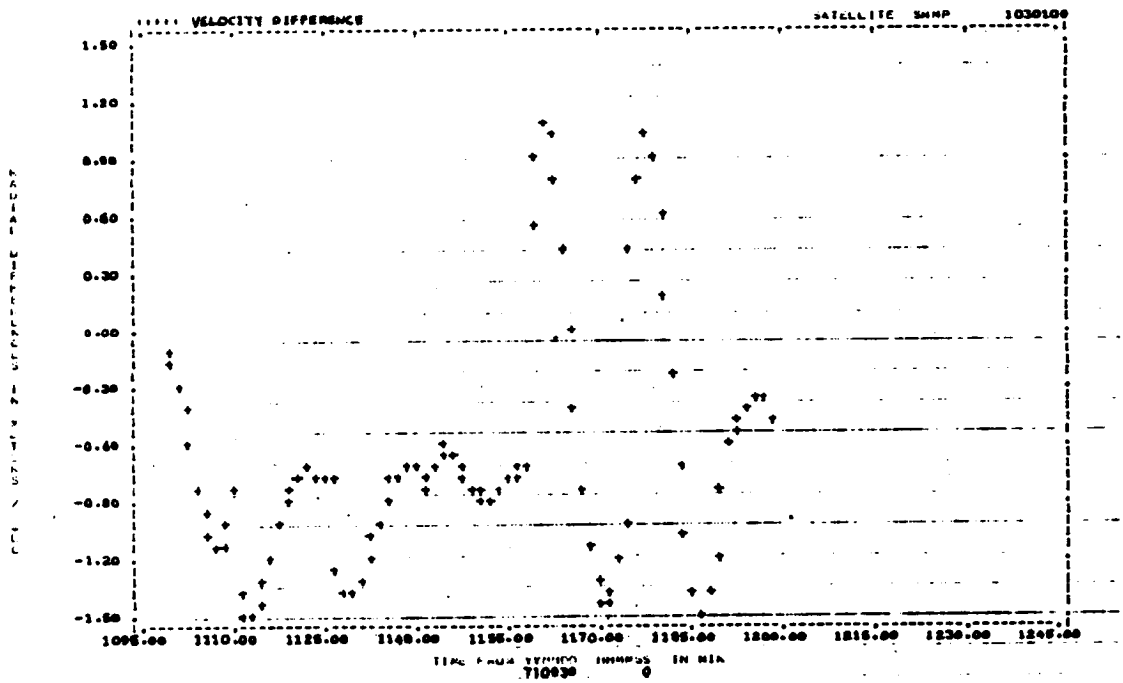

Figure 3-32. Errors in the Representation of the Radial Component of Velocity Using a 29-Term Fourier Series with a 16-Minute Grid Spacing and a (-.5, +.5) Interpolation Interval

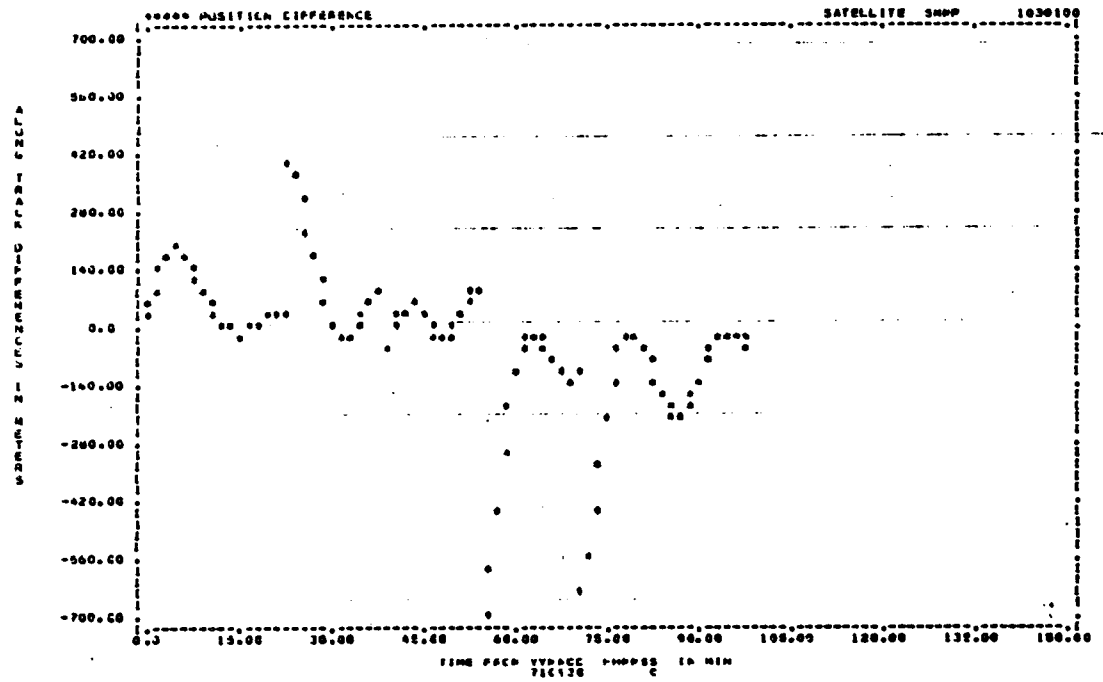

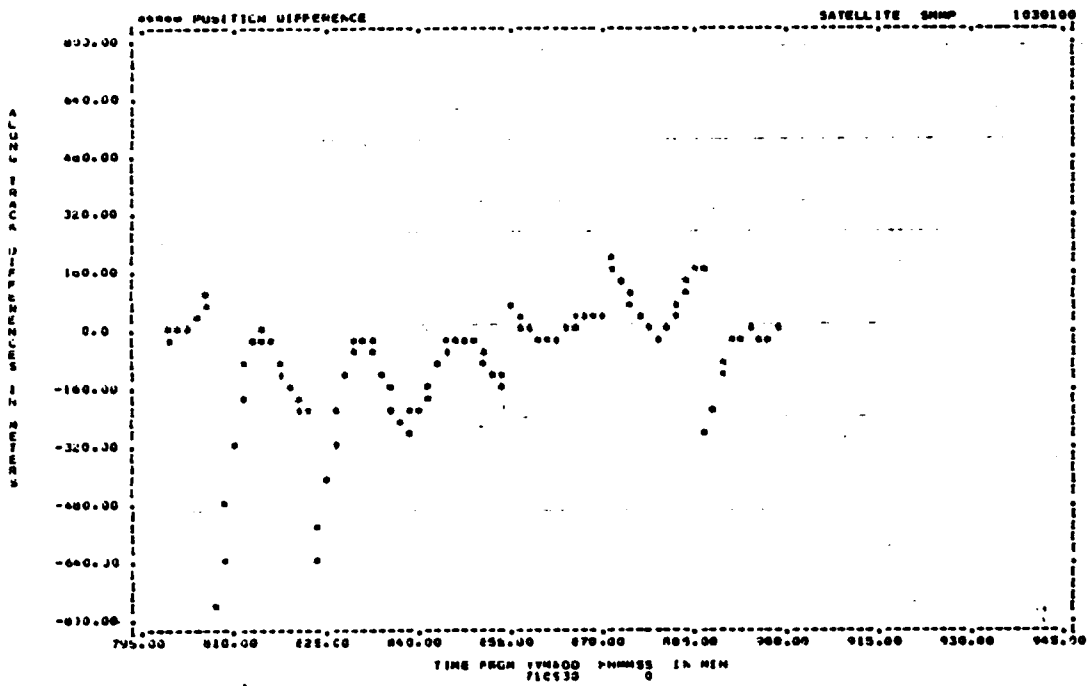

Figure 3-33. Errors in the Representation of the Along-Track Component of Position Using a 29-Term Fourier Series with Position Residuals, a 16-Minute Grid Spacing, and a (-.5, +.5) Interpolation Interval

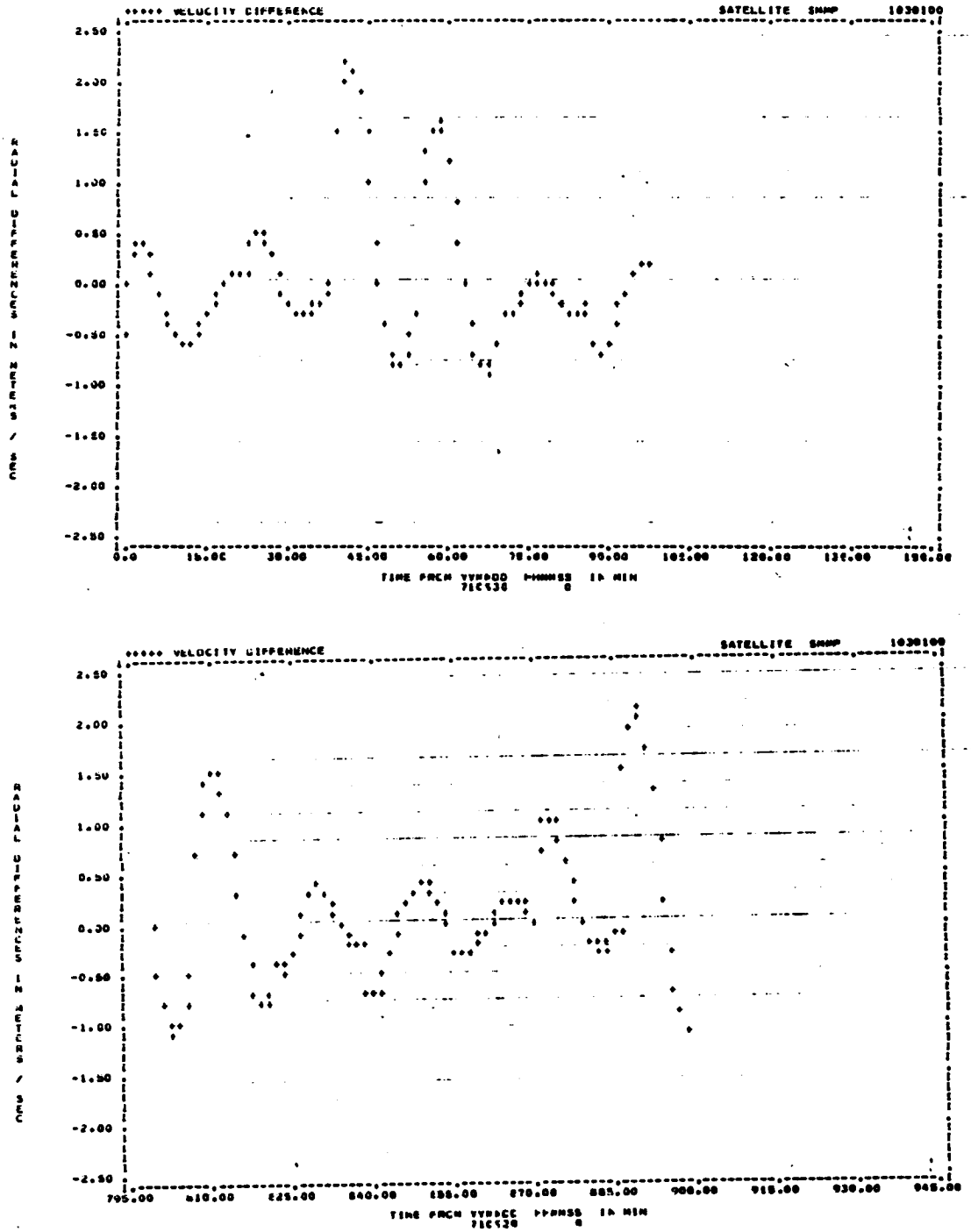

Figure 3-34. Errors in the Representation of the Radial Component of Velocity Using a 29-Term Fourier Series with Position Residuals, a 16-Minute Grid Spacing, and a (-.5, +.5) Interpolation Interval

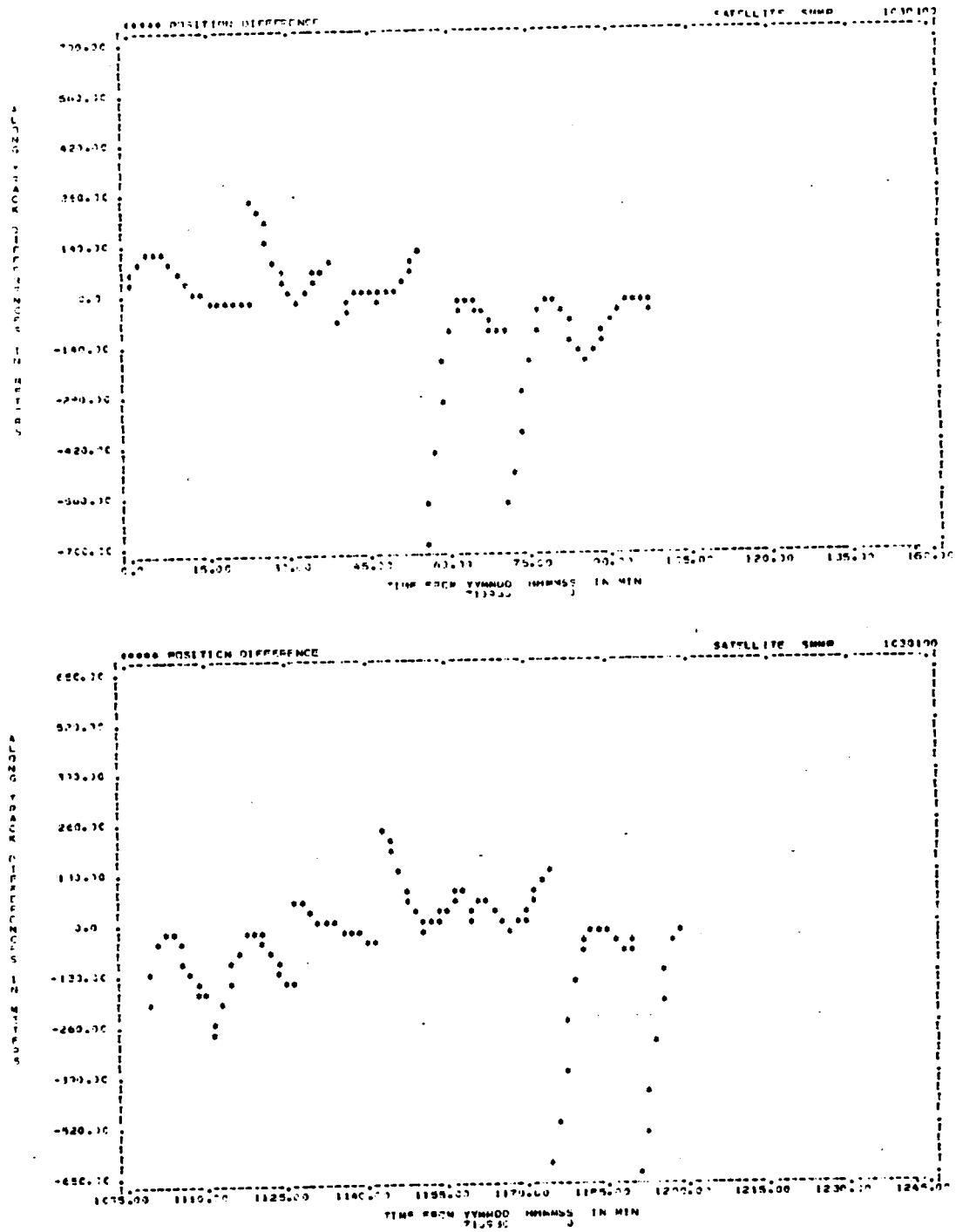

Figure 3-35. Errors in the Representation of the Along-Track Component of Position Using a 29-Term Fourier Series with Position and Velocity Residuals, a 16-Minute Grid Spacing, and a (-.5, +.5) Interpolation Interval

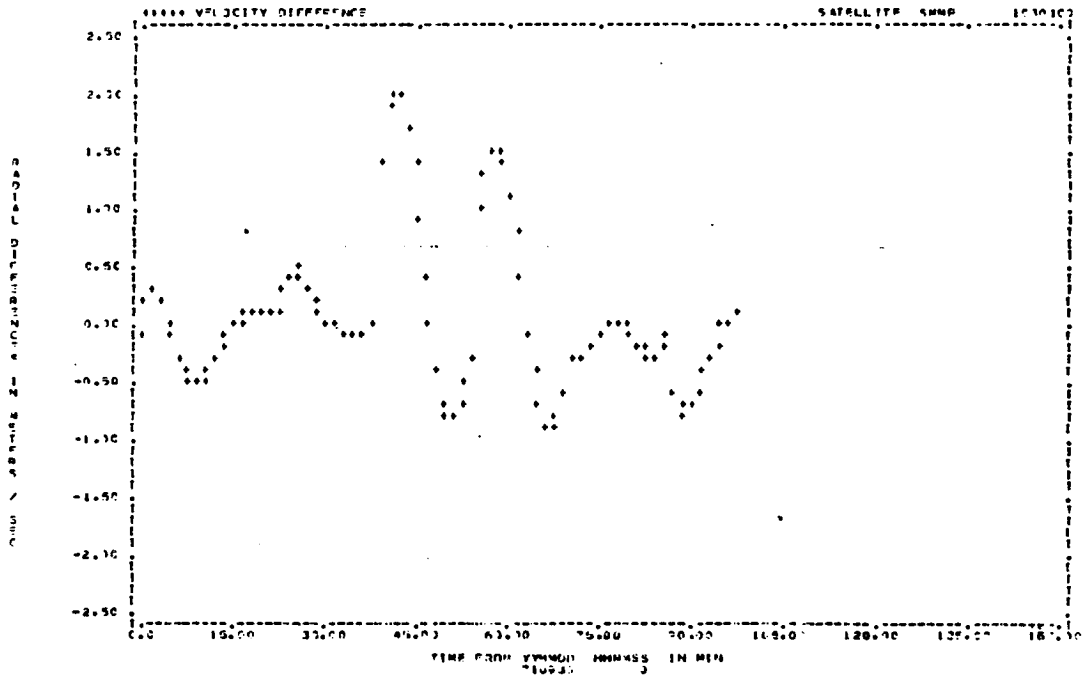

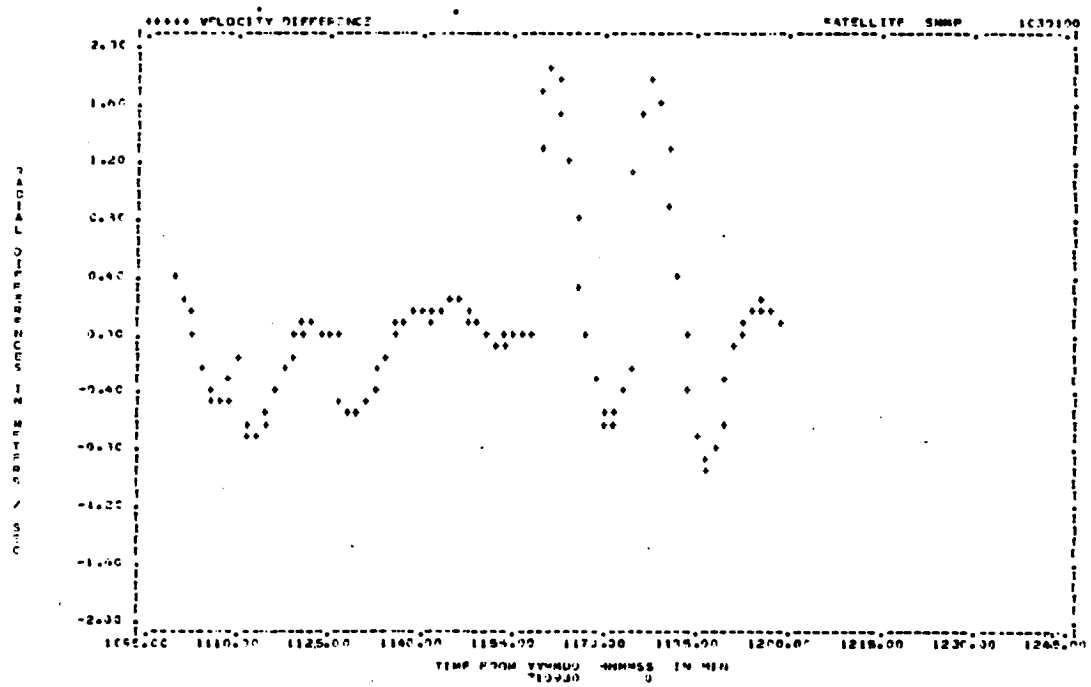

Figure 3-36. Errors in the Representation of the Radial Component of Velocity Using a 29-Term Fourier Series with Position and Velocity Residuals, a 16-Minute Grid Spacing, and a (-.5, +.5) Interpolation Interval

SECTION 4 - INFLUENCE OF DRAG, GRAVITY, AND ORBITAL ECCENTRICITY

In Section 3 the accuracy of several variations in the OBC interpolation method were discussed. Specifically, the effect of a number of terms in the Fourier series, the grid interval, and the interpolation range were studied. In the present section, the influence of atmospheric drag, changes in gravity model, orbital eccentricity, and mean orbital frequency are studied.

4.1 EFFECT OF INCREASED ATMOSPHERIC DRAG

In this study the same state vector is used as in the studies discussed in Section 3, but with a different cross-sectional area and mass (see Case 2, Table 3-1). A smaller spacecraft weight (735 kilograms) and a greater surface area (17.3 meters^2) are used with an increased drag coefficient (2.5). The results of this analysis are discussed below. The interpolation interval is (-0.25, +0.75) with respect to the second grid point, the grid spacing is 16-minutes, and the Fourier series consists of 29 terms. The results are summarized in Table 4-1.

4.1.1 No Residuals

The position rms errors in this case are 0.14 kilometers for the radial, 0.135 kilometers for the cross-track, and 0.473 kilometers for the along-track components. The rms velocity errors are 0.667×10^{-3} kilometers/second, 0.144×10^{-3} kilometers/second, and 0.431×10^{-3} kilometers/second, respectively, for the radial, cross-track, and along-track components. The minimum and maximum position differences are 0.309×10^{-4} and 0.519 kilometers for the radial component, 0.924×10^{-5} and 0.393 kilometers for the cross-track component, and 0.159×10^{-3} and 1.32 kilometers for the along-track component.

Table 4-1. Comparison of SMM Representation Accuracies for Different Force Models

TEST CASE	RESIDUALS	RMS POSITION ERROR				RMS VELOCITY ERROR				MAXIMUM POSITION ERROR			
		H (km)	C (km)	L (km)	$\Delta\vec{R}$ (km)	H (m/s)	C (m/s)	L (m/s)	$\Delta\dot{\vec{R}}$ (m/s)	H (km)	C (km)	L (km)	$\Delta\vec{R}$ (km)
2	NONE	0.14099	0.13530	0.47373	0.51245	0.66767	0.14474	0.43164	0.80811	0.51929	0.39321	1.32070	1.35462
2	$\vec{r}$	0.11730	0.02340	0.10052	0.15624	0.57634	0.11636	0.45372	0.74268	0.51270	0.11597	0.39619	0.55206
2	$\vec{r}, \dot{\vec{r}}$	0.10044	0.00056	0.08325	0.13046	0.45360	0.00262	0.41197	0.61277	0.29799	0.00322	0.20855	0.30295
3	NONE	0.14389	0.13190	0.49396	0.53113	0.68234	0.13809	0.43134	0.81897	0.51861	0.36673	1.46152	1.49835
3	$\vec{r}$	0.11850	0.02188	0.10194	0.15783	0.58511	0.11073	0.45628	0.75020	0.55341	0.10110	0.41349	0.59517
3	$\vec{r}, \dot{\vec{r}}$	0.10049	0.00066	0.08327	0.13061	0.45380	0.00333	0.41210	0.61300	0.29801	0.00355	0.20951	0.30242
4	NONE	0.10688	0.12410	0.45052	0.47937	0.50466	0.12430	0.16989	0.54680	0.32742	0.29847	1.36319	1.36349
4	$\vec{r}$	0.07415	0.01940	0.05677	0.09538	0.39259	0.10010	0.22009	0.46107	0.36737	0.09264	0.27452	0.40131
4	$\vec{r}, \dot{\vec{r}}$	0.04885	0.00054	0.02211	0.05363	0.20482	0.00250	0.13003	0.24262	0.14324	0.00267	0.21249	0.25143
4*	NONE	0.14014	0.12944	0.47392	0.51087	0.66705	0.13599	0.42981	0.80510	0.50914	0.37534	1.33087	1.36636
4*	$\vec{r}$	0.11715	0.02161	0.10049	0.15585	0.57577	0.10920	0.45261	0.74047	0.51976	0.11099	0.39238	0.55758
4*	$\vec{r}, \dot{\vec{r}}$	0.10044	0.00056	0.08325	0.13046	0.45360	0.00262	0.41197	0.61277	0.29799	0.00323	0.26855	0.30295

*A MEAN ORBITAL FREQUENCY OF 0.00111 8344 WAS USED INSTEAD OF COMPUTED VALUE OF 0.0010947826.

NOTE: ALL COMPARISONS WERE OVER 3 DAYS USING A 29 TERM FOURIER SERIES REPRESENTATION FOR THE GRID POINTS, 16 MINUTE GRID INTERVALS, AND (−0.25, +0.75) INTERPOLATION INTERVALS

4.1.2 Position Residuals

When only position residuals are available, the rms position errors are 0.117 kilometers for the radial component, 0.023 kilometers for the cross-track component, and 0.100 kilometers for the along-track component. The rms velocity errors are 0.576×10^{-3} kilometers/second, 0.116×10^{-3} kilometers/second, and 0.453×10^{-3} kilometers/second, respectively, for the radial, cross-track, and along-track components. The minimum and maximum position differences are 0.535×10^{-6} and 0.512 kilometers for the radial component, 0.797×10^{-9} and 0.115 kilometers for the cross-track component, and 0.422×10^{-8} and 0.396 kilometers for the along-track components.

4.1.3 Position and Velocity Residuals

When information on both position and velocity residuals is available, the rms position errors are 0.100 kilometers for the radial, 0.567×10^{-3} kilometers for the cross-track, and 0.83 kilometers for the along-track components. The rms velocity errors are 0.453×10^{-3} kilometers/second, 0.262×10^{-5} kilometers/second, and 0.411×10^{-3} kilometers/second, respectively, for the radial, cross-track, and along-track components. The minimum and maximum position differences are 0.109×10^{-5} and 0.297 kilometers, 0.768×10^{-9} and 0.322×10^{-2} kilometers, and 0.422×10^{-8} and 0.208 kilometers, respectively, for the radial, cross-track, and along-track components.

The plots showing the along-track position and radial velocity differences between the high-precision and the SMM-OBC interpolated trajectories are presented in Figures 4-1 through 4-6. Comparison with results obtained using Case 1 indicates that the increased drag does not degrade the accuracy of the representations. The results of this analysis are summarized in Table 4-1.

4.2 EFFECT OF INCREASED GRAVITY MODEL

In this comparison the state vectors and state parameters are the same as those discussed in the preceding section. However, the force field is a

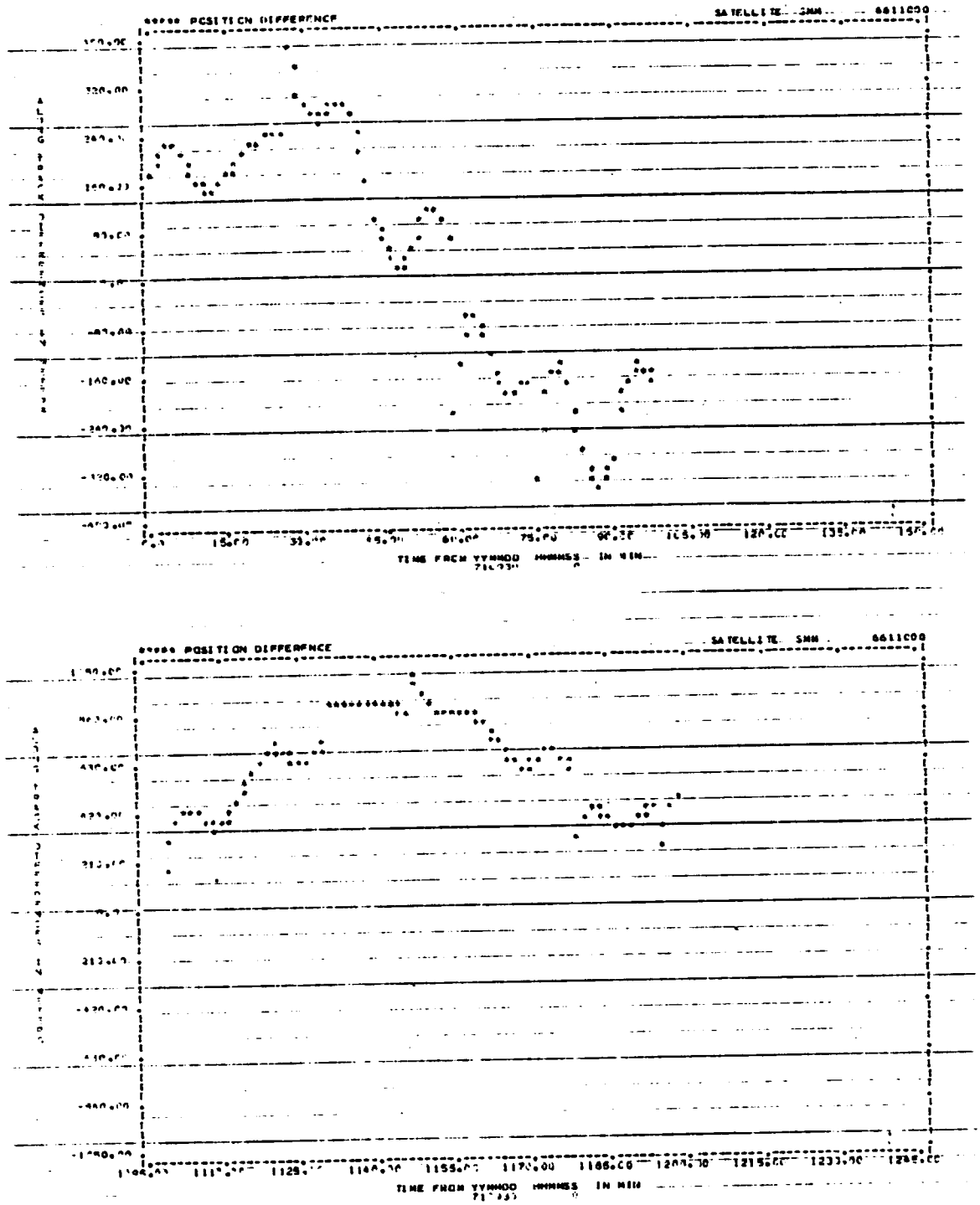

Figure 4-1. Errors in the Representation of the Along-Track Component of Position Using a 29-Term Fourier Series and a 16-Minute Grid Spacing in the Case of Increased Drag Effects

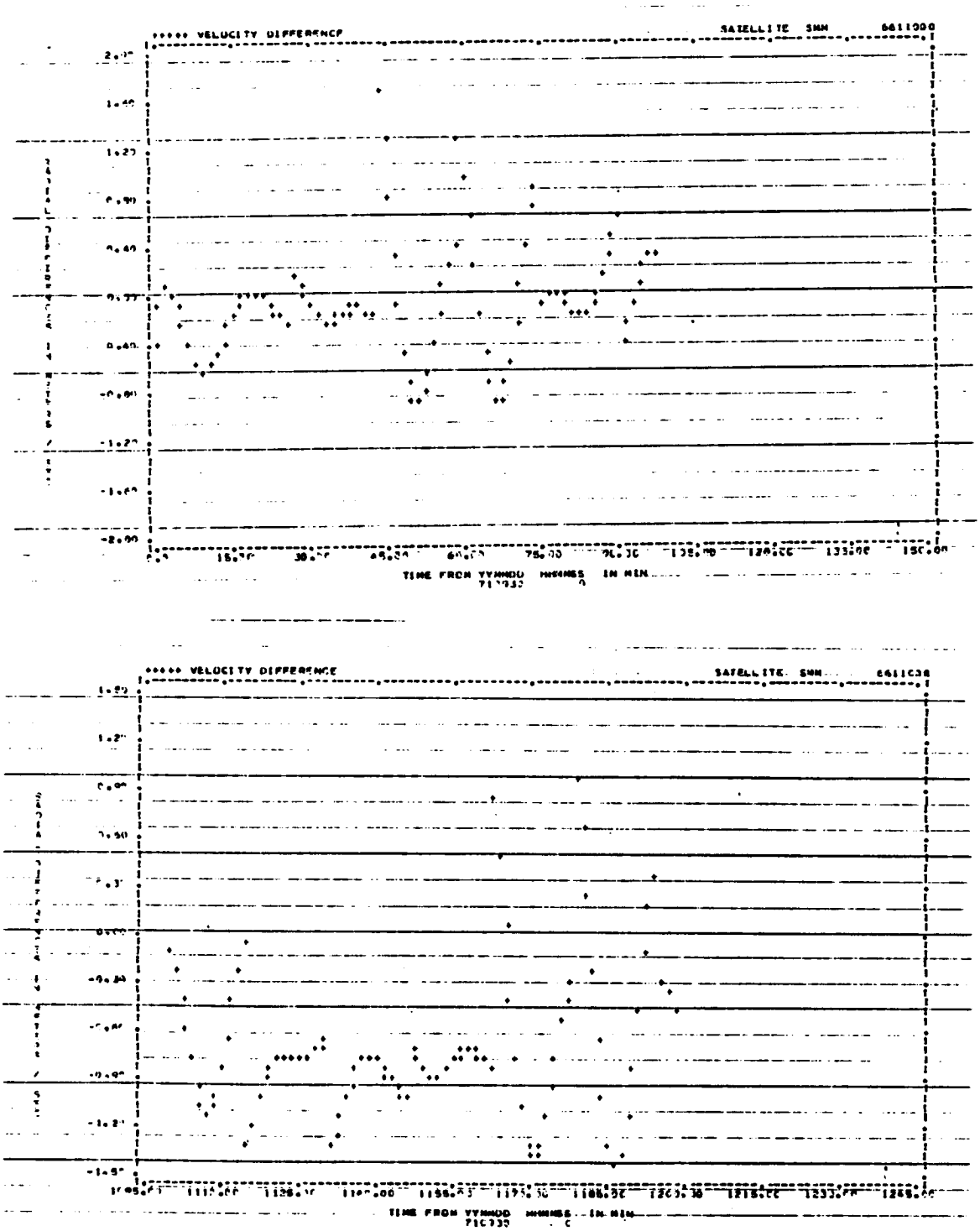

Figure 4-2. Errors in the Representation of the Radial Component of Velocity Using a 29-Term Fourier Series and a 16-Minute Grid Spacing in the Case of Increased Drag Effects

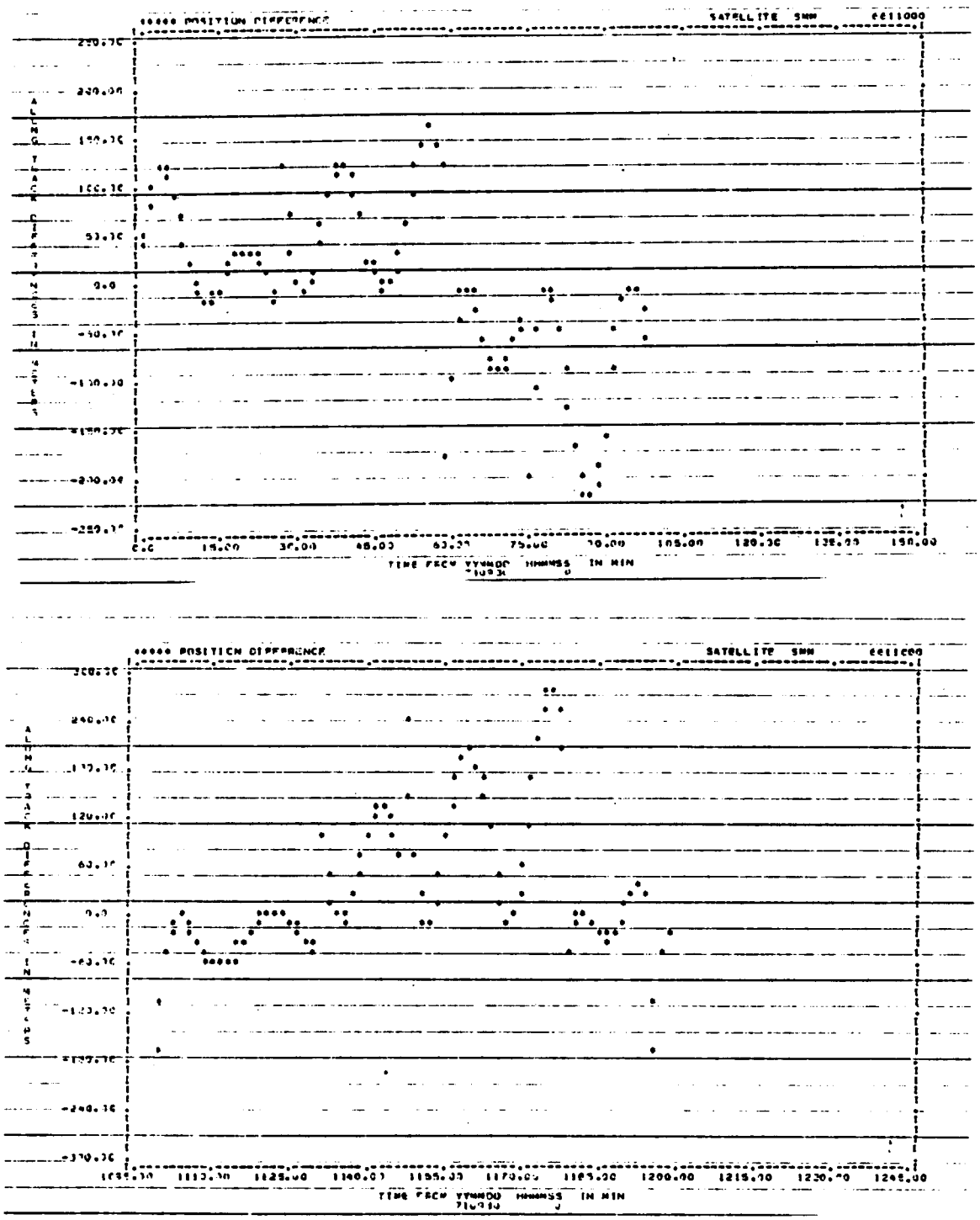

Figure 4-3. Errors in the Representation of the Along-Track Component of Position Using a 29-Term Fourier Series with Position Residuals and a 16-Minute Grid Spacing in the Case of Increased Drag Effects

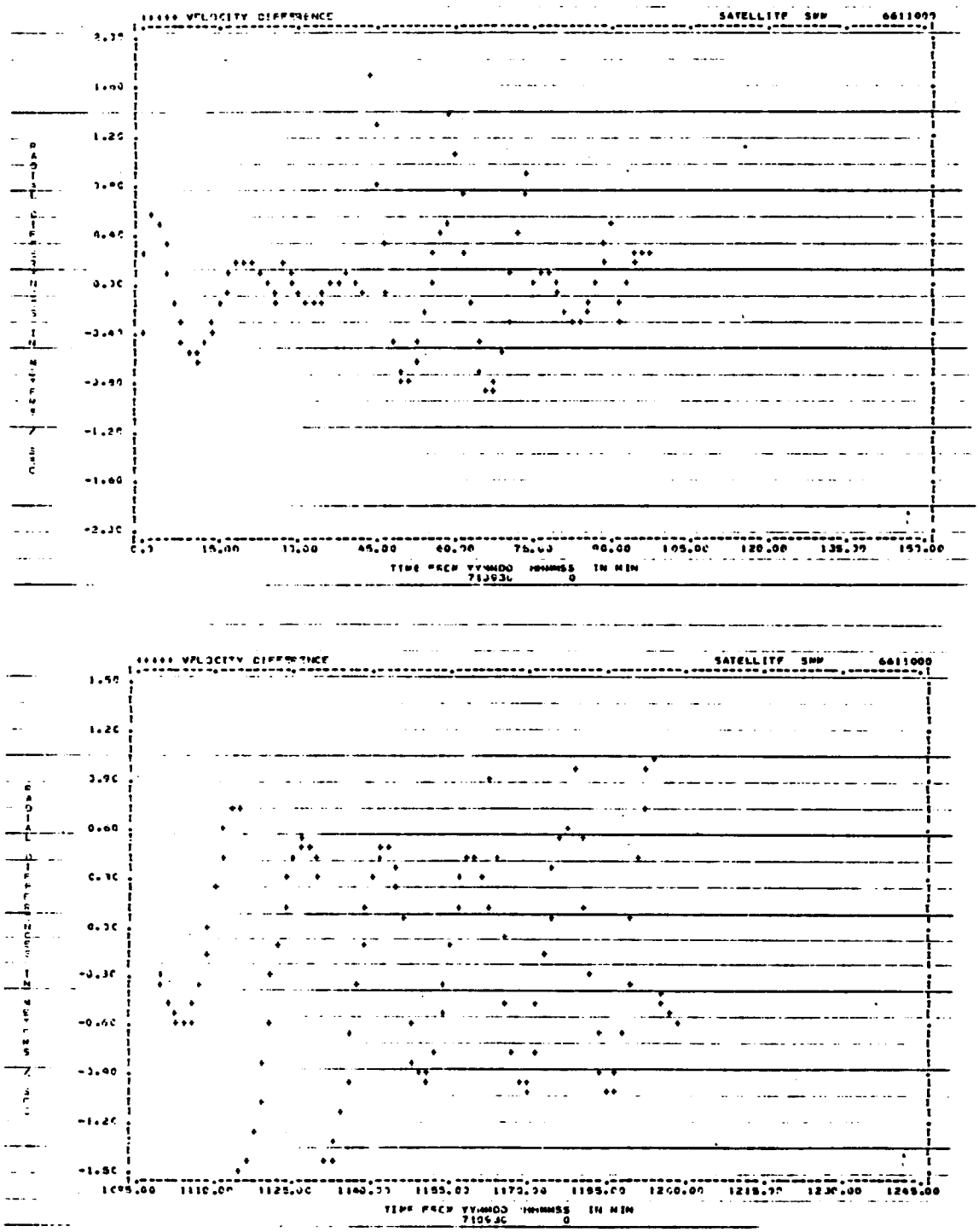

Figure 4-4. Errors in the Representation of the Radial Component of Velocity Using a 29-Term Fourier Series with Position Residuals and a 16-Minute Grid Spacing in the Case of Increased Drag Effects

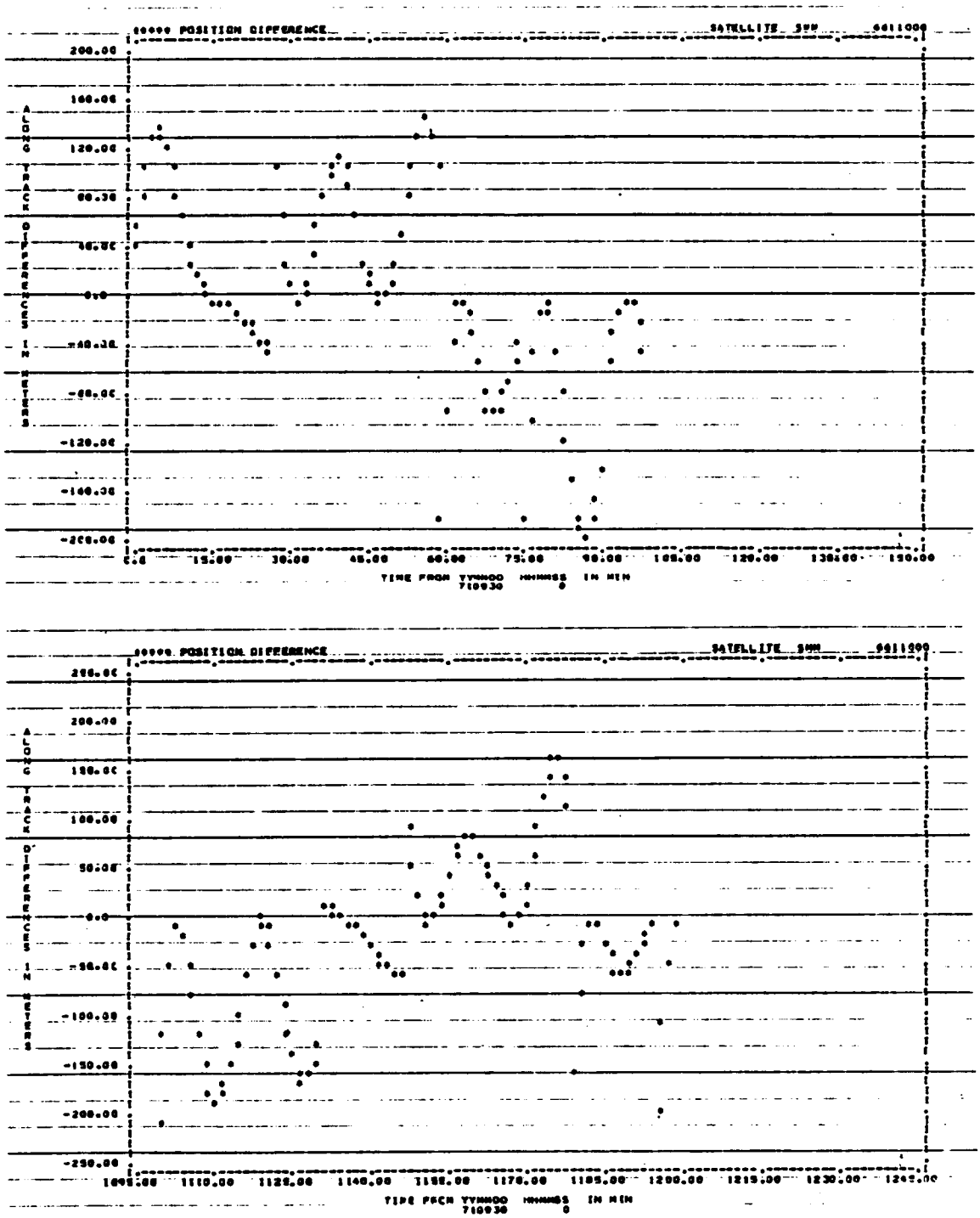

Figure 4-5. Errors in the Representation of the Along-Track Component of Position Using a 29-Term Fourier Series with Position and Velocity Residuals and a 16-Minute Grid Spacing in the Case of Increased Drag Effects

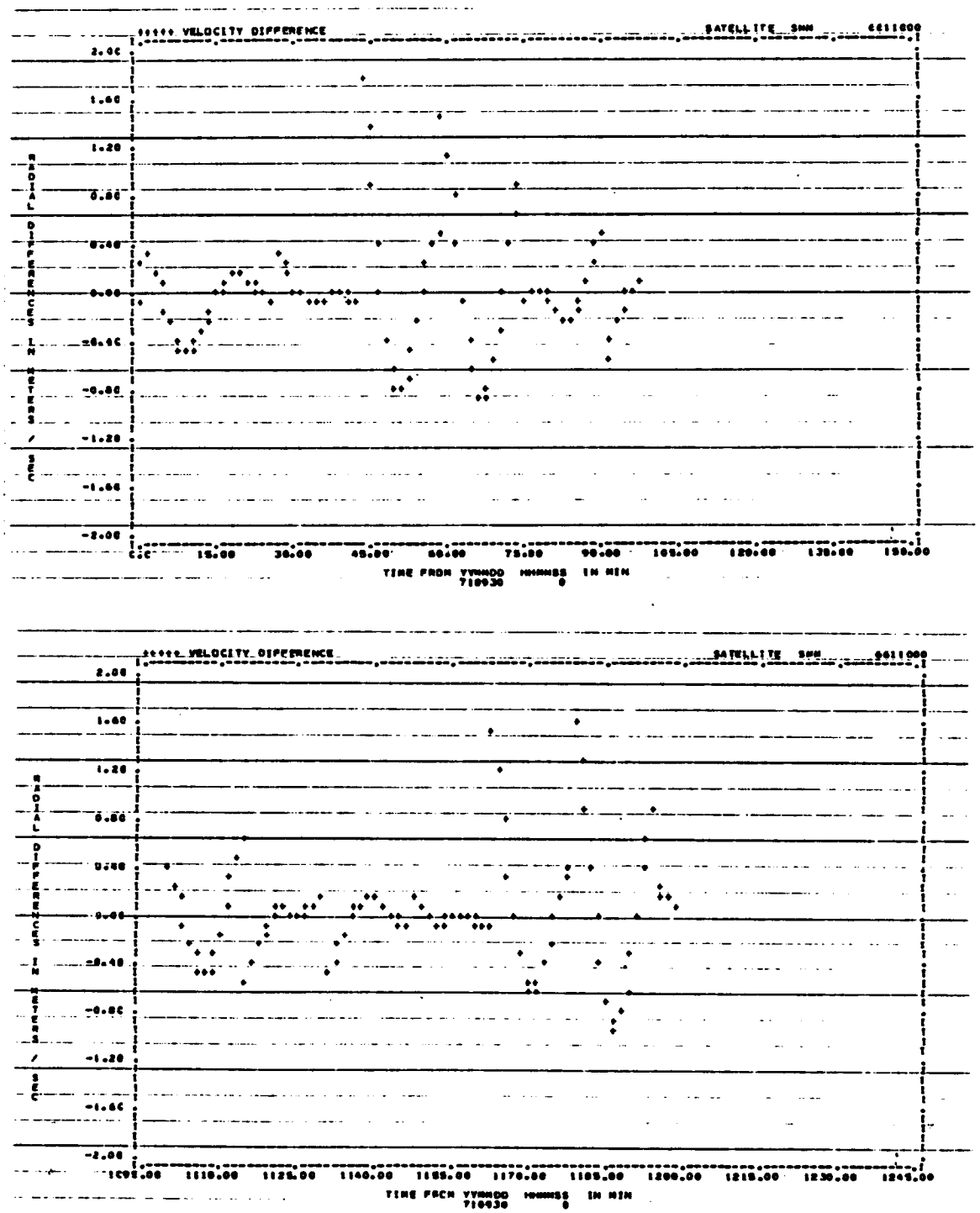

Figure 4-6. Errors in the Representation of the Radial Component of Velocity Using a 29-Term Fourier Series with Position and Velocity Residuals and a 16-Minute Grid Spacing in the Case of Increased Drag Effects

15 x 15 nonspherical geopotential field. The results of the investigation are discussed below. The complete result is presented in Table 4-1. The orbital frequency in this case was 0.1118344×10^{-2} radians per day. The state vectors and other parameters are those shown under Case 3 in Table 3-1. A 29-term Fourier series is used with a 16-minute grid spacing and a (-0.25, +0.75) interpolation interval.

4.2.1 No Residuals

When no position or velocity residuals are used, the rms position errors are found to be 0.143 kilometers for the radial component, 0.131 kilometers for the cross-track, and 0.493 kilometers for the along-track components. The rms velocity errors are 0.682×10^{-3} kilometers/second, 0.138×10^{-3} kilometers/second, and 0.431×10^{-3} kilometers/second for the radial, cross-track, and along-track components. The minimum and maximum position differences are 0.538×10^{-4} and 0.518 kilometers, 0.469×10^{-4} and 0.365 kilometers, and 0.105×10^{-3} and 1.46 kilometers, respectively, for the radial, cross-track and along-track components.

4.2.2 Position Residuals

When only position residuals are used, the rms position errors are seen to be 0.118 kilometers for the radial component, 0.021 kilometers for the cross-track component, and 0.101 kilometers for the along-track component, while the velocity rms errors are 0.585×10^{-3} kilometers/second, 0.11×10^{-3} kilometers/second, and, 0.456×10^{-3} kilometers/second, respectively, for the radial, cross-track, and along-track components. The minimum and maximum position differences are 0.13×10^{-5} and 0.553 kilometers, 0.172×10^{-7} and 0.1 kilometer, and, 0.186×10^{-8} and 0.413 kilometers, respectively, for the radial, cross-track, and along-track components.

4.2.3 Position and Velocity Residuals

In this case when all the position and velocity residuals are used the rms position errors are found to be 0.100 kilometers for the radial component, 0.664×10^{-3} kilometers for the cross-track component, and 0.083 kilometers for the along-track component. The rms velocity errors are found to be 0.453×10^{-3} kilometers/second for the radial, 0.333×10^{-5} kilometers/second for the cross-track, and 0.412×10^{-3} kilometers/second for the along-track components. The minimum and maximum position differences are 0.13×10^{-5} and 0.298 kilometers, 0.173×10^{-7} and 0.355×10^{-2}, and, 0.187×10^{-8} and 0.209 kilometers for the radial, cross-track, and along-track components, respectively.

Comparison of these results with those discussed previously indicates that increased gravitational effects do not degrade the accuracy of the respresentation algorithms. The along-track position and radial velocity differences in the high-precision and the SMM-OBC interpolated trajectories are given in Figures 4-7 through 4-12 for representative time spans.

4.3 EFFECT OF ORBITAL ECCENTRICITY

The state vectors and state parameters are those under Case 4 presented in Table 3-1. The force field is a 15×15 nonspherical geopotential field. The mean orbital frequency was calculated to be 0.0010947826 radians per second, using the maximum entropy method (Reference 8). The results of this analysis are discussed below, and may also be found in full in Table 4-1. A 29-term Fourier series with 16-minute grid spacing and (-0.25, +0.75) interpolation interval was used.

4.3.1 No Residuals

In this case, when position and velocity residuals are not used, the rms position errors are found to be 0.106 kilometers for the radial component, 0.124 kilometers for the cross-track component, and 0.45 kilometers for the along-track

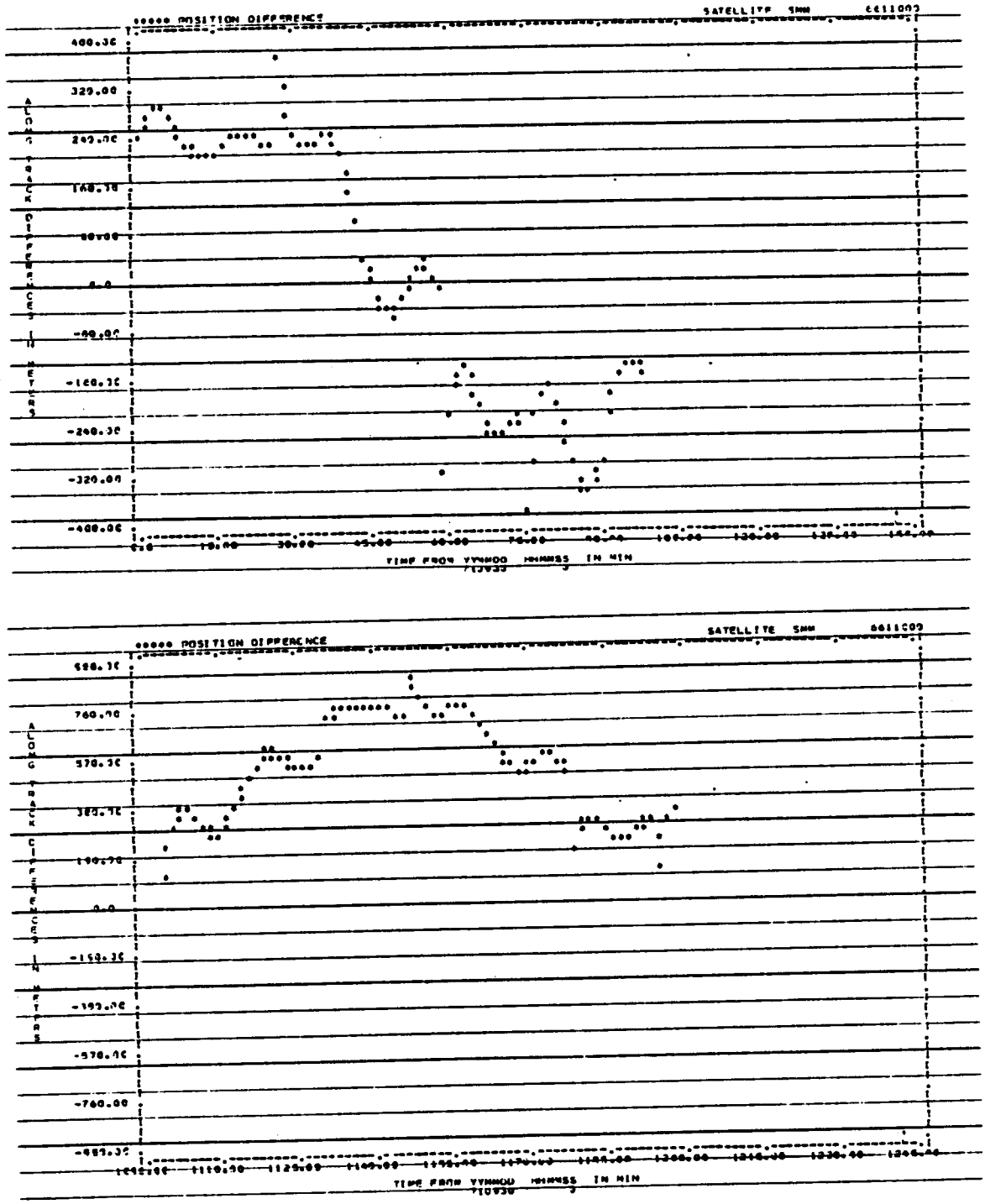

Figure 4-7. Errors in the Representation of the Along-Track Component of Position Using a 29-Term Fourier Series with a 16-Minute Grid Spacing in the Case of Increased Gravitational Effects

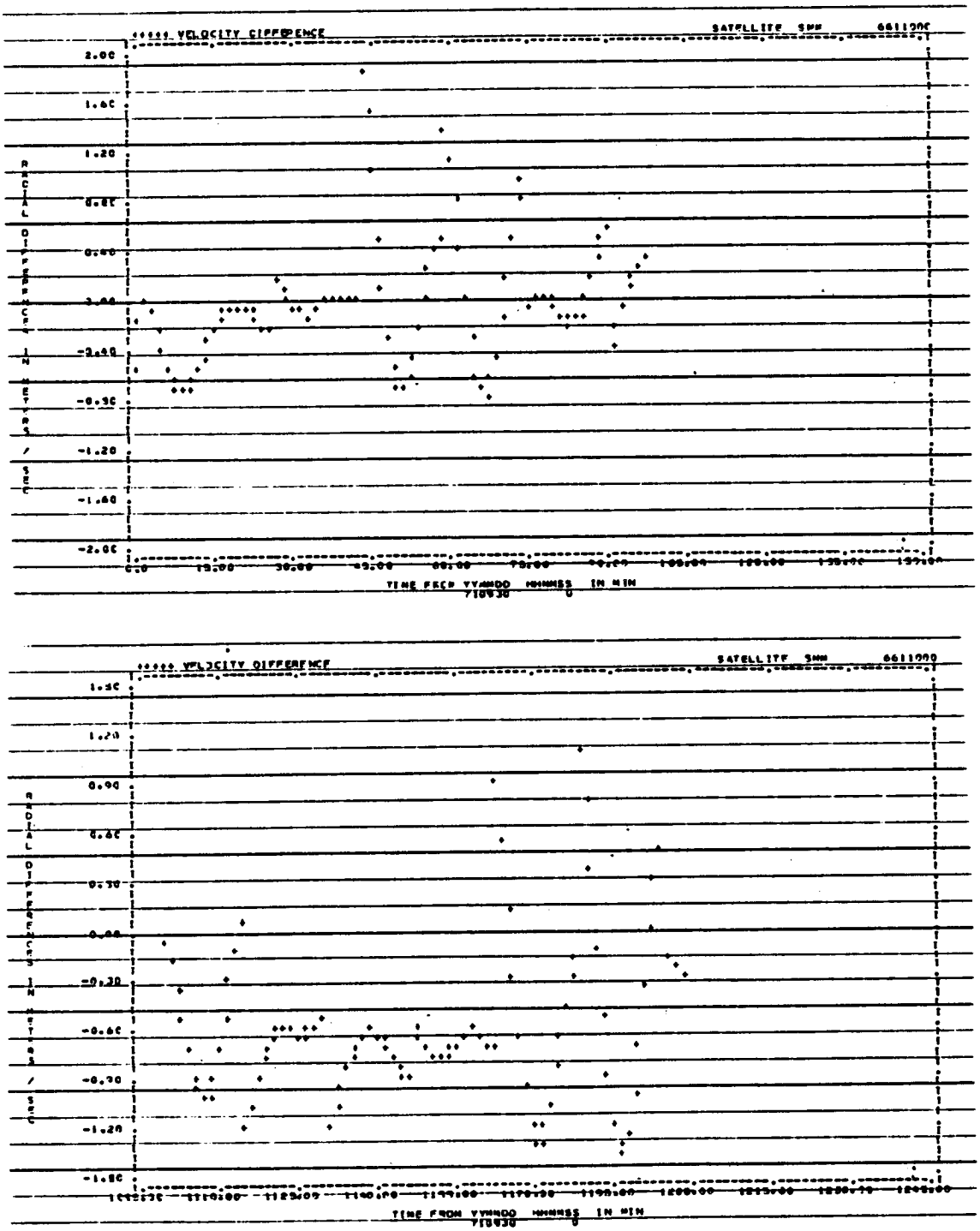

Figure 4-8. Errors in the Representation of the Radial Component of Velocity Using a 29-Term Fourier Series with a 16-Minute Grid Spacing in the Case of Increased Gravitational Effects

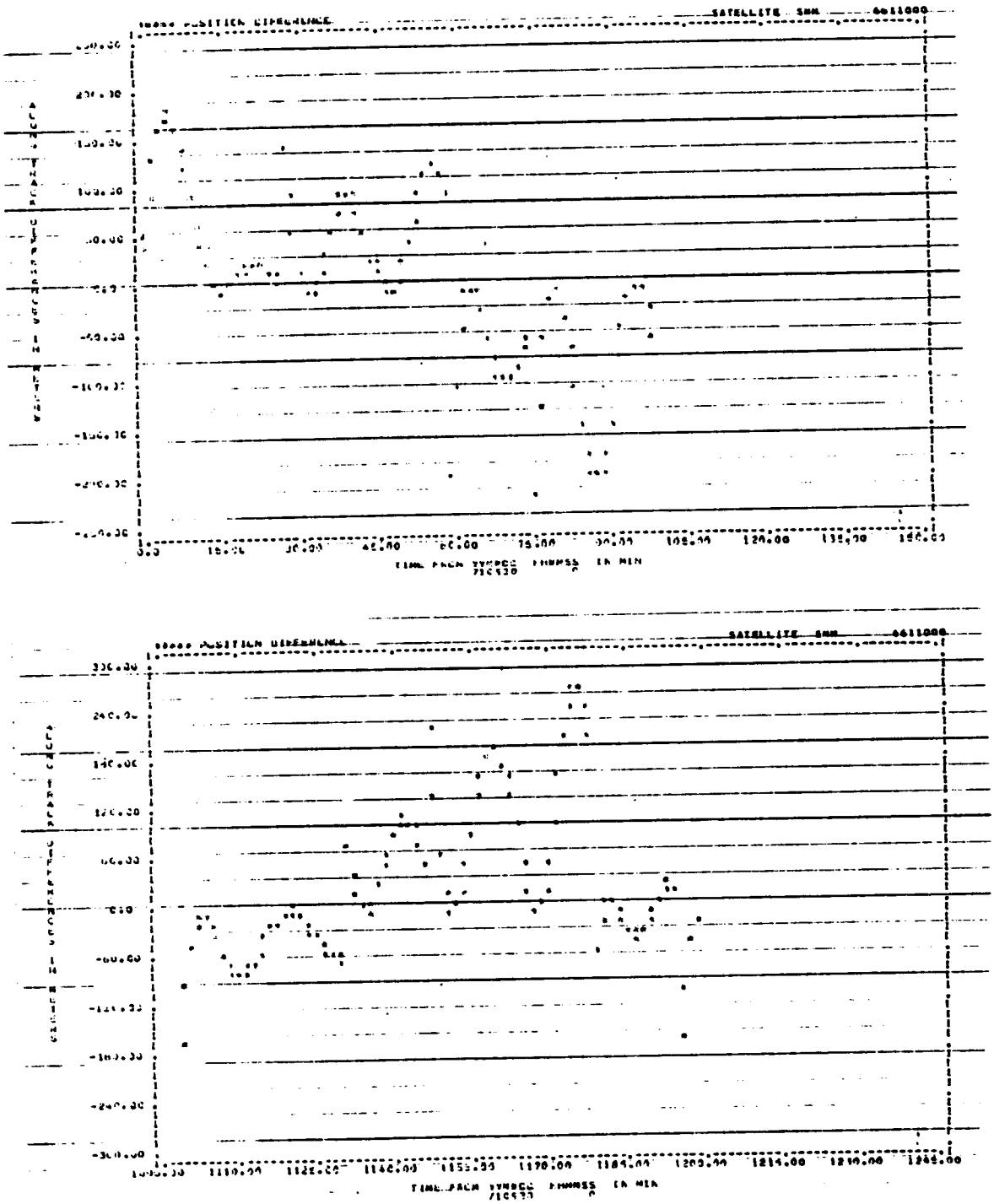

Figure 4-9. Errors in the Representation of the Along-Track Component of Position Using a 29-Term Fourier Series with Position Residuals and a 16-Minute Grid Spacing in the Case of Increased Gravitational Effects

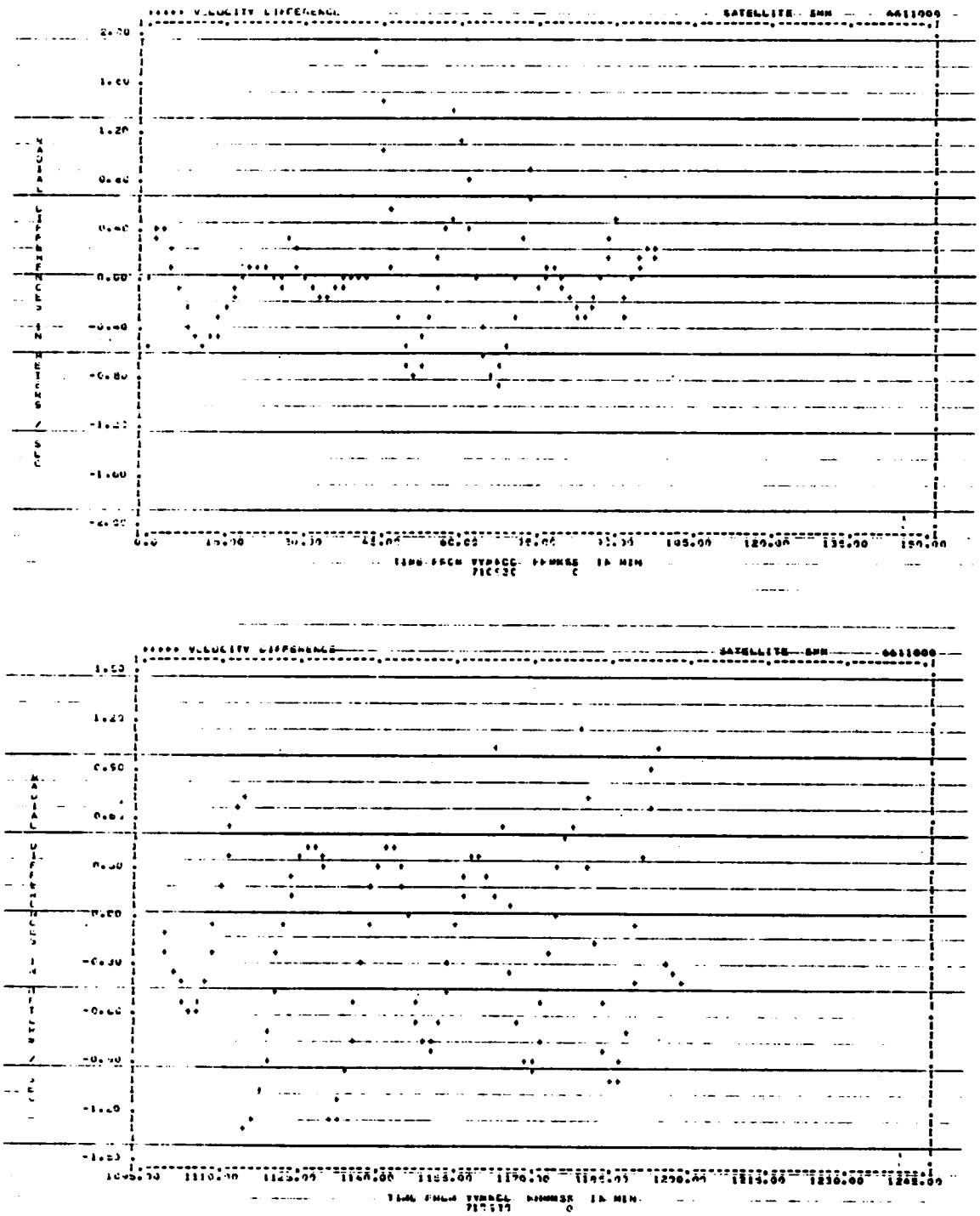

Figure 4-10. Errors in the Representation of the Radial Component of Velocity Using a 29-Term Fourier Series with Position Residuals and a 16-Minute Grid Spacing in the Case of Increased Gravitational Effects

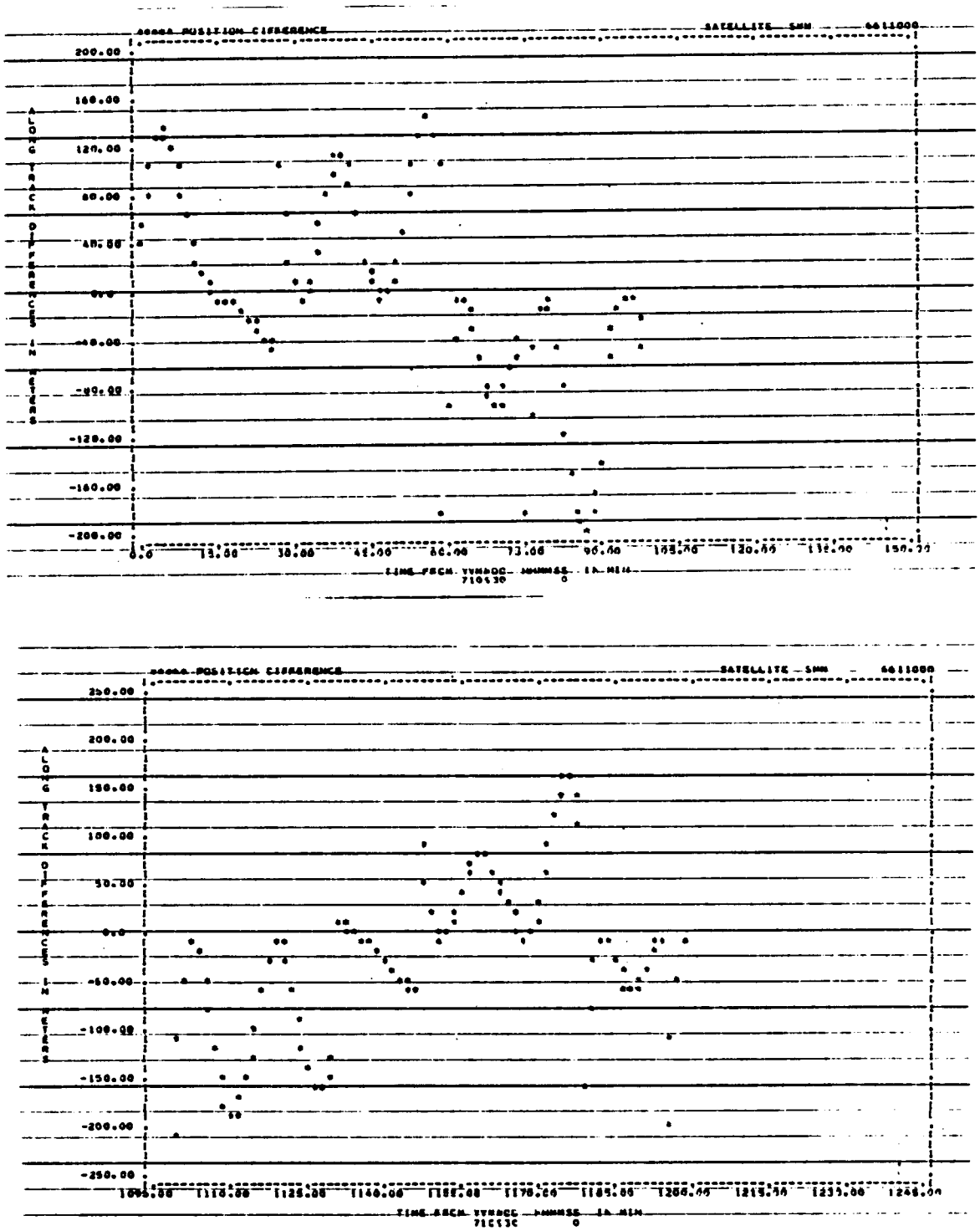

Figure 4-11. Errors in the Representation of the Along-Track Component of Position Using a 29-Term Fourier Series with Position and Velocity Residuals and a 16-Minute Grid Spacing in the Case of Increased Gravitational Effects

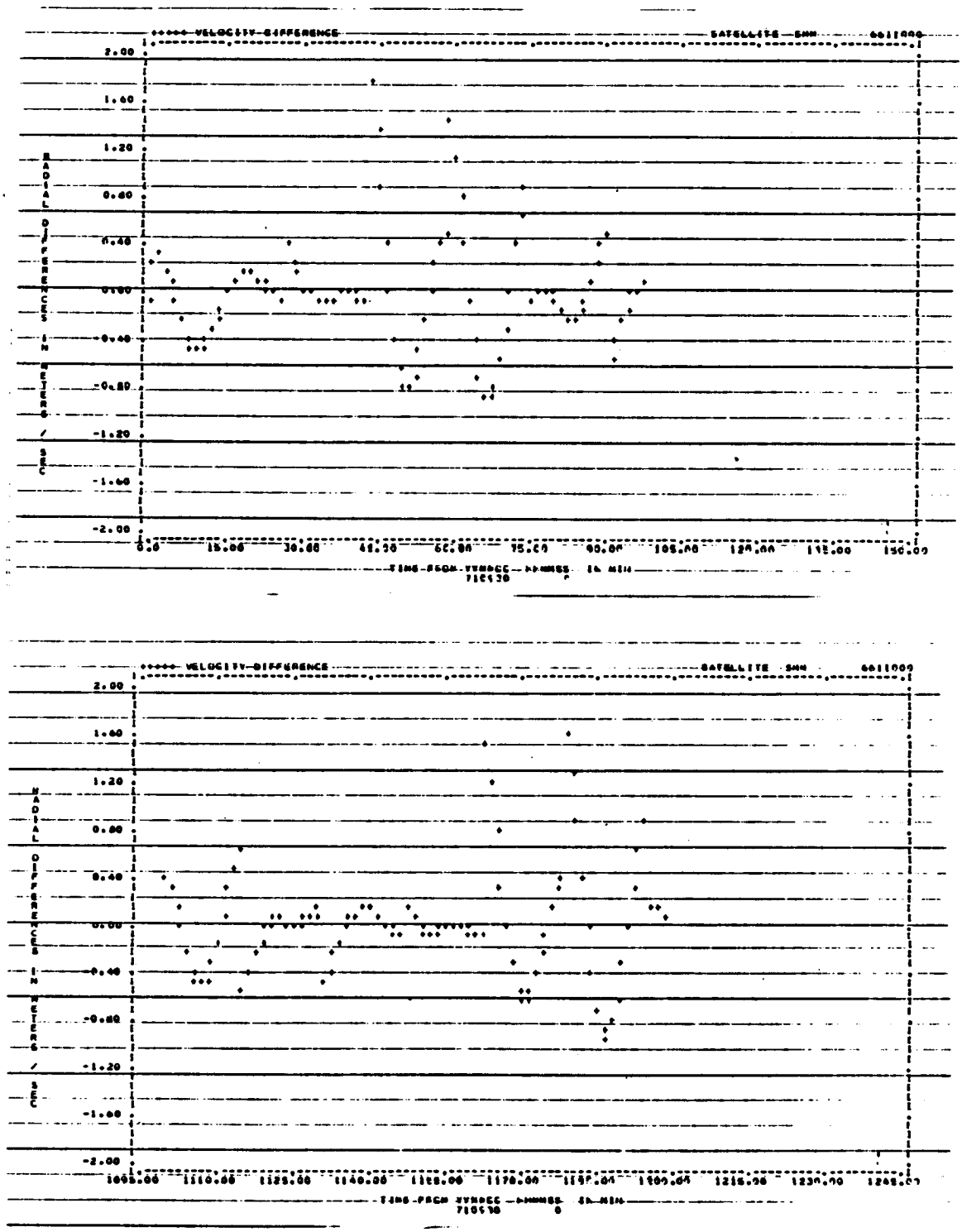

Figure 4-12. Errors in the Representation of the Radial Component of Velocity Using a 29-Term Fourier Series with Position and Velocity Residuals and a 16-Minute Grid Spacing in the Case of Increased Gravitational Effects

component. The rms velocity errors are 0.504×10^{-3} kilometers/second for the radial, 0.124×10^{-3} kilometers/second for the cross-track, and 0.169×10^{-3} kilometers/second for the along-track components. The minimum and maximum position errors are 0.632×10^{-5} and 0.327 kilometers, 0.279×10^{-5} and 0.298 kilometers, and 0.626×10^{-4} and 1.36 kilometers, respectively, for the radial, cross-track and along-track components.

4.3.2 Position Residuals

When position residuals are used, the rms position errors are found to be 0.074 kilometers for the radial component, 0.019 kilometers for the cross-track component, and 0.056 kilometers for the along-track component. The velocity rms errors are found to be 0.392×10^{-3} kilometers/second for the radial component, 0.1×10^{-3} kilometers/second for the cross-track component, and 0.22×10^{-3} kilometers/second for the along-track component. The minimum and maximum position differences are 0.174×10^{-5} and 0.367 kilometers, 0.154×10^{-7} and 0.092 kilometers, and, 0.149×10^{-5} and 0.274 kilometers, respectively, for the radial, cross-track, and along-track components.

4.3.3 Position and Velocity Residuals

When both position and velocity residuals are used, the rms position errors are found to be 0.048 kilometers, 0.544×10^{-3} kilometers, and 0.022 kilometers, respectively, for the radial, cross-track, and along-track components. The rms velocity errors are 0.204×10^{-3} kilometers/second, 0.25×10^{-5} kilometers/second, and 0.13×10^{-3} kilometers/second, for the radial, cross-track, and along-track components, respectively. The minimum and maximum position differences are 0.174×10^{-7} and 0.267×10^{-2} kilometers for the cross-track components, and 0.149×10^{-5} and 0.212 kilometers for the along-track component.

The plots representing the differences in the high-precision and the SMM-OBC interpolated trajectories are given in Figures 4-13 through 4-18.

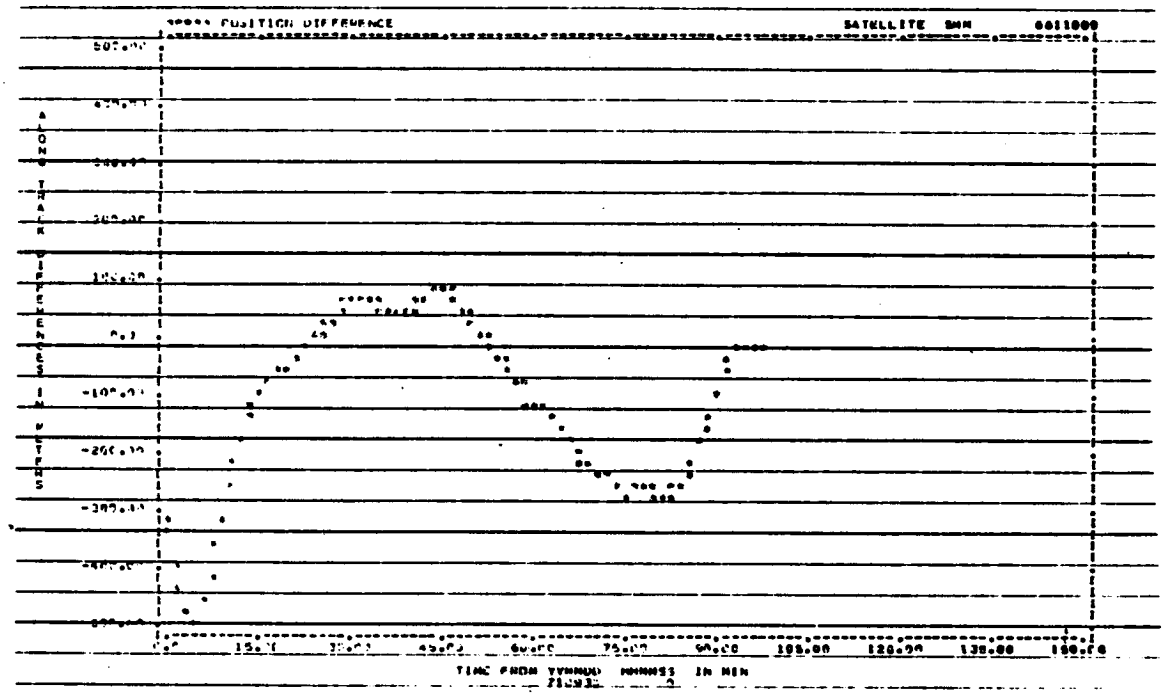

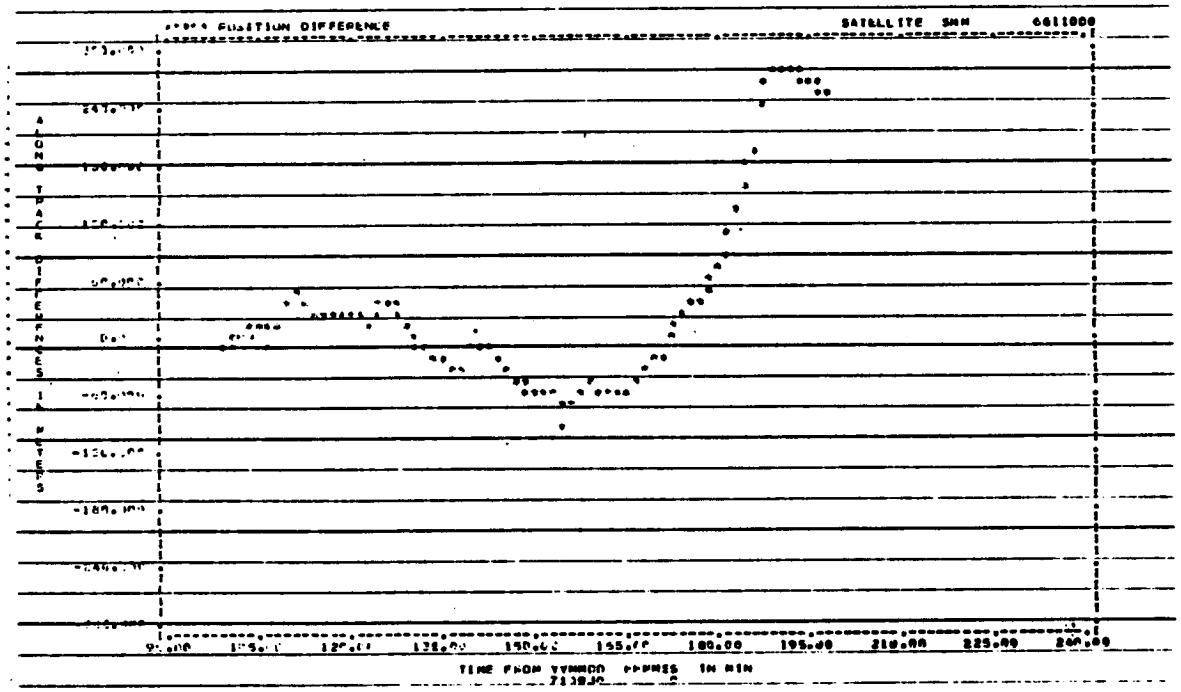

Figure 4-13. Errors in the Representation of the Along-Track Component of Position Using a 29-Term Fourier Series with a 16-Minute Grid Spacing for Case 4 (1 of 2)

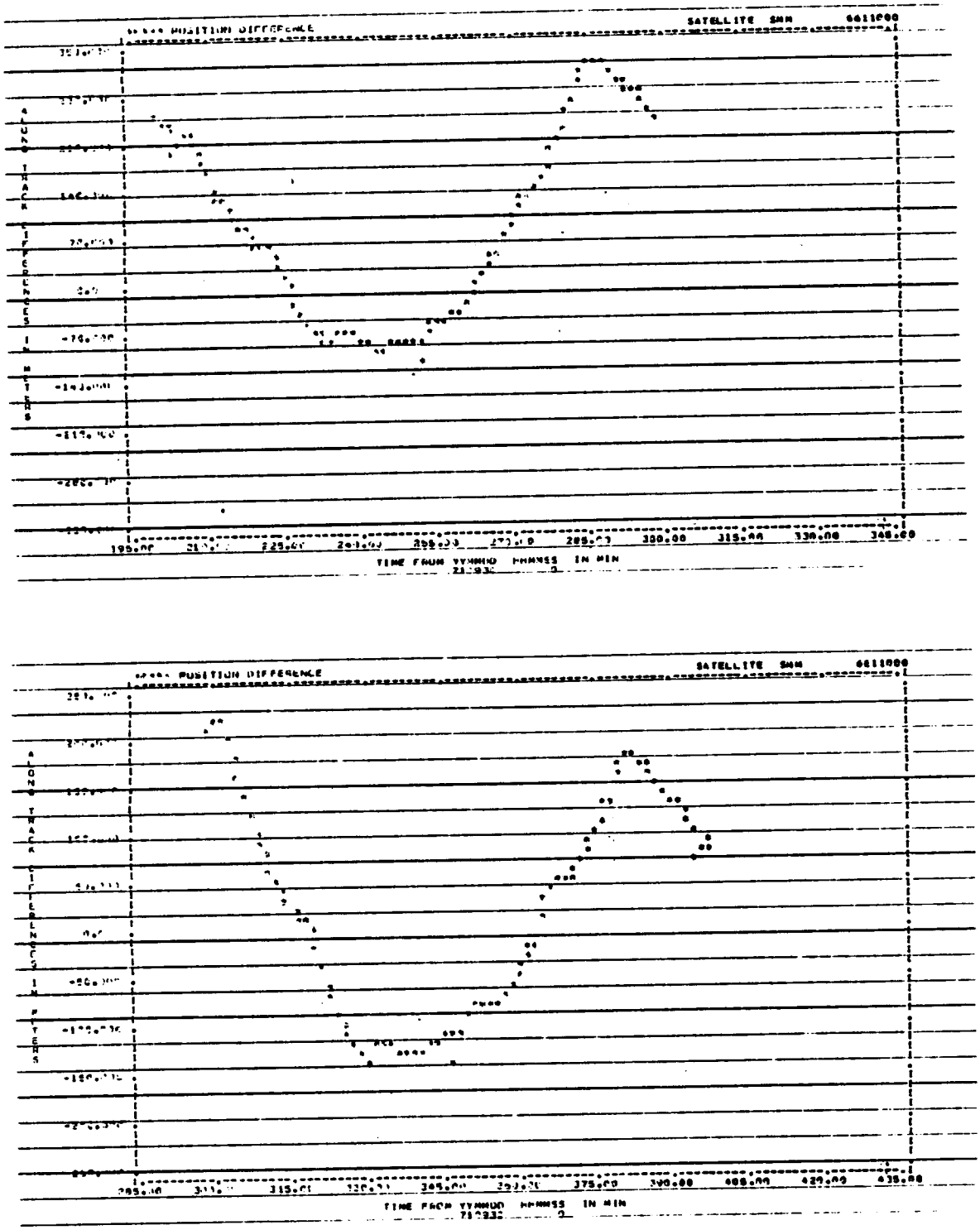

Figure 4-13. Errors in the Representation of the Along-Track Component of Position Using a 29-Term Fourier Series with a 16-Minute Grid Spacing for Case 4 (2 of 2)

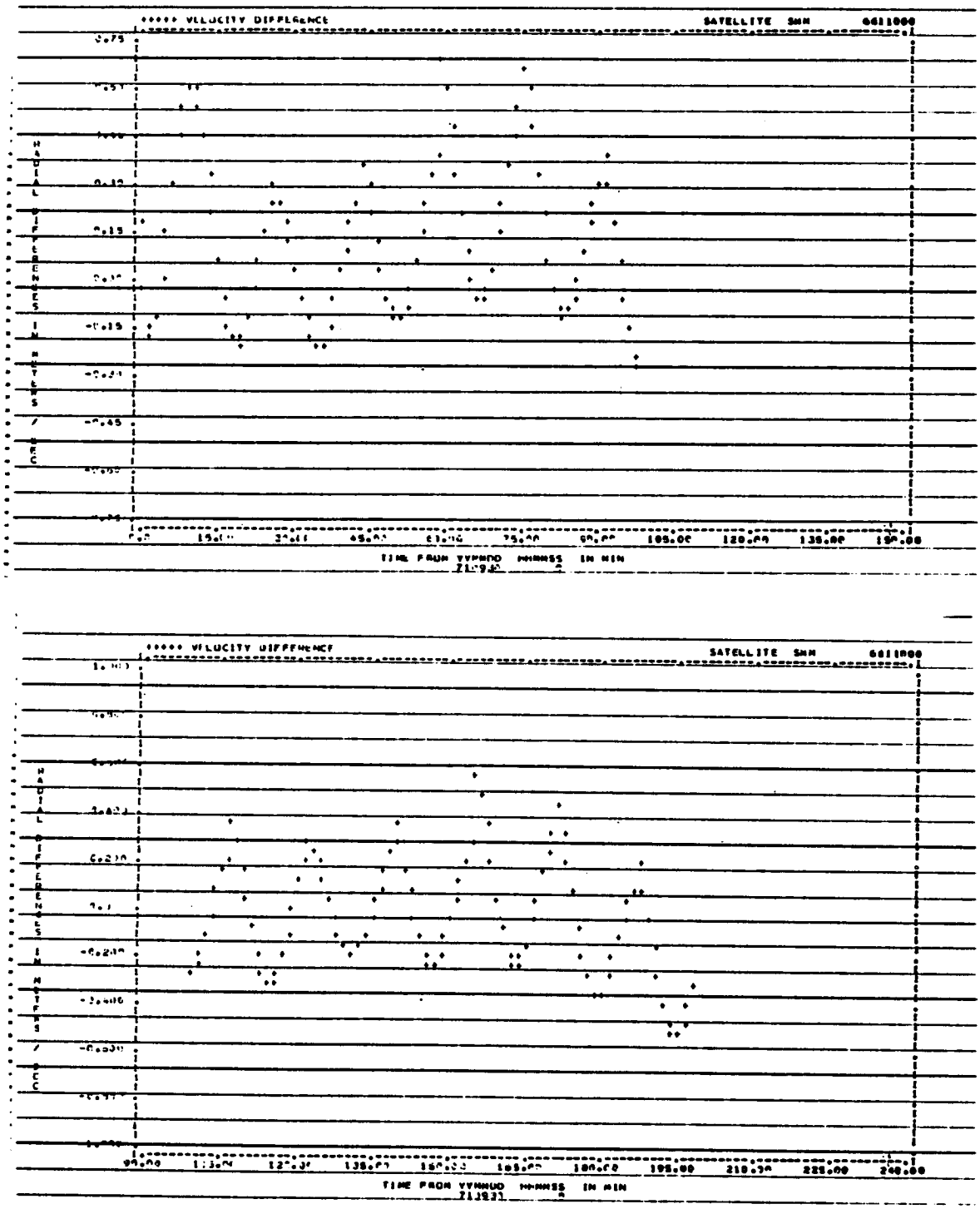

Figure 4-14. Errors in the Representation of the Radial Component of Velocity Using a 29-Term Fourier Series with a 16-Minute Grid Spacing for Case 4 (1 of 2)

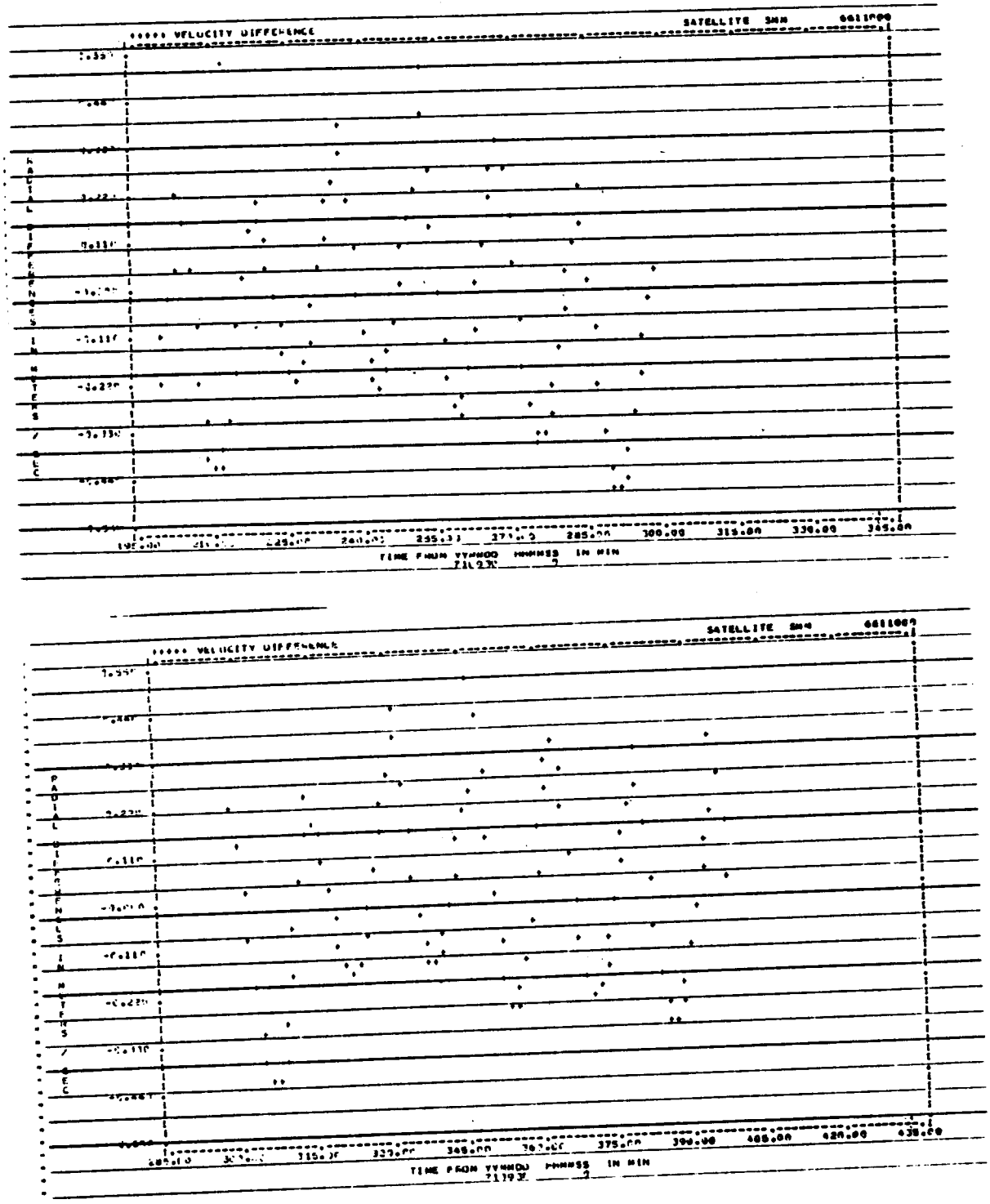

Figure 4-14. Errors in the Representation of the Radial Component of Velocity Using a 29-Term Fourier Series with a 16-Minute Grid Spacing for Case 4 (2 of 2)

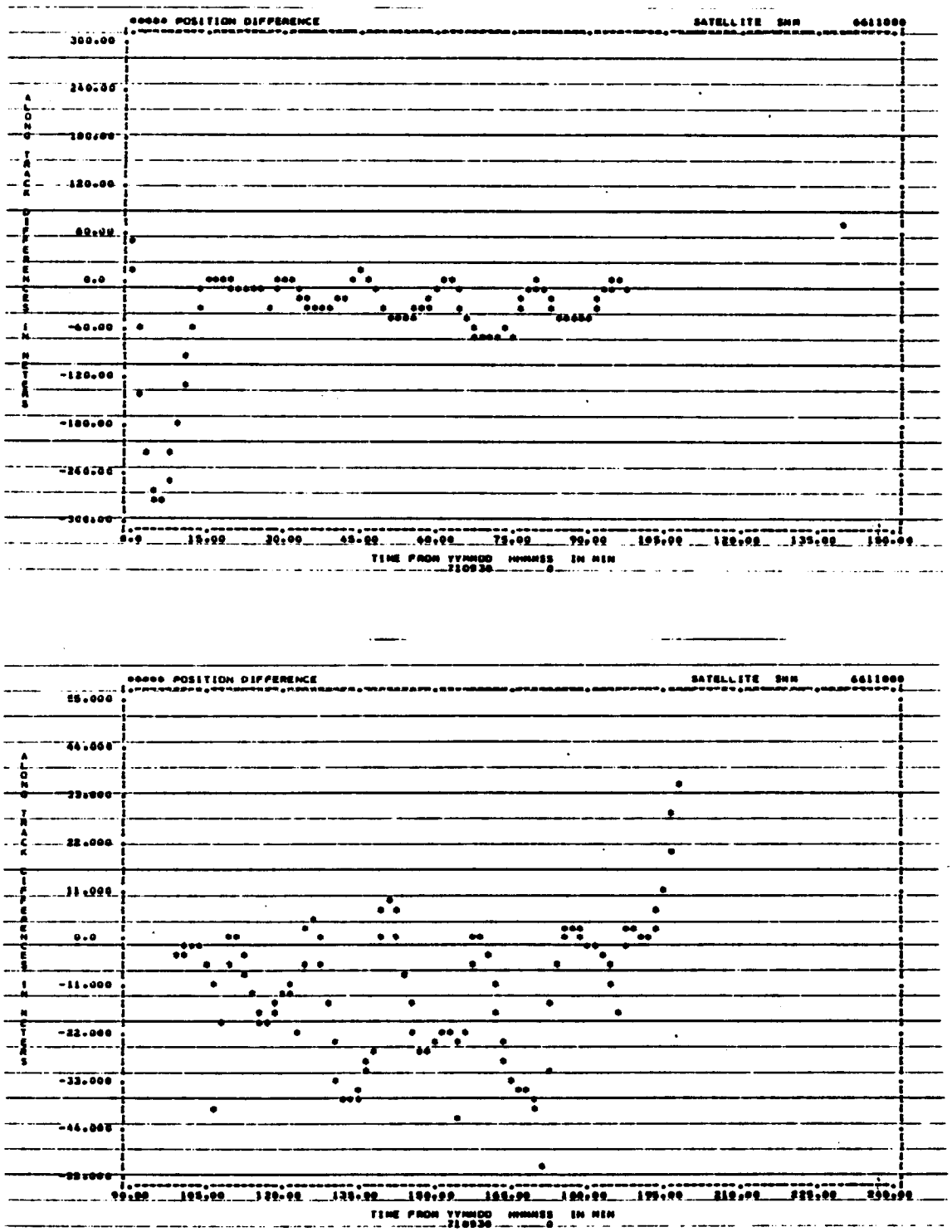

Figure 4-15. Errors in the Representation of the Along-Track Component of Position Using a 29-Term Fourier Series with Position Residuals and a 16-Minute Grid Spacing for Case 4 (1 of 2)

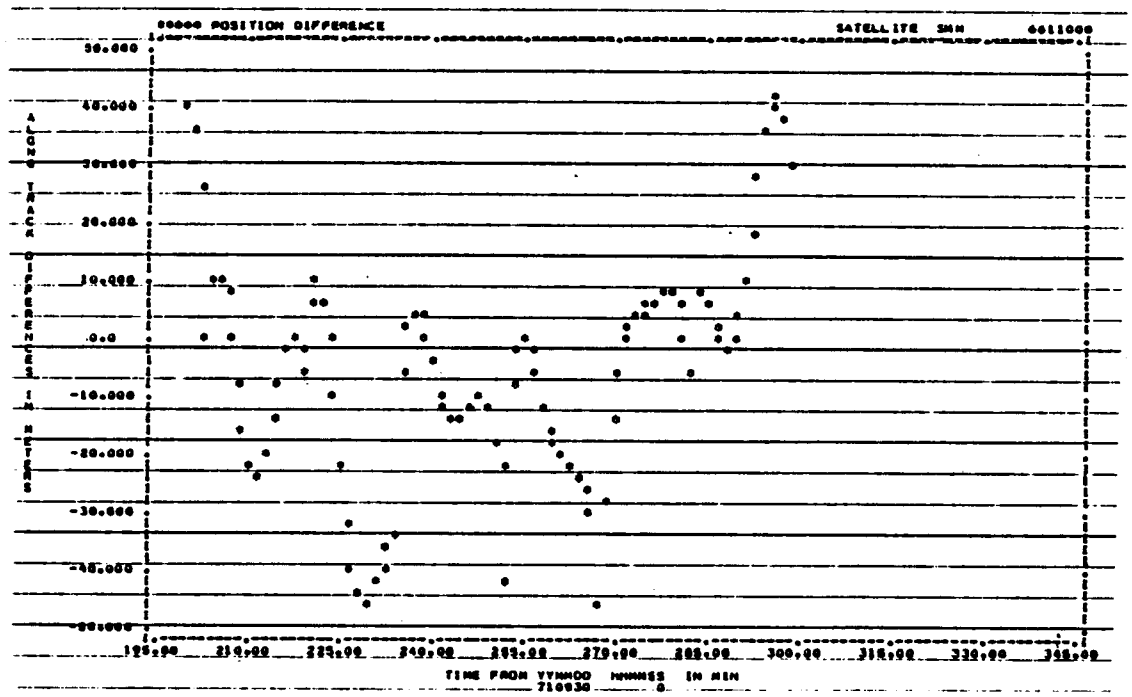

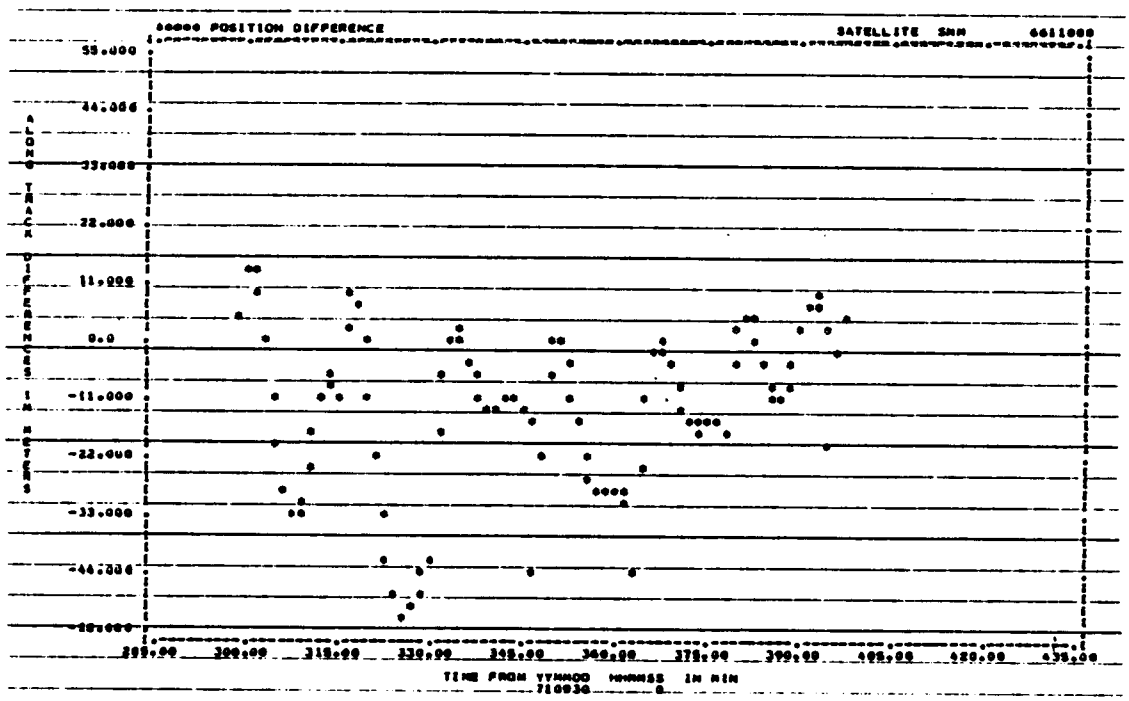

Figure 4-15. Errors in the Representation of the Along-Track Component of Position Using a 29-Term Fourier Series with Position Residuals and a 16-Minute Grid Spacing for Case 4 (2 of 2)

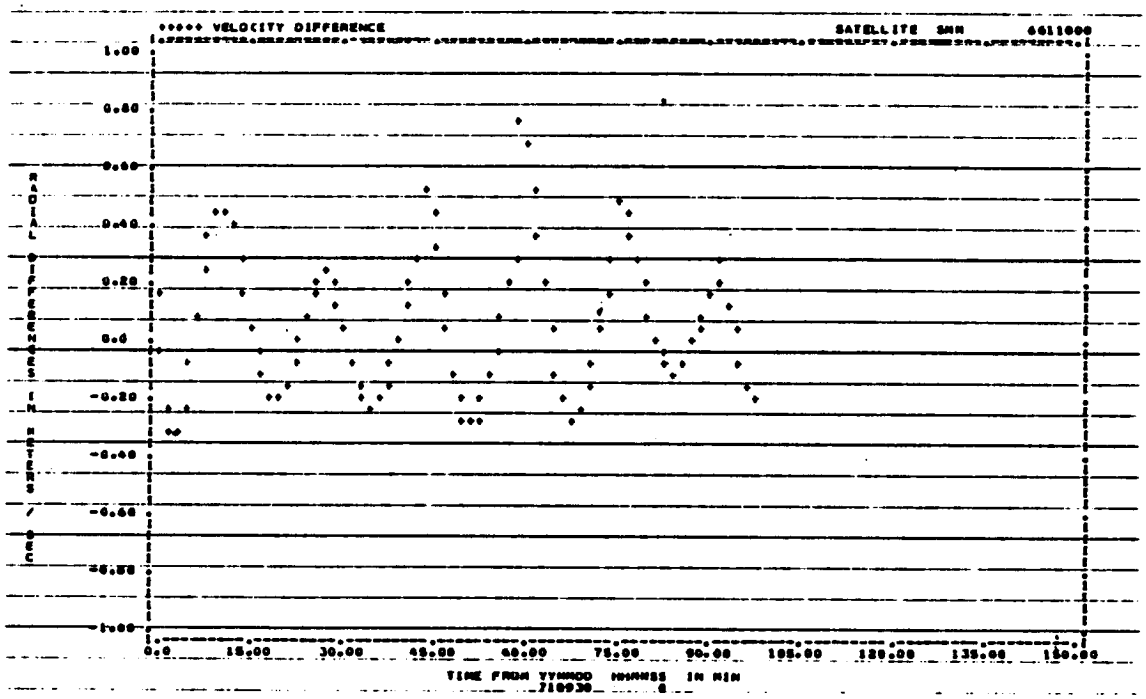

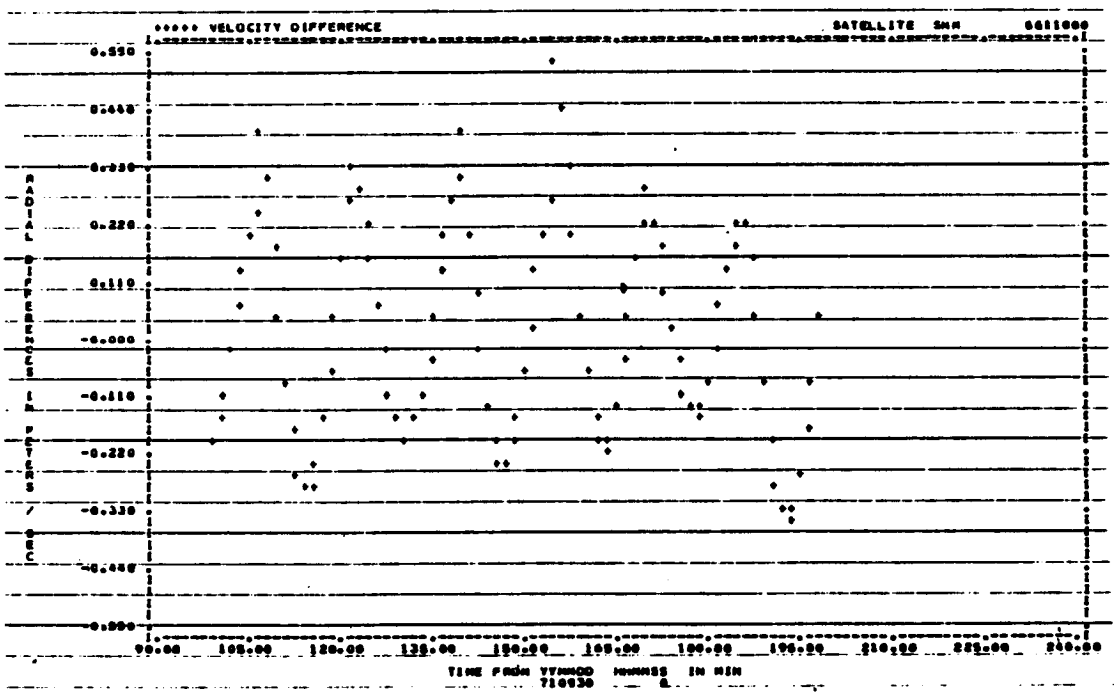

Figure 4-16. Errors in the Representation of the Radial Component of Velocity Using a 29-Term Fourier Series with Position Residuals and a 16-Minute Grid Spacing for Case 4 (1 of 2)

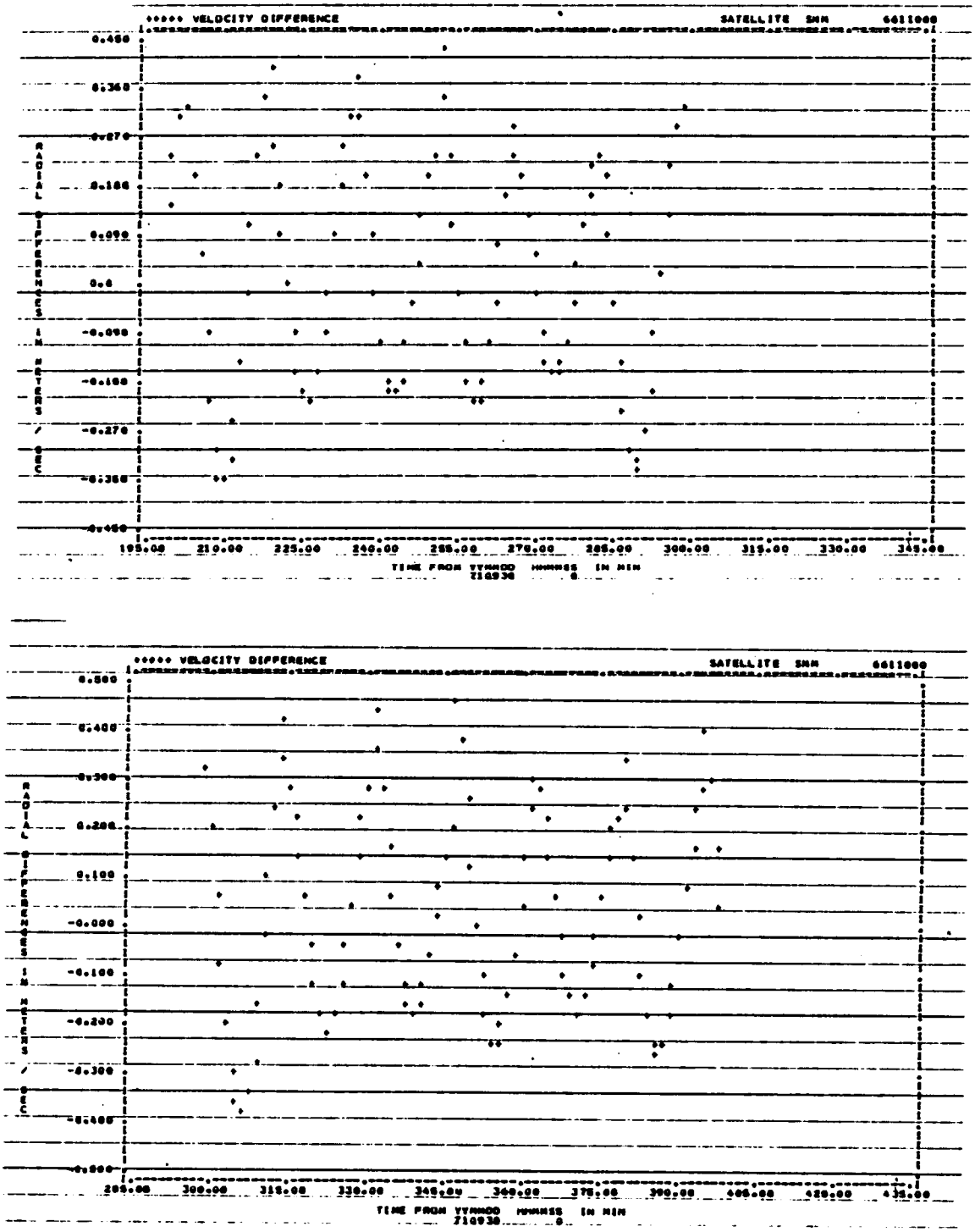

Figure 4-16. Errors in the Representation of the Radial Component of Velocity Using a 29-Term Fourier Series with Position Residuals and a 16-Minute Grid Spacing for Case 4 (2 of 2)

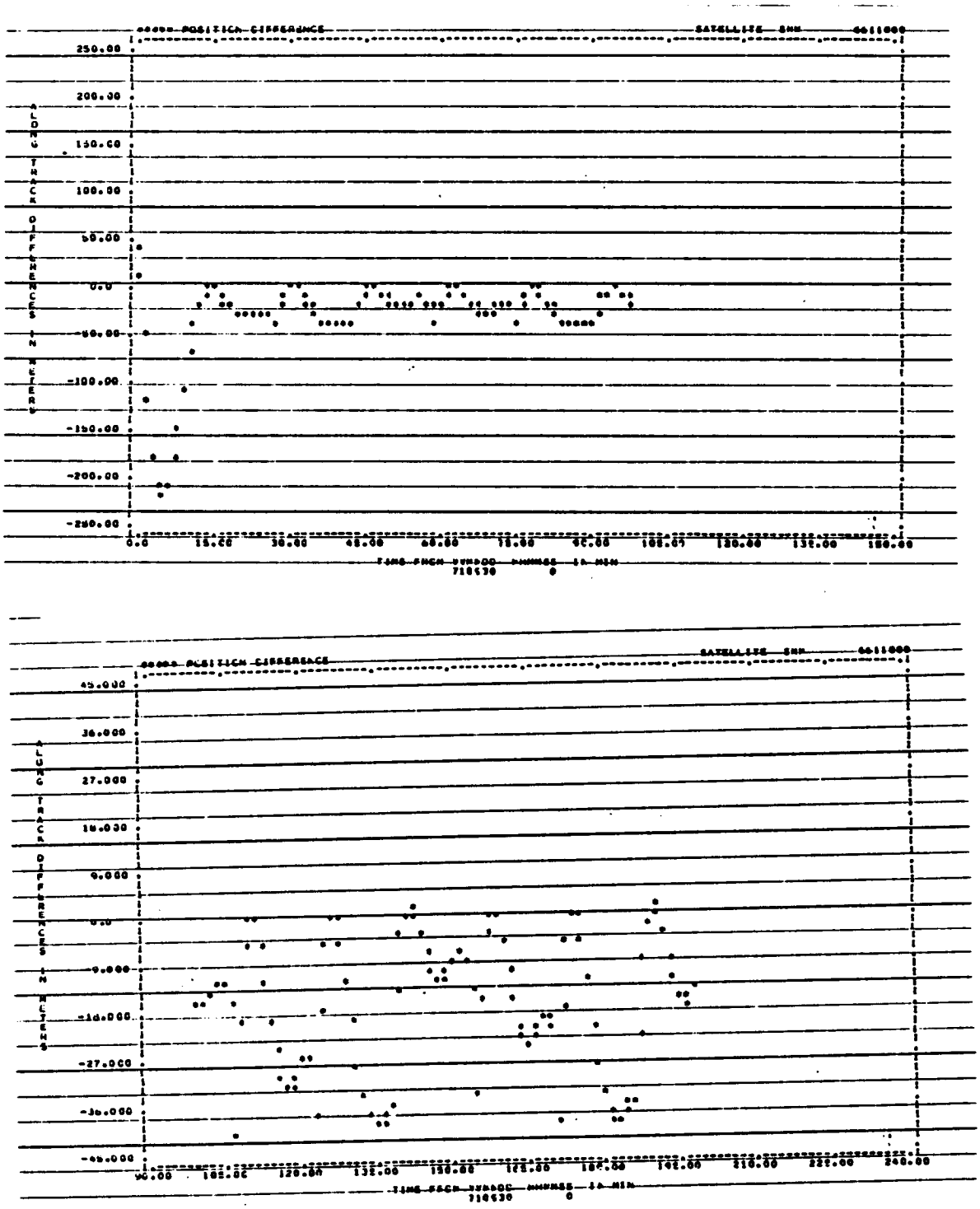

Figure 4-17. Errors in the Representation of the Along-Track Component of Position Using a 29-Term Fourier Series with Position and Velocity Residuals and a 16-Minute Grid Spacing for Case 4 (1 of 2)

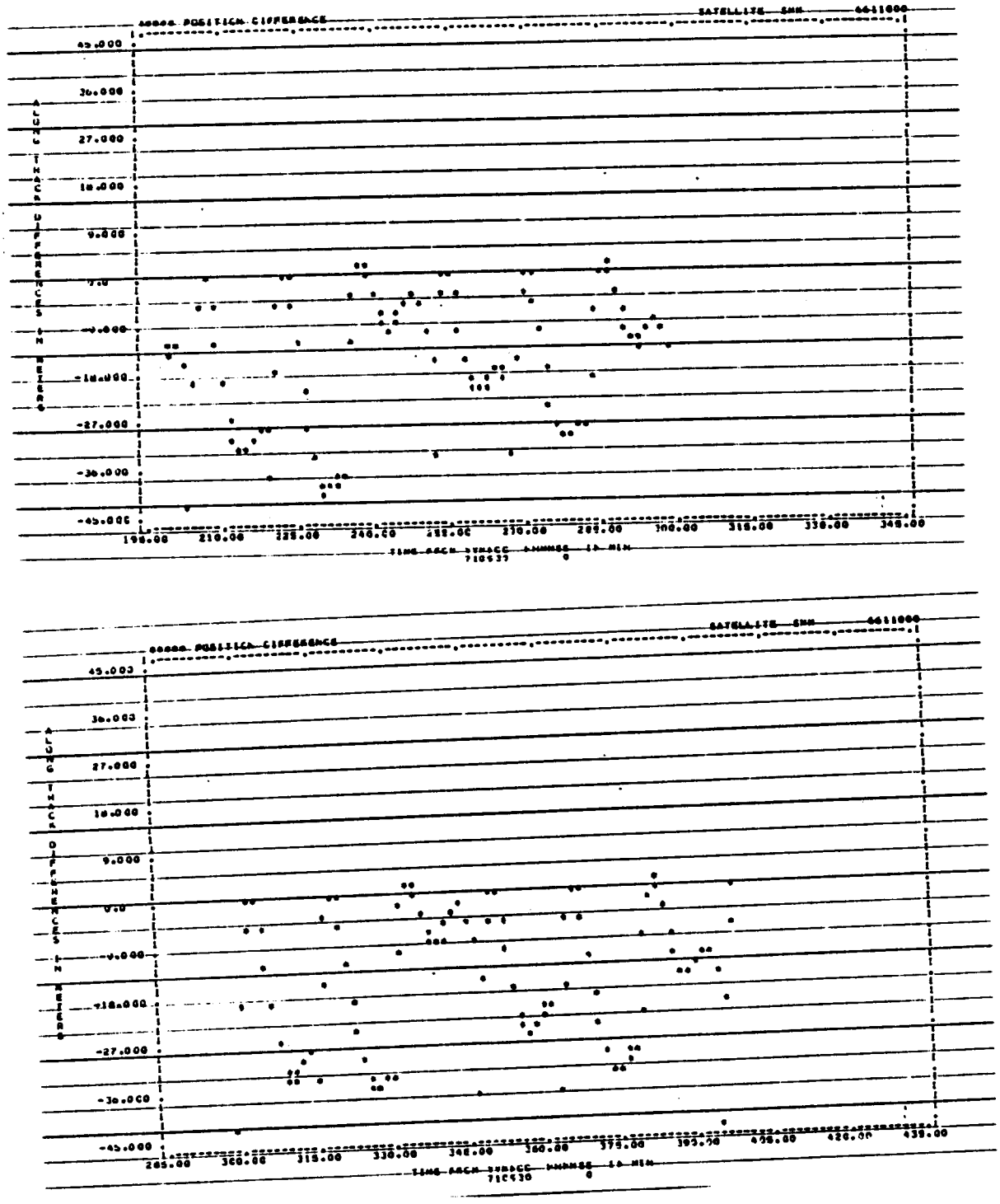

Figure 4-17. Errors in the Representation of the Along-Track Component of Position Using a 29-Term Fourier Series with Position and Velocity Residuals and a 16-Minute Grid Spacing for Case 4 (2 of 2)

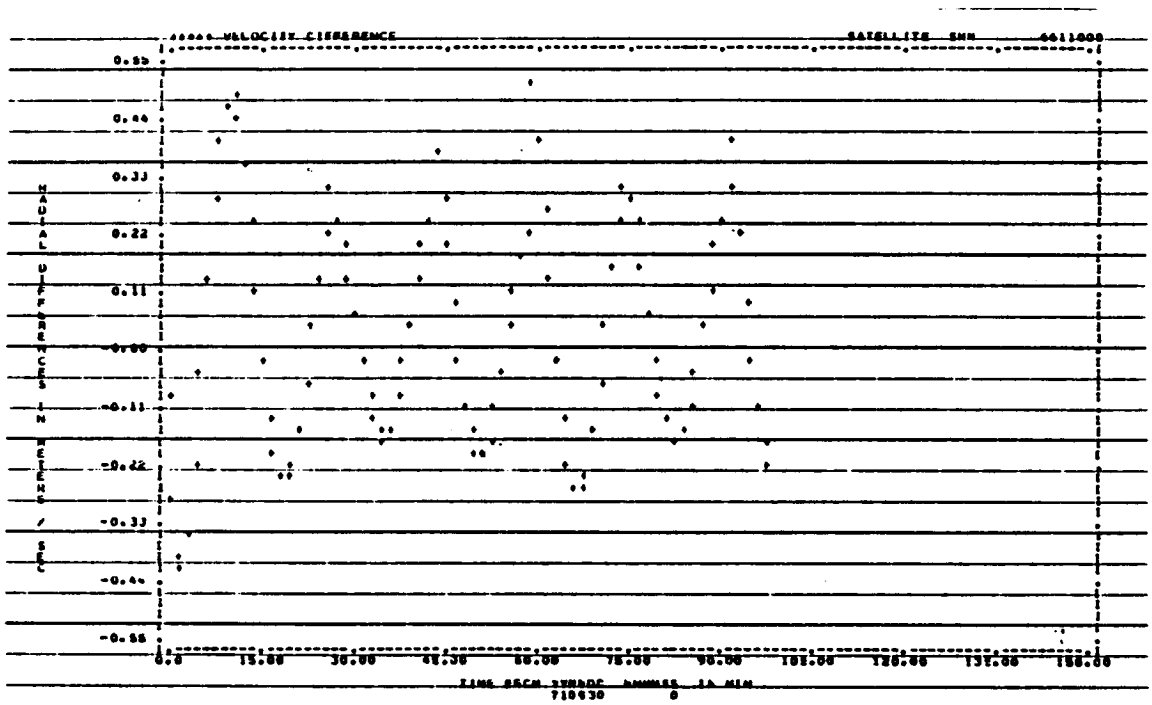

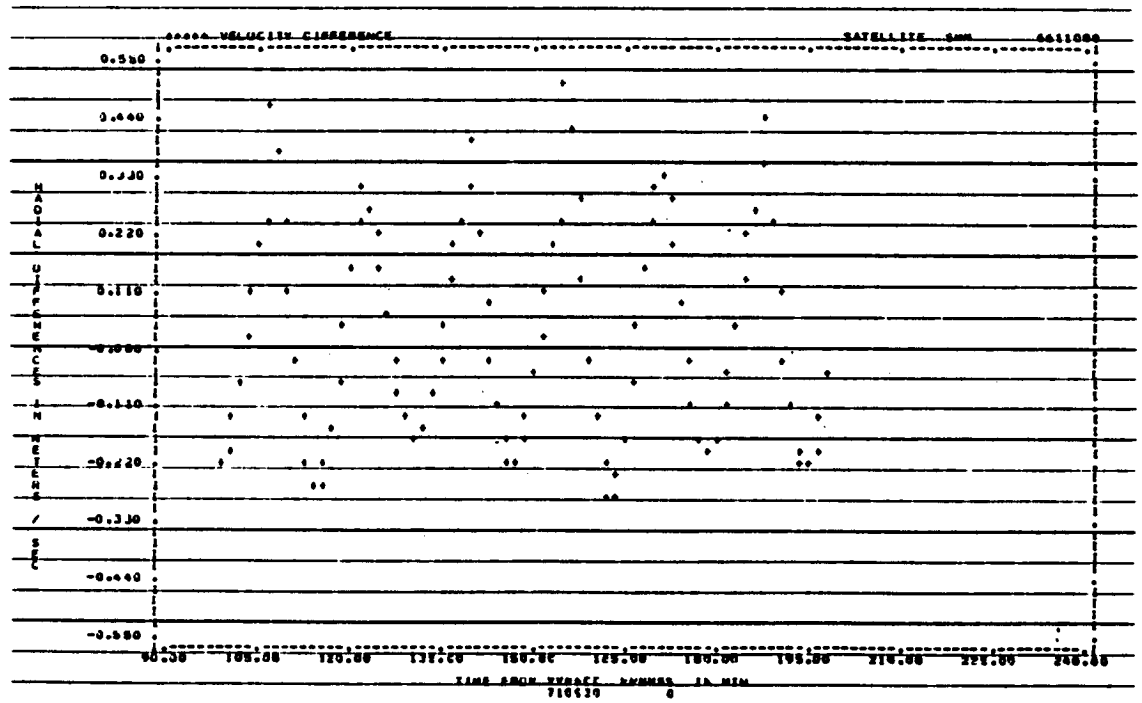

Figure 4-18. Errors in the Representation of the Radial Component of Velocity Using a 29-Term Fourier Series with Position and Velocity Residuals and a 16-Minute Grid Spacing for Case 4 (1 of 2)

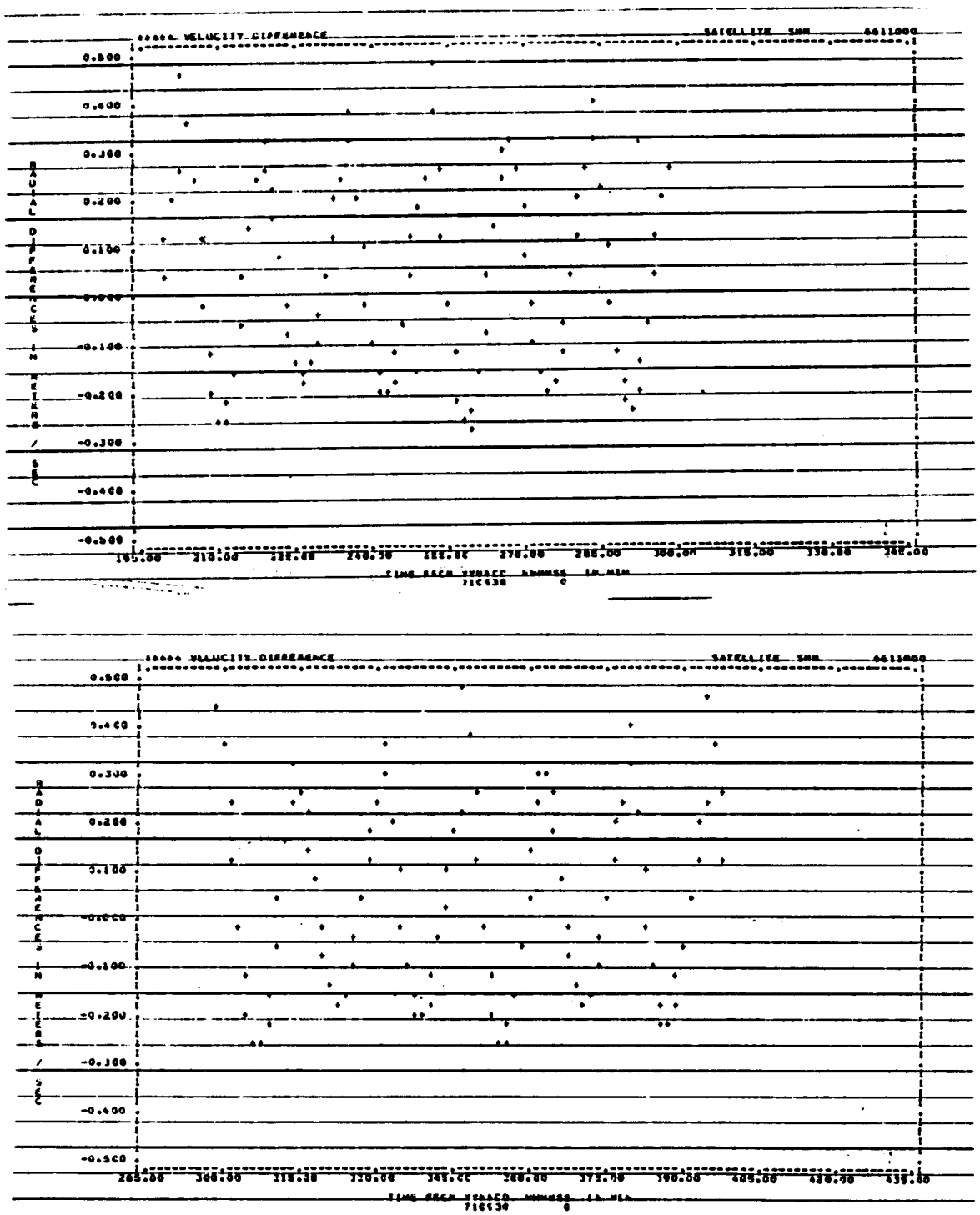

Figure 4-18. Errors in the Representation of the Radial Component of Velocity Using a 29-Term Fourier Series with Position and Velocity Residuals and a 16-Minute Grid Spacing for Case 4 (2 of 2)

Comparison with results presented previously indicates that the accuracy of the ephemeris representation is not highly sensitive to changes in the orbital parameters.

4.4 EFFECT OF VARYING MEAN ORBITAL FREQUENCY

In Section 4.3 SMM ephemeris representation accuracy is evaluated using new state vectors and state parameters. In the present section the same state parameters are used (Case 4 in Table 3-1), except with a newly assigned mean orbital frequency (0.001118344 radians/second). The results are presented in Table 4-1.

4.4.1 No Residuals

When position or velocity residuals are not used, the rms position errors are 0.14 kilometers for the radial component, 0.129 kilometers for the cross-track component, and 0.473 kilometers for the along-track component. The rms velocity errors are 0.667×10^{-3} kilometers/second, 0.135×10^{-3} kilometers/second, and 0.429×10^{-3} kilometers/second, respectively, for the radial, cross-track, and along-track components. The minimum and maximum position differences are 0.447×10^{-5} and 0.509 kilometers, 0.364×10^{-4} and 0.375 kilometers, and, 0.13×10^{-3} and 1.33 kilometers, respectively, for the radial, cross-track, and along-track components.

4.4.2 Position Residuals

When only position residuals are used, the rms position errors are 0.117 kilometers, 0.021 kilometers, and 0.100 kilometers, respectively, for the radial, cross-track, and along-track components. The rms velocity errors are 0.575×10^{-3} kilometers/second for the radial component, 0.109×10^{-3} kilometers/second for the cross-track component, and 0.452×10^{-3} kilometers/second for the along-track component. The minimum and maximum position differences are 0.196×10^{-5} and 0.519 kilometers, 0.813×10^{-7} and

0.11 kilometers, and, 0.228×10^{-8} and 0.392 kilometers for the radial, cross-track and along-track components, respectively.

4.4.3 Position and Velocity Residuals

When both position and velocity residuals are used, the rms position errors are 0.100 kilometers for the radial, 0.567×10^{-3} kilometers for the cross-track, and 0.083 kilometers for the along-track components. The velocity rms errors are 0.453×10^{-3} kilometers/second for the radial component, 0.262×10^{-5} kilometers/second for the cross-track component, and 411×10^{-3} kilometers/second for the along-track component. The minimum and maximum position differences are 0.163×10^{-5} and 0.297 kilometers, 0.347×10^{-9} and 0.323×10^{-2} kilometers, and 0.228×10^{-8} and 0.268 kilometers, for the radial, cross-track, and along-track components, respectively.

Comparison with previously presented results indicates that the representation accuracy is not highly sensitive to small changes in the mean orbital frequency. The differences in the high-precision and the SMM-OBC interpolated trajectories are nearly identical to those in Figures 4-1 through 4-12 and therefore are not reproduced.

SECTION 5 - EXAMINATION OF RESULTS

This section summarizes the results presented in previous sections, uses these results to recommend an ephemeris representation for SMM, and indicates areas for future study.

5.1 SUMMARY OF RESULTS

The following results were derived from the current evaluation:

- A Cartesian ephemeris representation which uses a Fourier series with position and velocity residuals for grid points yields an rms accuracy of 0.13 km over a 3-day SMM trajectory. Using a Fourier series with position residuals at the grid points yields an rms accuracy of 0.16 km. A Fourier series representation for the grid points yields an rms accuracy of 0.5 km.

- For representation of the major features of the SMM trajectory, a 29-term Fourier series (N = 3, M = 4 in Equation (2-4)) is as accurate as a 36-term Fourier series (N = 3, M = 5). Further, a 16-minute interpolation grid interval is nearly as accurate as a 10-minute grid interval in the case where grid point residuals are not used, in addition to being faster in terms of computational time. Further a (-0.25, +0.75) interpolation interval with respect to the second grid point is superior to a (-0.5, +0.5) interpolation interval in terms of the accuracy of the result.

- Keeping the above results in view, analysis was made (see Table 4-1) of other factors (e.g., atmospheric drag, higher order gravity field, orbital eccentricity, and mean orbital frequency) that might affect SMM representation accuracies. The results of this analysis indicate that the representation accuracy is not significantly degraded

by increased drag, increased gravitational effects, small changes in orbital parameters, or small errors in the mean orbital frequency.

5.2 CONCLUSIONS AND RECOMMENDATIONS

From results presented in Tables 3-2 and 4-1, it is evident that an onboard interpolation using the present interpolation scheme with a Fourier series representation for the grid points can produce the required rms accuracy of 2 kilometers. Uplinking position residuals will significantly increase the accuracy (almost 10-fold). The addition of velocity residuals will further improve the result. A comparison of uplink data set length and onboard computer timing requirements is given in Table 5-1. In view of the cost and core requirements, it is suggested that no residuals be uplinked.

5.3 AREAS FOR FURTHER INVESTIGATION

Examination of the graphs of the position error for the case when only a Fourier series is used at the grid points indicates that the dominant error has a periodicity of 1 day and an amplitude of about 0.5 km. In Figure 5-1, a condensed plot of the error in the x position component for Case 4 is presented. The fact that the major residual error source (probably arising from the C_{21} and S_{21} geopotential effects) is not modeled in the Fourier series explains the insensitivity of the representation accuracy to the factors mentioned above. Improvement of the representation accuracy without the use of residuals will require modeling this effect. Therefore the following approaches for future improvement of ephemeris representation accuracy are recommended.

5.3.1 Cartesian Coordinate Representations

The Cartesian ephemeris components could be represented by a trigonometric series based on the dominant perturbing frequencies. For low Earth satellites such as SMM, these would include the spacecraft orbital frequency and its first few harmonics and the Earth's rotational frequency to model nonspherical

Table 5-1. Summary of SMM Results

Fourier Series (Terms)	Residuals	Case	RMS Position Error (km)	RMS Velocity Error (m/sec)	Maximum Position Error (km)	Uplink Coefficients	Uplink Residuals/ 3 Days	Uplink Data Set Length*
29	$\vec{r}, \dot{\vec{r}}$	1	0.13	0.61	0.30	174	1620	1968
29	$\vec{r}, \dot{\vec{r}}$	2	0.13	0.61	0.30	174	1620	1968
29	$\vec{r}$	1	0.16	0.74	0.55	174	810	1158
29	$\vec{r}$	2	0.15	0.74	0.55	174	810	1158
36	-	1	0.50	0.80	1.34	216	0	432
29	-	1	0.51	0.80	1.34	174	0	348
29	-	2	0.51	0.80	1.36	174	0	348
29	-	3	0.53	0.82	1.50	174	0	348
29	-	4	0.48	0.55	1.36	174	0	348

*Single-precision OBC words

Note: All comparisons are over a 3 day arc using a 4-point Hermite interpolation with a Cartesian/Fourier representation for the grid point values spaced at 16 minute intervals.

gravitational effects. For geosynchronous satellites such as TDRS, these would include the spacecraft orbital frequency and its first few harmonics and the lunar frequency.

Investigation of such a representation was not pursued for SMM because a trigonometric series involving two primary frequencies would require the additional computation in the OBC of 1 sine and 1 cosine which is prohibitively expensive in the case of the NSSC-1. However, in such cases where the OBC ephemeris computation budget is small, a polynomial approximation to the longer frequency effects might yield a significant improvement in accuracy without much additional OBC cost.

For medium to high eccentricity orbits, trigonometric series in terms of the true anomaly should produce more compact representations than series in terms of time (or equivalently mean anomaly).

In the current study an interpolation scheme was adopted to save computational time in the OBC. In cases for which there is a less stringent budget for ephemeris representation, the trigonometric series could be directly evaluated at each request time thereby considerably simplifying the required OBC logic.

5.3.2 Orbital Element Representations

The orbital elements could be represented by mean elements to account for secular and long-period motion plus a Fourier or Chebyshev series representation for the short-period motion.

APPENDIX A - SMM ONBOARD COMPUTATION ALGORITHM

The purpose of this appendix is to describe the recommended algorithm for spacecraft ephemeris computation onboard the Solar Maximum Mission (SMM) satellite, the first of a series of Multimission Modular Spacecraft (MMS) satellites.

The selection was aimed at satisfying the SMM mission requirement. The selection was based on the following assumptions: (1) a 2 kilometer root-mean-squared position vector representation accuracy requirement during the normal upload period (3 days), and (2) the need for inertial Cartesian coordinates (i.e., position and velocity components) only, at a moderately frequent interval in the range of several tens of seconds.

The selected algorithm uses a Cartesian coordinate representation with a Fourier-power series data compression technique along with a four-point Hermite interpolator (Reference 1) and is an extension of the Air Force Block 5D algorithm (Reference 7). Apart from data compression, the Fourier-power representation also permits (with reduced accuracy) extrapolation beyond the normal upload period. The approximate onboard computational time per interpolation, exclusive of overhead, is estimated to be about 20 milliseconds. In addition, grid point computations, performed once per grid interval, cost about 120 milliseconds. The onboard core storage requirement for a 3-day upload is estimated to be about 350 single precision words.

The ground upload data set will consist of: (1) a reference time indicating the start time of the ephemeris file (t_R), (2) a grid interval (g), (3) the grid interval inverse (g^{-1}), (4) a mean orbital frequency (w), and (5) six sets of 29 Fourier-power coefficients (one set each for x, y, z, $\dot{x}$, $\dot{y}$, and $\dot{z}$, the set consisting of the coefficients A_1 through A_5, A_7 through A_{11}, A_{13} through A_{17}, A_{19} through A_{22}, A_{24} through A_{27}, A_{29} through A_{31}, and A_{33} through A_{35}, in Equation 2-5, all in double-precision words on the OBC.

A block diagram of the OBC orbit representation program is given in Figure A-1. The revised requirement specification for the SMM OBC algorithm follows.

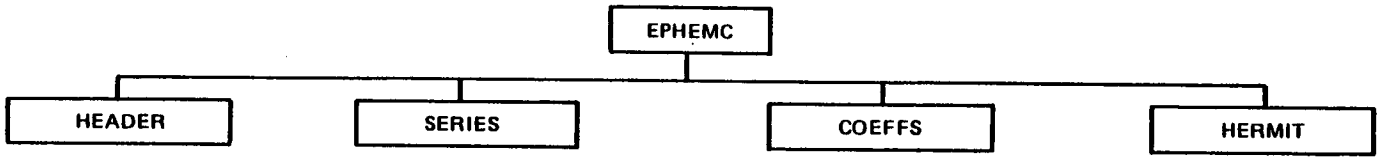

A. HEADER CALLED TO READ NEWLY UPLINKED DATA

B. SERIES CALLED EACH TIME A NEW GRID POINT IS REQUIRED

1. FOURIER-POWER SERIES EVALUATED TO GIVE STATE VECTOR FOR GRID TIME

2. RESIDUAL VECTOR ADDED TO ABOVE VECTOR TO BETTER APPROXIMATE EPHEMERIS VECTOR (OPTIONAL)

C. COEFFS CALLED TO COMPUTE HERMITEAN INTERPOLATION COEFFICIENTS IF A NEW GRID POINT WAS EVALUATED

D. HERMIT INTERPOLATES FOR STATE VECTOR AT REQUESTED TIME

E. PROGRAM MOVES THE 4-POINT TIME GRID THROUGH TIME BY SUCCESSIVE CALLS TO SERIES UNTIL REQUEST TIME IS APPROPRIATELY SURROUNDED BY THE 4 POINTS

Figure A-1. Structure of Orbit Representation Program

REQUIREMENT SPECIFICATION
SMM OBC APPLICATIONS PROCESSOR: EPHEMERIS COMPUTATION

- Title: Onboard Spacecraft Ephemeris Computation (EPHEMC)
  Contributor: P. S. Desai P S Desai
  Reviewed by: A. C. Long ACL
  Date: January 28, 1976, revised December 15, 1977

- Function: This module computes the SMM spacecraft ephemeris (Cartesian position and velocity components) at a requested time, using orbit uplink data stored in memory.

- Real-Time Inputs: The time at which the ephemeris information is desired,[1] t, and a logical flag IFIRST (which = .TRUE. at the first call after the orbit data base is changed using a recent uplink data set)

- Data Base: The following data are used; all of these data must be uplinked from the ground periodically (e.g., nominally once every 3 days) and they must be stored in COMMON via a call to HEADER.

FORTRAN Name	Symbol	Precision[2]	Description
TREF	t_R	ms	Reference time (absolute S/C clock time) in seconds
TFIRST	t_F	32 μs	Time relative to t_R of first time for which Fourier coefficients are valid
TEND	t_E	32 μs	Relative time of last time for which Fourier coefficients are valid
GRID	g	32 μs	Grid interval in seconds
GRIDIN	g^{-1}	10^{-13} sec^{-1}	Reciprocal of the grid interval

[1]Successive values of t must be in increasing order.

[2]Units are as follows: ms = millisecond, μs = microsecond, sec = second.

FORTRAN Name	Symbol	Precision	Description
OMEG	w	10^{-13} rad/sec	Mean orbital frequency
AB(29, 6)	A, B	**	Fourier-power coefficients

- Real-Time Outputs: Spacecraft Cartesian coordinates (x, y, z, $\dot{x}$, $\dot{y}$, $\dot{z}$) at the requested time (in kilometers and meters/second) and a logical flag INTERP (which = .TRUE. for interpolated coordinates, = .FALSE. for extrapolated coordinates. Also, an error flag or error return is indicated when the request time is outside the specified span of applicability (i.e., from $t_R + t_F$ to $t_R + t_E$).

- Interface With Other Software Elements: None. EPHEMC, along with its associated submodules HEADER, SERIES,† COEFFS, HERMIT, and COMMON block EPHCOM, forms a self-contained module that can be used by the EXECUTIVE without calling on any other applications modules.

- Hardware and Sequencing Requirements: TBD. It may help to know that each call to SERIES and COEFFS (occurring once every grid interval, or about 16 minutes) costs about 120 milliseconds, while each call to HERMIT (occurring every interpolation interval, or about 1 minute) costs about 20 milliseconds.††

*Units are as follows: rad = radians, sec = seconds.

**Precision is such as to yield 0.1 meters and 0.1 millimeters/second in $\vec{r}$ and $\dot{\vec{r}}$, respectively.

†This submodule calls the sin and cos functions.

††These figures are based on a 200 μs DP multiplication time; this is subject to revision.

- Implementation Requirements:

Quantity	Type	Expected Range of Values	Units	Scaling**	
				Power of 10	Power of 2
t_R	D	$0 - 1.6 \times 10^7$	sec	3	10
t_F	D	$(-3) - 0 \times 10^5$	sec	4	15
t_E	D	$1 - 3 \times 10^5$	sec	4	15
g	D	400 - 16,000†	sec	4	15
g^{-1}	D	$0.0625 - 2.5 \times 10^{-3}$	sec^{-1}	12	42
w	D	$1 - 1.2 \times 10^{-3}$	rad/sec	12	42
A, B	D	Variable, but well within the DW (double word) limit after scaling	km, m/sec	4	14
			km/sec, m/sec^2	10	32
			km/sec^2, m/sec^3	15	50
			km/sec^3, m/sec^4	20	68
			km/sec^4, m/sec^5	25	86
			km/sec^5, m/sec^6	30	104

All operations should be in double precision.

**The powers of 10 and 2 given here do not necessarily correspond exactly with one another. In actual OBC coding, the power of 2 will be used.

The suggested scaling allows for a millisecond time precision; in practice, a 16 millisecond precision is expected. This means that the 5th bit from the right will change every 16 milliseconds.

†Typical values are 960 seconds (SMM).

- Algorithm Description: The onboard ephemeris algorithm for SMM is given below. It consists of a main routine (EPHEMC) and the four subroutines HEADER, SERIES, COEFFS, and HERMIT. Also, one COMMON block is needed for communication among ephemeris modules; this COMMON block is defined later. All variables and operations are to be in double precision or simulated double precision on the OBC. The design described here attempts to satisfy OBC constraints, such as the 4K limit on each module and each COMMON block and the limit of eight control statements. After coding, a final verification must be made that the constraints are not exceeded.

1. EPHEMC: The input to the main routine EPHEMC is the request time, t, and the output is the set of spacecraft coordinates ($x, y, z, \dot{x}, \dot{y}, \dot{z}$) at time t and an optional flag INTERP indicating interpolated or extrapolated coordinates. It is assumed that successive input time values will be in increasing sequence. In fact, in view of the high grid point computational cost, this is also a recommended method of using this ephemeris algorithm. The input times will be constrained to vary from $t_R + t_F$ (e.g., $t_R - 1.5x86,400$) to $t_R + t_E$ (e.g., $t_R + 1.5x86,400$). Steps followed by the main routine are as follows:

   a. At the first call,† subroutine HEADER will be called. Next, an internal variable t_0 will be set equal to $-g + t_F$ and the flags ENDFIL, NEW, and INTERP will be set to .FALSE., .TRUE., and .TRUE., respectively. Then, in a loop for I = 1 to 4, the following operations will be performed:

      (1) The switch IGRID will be set equal to I

      (2) The quantity t_0 will be incremented by g

†A variable IFIRST must be set by the calling routine before calling EPHEMC.

(3) The quantity $t_g(I)$ will be set equal to t_0

(4) Subroutine SERIES will be called

b. The relative time for computation will be evaluated as follows:

$$t_c = t - t_R$$

If t_c is greater than t_E or less than $t_g(1)$, an error exit is taken.

c. If t_c is less than $t_g(2) + 3g/4$, go to step (e). Otherwise, NEW is set equal to .TRUE. and the values $t_g(2\text{-}4)$ and $x_g(1\text{-}6, 2\text{-}4)$ are loaded into $t_g(1\text{-}3)$ and $x_g(1\text{-}6, 1\text{-}3)$, respectively. The value $t_g(4)$ is set equal to $t_g(4) + g$, IGRID is set equal to 4, and SERIES is called.

d. Go to step (c).

e. If NEW is equal to .FALSE., go to step (f); otherwise, set NEW = .FALSE. and call subroutine COEFFS.

f. Call subroutine HERMIT.

g. The quantities $x_c(1\text{-}3)$ and $v_c(1\text{-}3)$, which are returned by subroutine HERMIT via COMMON, are loaded into the output variables x, y, z, $\dot{x}$, $\dot{y}$, and $\dot{z}$ and a return is taken.

2. HEADER: This routine will read the input ground update file, compute g_2,* and store t_R, t_E, T_F, w, g, g^{-1}, g_2, and the 174-Fourier-power coefficients, AB, in a COMMON block. The satellite ID and other protocol information may also be read from the header.

*Here, $g_2 = g/1000$.

3. SERIES: This subroutine evaluates the Fourier-power series using coefficients stored in COMMON by subroutine HEADER. First, an internal variable t is set equal to t_g(IGRID). Next, S = sinwt and C = cos wt are computed. Finally, the following computations are carried out for the three position and three velocity coordinates.

$$
\begin{aligned}
x_g(I,IGRID) = {} & A_1(I) + t\Big\{A_2(I) + t\Big[A_3(I) + t\big(A_4(I) + t\,A_5(I)\big)\Big]\Big\} \\
& + S\Big\{A_7(I) + t\Big[A_8(I) + t\big(A_9(I) + t\big(A_{10}(I) + t\,A_{11}(I)\big)\big)\Big]\Big\} \\
& + C\Big\{A_{13}(I) + t\Big[A_{14}(I) + t\big(A_{15}(I) + t\big(A_{16}(I) + t\,A_{17}(I)\big)\big)\Big]\Big\} \\
& + S\Big\{S\Big[A_{19}(I) + t\big(A_{20}(I) + t\big(A_{21}(I) + t\,A_{22}(I)\big)\big)\Big] \\
& + S\Big[S\big(A_{29}(I) + t\big(A_{30}(I) + t\,A_{31}(I)\big)\big) \\
& + C\big(A_{33}(I) + t\big(A_{34}(I) + t\,A_{35}(I)\big)\big)\Big]\Big\}
\end{aligned}
$$

4. COEFFS: In this subroutine, the Hermitean coefficient matrix Y(6,3) is filled using the grid point values x_g(6,4) as follows.

For J = 1 to 3, the following computations are carried out:

$$Y(1,J) = \frac{56.}{108.} xg(J,1) - \frac{11.}{4.} xg(J,2) + 2. xg(J,3) + \frac{25.}{108.} xg(J,4)$$
$$+ g_2\left[\frac{1.}{9.} xg(J+3,1) - xg(J+3,2) - xg(J+3,3) - \frac{1.}{18.} xg(J+3,4)\right]$$

$$Y(2,J) = \frac{-124.}{108.} xg(J,1) + \frac{1.}{4.} xg(J,2) + xg(J,3) - \frac{11.}{108.} xg(J,4)$$
$$+ g_2\left[-\frac{2.}{9.} xg(J+3,1) - \frac{7.}{4.} xg(J+3,2) + \frac{1.}{36.} xg(J+3,4)\right]$$

$$Y(3,J) = \frac{50.}{108.} xg(J,1) + \frac{5.}{2.} xg(J,2) - \frac{5.}{2.} xg(J,3) - \frac{50.}{108.} xg(J,4)$$
$$+ g_2\left[\frac{1.}{36.} xg(J+3,1) + 2. xg(J+3,2) + \frac{7.}{4.} xg(J+3,3) + \frac{1.}{9.} xg(J+3,4)\right]$$

$$Y(4,J) = \frac{59.}{108.} xg(J,1) - \frac{1.}{2.} xg(J,2) - \frac{1.}{4.} xg(J,3) + \frac{22.}{108.} xg(J,4)$$
$$+ g_2\left[\frac{7.}{36.} xg(J+3,1) + \frac{1.}{2.} xg(J+3,2) - \frac{1.}{4.} xg(J+3,3) - \frac{1.}{18.} xg(J+3,4)\right]$$

$$Y(5,J) = \frac{-52.}{108.} xg(J,1) - \frac{3.}{4.} xg(J,2) + xg(J,3) + \frac{25.}{108.} xg(J,4)$$
$$+ g_2\left[\frac{-5.}{36.} xg(J+3,1) - xg(J+3,2) - \frac{3.}{4.} xg(J+3,3) - \frac{1.}{18.} xg(J+3,4)\right]$$

$$Y(6,J) = \frac{11.}{108.} xg(J,1) + \frac{1.}{4.} xg(J,2) - \frac{1.}{4.} xg(J,3) - \frac{11.}{108.} xg(J,4)$$
$$+ g_2\left[\frac{1.}{36.} xg(J+3,1) + \frac{1.}{4.} xg(J+3,2) + \frac{1.}{4.} xg(J+3,3) + \frac{1.}{36.} xg(J+3,4)\right]$$

In actual coding, preevaluated values of numerical factors such as 59./108., etc., should be used in order to reduce onboard computations. Reciprocals of 2.0 and its powers may be treated as division.

Thus, the last equation given above would appear as

$$Y(6,J) = 1018518519. \times 10^{-10}\left[x_g(J,1) - x_g(J,4)\right] + \frac{x_g(J,2) - x_g(J,3)}{4.}$$

$$+ g_2\left\{277777778. \times 10^{-10}\left[x_g(J+3,1) + x_g(J+3,4)\right] + \frac{x_g(J+3,2) + x_g(J+3,3)}{4.}\right\}$$

5. HERMIT: This subroutine interpolates for position and velocity at the request time t_c, using the Hermitean coefficient matrix, Y. First, an internal variable p, representing the relative time ratio, is computed as follows:

$$p = g^{-1}(t_c - t_g(2))$$

where g^{-1} has been stored in COMMON by subroutine HEADER.

Next, for I = 1 to 3, the position and velocity components are computed as

$$x_c(I) = x_g(I,2) + p\left\{g_2 x_g(I+3,2) + p\left[Y(1,I) + p(Y(2,I) + p(Y(3,I) + p(Y(4,I) + p(Y(5,I) + pY(6,I)))))\right]\right\}$$

$$v_c(I) = x_g(I+3,2) + g^{-1}\left\{p\left[2.Y(1,I) + p(3.Y(2,I) + p(4.Y(3,I) + p(5.Y(4,I) + p(6.Y(5,I) + p.7\,Y(6,I)))))\right]\right\} \times 10^3$$

In order to save time at the expense of a slightly increased core size, the quantities 3Y(2,1-3), 5Y(4,1-3), 6Y(5,1-3), and 7Y(6,1-3) should be stored in COMMON by subroutine COEFFS and simply accessed when evaluating v_c, above. (The units for x_c and v_c are kilometers and meters/second, respectively.)

7. COMMON: A COMMON block /EPHCOM/ will be used for the following information:

Variable	Type*	Starting Location	Description
t_R	D	R1	Reference time
g	D	2	Grid interval
g^{-1}	D	3	Reciprocal of the grid interval
w	D	4	Orbital frequency
AB(29,6)	D	5	Fourier-power coefficients
$t_g(4)$	D	221	Grid times
$x_g(6,4)$	D	225	Grid Cartesian coordinates
t_c	D	249	Relative request time
Y(6,3)	D	250	Hermitean coefficient matrix
$x_c(3)$	D	268	Computed position (km)
$v_c(3)$	D	271	Computed velocity (m/sec)
g_2	D	274	Grid interval divided by 1000.
YY(4,3)	D	275	Values of 3Y(2,1-3), 5Y(4,1-3), 6Y(5,1-3), and 7Y(6,1-3)
t_E	D	276	Span of applicability--relative end time
t_F	D	277	Relative time of first residual
IGRID	I	I1	Current grid point
ENDFIL	L	L1	"End-of-residual-file" indicator
NEW	L	2	"Coefficients required" indicator
IFIRST	L	3	Call indicator: IFIRST = .TRUE., first call IFIRST = .FALSE., subsequent calls

*D = double-precision on the OBC; = REAL*4 on the PDP or the IBM S/360.
I = integer on the OBC; = INTEGER*2 on the PDP or the IBM S/360.
L = LOGICAL on all machines.

APPENDIX B - RECENT TRACKING AND DATA RELAY SATELLITE (TDRS) RESULTS

In Reference 4 we have discussed several ephemeris representations for the TDRSS-spacecraft. Both interpolation and extrapolation accuracies were evaluated by comparison with a high-precision ephemeris. Comparison of the trigonometric (Fourier) series representation of the Cartesian variables using coeffecients A_1, A_7, A_8, A_{13}, A_{14}, A_{19}, and A_{24} in Equation (2-5) with a high precision ephemeris obtained from the GTDS did not show significant differences in the position and velocity errors using Fourier series coefficients determined from high precision data spaced at 100- , and 150-minute intervals. Consequently, it was recommended that a 150-minute data interval be used. In view of the above results, we have attempted to compute Fourier series coefficients using data spaced at 200-minute intervals. An updated table along with the earlier results are given in Table B-1. For completeness the TDRSS state vectors are also presented in Table B-2. The result shows that even a 200-minute (data) interval is acceptable in terms of accuracy needs and hence can be used, further reducing the computational cost.

Table B-1. Summary of TDRSS Representation Accuracies

REPRESENTATION	INTER-POLATOR	GRID SPACING (MIN)	RMS POSITION ERROR				RMS VELOCITY ERROR				MAXIMUM POSITION ERROR			
			H (km)	C (km)	L (km)	$\Delta\vec{R}$ (km)	H (m/s)	C (m/s)	L (m/s)	$\Delta\vec{R}$ (m/s)	H (km)	C (km)	L (km)	$\Delta\vec{R}$ (km)
MEAN ELEMENT	6TH ORDER ADAMS	1440	1.2162	0.1906	0.6257	1.3809	0.03074	0.01225	0.09313	0.09883	1.7727	0.2810	1.3337	1.9090
MEAN ELEMENT	2-POINT HERMITE	5760	1.2151	0.2284	0.6416	1.3929	0.03276	0.01040	0.09304	0.09919	1.7578	0.3596	1.3327	1.9086
MEAN ELEMENT	3-POINT HERMITE	2880	1.2162	0.1906	0.6255	1.3808	0.03071	0.01225	0.09313	0.09883	1.7729	0.2808	1.3332	1.9086
MEAN ELEMENT	5 POINT LAGRANGE	1440	1.2163	0.1904	0.6249	1.3810	0.03075	0.01227	0.09313	0.09884	1.7730	0.2808	1.1333	1.9086
CARTESIAN/ FOURIER (7 COEF-FICIENTS)	NONE	50	0.1407	0.1630	0.3392	0.4017	0.02103	0.01065	0.01761	0.02942	0.4158	0.4839	0.6281	0.6453
CARTESIAN/ FOURIER (7 COEF-FICIENTS)	NONE	100	0.1407	0.1636	0.3395	0.4022	0.02108	0.01065	0.01757	0.02943	0.3892	0.4572	0.6300	0.6482
CARTESIAN/ FOURIER (7 COEF-FICIENTS)	NONE	150	0.1401	0.1666	0.3406	0.4042	0.02083	0.01066	0.01794	0.02949	0.3749	0.5659	0.6306	0.6844
CARTESIAN/ FOURIER (7 COEF-FICIENTS)	NONE	200	0.1417	0.1670	0.3403	0.4047	0.02069	0.01066	0.01807	0.02947	0.3874	0.5412	0.6343	0.6527

Table B-2. State Vector for the TDRSS

Parameter	Value
Epoch	740228.
Semimajor axis (kilometers)	42163.79344
Eccentricity	0.25304×10^{-3}
Inclination (degrees)	2.0
Longitude of ascending node (degrees)	133.63074
Argument of perigee (degrees)	301.633
Mean anomaly (degrees)	351.633
Latitude (degrees)	1.8 South
Longitude (degrees)	91 West
Period (approximate) (minutes)	1440.00
Spacecraft area (kilometers^2)	0.3×10^{-4}
Spacecraft mass (kilograms)	1402.00

REFERENCES

1. Computer Sciences Corporation, CSC/TM-76/6074, Evaluation of Ephemeris Representations for the Multimission Modular Spacecraft (MMS), P. S. Desai and A. C. Long, August 1976

2. --, Interoffice Correspondence, Evaluation of Onboard Ephemeris Representations, P. Desai and A. Long, October 14, 1975

3. --, Interoffice Correspondence, Evaluation of Ephemeris Representations, A. Long and P. Desai, January 6, 1976

4. --, CSC/TM-77/6236, Evaluation of Ephemeris Representations for Tracking and Data Relay Satellite System (TDRSS) Spacecraft, N. Kumar, September 1977

5. J. D. Vedder, "Representation and Interpolation of Predicted Satellite Ephemerides", Journal of Spacecraft and Rockets, vol. 12, no. 8, August 6, 1975

6. A. J. Fuchs, Goddard Space Flight Center, Private Communication, June 1977

7. Computer Sciences Corporation, CSC/SD-77/6078, Systems Description of the Orbit Representation Program, C. Shenitz, July 1977

8. --, CSC/TM-77/6297, Maximum Entropy Spectral Analysis, D. L. Hall, November 1977